Delineating a Functional Role for the Urinary Biomarker Lipocalin 2 in Prostate Cancer

Allon Hazan
2014

A thesis submitted in accordance with regulations for the degree of PhD.

Centre for Cutaneous Research
Blizard Institute of Cell and Molecular Science
Barts and The London School of Medicine and Dentistry
Queen Mary College
University of London

Declaration of Originality of This Research

I hereby declare that the work presented in this thesis is entirely my own.

……..

Allon Hazan

March 2014

Abstract

Prostate cancer (PCa) is the most commonly diagnosed cancer amongst Western males. PCa progression is strongly linked to steroid receptor signalling, however the modulation of steroid receptor expression in PCa is incompletely understood.

Lipocalin 2 (LCN2) is a secreted protein which binds to Fe^{3+}-containing siderophores and was originally identified as part of the innate immune response. LCN2 has been proposed as a potential biomarker for a range of cancers. However, LCN2 effects appear to be tissue specific. LCN2 expression is associated with poor prognosis in breast cancer, but with good prognosis in pancreatic cancer where it has been used therapeutically. The role of LCN2 in prostate cancer is poorly understood, in particular its effects on steroid receptor regulation.

To elucidate the role of LCN2 in prostate cancer, the LCN2 gene was ectopically expressed in LNCaP cells to generate the LNCaP-LCN2 cell line. LNCaP-LCN2 cells had elevated androgen receptor expression which was linked to increased levels of KLK3 (PSA). LNCaP-LCN2 cells also had reduced levels of Estrogen receptor α (ERα), but increased expression of ERβ. This was combined with higher levels of E-cadherin, but not to changes in other EMT markers.

Reciprocally, LCN2 was suppressed using RNAi in the PC3 cell line to generate PC3-shLCN2 cells. PC3-shLCN2 displayed a distinct change in morphology, with increased cell size and a sub-population of multi-nucleated and highly enlarged cells. PC3-shLCN2 cells had reduced proliferation, and lost the ability to form colonies in a 3D substrate. With regards to steroid receptors, PC3-shLCN2 cells had increased ERα expression, but reduced ERβ expression. This was also combined with a loss of E-cadherin and EGFR.

Microarray analysis of PC3-shLCN2 cells identified changes to expression of a wide range of genes including VEGF-R, SPARC and KLK6. Functional grouping of differentially expressed genes suggests that LCN2 in involved in a range of cellular processes including hormone receptor response, Wnt signalling and cell cytoskeletal integrity. Many, but not all genes identified by microarray were responsive to recombinant LCN2 protein indicating a paracrine function for the protein.

Treatment of PC3 cells with the iron chelator Deferoxamine resulted in phenotypic changes similar to those found in PC3-shLCN2 cells which suggest that LCN2 functions in part due to intracellular iron regulation. In summary, the data presented in this thesis suggests that LCN2 has both pro- and anti- tumourigenic properties in prostate cancer and that the

protein is involved in a much wider range of functions than previously described.

Acknowledgements

I sincerely thank all the people who have helped me in producing this thesis, and who have supported me over the course of this PhD. I would particularly wish to thank my supervisors Dr. Graham Neill and Prof. Mike Philpott for their fantastically invaluable advice and guidance throughout. I am particularly indebted to the other members of both the Neill and Philpott groups, especially Dr. Sandeep Nadendla and Dr. Muhammad Rahman for teaching me techniques and contributing to the development of the project. I also wish to thank Neill group members Dr. Dimalee Herath, Dr. Margherita Ruocco, Matt Ward and Mahvesh Javaid for all their help and assistance. I also wish to thank all the staff at the Blizard Building, including Gary Warnes for his help with FACS analysis. A special thanks goes to Dr. Joanne Selway and Avijit Roy for their help with MetaCore analysis.

This thesis would not be possible without the support and love of my family and friends. Thank you for putting up with me for the past few years, and cheering me up when everything seemed to go wrong. This thesis is dedicated to you.

List of Abbreviations

AD	**Androgen Dependent**
AGR2	**Anterior Gradient Protein 2 homolog**
AI	**Androgen Independent**
AR	**Androgen Receptor**
ARE	**Androgen response element**
BCa	**Breast Cancer**
BCC	**Basal Cell Carcinoma**
BCL2	**B-cell lymphoma 2**
BOCT	**SLC22A17 solute carrier family 22, member 17**
bp	**Base Pairs**
BRCA1	**Breast cancer 1, early onset**
CSC	**Cancer Stem Cell**
CD44	**Cluster of Differentiation 44**
CO_2	**Carbon Dioxide**
DFX	**Deferoxamine**
DHT	**Dihydrotestosterone**
DNA	**Deoxyribose Nucleic Acid**
EGF	**Epidermal Growth Factor**
EGFR	**Epidermal Growth Factor Receptor**
EIF4BP1	**Eukaryotic translation initiation factor 4E-binding protein 1**
ELISA	**Enzyme-Linked Immunosorbent Assay**
EMT	**Epithelial to Mesenchymal Transition**
ER	**Estrogen Receptor**
ERE	**Estrogen Receptor Element**
ERK	**Extracellular-signal-regulated kinase**
FACS	**Fluorescence-activated cell sorting**
FBS	**Foetal Bovine Serum**
Fe^{3+}	**Iron 3+ ion**
g	**Gram**

GAPDH	**Glyceraldehyde 3-phosphate dehydrogenase**
HIF-1α	**Hypoxia-inducible factor 1α**
Hh	**Hedgehog**
HIP	**Hedgehog Interacting Protein**
hrs	**Hours**
IGF	**Insulin-like Growth Factor**
IκB	**Inhibitor of kappa B**
IKK	**IκB kinase**
IL1β	**Interleukin 1β**
KAAD-cyc	**KAAD-Cyclopamine**
KLK	**Kallikrien**
LCN2	**Lipocalin 2**
LCN2-R	**Lipocalin 2 Receptor**
M	**Molar**
MAP	**Mitogen-activated protein Kinase**
µl	**Microlitre**
m-RNA	**Messenger- RNA**
mins	**Minutes**
mTOR	**Mammalian Target of Rapamycin**
NF-κB	**Nuclear factor kappa-B**
nm	**Nanometre**
p-	**Phospho-**
PCa	**Prostate Cancer**
PCR	**Polymerase Chain Reaction**
PIN	**Prostatic intraepithelial neoplasia**
PSA	**Prostate Specific Antigen**
PTCH1	**Patched 1**
PTEN	**Phosphatase and tensin homolog**
qPCR	**Quantitative Polymerase Chain Reaction**
RNA	**Ribonucleic Acid**
RT-PCR	**Reverse transcriptase polymerase chain reaction**

SHBG	**Albumin sex hormone binding globulin**
SHH	**Sonic Hedgehog**
shRNA	**Short hairpin RNA**
siRNA	**Short interfering RNA**
SMO	**Smoothened**
SPARC	**Secreted protein acidic and rich in cysteine**
SUFU	**Suppressor of Fused Homolog**
TCF	**T-Cell factor**
TGFβ	**Transforming growth factor beta**
TGFβR	**Transforming growth factor beta receptor**
TNM	**Tumour-node-metastasis**
TP53	**Tumour Protein 53**
TSC1	**Tuberous sclerosis 1**
TWIST1	**Twist-related protein 1**
VEGF	**Vascular endothelial growth factor**
VEGFR	**Vascular endothelial growth factor receptor**
v/v	**volume/volume**
w/v	**weight/volume**
ZEB1	**Zinc finger E-box-binding homeobox 1**

Presentations and Publications

This data has been presented at the following scientific publications;

> **GLI1 confers profound phenotypic changes upon LNCaP prostate cancer cells that include the acquisition of a hormone independent state.** Nadendla,S.K., Hazan, A., Ward, M., Harper, L. J., Moutasim K., Bianchi, L.S., Naase, M., Ghali, L., Thomas, G.J., Prowse, D.M., Philpott, M.P., Neill, G.W., PLoS One, 6, e20271.

These data has been presented at the following scientific meetings;

GLI1 confers profound phenotypic changes upon LNCaP prostate cancer cells that include the acquisition of a hormone independent state

Sandeep Nadendla, Allon Hazan, Matt Ward, M., Lucy Harper, Kemal Moutasim Lucia Bianchi, Mohammed Naase, Lucy Ghali, Gareth Thomas, David Prowse, Mike Philpott, Graham Neill.

Young Prostate Researchers Symposium, Cambridge, November 2010 (Poster)

The role of LCN2 in Prostate Cancer

Allon Hazan, Sandeep Nadendla, Mike Philpott and Graham Neill.

Graduate Day, QMUL, May 2011 (Poster)

The role of LCN2 in Prostate Cancer

Allon Hazan, Sandeep Nadendla, Mike Philpott and Graham Neill.

William Harvey Day, Bart's Hospital, October 2011 (Poster)

Lipocalin 2 Regulates Multiple Tumour-associated Mechanisms in Prostate Cancer Cells. Allon Hazan, Sandeep Nadendla, Joanne Selway, Avijit Roy, Matt Ward, Mike P. Philpott, Graham W. Neil. Graduate Day, QMUL, May 2012 (Poster)

Lipocalin 2 Regulates Multiple Tumour-associated Mechanisms in Prostate Cancer Cells. Allon Hazan, Sandeep Nadendla, Mahvesh Javaid, Luis Beltran, Joanne Selway, Avijit Roy, Matt Ward, Mike P. Philpott, Graham W. Neil. M, L,

William Harvey Day, Barts Hospital October 2012 (Poster)

The Biomarker LCN2 Regulates Multiple Tumor-associated Genes and Mechanisms in Prostate Cancer Cells

Allon Hazan, Joanne Selway, Sandeep Nadendla, Mike Philpott & Graham Neill.

Joint AACR-JCA Conference- Breakthroughs in Basic and Translational Cancer Research- Maui, USA. February 2013. (Poster)

The Biomarker LCN2 Regulates Multiple Tumor-associated Genes and Mechanisms in Prostate Cancer Cells

Allon Hazan, Joanne Selway, Sandeep Nadendla, Mahvesh Javaid, Mike Philpott & Graham Neill. William Harvey Day November 2013 (Poster)

List of Figures and Tables

Chapter 1
Introduction

1.1 Anatomy and function of the prostate

The prostate is a critical component of the male reproductive system and is common to all mammals. In humans, the prostate gland is approximately 4.5-5 cm in diameter, and is of a similar size and shape to a chestnut and is found directly beneath the bladder (Myers, 2000).

The primary function of the prostate gland is to secrete an alkaline fluid which is a major constituent of semen. This alkaline microenvironment increases the lifespan of spermatozoa by neutralising the slightly acidic environment found in the female reproductive tract which is present as an anti-microbial fluid (Myers, 2000). Without the alkaline fluid, sperm would be unable to survive long enough for fertilization to occur. Neutralisation thereby provides an optimal pH for reproduction. The alkaline fluid contains acid phosphatases, a range of proteolytic enzymes and zinc (Owen and Katz, 2005). Also present is prostate specific antigen (PSA), which is critical to maintaining the liquidity of semen, and allows sperm cells to swim unhindered (Lilja, 2003).

As the prostate's role is primarily reproductive, the size of the prostate is relatively small in pre-pubescent males, but enlarges rapidly upon the onset of puberty (McLaughlin et al., 2005, Myers, 2000). In post-pubescent males, the prostate is approximately 10-20g in weight and has an inverted conical shape, with the base at the bladder neck and the apex at the urogenital diaphragm (Leissner and Tisell, 1979). The prostate gland is not uniform in physiology; rather it can be divided into zones. These zones are the peripheral zone (which comprises ~75% of tissue), transitional zone and central zone (Figure 1.1) (McNeal, 1981). Surrounding these

areas is the stroma. Each of these zones has specific functions and change in size and volume through puberty. In terms of pathology, prostatic tissue forms a honeycomb-like structure, consisting of ducts, comprised of epithelial tissue forming roughly spherical structures. These ducts are relatively simple structures, comprising of a few tissue layers, surrounded by stromal tissue which connects the ducts and creates structure (Myers, 2000). Luminal cells are responsible for producing PSA and alkaline fluid, which drain into the ducts, which are connected to the ejaculatory duct. The urethra runs through the centre of the prostate from top to bottom. The urethra and ejaculatory ducts are connected through small openings which allow passage of the seminal fluid (McNeal, 1981).

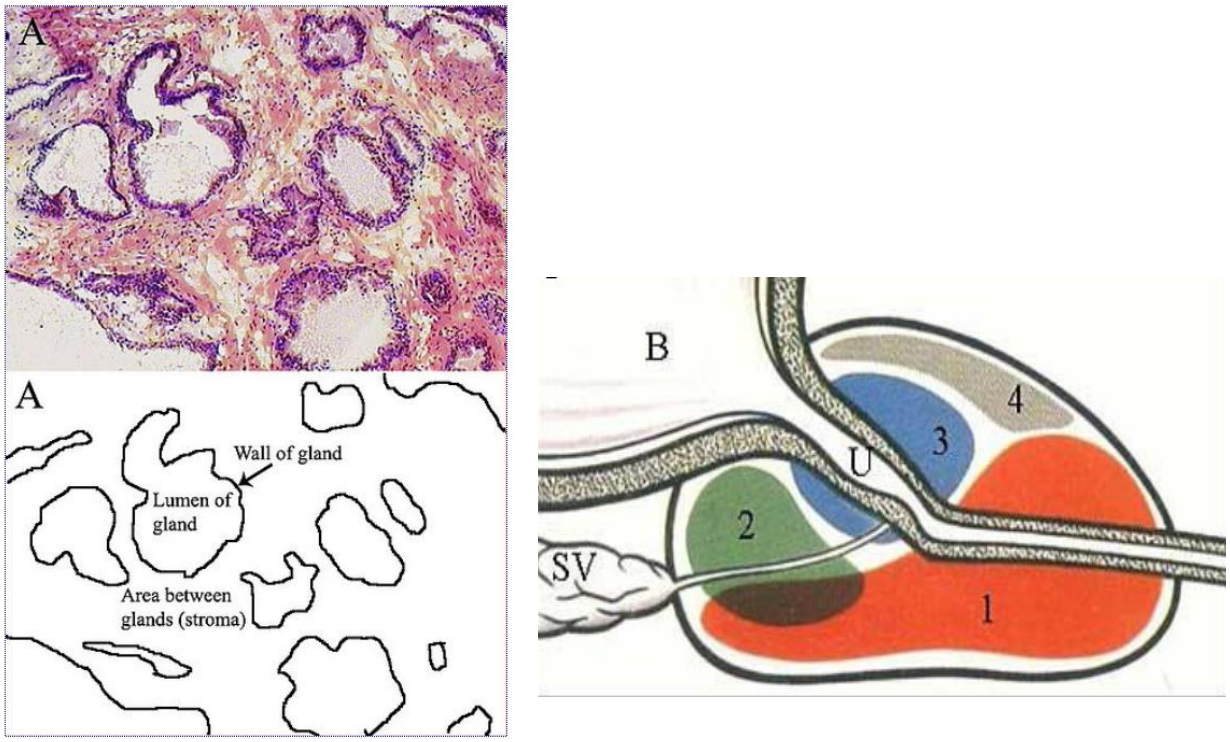

Figure 1.1 Histology and anatomy of the prostate: A- Haematoxylin and Eosin straining of healthy prostate tissue. Walls of glands/ducts are stained purple. Stromal regions are stained pink (commons free-of-use image). B Prostatic zones: 1= Peripheral Zone, 2= Central Zone, 3= Transitional Zone, 4= Anterior Fibro muscular Zone. B= Bladder, U= Urethra, SV= Seminal Vesicle (adapted from Algaba, 1991)

1.2 Histology and cell types of the prostate gland.

The prostate is relatively simple in terms of cellular composition. The majority of prostate tissue is comprised of a layer of epithelial tissue which form the secretory ducts surrounded by connective and stromal tissue. The stroma surrounds and connects epithelial tissue and is consists of a fibroblasts, smooth muscle tissue and endothelial cells (Myers, 2000). As well as providing structural support, the stroma is also believed to interact with the epithelial layers and induce signalling(Lee, 1996).

The inner layer of the epithelial tissue is formed of cuboidal luminal cells (Figure 1.2)(Lang et al., 2001). These cells are relatively differentiated, and are responsible for producing PSA. The luminal cells are surrounded by a layer of flat, and less differentiated basal cells. These basal cells provide a structural attachment base for luminal cells, and also provide a source of new, undifferentiated cells. The basal layer is also believed to contain purported prostate stem cells (Signoretti et al., 2000, Collins et al., 2005). In addition, the basal layer also contains transit amplifying cells, which are partially differentiated into luminal cells. Interspersed within the basal layer are a small number of neuroendocrine cells. As their name suggests, neuroendocrine cells have a dendritic appearance (Abrahamsson, 1999, Bonkhoff, 1998), and express a number of neuropeptides. The role of neuroendocrine cells is not fully resolved, but it is believed that they are involved in tissue maintenance and differentiation. Indeed, they are known to secrete growth factors such as VEGF and a wide range of signalling peptides (Sun et al., 2009).

Luminal and basal cells differ markedly with regards to gene expression. The two cell types express different keratins: Basal cells are known to express both Keratin 5 and 18, whereas luminal cells express Keratin 18. In keeping with their role of tissue

generation, basal cells express the proliferation marker Ki67, whereas the terminally differentiated luminal cells do not (Sherwood et al., 1991, Tran et al., 2002).

Basal and luminal cells differ in their expression of cell adhesion and structural molecules. The adhesion molecule E-cadherin is expressed at high levels in luminal cells, but does not express the filament vimentin, whereas basal cells express vimentin but not E-cadherin (Tomita et al., 2000). This is also true of the cell surface basal marker CD44 which is not expressed in luminal cells but is in basal cells (Collins et al., 2005).

One of the key differences between luminal and basal cells is in the expression of both androgen Receptor (AR) and PSA (Liu et al., 2002). Basal cells express neither AR nor PSA, and this ability is only conferred on cells which have differentiated fully to luminal cells (transit amplifying cells also express neither AR nor PSA) (Goldstein et al., 2010, Smith and Catalona, 1994).

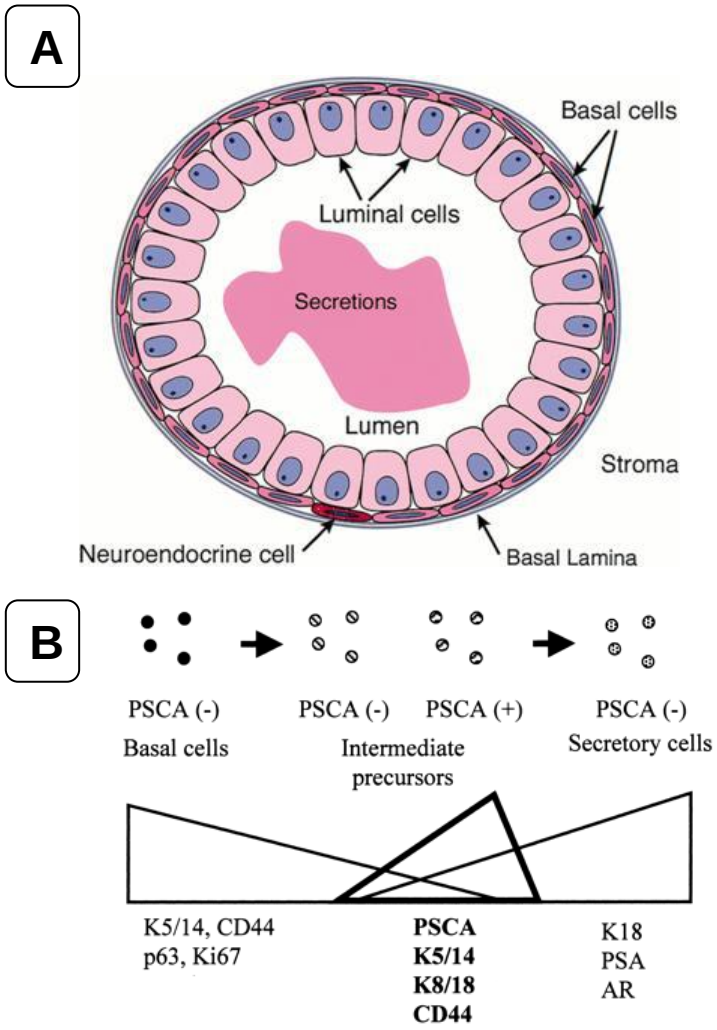

Figure 1.2 Overview of cell types in the prostate. A- Cross section of a prostate secretory duct. The prostate secretory duct is comprised of cuboidal luminal epithelial cells surrounded by a layer of basal cells interspersed with neuroendocrine cells. B- Changes in expression of key genes from basal to secretory cells. Basal cells express CD44, which is lost in secretory cells. Secretory cells gain expression of PSA and AR (Modified from Tran et al,. 2002).

1.3 Prostate cancer: Epidemiology, causes and classification.

Prostate cancer (PCa) is the most commonly diagnosed form of cancer amongst Western males. According to recent statistics, approximately 40,000 men were diagnosed with PCa every year in the Britain alone, making up 25% of all cancer diagnoses for males (Cancer research UK statistics,-www. cancerresearchuk.org/cancer-info/cancerstats/types/prostate/incidence/).Worldwide, around 1 million people are diagnosed with PCa every year. Prostate cancer survival rates are improving, but nevertheless, PCa still has a high mortality rate. In Britain, approximately 10,000 men die each year as a direct result of the disease (Cancer research UK statistics).

Whether a man will develop prostate cancer is dependent on a range of factors. By far the greatest risk is associated with advanced age. Only 1% of new prostate cancer diagnoses are in patients under 50 years. The incidence of PCa increases rapidly, with over 75% of cases being diagnosed in men over 65 (Bray et al., 2010). Over recent decades, diagnosis of PCa has increased dramatically due to a combination of ageing populations in developed countries and improved screening techniques.

In addition to age, there are a number of factors which increase the risk of developing prostate cancer. Only around 5% of PCa is associated with hereditary genetic mutations. Of these, mutations in either BRCA1 or BRCA2 are commonly found a source of PCa development, and can increase the risk of PCa development by up to 5 times (Levy-Lahad et al., 2000). These mutations are usually associated with breast cancer, and indeed having a mother with breast cancer has been associated with an ~20% increased risk (Hemminki and Chen, 2005).Having a father

or brother with PCa also greatly increases the probability of developing the condition oneself by between 100-200% (Hemminki and Chen, 2005).

PCa has widely variable rates in different countries, with Western developed countries showing the highest incidence and Eastern countries such as Japan having significantly fewer cases (Jadvar, 2011). This distinction is believed to derive mostly from differences to diet and activity rather than genetic factors as men with Asian ancestry living in the USA or Europe show similar levels of diagnosis to the Caucasian population (Jadvar, 2011). Diet has been shown to be a partial determinant for PCa in a number of studies. Soya based products- consumed frequently in Asia- have been shown to reduce PCa incidence by 26-30% in Asian males (Yan and Spitznagel, 2009). Carotenoids including vitamin A have also shown to reduce risk (Giovannucci et al., 1995). Other more tenuous preventatives have included green tea, coffee and omega-3 fish oils (Jian et al., 2004, Berquin et al., 2007). As with all diet based studies however it is difficult to confirm whether these effects are purely due to food intake or overall lifestyle differences. Relative to other cancer types, smoking is not a major factor in PCa, although it may increase risk moderately (Huncharek et al., 2010). In a very large study, Roddam et al. (2008) showed no correlation between circulating androgens or estrogens and the risk of developing PCa (Roddam et al., 2008).

The vast majority (>95%) of prostate cancers are adenocarcinomas, or neoplasia of glandular epithelial tissue. The remaining 5% of tumours are mostly neuroendocrine tumours (Jadvar, 2011). PCa sarcomas are relatively rare but not totally absent. Approximately 75% of PCa tumours originate in the peripheral zone of the prostate, with a further 20% originating in the central zone. Tumours arising from the central

zone are relatively rare (2-3% of cases), but have been shown to be more aggressive in behaviour (Cohen et al., 2008).

A potential precursor to prostate cancer is known as Prostatic intraepithelial neoplasia (PIN). This is a more benign disease whereby there is increased cell proliferation, but where the basal layer of the prostate remains intact (Montironi et al., 2007). In PCa, the basal layer is often disrupted or even absent. Whether PIN necessarily precedes carcinogenesis itself is however still under discussion (Herawi et al., 2006).

Until fairly recently, the origin of PCa was believed to be in the luminal cells (Stoyanova et al., 2013). This was due to the similarity of histological sections of tumours with epithelial cells. However, a number of studies (Goldstein et al., 2010) have since demonstrated that basal cells are also implicated. Indeed, other studies have shown interaction between the basal and epithelial layers in stimulating PCa tumour growth (Tuxhorn et al., 2002a, Tuxhorn et al., 2002b).

Prostate cancer grade is determined histologically by the Gleason grading system which ranges from 1 to 5, where 5 has the least differentiation and the poorest prognosis. Two samples are usually identified based on the most common and second most common patterns. The scores are then combined to give a total score from 2-10. For example, a high scoring grade may hence be labelled as 5+2=7. A further, more clinical scoring system known as tumour-node-metastasis (TNM) system. TNM classification is based on the presence and size of primary tumours, evaluation of lymph nodes, and the presence and distance of metastases. TMN and Gleason scores may be combined to assess a disease stage, ranging from stage I to stage IV, with stage IV being the most severe (Thorson and Humphrey, 2000).

Diagnosis of PCa is most commonly performed through either physical examination or punch biopsies, or through the PSA blood test (Velonas et al., 2013). At early stages, PCa is often associated with increased sensitivity to androgens, and to an increase in the expression of AR (Feldman and Feldman, 2001). Under normal conditions, AR is sequestered in the cytoplasm by Hsp90 and Hsp70 (Reebye et al., 2012). Upon binding of AR to testosterone or dihydrotestosterone (DHT), AR is released and relocates to the nucleus where it is dimerised and acts as a transcription factor, binding to androgen-response elements enabling the transcription of numerous genes, including PSA (Figure 1.3). The increase in PSA is therefore a good initial indicator for determining abnormal proliferation. While the PSA test has disadvantages, as it does not detect all prostate cancers, and in many cases produces many false positives, the PSA test has enabled the early detection and treatment of PCa for thousands of men. Indeed, the PSA test is now freely available for all men over 50 in the UK. Diagnosis can be followed up with a biopsy test to rule out false positives due to temporary infection and to test for tumour grade.

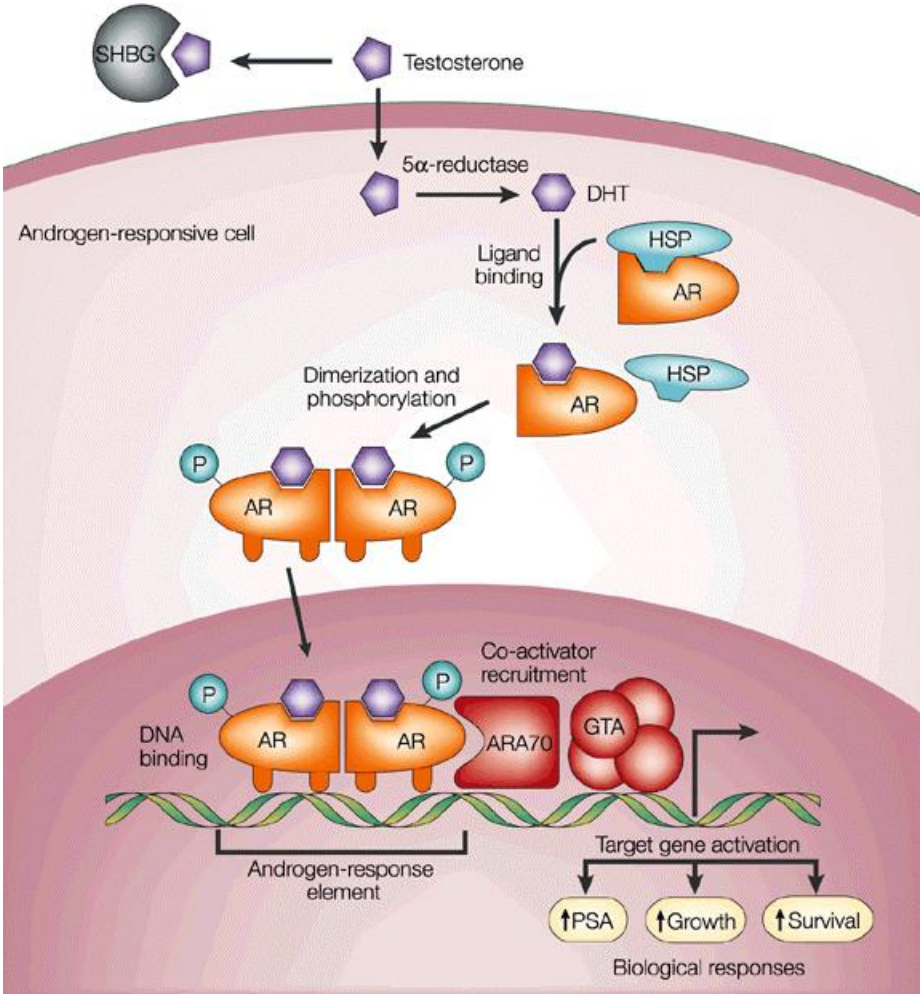

Figure 1.3 Mechanisms of androgen receptor function. The majority of testosterone (97%) circulates in the bloodstream where it binds to one of two proteins: or albumin sex hormone binding globulin (SHBG). Testosterone is reduced into dihydrotestosterone (DHT) by 5α-reductase. DHT is 2-3 times more potent than normal testosterone. DHT binds to AR facilitating the dissociation of AR from heat shock proteins (HSP), thus allowing it to dimerise and translocate into the nucleus. Here, the DHT/AR complex engages with specific chromatin regions, androgen response elements (AREs), to control target gene expression such as PSA and genes responsible for growth and Survival (Adopted from Feldman and Feldman, 2001).

1.4 Treatment of prostate cancer: The problem of Androgen independence and metastasis

Cancer of the prostate alone is not usually fatal as the prostate is not a vital organ such as the liver or lungs. As such, early stage PCa is focused on tumour management and hormone starvation. The majority of prostate cancers express both androgen receptor and hence PSA. Indeed, cancer cells require AR's ability to bind to DHT to enable cell division and drive growth. Therefore, first line treatment for PCa involves hormone deprivation therapy (Attard et al., 2011). Patients may undergo a prostatectomy or radiotherapy, thereby cutting off the supply of androgens(Tammela, 2012). Alternatively, AR signalling is blocked by chemical inhibitors. Clinically, the most common inhibitor in use currently is bicalutamide (Casodex®) (Wirth et al., 2007). Bicalutamide is an anti-androgen which is able to preferentially bind to AR, thereby inhibiting the binding of DHT. Over time this leads to hormone starvation and eventually tumour reduction and can even act as a total cure.

While hormone deprivation treatment is highly effective in treating low grade prostate cancer, this method often not able to totally clear the disease completely. As mentioned in section 1.3, many PCa tumours require the expression of androgen receptor for growth. In many cancers however, particularly in those patients which have already undergone hormone refractory treatment, cells become androgen independent (AI). In this case, cells remove the need for androgen signalling and are able to evade drugs such as bicalutamide (Garcia and Rini, 2012). There are a number of proposed theories as to how cells become androgen independent, and there is considerable variation between patients (Reviewed (Pienta and Bradley, 2006). A well-defined mechanism for AI is termed the bypass pathway, whereby

through mutation, the anti-apoptotic protein BCL2 is over expressed, preventing cells from apoptosing after steroid withdrawal. Alternative mechanisms include AR being able to bind to non-steroids such as EGF and signal independently of testosterone (Pienta and Bradley, 2006).

As mentioned in section 1.3, prostatic tumours by themselves are rarely fatal. Disease progression therefore is dependent on the tumour metastasising to other areas of the body. In prostate cancer, approximately 90% of advanced patients have metastases in bone tissue. Other common metastases are to lung (46%) and liver (25%) (Bubendorf et al., 2000). The reasons why PCa cells specifically target the bone as opposed to other tissue is still not fully resolved. However, studies have suggested that PCa cells are attracted by cell surface integrins such as avβiii which are present on bone cells, and enable attachment of the cancer cell to the bone tissue (McCabe et al., 2007, Schneider et al., 2011). Bone cells also produce a number of chemoattractants such as SPARC (Derosa et al., 2012, Shin et al., 2013). Conversely, PCa cells are also able to modify the bone tissue environment. One way in which this is done is by secreting factors such as Wnts, which activate osteogenic pathways, allowing entry into the tissue (Dai et al., 2008).

Metastatic PCa cells often show signs traditionally associated with epithelial-mesenchymal-transition (EMT). As the name suggest, EMT is process whereby epithelial cells change gene expression and morphology, and instead express mesenchymal markers and have increased migration and plasticity. EMT is a necessary cellular function associated with processes such as wound repair and development which are hijacked by cancer cells (Micalizzi et al., 2010). Common

characteristics of EMT include the loss of E-cadherin expression, as well as increased expression of E-cadherin inhibitors such as SNAI1, TWIST1 and ZEB1. Conversely, cells in EMT increase expression of N-cadherin and other intracellular filaments such as vimentin (Thiery et al., 2009).

There are a number of causes for EMT involving a range of cell signalling mechanisms which are often interlinked. One well established mechanism is via the receptor TBFβR. Upon binding to its ligand TGF, TGFβR is able to activate the transcription factors known as Smads (Heldin et al., 2012, Xu et al., 2009). These transcription factors are then able to relocate to the nucleus where they are able to both inhibit epithelial marker genes and drive mesenchymal marker expression. Smad proteins have also been shown to interact with other EMT genes such as ZEB1 (Xu et al., 2009). While the TGFβ-Smad pathway is known as the canonical pathway, TGFβ is also known to activate a range of other signalling mechanisms such as the MAP-Kinase pathway, which is also able to interact with SNAI1(Vincent et al., 2009) (Figure. 1.4).

1.5 Cell lines used in prostate cancer research

Ideally, all studies of prostate cancer would be performed *in vivo*. However, in order to obtain much more rapid, higher output, and less ethically problematic data, cell lines have been derived from patients which are able to proliferate almost indefinitely. Cell lines also have a benefit of being generated from human tissue, thereby removing any issues of species differentiation, as there is still some debate as to whether a mouse model is phenotypically similar to what occurs in the human prostate (Reviewed by (Ittmann et al., 2013). Numerous PCa cell lines exist, nevertheless, the lines LNCaP, PC3 and DU145 are by far the most commonly used in research (Table 1.2) (Sobel and Sadar, 2005).

The LNCaP cell line is derived from needle aspiration biopsy of a lymph node metastatic lesion from a 50-year-old white man (Horoszewicz et al., 1980). Cells grown relatively sparsely in tissue culture conditions and are often elongated and maintain a degree of polarity. LNCaP cells show less tumorigenicity than most other PCa cell lines. LNCaP cells attach poorly to plastic and can LNCaP cells are notable for their expression of androgen receptor and PSA. LNCaPs also express Estrogen receptor α. However, LNCaP cells do have a mutation at T877A which leads to more non-specific steroid binding (Sobel and Sadar, 2005). As a result of AR expression, LNCaP cells require androgens and other steroids in order to proliferate normally, and will have significantly reduced growth in steroid free media. With regards to karyotype, there is a large degree of aneuploidy, with cells containing ~33-90 chromosomes. The cell line does however have a wild type p53. The LNCaP cell line is also the parent population for many other lines, some of which have been generated to be androgen independent such as LNCaP-AI and LNCaP-104s (Sobel and Sadar, 2005).

PC-3 cell line was derived from a lumbar vertebral metastasis in a 62-year-old white man (Kaighn et al., 1978). This cell line is highly tumourigenic, and is greatly metastatic in xenograft models. Cells form moderately tight colonies and cells are often somewhat irregular in shape. A key feature of PC3 cells is that they do not express androgen receptor or PSA, and are able to proliferate in only 1% serum (Sobel and Sadar, 2005). Aneuploidy is ubiquitous in the cell line, with an average chromosome number of 58 PC3 cells contain a mutation in the TP53 gene which causes a frame-shift mutation resulting in a premature stop codon (van Bokhoven et al., 2003). PC3 is also the parental line for other derivative cell lines such as ALVA-31 and PC3-1A (Sobel and Sadar, 2005).

The DU-145 cell line was derived from a tumour mass excised from the brain metastasis of a 69-year-old white man with both prostate cancer and lymphocytic leukaemia (Stone et al., 1978). DU145 cells are epithelial in origin and were the first PCa cell line to be fully described. DU145 cells do not express AR or PSA, but are not as tumorigenic as PC3 cells but do proliferate rapidly. Aneuploidy is also present. DU145 cells are heterozygous for p53, which is partially active. Due to the rare nature of the brain origin of DU145, there is some debate as to whether this cell line accurately models prostate cancer but it does serve as a model for cell signalling (Sobel and Sadar, 2005).

Other prostate cell lines sometimes referred to literature include PNT2, which is derived from normal prostate epithelial tissue from a 33 year old male immortalised with an SV40 virus. These cells are non-tumourigenic, and express AR and PSA (Sobel and Sadar, 2005). VCaP cells are a cell line which is derived from a vertebral lesion of a 59 year old male, but express AR and PSA.

Cell Line	AR expression	P53 status	Tumorigenicity
LNCaP	Yes	Wild type	Low
PC3	No	Null	High
DU145	No	Mutated	Moderate
PNT2	Yes	Wild type	None

Table 1.1 Overview of commonly used prostate cell lines

1.6 Key signalling mechanisms in prostate cancer:

1.6 NF-κB signalling

Nuclear factor kappa-B (NF-κB) is a transcription factor complex which sits at the centre of a wide range of cellular processes (Sen and Baltimore, 1986). NF-κB is most commonly associated with rapid cellular responses such as innate immunity and inflammation. NF-κB itself is a complex comprised of p50 and RelA (Gilmore, 2006). Under non-activating conditions, the NF-κB complex is sequestered in the cytoplasm by IκB (Perkins, 2007). Stimulation via cell surface receptors, leads to the activation of IKK, which in turn phosphorylates IκB. Phosphorylation enables IκB to be targeted for proteasomal degradation, allowing NF-κB into the nucleus where it associates with co-activators and binds to DNA and helps drive transcription (Senftleben et al., 2001) (Figure 1.4). The NF-κB pathway has been shown to have a large amount of both upstream and downstream cross-talk between other signalling pathways. IKK has been shown to be activated by the p53 pathway (Kawauchi et al., 2008) and mTOR/AKT signalling (Lee et al., 2007). NFκB is also known to

regulate a range of other pathways including inducing transcription Hypoxia-inducible factor 1α (HIF-1α) (Rius et al., 2008). NF-κB also activates transcription of interleukin 1β (IL1β) (Cowland et al., 2006). Indeed, IL1β itself is an activator of the NF-κB pathway, creating a positive feedback loop (Hartupee et al., 2008, Niu et al., 2004).

With regards to prostate cancer NF-κB has been shown to be indicative of a poor prognosis in patients (Karin et al., 2002). It is also a key component of inflammation in cancer. NF-κB has also been shown to lead to an androgen independent phenotype, and is up-regulated in hormone refractory patients (Suh and Rabson, 2004, Zhang et al., 2009). A study by Nadiminty et al (2012) demonstrated that NF-κB itself interacts with the N-terminal of AR, enabling its translocation to the nucleus and also assists in recruiting co-activators to AR transcription sites, and can enable the transcription of androgen independence linked genes (Nadiminty et al., 2010). Also, NF- κB over expression has been assist in AR entering the nucleus, and is present at greater levels in androgen independent PCa cell lines (Jain et al., 2012). As with any pathway however, the precise role of NF-κB is likely to be dependent on the presence and absence of other factors.

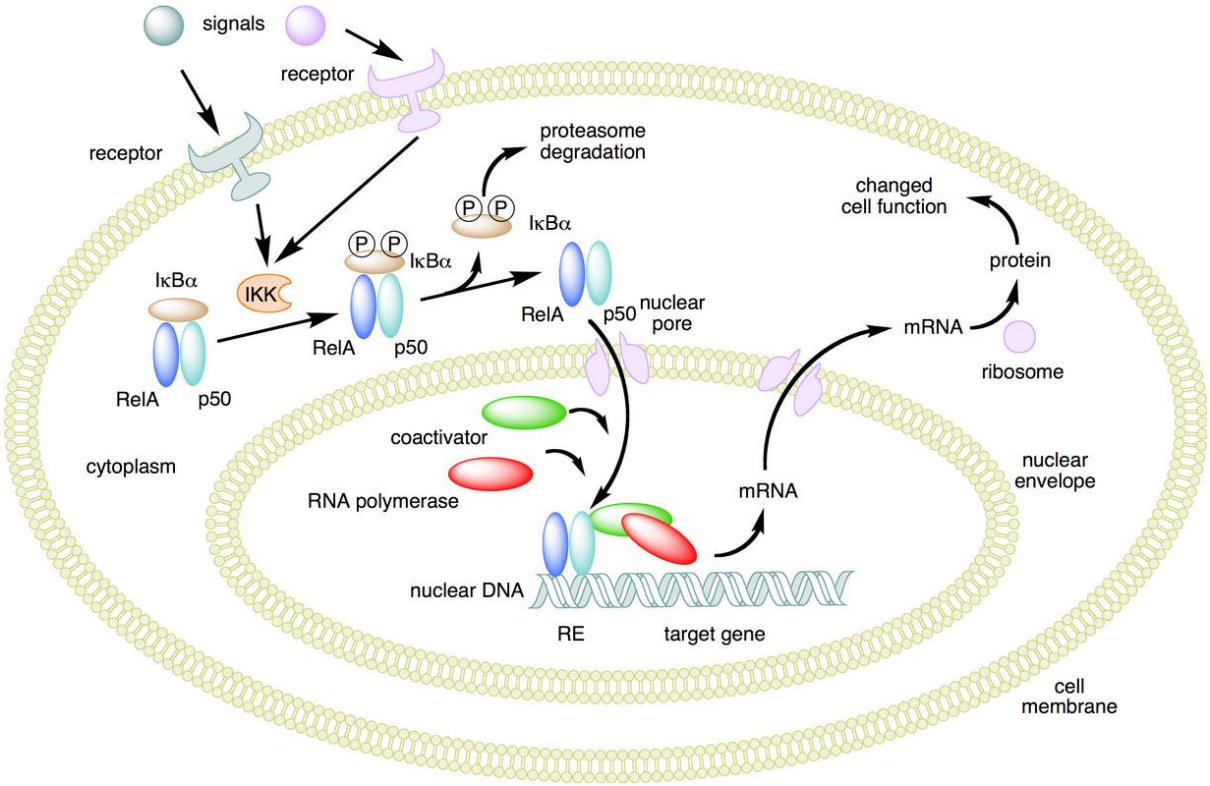

Figure 1.4 The NF-κB pathway. Under non-stimulating conditions, the NF-κB complex, comprising of RelA and p50 is sequestered in the cytoplasm by IκB. When activated, IκB is phosphorylated by IKK, and is targeted for proteasomal degradation. The NF-κB complex is then free to enter the nucleus, where it binds to co-activators and drives mRNA expression (Commons free image).

1.8 Hedgehog Signalling: Mechanism of action

The hedgehog (Hh) signalling pathway plays an essential role in the regulation of, differentiation, proliferation patterning and growth of the embryo, and is a key regulator of cell proliferation. The hedgehog pathway was first identified in *Drosophila Melanogaster* studies, where Hh mutant larvae had a hairy or hedgehog like appearance for which Nüsslein-Volhard and Wieschaus won the Nobel prize (Nusslein-Volhard and Wieschaus, 1980). It was later found that Hh is actually a secreted protein (Bumcrot et al., 1995). Hh is highly conserved across animals (Krauss et al., 1993, Ingham et al., 2011), however whereas *D. Melanogaster* has only a single Hh protein, in humans there are 3 sub-types namely Sonic Hedgehog (SHH), Desert Hedgehog (DHH) and Indian Hedgehog (IHH), of which SHH is by far the most studied (Krauss et al., 1993).

After being secreted, SHH binds to the transmembrane protein PTCH1 (a homologue of Patched in *D.Melanogaste*r). Under non-stimulating conditions, one of PTCH1's main functions is to sequester SMO (Figure 1.6) (a homologue of Smoothened in *D.Melanogaste*r, thereby inhibiting its activity. Upon binding to SHH, SMO is released, allowing to be targeted for phosphorylation by CK1α and GRK2 protein kinases at the C-terminal end which induces conformational changes allowing SMO to translocate to the primary cilium (Figure 1.5) (Chen et al., 2004). Following migration to the cilium, SMO is then able to interact with Suppressor of Fused Homolog (SUFU). Under non stimulating conditions, SUFU is located in the cytoplasm where it is bound to group of proteins called GLI1, GLI2 or GLI3 (grouped as GLI). When these proteins are bound, GLI is phosphorylated and is targeted for proteasomal degradation by ubiquitination (Rahnama et al., 2006). However, under stimulating conditions, SMO preferentially binds to SUFU, freeing GLI and causing

conformational change GLI so that is not degraded and is also able to enter the nucleus (Alcedo et al., 2000) (Figure 1.5).

The GLI (GLI1, 2 and 3) proteins are zinc-finger transcription factors which are the primary effectors of the Hedgehog signalling pathway. GLI1 was first isolated in human glioma cells (hence the name), where it was found to be highly up regulated (Rahnama et al., 2006, Kinzler et al., 1987). Both GLI1 and GLI2 are generally considered to be transcriptional promoters and share the same DNA consensus binding sequence of GACCACCCA (Kinzler and Vogelstein, 1990). GLI3 on the other hand is usually described as a transcriptional repressor. In most unstimulated cells, GLI2 is the member which is most highly expressed, whereas in Hh stimulated cells, active GLI2 will drive the transcription of GLI1. GLI1 and GLI2 share many overlapping characteristics and active forms are both able to transcribe PTCH1, thereby generating a positive feedback look (Liu et al., 1998). However, to prevent hyper-stimulation, GLI1 also transcribes Hedgehog interacting protein (Hip) which also binds and sequesters SHH as an alternative to PTCH1 (Olsen et al., 2004). GLI1 has also been implicated in the transcription of cell cycle factors such as Cyclin D2 and FOXM1 (Teh et al., 2002). GLI expression is also linked to the suppression of apoptosis, and has been shown to increase expression of BCL2 However, while the overall Hh is relatively well understood, the actual global transcriptional effects of GLI1 and GLI2 are still poorly understood.

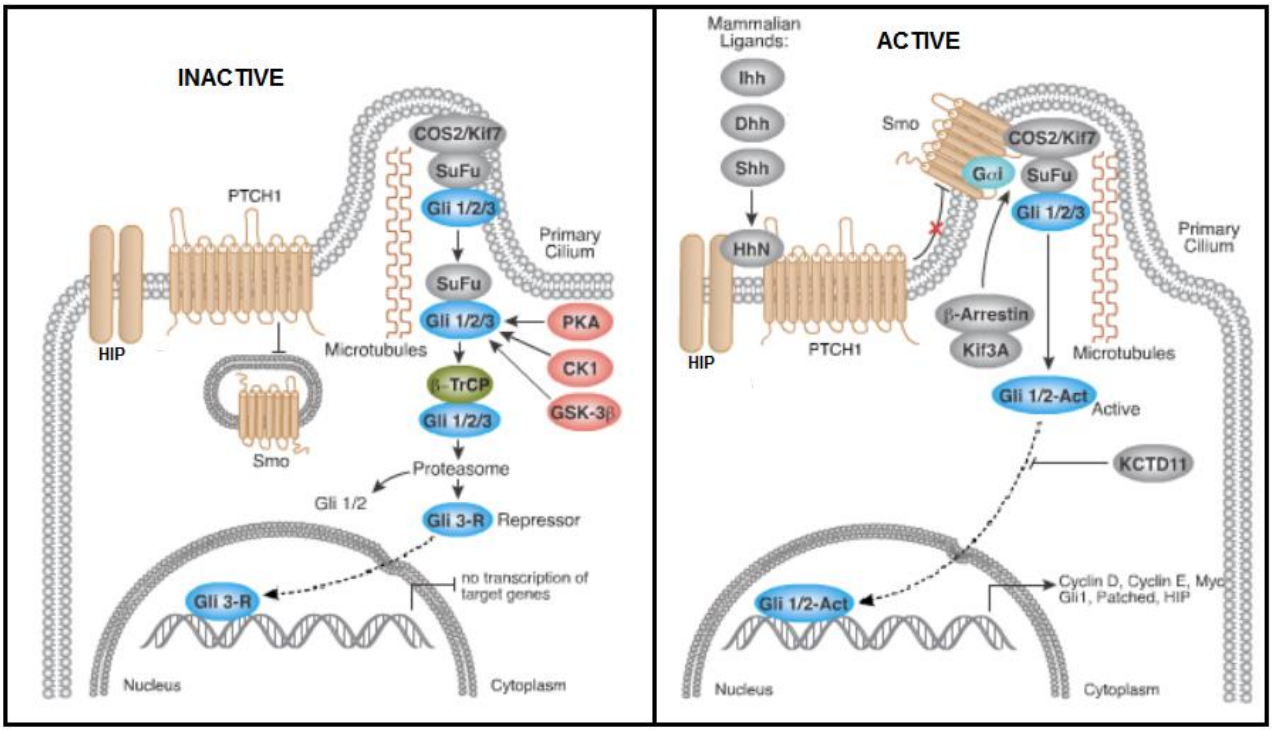

Figure 1.5 Overview of the Hedgehog pathway. Left panel- When inactive, PTCH1 sequesters SMO in the cytoplasm. GLI1/2 is bound by SUFU, and by destruction complexes including GSK-3β which targets it to the proteasome leaving only GLI3 to act as a repressor. When active (right panel), the Hedgehog family bind and inhibit PTCH, allowing SMO to migrate to cilia where it prevents SUFU function and aids in GLI modification and activation. Active GLI1/2 enters the nucleus where it drives transcription of PTCH, Cyclin D1 and HIP (Modified from cellsignal.com/reference/pathway/Hedgehog.html)

1.9 Hedgehog signalling in development and disease

The hedgehog pathway was initially identified with regards to embryonic development. The Hh pathway is critical in the formation of skeletal tissue, in colon and gastroenterinal tissue development and in the patterning of organs such as the lungs (Heussler and Suri, 2003, Laufer et al., 1994, Marigo et al., 1996). Expression of SHH in embryonic limb buds in particular is now widely accepted to help differentiate tissue and is the leading determinant in digit formation in the hands and feet (Marigo et al., 1996). The Hh pathway is also active in adult cells albeit at lower levels, where it performs a wide range of functions. GLI1 is expressed in the hair follicle root sheath (Ghali et al., 1999), and is also necessary for the maintenance of tissues with high turnover such as neural and gut tissues (Ramalho-Santos et al., 2000). Hh signalling also has roles in bone fracture repair (Wang et al., 2010).

Due to the Hh pathway's critical involvement in development, it therefore follows that it is associated with a number of congenital disorders such as polydactyly (having extra fingers), as well as neurological conditions involving malformation of the fore lobe of the brain (Ming et al., 2002, Traiffort et al., 2004).

Aside from developmental diseases, by far the most investigated role of the Hh pathway is in cancer. One of the first links to cancer came from patients with Gorlin syndrome (Ming et al., 2002). Gorlin syndrome is an autosomal inherited disorder with symptoms which include skeletal deformations, particularly in the ribs and vertebrae. However, the man symptom of the syndrome is the propensity to develop numerous basal cell carcinomas (BCCs), and patients are highly susceptible to ultraviolet sunlight. Genetic studies on Gorlin patients revealed that sufferers have mutations in the PTCH1 gene which inactivates one allele (Ming et al., 2002).

Subsequent loss of heterozygosity then leads to the constitutive activation of Hh pathway, giving rise to tumours. Gorlin syndrome is a relatively rare disease (~1 in 20,000), however novel BCC tumours are the most common form of any cancer, with an incidence rate of ~75/100,000 people (Traiffort et al., 2004). While incidence is high, survival rates are very high, in part due to very low rates of metastasis (only 1-2% of cases) and relatively easy surgical removal. Nevertheless, surgery can lead to bad scarring, especially on the head and face. The prevalence of BCCs increases with both exposure to sunlight and the fairness of skin (as a result, Australia has greatly increased incidence). Johnson et al demonstrated that ~85% of BCCs have mutations in the PTCH1 gene, and a further 10% have mutations in SMO (Johnson et al., 1996). Both mutations lead to the Hh pathway being over-stimulated and the proliferation of tumour tissue. Within the pathway, both GLI1 and GLI2 have been directly implicated in the formation of BCC tumours (Dahmane et al., 1997). Mouse studies whereby GLI1 was overexpressed generated skin tumours with a high level of similarity to BCCs (Nilsson et al, 2000). Heterozygous Ptch1+/- mice are also more prone to develop tumours following ultraviolet exposure .

Although many BCCs are excised surgically, in order to prevent scarring and recurrence drugs have since been developed which target the Hh pathway. The majority of pharmacological inhibitors target SMO. Cyclopamine was originally identified after it was found that sheep which had eaten the plants had only one eye and numerous other defects (Taipale et al., 2000). It was later found that Cyclopamine is a naturally occurring small molecular inhibitor of SMO, and hence Hh signalling. Subsequently, KAAD-Cyclopamine has been developed as a more potent artificial derivative. Other SMO inhibitors such as SANT-1 and Sonidegib have also been tested with mixed success (Yang et al., 2010). Drugs have also been

developed which target the GLI family specifically. GANT-61 has been shown to inhibit GLI 1,2 and 3 in pancreatic cancer xenograft model (Fu et al., 2013), however to date, there have been no *in vivo* studies published.

1.10 The Hedgehog Pathway in Prostate Cancer

As well as BCCs, the Hh pathway has been implicated in a number of other cancers including breast, medulloblastomas and lung (Yang et al., 2010). The Hh pathway has also been shown to be active in prostate cancer. The Hh pathway is active in the embryonic development of the prostate gland where it regulates gland polarity and ductal budding. The pathway continues to be active in the adult where it is necessary for epithelial upkeep and regeneration, although levels are lower than in the embryo. Unlike in BCCs, the Hh pathway in prostate cancer is not usually associated with PTCH1 or SMO mutations, indeed mutations of these genes are virtually absent in patients. Mutations to SUFU have however been observed at low frequency (Chen et al., 2011).

Currently, there are a number of mechanisms proposed for the development of Hh based prostate cancer growth, often labelled type I, II, III and IIIb (Figure 1.6). Type I, or 'ligand independent growth' is similar to BCCs as mentioned above, whereby mutations, usually SUFU in PCa lead to constitutive activation of the Hh and GLI pathways. Type II growth or 'ligand dependent autocrine growth' is where Shh activates the Hh pathway, leading to GLI1 and GLI2 expressing both more PTCH1 and Shh, thereby creating a positive feedback loop and over-proliferation of cells. Type II growth has previously been detected in PCa (Kharkodar et al 2004), however the precise reasons which stimulate initial elevated Shh growth is still relatively

unclear. Factors such as NF-κB have been proposed in PCa, and elevated Shh may be as a result of mutations in other signalling pathways.

Type III or 'ligand dependent paracrine' growth states that rather than single cancer cell mutations, growth is dependent on stromal cell activation (Figure 1.6). Shh secreted from the cancer cell is able to activate the Hh/GLI1 pathway in surrounding stromal cells. GLI1 then initiates the production and secretion of other growth factors such as VEGF, Wnts and IGF from the stromal cells. These growth factors then promote the growth of the cancer cells. Conversely, the stromal cells themselves may secrete Shh (This hypothesis is sometimes known as Type IIIB). This theory of cancer growth is based on developmental studies which have shown that Shh secreted by the epithelium is received by the mesenchymal stroma and directly stimulates proliferation in the mesenchymal tissue. This form of signalling has been detected in number of cancer subtypes including pancreatic cancer, and have also recently been shown to be present in prostate cancer. A study Zunich et al (2012) demonstrated that osteoblasts derived from bone tissue used paracrine signalling to promote the Hh pathway in the LNCaP cell line and propose this mechanism as a partial driver or bone metastasis.

Aside from autocrine/paracrine signalling, a further mechanism of Hh mediated growth is through cancer stem cells. The cancer stem cell (CSC) theory states that rather than all cells within a tumour being proliferative, the growth of the tumour is driven by a small subset of cells which possess stem-like qualities which enable them to produce progeny but retain self-renewing qualities. The hedgehog pathway is a key in the maintenance of stem cell in normal tissues, and helps drive growth, particularly in embryogenesis (Taipale and Beachy, 2001, Zhou and Kalderon, 2011). (Taipale and Beachy, 2001, Zhang and Kalderon, 2001). The Hh pathway

was also been implicated in the formation of CSCs in a number of different cancer types, particularly gliomas, breast and most notably chronic myelogenous leukemia(Merchant and Matsui, 2010). The Hh pathway has been shown to activate a number of key CSC related genes, including nestin, CD44 and BMI1 (Yang et al., 2010). The Hh pathway also works with the Wnt pathway to maintain the CSC phenotype and the two pathways are thought to activate each other (Taipale and Beachy, 2001). In prostate cancer, the Hh pathway has been implicated in the maintenance of a CSC phenotype, where GLI1 has been shown to co-localise with the stem cell marker CD44. In 2011, Chang and colleagues demonstrated that Shh overexpression in mice prostate led to the development of tumours with strong indicators of CSCs, such as a p63+ and CD44+ state (Chang et al., 2011) .

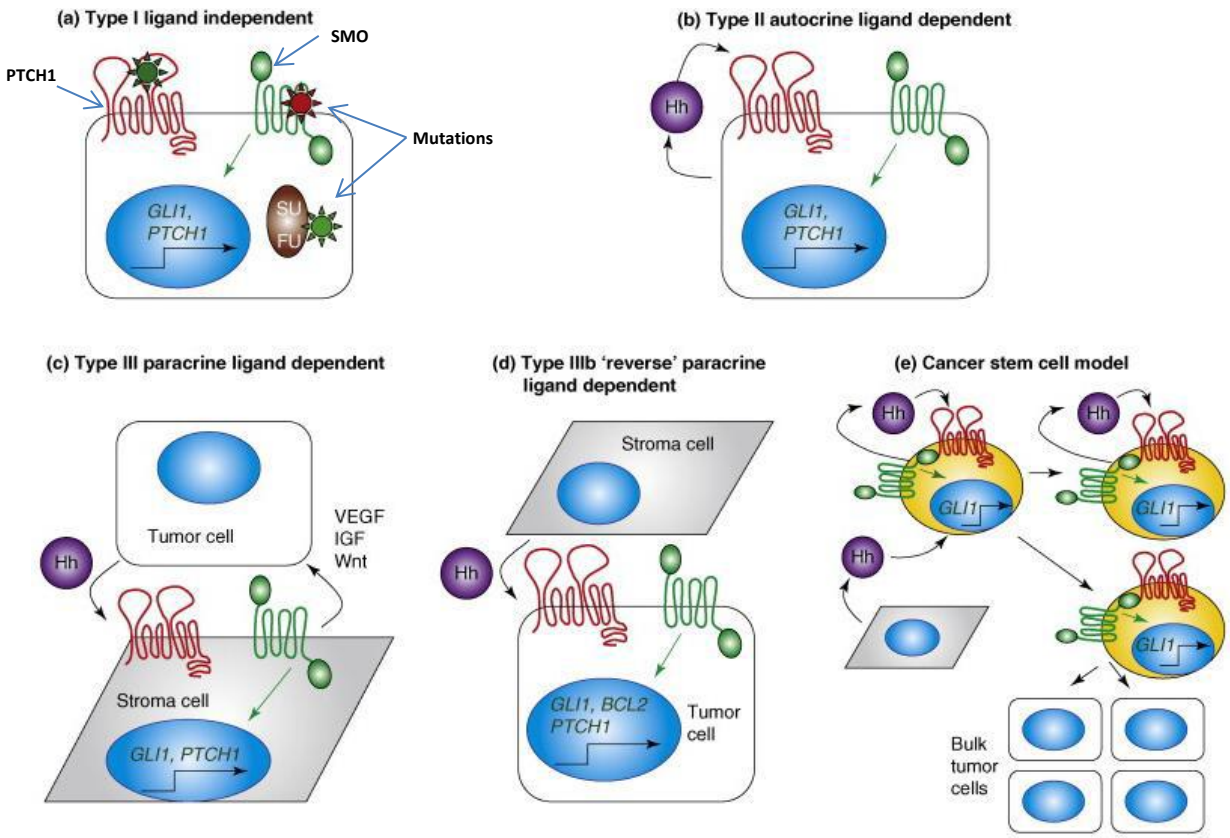

Figure 1.6: Different methods of Hedgehog signalling in [**a**] Type I ligand independent cancer: Mutations in either PTCH1, SMO or SUFU lead to the constitutive activation of GLI1 [**b**] Type II ligand dependent autocrine -cancer cells produce Hh, which is able to activate the pathway in the same cells. [**c**] Type III ligand dependent paracrine- cancer cells secrete Hh which activates the GLI1 pathway in stromal cells. Stromal cells then feed back to the cancer cell with signals such as Wnt, Vascular endothelial growth factor (VEGF) and Insulin growth factor (IGF) [**d**] Reciprocally, in type IIIb ligand dependent paracrine tumours stromal cells secrete Hh activating the pathway in the cancer cell. [**e**] Hh signalling in self-renewing cancer stem cells that may come from the stroma or the cancer cell itself. The expression of GLI1 can lead to activation of stem-like phenotypes which provide the tumour with ability to grow indefinitely (modified from Scales & de Sauvage 2009).

1.11 The cell of origin in prostate cancer- links to androgen independence and Hedgehog signalling.

One of the unresolved questions surrounding prostate cancer in general is the cell of origin for tumours, and whether PCa starts in epithelial or basal cells. Initial prostate tumour growth often shows signs of being derived from epithelial cells, including expression of androgen receptor and high PSA production. On the other hand, basal cells have also been proposed as the cell of origin for some tumours due to their ability to proliferate and differentiate. Increasingly, there is evidence that rather than one or the other, prostate cancer has a large degree of heterogeneity and that both cell types can function as a cell of origin, but that the resultant tumours have differing characteristics (Goldstein et al., 2010). Tumours with a cell of origin derived from luminal cells lead to a generally poorer prognosis and more rapid early tumour growth (Wang et al., 2013b). Basal cell origin tumours on the other hand may be more prone to metastases and androgen independence. It has also been shown that the basal and luminal cells promote each other's growth. A further idea is basal tumour cells are able to acquire a more luminal like morphology, or vice versa. Wang and colleagues (2009) demonstrated basal-luminal transition may be dependent on the expression of homeobox genes particularly Nkx3-1 (Wang et al., 2009). Xin (2013) also demonstrated while basal cells may be the cell of origin, particularly in metastases, basal-luminal transition often occurs in distal tumours driving their more rapid growth (Xin, 2013). However, one caveat of this theory is that it tends to only explain androgen responsive tumours. Androgen independent tumours on the other hand appear to acquire more basal characteristics, especially loss of AR expression.

The mechanisms which stimulate cells to become androgen independent or to lose AR expression completely are still relatively unknown. The Wnt pathway (particularly Wnt11) has been shown to mutually inhibit the expression of AR (Zhu et al., 2004). Bernard et al (2003) also showed that c-Myc expression results in an androgen independent state in LNCaP cells (Bernard et al., 2003).

In 2008, Shaw et al found that androgen independent PCa cells were sensitive to the (Shaw and Prowse, 2008) Hh antagonist Cyclopamine, suggesting an active Hh pathway, and that high levels of PTCH1 are present in circulating androgen independent PCa cells. The team also found that Hh and HER2 (ErbB2) signalling worked synergistically to promote an androgen independent phenotype. Subsequently, Chen et al (2010) found that Cyclopamine treatment resulted in dose-dependent modulation of the expression of genes that are regulated by androgen and that targeted suppression of SMO by siRNA reduced expression of androgen-inducible KLK2 and KLK3 in androgen deprived cells without affecting the expression of androgen receptor (AR) (Chen et al., 2010). It was also found that GLI2 itself co-localised with AR as evidenced by immunoprecipitation. As well as regulating AR, Hh has also been strongly associated with a further change which is believed to occur in epithelial-basal transition, namely EMT. This link between Hh signalling and EMT has been shown in other cancer types (e.g. gastric cancer), but relatively little information exists with regards to prostate cancer (Gonnissen et al., 2013).

1.12 Aims of study

Based on previous findings, members of the Neill lab, especially Dr. Sandeep Nadendla hypothesised that Hh signalling (specifically GLI1) was regulating both AR expression and EMT, and was responsible for cells controlling a basal phenotype. Levels of GLI1 was were analysed in a range of PCa cell lines and it was found that GLI1 activity was higher in androgen receptor cell lines (PC3 and DU145) than in cell lines where AR was expressed (LNCaP, PNT2). GLI1 was ectopically expressed in the LNCaP cell line to generate an LNCaP-GLI1 cell line, leading to a notable change of phenotype whereby cell colonies formed a basal-like or cobblestone morphology, and formed tight and distinct colonies whereas standard LNCaP cells are less compact (Nadendla et al., 2011).LNCaP-GLI1 cells proliferated a much higher rate than controls . As well as morphological changes, LNCaP-GLI1 cells also lost the expression of AR and were resistant to bicalutamide. Also, LNCaP-GLI1 cells displayed strong signs of an EMT phenotype including a loss of E-cadherin, and an increase in vimentin. LNCaP-GLI1 cells showed expression of basal cell markers, particularly CD44 and ΔNP63 (Nadendla et al., 2010). Microarray analysis on LNCaP-GLI1 cells further confirmed an androgen independent and EMT phenotype as well as a range of other gene expression changes. The initial aim of this study therefore was to investigate whether this change was potentially reversible and whether subsequent silencing of GLI1 would change morphological or gene expression and for LNCaP-GLI1 cells to return to a more luminal phenotype.

In addition to the considerable morphological and phenotypic changes and the switch to an AI state GLI1 appeared to mediate a range of biological processes including proliferation, apoptosis and EMT. To obtain a global view of gene expression in LNCaP-GLI1 cells, and to elucidate the pathways being activated/deactivate, a genome wide mRNA microarray was carried out by S. Nadendla (Thesis: Sandeep Nadendla, 2011) comparing gene expression profiles between LNCaP-pBP and LNCaP-GLI1, (also PC3 and DU145 cell lines). As mentioned above, when gene expression was analysed, a 10-fold cut off yielded 262 differentially regulated transcripts (144 up and 120 down) in LNCaP-GLI1 cells compared to LNCaP-pBP cells. Of the genes that were up regulated, the gene LCN2 was shown to have a 55 fold increase in LNCaP-GLI1 compared to LNCaP-pBP cells (Nadendla et al., 2011). When gene ontologies were grouped, LCN2 was the only gene that appeared in both the Androgen independence and the EMT signatures. Indeed, when the Androgen independence associated genes were delineated separately, LCN2 showed a response to GLI1 far greater than any other genes in the group (Figure 1.7). LCN2 therefore appeared to be a good candidate for further investigation with regards to both EMT and AI and it was hypothesised that LCN2 may be responsible, at least in part for the effects seen in LNCaP-GLI1 cells. As such, LCN2 was chosen as a candidate for further investigation (See chapters 4-8).

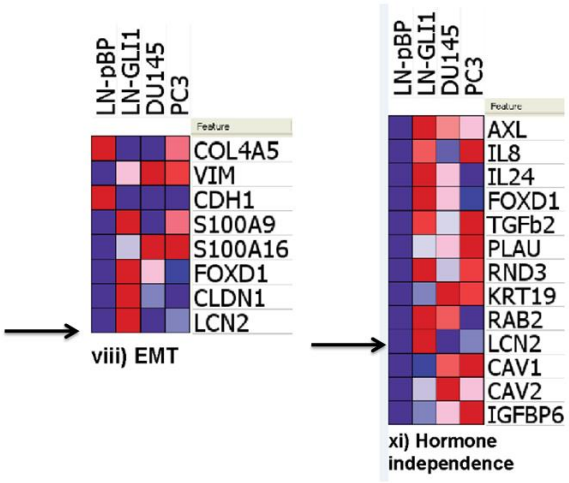

Figure 1.7: Partial heat map of genes grouped according to gene ontology that are regulated by Gli1 in LNCaP cells. Analysis was carried out on LNCaP (LN-GLI1), DU145 and PC3 cells. Red colours represent the higher fold expression values. Blue colours represent decreases in expression. Data is representative of average of triplicate values. All values relative to LNCaP-pBP. (Taken from Nadendla et al,. 2011).

1.13 The Lipocalin Family

Lipocalin 2 is a member of the Lipocalin family of proteins. This family is comprised of approximately 30 structurally dissimilar proteins which are mostly secreted and associated with the transport binding and of small hydrophobic molecules (Flower et al., 2000). The term 'Lipocalin' is somewhat broad, encompassing a range of proteins which share as little as 20-30% homology to each other. Despite their differences in amino acid composition, all members of the lipocalin family share a similar 3D structure. All members of the family contain a 'Lipocalin fold'. This structure comprises of an 8 β-sheets, which form hydrogen bonds to form an anti-parallel β-barrel structure which forms a cup like structure, inside of which is a binding site for specific ligands (Flower, 2000). The Lipocalin structure is found in all eukaryotes and in gram negative bacteria, although actual sequence similarity both at the genetic and protein level differ greatly between species (Flower, 1996). Most lipocalins also have an L1 loop, which is a linking structure which also functions as a cap or lid which can either prevent entry into or out of the binding domain(Flower, 2000). As many proteins within the Lipocalin family were identified before the group was defined, the majority of proteins, somewhat confusingly do not contain the name Lipocalin. Members of the family include Apoplipoprotein (which binds to progesterone and other steroids) and CRABP2-a retinoic acid binding protein produced in eye tissue (Chakraborty et al., 2012). Of genes with the name Lipocalin (LCN), LCN1, 2, 6 8,9 12 10 and 15 have been identified. However of these, only LCN1 (an endonuclease produced in tear ducts) and LCN2 have been described functionally (Glasgow et al., 2002).

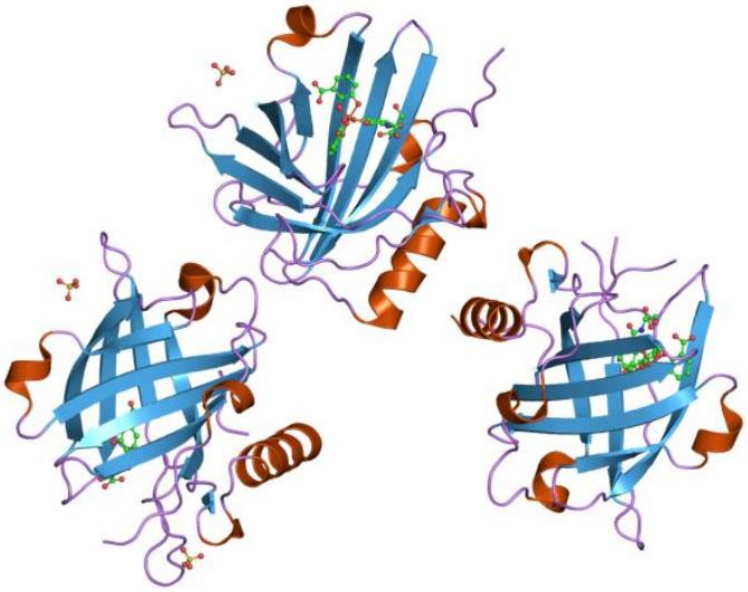

Figure 1.8- 3D structure of LCN2 bound to iron-associated siderophores: LCN2 forms a cup like structure formed of 8-β sheets (in blue). The L1 loop (purple) acts as lid-like structure regulating entry. Siderophores (green) are able to enter LCN2 where they are tightly bound. (Image license free from http://www.ebi.ac.uk/pdbe-srv/view/images/entry/1l6m600.png)

1.14 Structure of LCN2

Lipocalin 2 is labelled under a range of different names which reflect its initial discovery and characterisation, specifically 24p3, NGAL and Uterocalin. The first name given to lipocalin 2 was 24p3. This name was proposed by Hraba-Renevey and colleagues in the first identification of a 24kDA protein which was found to be over-expressed in SV-40 virally induced mouse kidney cells (Hraba-Renevey et al., 1989). Later, Flower et al identified this protein as a member of the lipocalin family (Flower et al., 1991). In 1994, Borregard et al. described a human homologue of 24p3. This protein formed part of the gelatinase (i.e. MMP9) complex found in

neutrophils. Thus, this protein was termed Neutrophil-gelatinase-associated-Lipocalin or NGAL (Kjeldsen et al., 1994). NGAL is still commonly used, especially in the renal biology field. Uterocalin is a further name which found in older literature but has since dropped out of use.

Regarding the 3D structure of lipocalin 2, the protein differs from other lipocalins due to the presence of a 20 a.a. N-terminal signal peptide, although the lipocalin domain itself still makes up ~75% of the protein (Coles et al., 1999). LCN2 forms a cup like structure as with other members of the family toward the base of the cup structure is a bulge consisting of a concentration of hydrophobic amino acids tryptophan, phenylalanine threonine and valine. The entrance of the cup structure on the other hand is has a number of polar residues such as Lysine 125 which project inwards which may help in providing affinity for substrates (Goetz et al., 2000). In this respect LCN2 differs from other members of the family. The LCN2 protein is a relatively small protein of only 198a.a. in length. It is important to note that much of the work performed on Lipocalin2 has been performed in mice. However in terms of residues, mouse Lcn2 shares only a 62% homology with the human form (Chakraborty et al., 2012, Kjeldsen et al., 2000). This is particularly relevant to functional studies as it not yet known whether this impacts on binding activity. Lipocalin 2 is usually described as a monomer of 25 kDa. In their initial description of LCN2, Kjeldsen et al. also described a 46 kDa homodimer and a homotrimer of 70 kDa which are linked by sulphur bonds, but these dimers have not been further investigated in terms of function (Kjeldsen et al., 1994).

1.15 Function of Lipocalin 2

LCN2 does not contain any known phosphorylation sites, nor does it act as a transcription factor (Goetz et al., 2000). LCN2 has been shown to be glycosylated, although this has not been well characterised (Miyamoto et al., 2011). In terms of cellular localisation, relatively little is known. While LCN2 is known to be secreted, within the cell LCN2 is believed to be located primarily within the cytoplasm, but has also been shown to be present within the nucleus. LCN2 does not contain a nuclear localization sequence, but may be able to shuttle in and out of the nucleus due to its small size.

Despite its small size and lack of phosphorylation activity, LCN2 has been associated with a range of cellular functions. LCN2 was first described as being associated with MMP9. MMP9 is a matrix metalloprotease which is involved in the remodelling and breakdown of the extra-cellular matrix, with particular affinity for collagen V (Yan et al., 2001). LCN2 is able to bind to MMP9 covalently (Figure 1.9), thereby stabilising it and preventing its MMP9's inhibition by TIMP1 (Van den Steen et al., 2006). Notably, this interaction does not occur in murine tissue, as the mouse Lcn2 does not contain the same cysteine residues necessary for binding.

LCN2's main function was derived in part from observations in LCN2-/- knockout mice. These mice looked phenotypically healthy. However they were found to be far more susceptible to bacterial infection than wild type mouse (Flo et al., 2004). Bacteria need a number of nutrients to survive, one of which is iron (specifically Fe^{3+}). However in a host organism, iron is not readily available in its free state, or is bound up inside other host cells or proteins. To combat this deficiency, bacteria produce and secrete siderophores. Siderophores are a broad range of organic

compounds that are able to incorporate Fe^{3+} into their structure. By producing siderophores and re-incorporating them, bacteria are able to scavenge any freely available iron, and thereby enable growth or proliferation . While some bacteria are only able to scavenge free iron, other bacteria such as *E.Coli, Listeria* and *Salmonella* are able to produce siderophores which have an even stronger affinity for iron, and are extract it from the host's own proteins and enzymes. To help fight against these bacterial attacks, animal cells produce LCN2. LCN2 is able to bind to siderophores, essentially trapping them and preventing their uptake by the bacteria (Flo et al., 2004, Richardson, 2005, Srinivasan et al., 2012) (Figure 1.9). Specifically, LCN2 has a higher affinity for catecholate siderophores which form larger molecules rather than hydroxamate siderophores such as deferoxamine which tend to form long chains (Flo et al., 2004).

Once LCN2 has bound the siderophores, its function is not simply to sequester them, but instead LCN2 is able to transport them back into the cell. Exactly how LCN2 is transported in and out of the cell is not fully understood, but two potential receptors have been identified: SLC22A17 (also known as BOCT or NGAL-R) and Megalin (Devireddy et al., 2005, Bao et al., 2010), which is also able to transport a wide range of other ligands. Once inside the cell, LCN2 is able to release the iron, which can drive a large number of different processes (discussed below). However, LCN2 is also able to capture non-iron bound siderophores and transport them inside the cell. When these are released they are free to bind to intracellular iron (Figure 1.9) If this happens too much, it has been proposed that this can lead to a critical loss of the mineral and potentially to apoptosis through up-regulation of the pro-apoptotic BIM (Devireddy et al 2005) although there is considerable debate as to whether LCN2 is pro- or anti-apoptotic overall is a matter of considerable debate. Briefly, the

apoptotic actions of LCN2 may be dependent on the exact type and concentration of siderophores –there is great variation in chemical structure and Fe3+ binding, or on tissue type (Tong et al., 2005, Tong et al., 2003). Alternatively the anti or pro-apoptotic effects may be due to pre-existing conditions within each cell type. Indeed even in identical conditions Lcn2 over-expressing cells have been shown to have opposing effects (Gwira et al., 2005). It should also be noted that there are likely to be considerable differences in LCN2's effects in culture conditions compared to whole tissue.

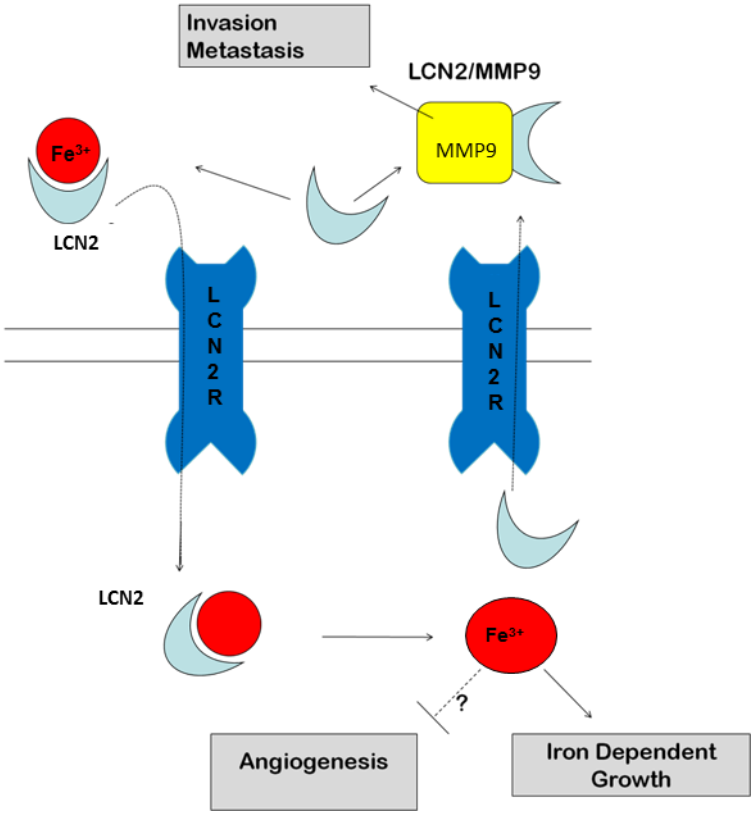

Figure 1.9 Basic overview of LCN2 function: LCN2 is secreted by cells where it is binds to iron containing siderophores. These are then shuttled back into cells via receptors such as Megalin or LCN2R. Siderophores are released from LCN2 which subsequently drive iron dependent growth and signalling. Alternatively, LCN2 is able to bind to and stabilise MMP9 leading to invasion or metastasis.

4.4 Lipocalin 2 in human physiology.

LCN2 is expressed in a range of tissues. GeneAtlas data, as well as other more specific studies show that in normal human physiology, the highest expression is in bone marrow, pancreatic islets and the trachea (Su et al., 2004). This represents LCN2's close association with neutrophils, which are generated in the bone marrow,

as well as its links to T-cells which are matured in the thyroid (Orabona et al., 2001). LCN2 not usually expressed at very high levels in other types of tissue, but can be up regulated in disease (see below). In mice, Lcn2 is expressed specifically in the basal layer of hair follicles, and not in other dermal layers. LCN2 is a secreted protein, and as such can be found in blood plasma. In one of the earliest descriptions of LCN2, Kjdelsen et al used LCN2 ELISA to determine an average blood plasma level of 72ng/ml, although there was high variation, and a range from 40 to 109ng/ml (Kjeldsen et al., 1994). This is has been subsequently confirmed in wider scale studies and average plasma levels are generally between 70-120 ng/ml depending on the exact methods used (Shapiro et al., 2010). LCN2 is also found in urine, albeit at lower levels. Urine LCN2 levels in healthy adults typically range from 20-30ng/ml (Bennett et al., 2008).

1.16 The Signalling mechanisms of Lipocalin 2

Since its discovery, LCN2 expression has been shown to be regulated by a range of different signalling mechanisms. These signalling pathways are however often connected, and indeed the literature concerning exactly what inhibits or promotes LCN2 expression is often either cell specific (especially between mouse and human) or completely contradictory. Despite this, what is becoming increasingly clear is that LCN2 is linked to many of the key pathways in cells.

Of all the potential regulators of LCN2, the transcription factor NF-κB is the most closely associated. Briefly, NF-κB. Under non-stimulating conditions, NF-κB is bound by its inhibitor IκB, which sequesters NFκB in the cytoplasm. Under activating conditions, due to a range of upstream receptor tyrosine kinases, IκB is phosphorylated by IKK in complex with NEMO. This enables IκB to be targeted for

proteasomal degradation by ubiquitinases. This frees NFκB which is able to enter the nucleus and activate transcription (See above, section 1.6) (Karin et al., 2002).

LCN2 was first linked to NFκB signalling by Cowland et al in 2003 who demonstrated that the LCN2 promoter contains an NFκB consensus binding site (Cowland et al., 2003). Interestingly, this study also showed that even though NFκB binding to the LCN2 promoter occurred after both IL1 β and TNFα activation, expression occurred only after Il1B activation. A follow up paper then demonstrated the requirement for IκBζ which is not induced by TNFα (Cowland et al., 2006). A number of other subsequent studies have also demonstrated a strong link between NFκB and LCN2 (Iannetti et al., 2008, Karlsen et al., 2010, Glaros et al., 2012, Borkham-Kamphorst et al., 2011). In many cases, a link to Il1β activation is emphasised, although IL-6 and IL-8 have also been proposed as activating LCN2 in an immune setting.

LCN2 has been shown to be regulated by Hypoxia Inducible factor 1α (HIF-1α)(Viau et al., 2010). HIF-1α is transcription factor which is stabilised in response to low oxygen concentrations. HIF-1α expression is tightly controlled by NF-κB. HIF-1α stability is regulated by procollagen-proline dioxygenase which hydroxylates HIF-1α targeting it for degradation (Maxwell and Salnikow, 2004), which is in turn regulated by intracellular iron levels . However, LCN2 itself has been shown to regulate HIF-1α expression and help drive angiogenesis related expression via VEGF (Yang et al., 2013). As such, there may be feedback mechanisms involved with LCN2, HIF-1α and iron regulation

Aside from NFκB, a range of other activators of LCN2 have proposed. A STAT1 binding site was observed at the LCN2 promoter by (Zhao and Stephens, 2013), who also indicated a role for ERK signalling, albeit indirectly through NFκB. The LCN2

promoter region also contains a binding site from the transcription factor C/EBP, which is also associated with NFκB. There are however 6 members of the C/EBP family labelled α to ζ. It was shown by Karlsen et al that C/EBPβ and C/EBPδ had no effect on LCN2 expression (Karlsen et al., 2010). On the other hand, the opposite has been shown by both Du et al (2010) and Zhang et al (2012) in the case of C/EBPβ only (Du et al., 2011, Zhang et al., 2012). Also, C/EBPζ has been identified as an LCN2 repressor (Wang et al., 2014).

Other regulation mechanisms for LCN2 include Wnt signalling. In mouse Lcn2, active Wnt signalling was found to reduce both mRNA and protein expression of Lcn2, and this appeared to have little effect on intracellular iron levels, although removal or iron itself did reduce Lcn2 expression, indicating that Wnt regulation is iron independent. This mechanism however has not been further explored and has not been demonstrated in humans.

Overall, it appears that the regulation of LCN2 is fairly complex, while NFκB is important, there are ever more links to other transcription factors being discovered at a growing rate.

1.17 Lipocalin 2 in non-cancer based disease

As LCN2 is a secreted protein, which is relatively easy and cheap to detect in either blood or urine, there has been significant focus on whether it may be used as a diagnostic markers for a wide array of different diseases and conditions which ranges from diabetes to HIV/AIDS (Where LCN2 plasma levels are lower in more severe patients(Landro et al., 2008)) . LCN2 has been implicated in heart disease and myocardial infarction, and also following organ transplantation. In both cases,

elevated LCN2 levels have been observed. LCN2 has most commonly been associated with severe organ dysfunction or injury.

To date, the most common practical application of LCN2 as a diagnostic tool has been with Acute Kidney injury (AKI). AKI is a rapid and extremely dangerous form of renal failure. However, being an internal organ, its symptoms are not easily observed. AKI is a somewhat broad term for the symptoms resulting in significant loss of renal function and nephron activity. AKI may result from drug side effects, trauma (especially in surgery) or sepsis. AKI is a major cause of hospital admission, and 10-20% of patients show some form of AKI especially amongst those aged 65+. It also has a high (up to 50%) mortality rate (Haase-Fielitz et al., 2009). AKI is usually assessed through blood creatinine levels, which is the standard method of diagnosis. However, creatinine levels are notoriously imprecise. Creatinine is also unable to finely distinguish between sepsis-related and non-sepsis AKI. It can also not define whether AKI is due to direct trauma or not. As such, other markers have been explored to help complement existing testing methods. LCN2 has emerged as one of the primary candidates for this detection, indeed, a large to be significantly majority of LCN2 based literature concerns just this one area (Note: LCN2 is still often called NGAL in AKI papers). NGAL has been shown elevated in AKI patients in a range of studies (Shapiro et al., 2010, Gabbard et al., 2010, Makris et al., 2009). In a major study, it was showed that urinary LCN2 levels at were significantly higher among patients who went on to develop AKI [155.5 (50.5-205.9) ng/mL vs. 8.0 (5.7-17.7) ng/mL]. LCN2 was also more sensitive to the sepsis status of AKI patients, which may be reflective of its anti-bacterial function (Bagshaw et al., 2010). There is however still considerable debate about the specifics of which patients shows greatest response, and how accurate blood vs urine readings are etc. LCN2 has

been trialled in patients but required better characterisation before it can be used in wide scale clinical settings. Nevertheless, a meta-analysis by Haase et al. did show that LCN2 is indeed a reliable indicator for AKI, especially in children (Haase et al., 2009). Despite the large volume of clinical studies on LCN2 and AKI, it is somewhat notable that there are relatively few studies on the actual biological effects of elevated LCN2 serum levels. Martines et al. (suggest that LCN2 is secreted to assist with iron imbalance, whereas Haase et al. propose that it is either anti-bacterial, or possibly even a non-functional marker (Haase et al., 2009, Martines et al., 2013). Also, there are very few cell-based studies in terms of LCN2's intracellular or extracellular effects in AKI.

LCN2 has also been associated with a host of other diseases or conditions including a range of skin conditions including in the basal layer of eczema and psoriasis patients, where LCN2 was up-regulated (Mallbris et al., 2002). More recently, LCN2 has even been linked to neurological disorders. LCN2 $^{-/-}$ mice exhibit signs of memory loss and anxiety (Ferreira et al., 2013). In humans, levels of LCN2 have been observed in patients with Alzheimer's disease, and positive correlation to cognitive impairment has been observed (Choi et al., 2011, Naude et al., 2012). Overall therefore, literature to date appears to support the idea that LCN2 is produced as a response to stress, this is particularly noticeable in acute trauma ,but is also present in more chronic conditions. However, the actual effects of this LCN2 production are still poorly understood. Whether the presence of LCN2 is purely anti-bacterial, or whether it contributes to cell survival is not yet fully understood but our understanding of LCN2's effects and regulation is steadily increasing.

1.18 Lipocalin 2 in cancer.

In recent years, LCN2 has attracted ever more attention in relation to cancer; both as an diagnostic marker, but also a potential mechanistic driver of the disease. Indeed, LCN2 has been associated with an ever-widening array of different cancer types. There is however also a large amount of variation between cancer sub-types. Indeed the literature surrounding LCN2 and cancer is often highly contradictory. In general, the data published so far suggests that the role of LCN2 is highly tissue specific and cannot be simply considered as “pro-” or “anti-” tumorigenic, but that a number of key features are common to most cancer types.

Non-solid tumours

Currently, there has been increased interest in the role of LCN2 due its role in Chronic myeloid leukaemia (Arlinghaus and Leng, 2008). Here, LCN2 has been shown to be a critical determinant of the BCR-ABL+ fusion gene’s function. Higher levels of LCN2 were also recorded in patients with more advanced disease state (Leng et al., 2008).

Pancreatic and Colorectal cancer

Significant efforts have been devoted to the role of LCN2 in Pancreatic cancer. Pancreatic cancer has an extremely high mortality rate of around 95%. Hence the need for an early diagnostic marker is of the utmost importance. Early studies by Moniaux et al. identified NGAL as having a strong positive correlation to tumour differentiation and severity, albeit in a relatively small number of patient samples (Moniaux et al., 2008). By contrast, in the same year Tong et al used ectopic expression of LCN2 in pancreatic cell lines to show that LCN2 inhibits both

angiogenesis and migration, and this correlated it its expression in well differentiated tumours, but not in poorly differentiated tumours (Tong et al., 2005). In a key follow up study, Tong et al provided some key mechanistic studies in cell lines whereby the presence of EGF led to a decrease in LCN2 expression (Tong et al., 2011). It was also found that EGF, by activating EGFR inhibited E-cadherin expression (via ZEB1), which in turn led to the activation of NF-κB and hence LCN2 transcription. Other studies have since strengthened the view that high LCN2 is favourable in pancreatic cancers, is related to reduced EMT (Figure 1.10) (Xu et al., 2012a). A picture is emerging which supports LCN2 being up-regulated in low grade tumours, but lost in higher grade. As such, LCN2 has been identified as a potential diagnostic marker from plasma (Slater et al., 2013, Kaur et al., 2013). Indeed, in one of the first practical applications of LCN2, Xu et al used an oncolytic virus containing LCN2 to transfect pancreatic cancer cells which dramatically reduced tumour growth in vitro and in vivo by increasing apoptosis of tumour cells, and some xenograft tumours were completely eradicated (Xu et al., 2012a). There are hence early trials currently ongoing investigating whether similar effects are seen in human patients follow that of rodent models.

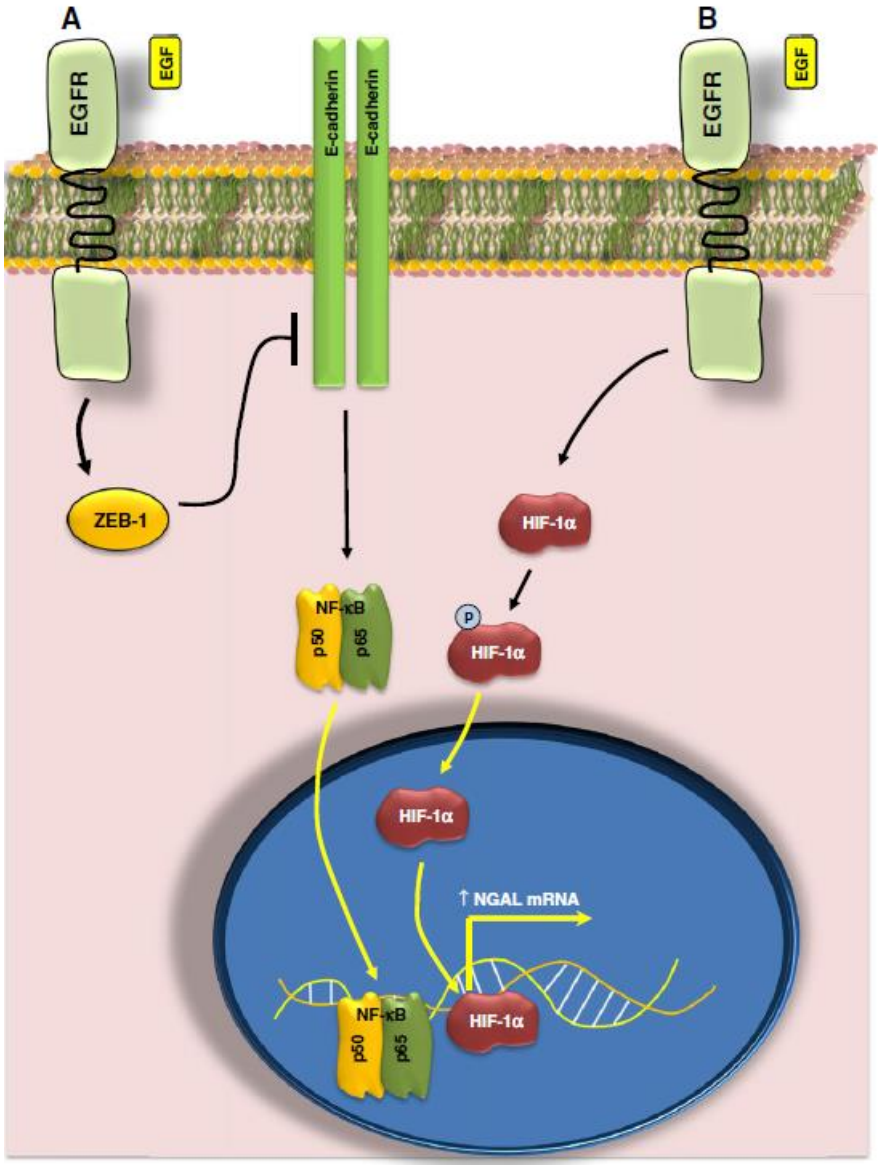

Figure 1.10 Potential regulation of LCN2 expression by EGFR and NF-κB. Stimulation of EGFR by EGF, this in turn inhibits E-cadherin expression via ZEB1 repression. E-cadherin may activate NF-κB (via IKK) which drives LCN2 transcription. In parallel, EGFR helps stabilise HIF-1α, possibly in response to iron levels which drives LCN2 expression. (Adapted from Chakroborty et al., 2012)

In contrast, in colorectal cancers LCN2 has been strongly associated with a poor prognosis (Barresi et al., 2011). A recent study has shown LCN2 as a good prognostic marker of both tumour grade and tumour size (Marti et al., 2013). Recently, Reilly et al. demonstrated that not only was LCN2 linked to advanced tumour grade, but that it was closely linked to the level of iron within the tumour tissue. The authors also indicate that a more wide scale testing of plasma LCN2 levels in relation to colorectal cancer patients is ongoing with results due in the coming years (Reilly et al., 2013).

LCN2 has also been associated in an increasing number of other cancers with mixed results. LCN2 expression was shown to have a negative correlation to differentiation in thyroid and endometrial cancers (Iannetti et al., 2008, Lin et al., 2011, Liao et al., 2013). Conversely LCN2 had a positive correlation to tumour differentiation in ovarian cancer, rectal and gastric cancer (Playford et al., 2006, Du et al., 2011).

Overall therefore, a picture is emerging that indicates that the role of LCN2 is likely to be tissue specific (Table 4.1). A distinction must also be drawn between having advanced or early stage tumours as the role of LCN2 may be different as the disease progresses.

Breast Cancer and steroid signalling.

Breast cancer is now the most commonly diagnosed cancer type among women (Siegel et al., 2013). While BCa is a highly complex disease, a strong component of its growth is its dependence on hormones and hormone receptors. The early stage of BCa is dependent on a range of steroid receptors, most notably Estrogen receptor (ER), Progesterone Receptor (PR) and receptor tyrosine kinases such as Her-2 (Alderton, 2012). Elevated levels of these receptors are strongly associated with

tumour severity and growth and as such are often targets for therapy (e.g. Herceptin). However, in many cases, especially in refractory tumours, cells are able to evade the need for steroid based growth by acquiring an ER-, PR- or HER2- status. Indeed, some tumours show no expression of all three types and are termed triple-negative. While the severity of these triple-negative tumours is debated and very heterogeneous, they are dangerous as they cannot be targeted by drugs such as Herceptin (Dawood et al., 2010).

The first study linking LCN2 to BCa by Stoesz et al showed that LCN2 expression was heterogeneous in human tissue, but appeared to be concentrated in the lumen. Moreover, while there was no correlation to HER2 status, there was a significant correlation between LCN2 and an ER- status (Stoesz et al., 1998). Following on from this study, a range of other groups have also shown a link between LCN2 and a steroid receptor negative status. Bauer et al, in a much larger study showed a very strong correlation between LCN2 expression *in vivo* and ER- status and poor histological grade, but also to higher HER2 levels (Bauer et al., 2008). Using a mouse model, Leng et al (2009) showed that Lcn2-/- mice had significantly less tumour growth and metastasis. The group also showed that HER2 itself is able to regulate LCN2 levels through NF-κB (Leng et al., 2009).

In a key study, Yang et al provided evidence of an positive correlation between LCN2 expression and BCa tumour grade. Further to this, the group also analysed an LCN2 over-expressing clone in MCF7 cells, and reciprocally used siRNA for temporary LCN2 suppression (Yang et al., 2009). Results obtained showed an inverse correlation between LCN2 and ERα. In addition, the group also noted that

LCN2-high clones had EMT-like characteristics with reduced E-cadherin and elevated vimentin levels. It was also demonstrated that EMT was being affected via the ER/Slug axis, and when ERα was subsequently over-expressed in LCN2 high cells, the EMT phenotype was reversed. This study also showed limited data of E-cadherin (but not ERα) being reduced by recombinant LCN2 protein. However in this instance, only a minor change was observed, and only after treatment with a very high concentration of 100μg/ml of protein. It should also be noted that there were significant. Differences in expression between clones created (Yang et al., 2009). Overall however, there is steadily increasing evidence between a negative correlation between LCN2 and ERα (Guo et al., 2012). What is less clear however is whether it is LCN2 affecting ERα or vice versa, or there being a potential feedback loop between the two genes. Both breast and prostate cancer share a common in characteristic in that steroid receptor negative status generally confers a poorer prognosis. To identify some of the common genetic features between the two cancer types, Creighton et al preformed microarray analysis on a large number of ER- breast cancer tissues and cell lines, and AR- prostate cancer cell lines. Of the many hundred genes found for each category, only 51 were found to be common to all AR- and ER- cells/tissues forming a “common signature of hormone independence”. Within this set, one of the most prominent genes was LCN2 (Figure 1.11) (Creighton, 2007).

Cancer Type	LCN2 correlation
Pancreatic	Generally positive correlation to good prognosis
Colorectal	Positive correlation to high tumour grade
Thyroid	Negative correlation to tumour differentiation
Ovarian	Positive correlation to tumour differentiation
Breast	Positive correlation to poor prognosis and ER- status
Prostate	Positive correlation to tumour grade

Table 1.2 Overview of LCN2 in different cancer types

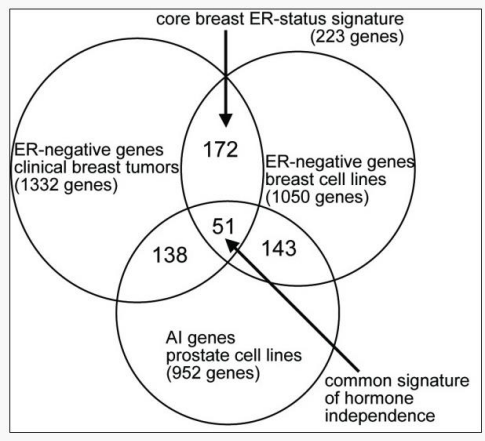

Genes with elevated mRNA levels in common signature of hormone independence

Entrez	Name	Title	Entrez	Name	Title
87	ACTN1	actinin, alpha 1	5329	PLAUR	plasminogen activator, urokinase receptor
136	ADORA2B	adenosine A2b receptor	5359	PLSCR1	phospholipid scramblase 1
390	ARHE	Rho family GTPase 3	5621	PRNP	Prion protein (p27–30)
824	CAPN2	calpain 2, (m/II) large subunit	6732	SRPK1	SFRS protein kinase 1
858	CAV2	caveolin 2	7272	TTK	TTK protein kinase
994	CDC25B	cell division cycle 25B	7296	TXNRD1	thioredoxin reductase 1
1075	CTSC	cathepsin C	7378	UP	uridine phosphorylase 1
1284	COL4A2	collagen, type IV, alpha 2	7398	USP1	ubiquitin specific peptidase 1
1786	DNMT1	DNA (cytosine-5-)-methyltransferase 1	8882	ZNF259	zinc finger protein 259
1969	EPHA2	EPH receptor A2	8898	MTMR2	myotubularin related protein 2
2000	ELF4	E74-like factor 4 (ets domain)	9056	SLC7A7	solute carrier family 7, member 7
2023	ENO1	enolase 1, (alpha)	9322	TRIP10	thyroid hormone receptor interactor 10
2037	EPB41L2	erythrocyte membrane protein band 4.1-like 2	10403	KNTC2	kinetochore associated 2
2131	EXT1	exostoses (multiple) 1	10479	SLC9A6	solute carrier family 9, member 6
2182	ACSL4	acyl-CoA synthetase long-chain member 4	10644	IMP-2	IGF-II mRNA-binding protein 2
2633	GBP1	guanylate binding protein 1, interferon-inducible	10946	SF3A3	splicing factor 3a, subunit 3, 60 kDa
2920	CXCL1	chemokine (C-X-C motif) ligand 2	25937	DKFZP586I1419	WW domain containing transcription regulator 1
3383	ICAM1	intercellular adhesion molecule 1 (CD54), human rhinovirus receptor	26031	OSBPL3	oxysterol binding protein-like 3
3569	IL6	interleukin 6 (interferon, beta 2)	26064	RAI14	retinoic acid induced 14
3575	IL7R	interleukin 7 receptor	29083	HSPC135	HSPC135 protein
3600	IL15	interleukin 15	29970	SCHIP1	schwannomin interacting protein 1
3801	KIFC3	kinesin family member C3	29980	DONSON	downstream neighbor of SON
3934	LCN2	lipocalin 2 (oncogene 24p3)	55003	PAK1IP1	PAK1 interacting protein 1
4478	MSN	moesin	56913	C1GALT1	glycoprotein-N-acetylgalactosamine 3-beta-galactosyltransferase
4907	NT5E	5'-nucleotidase, ecto (CD73)	140885	PTPNS1	protein tyrosine phosphatase, non-receptor type substrate 1
5271	SERPINB8	serpin peptidase inhibitor, clade B			

Figure 1.11 List of genes which associated with ER- and AI status in BCa cell lines and tissue and PCa cell lines. Right- Table of genes which form a 'common signature of hormone independence'. LCN2 highlighted in yellow (Adapted from Creighton et al, 2006)

1.19 Lipocalin 2 in Prostate cancer

Compared to other cancer types, the role of LCN2 in PCa is very poorly understood. To date, only two studies have directly addressed the issue. Mahadevan et al. did not assess the role of LCN2 in PCa directly, but rather used it as a model for identifying LCN2 regulation. In this study, the authors found that LCN2 was elevated in PCa cells through endoplasmic reticulum induced stress via the unfolded protein response. Moreover, they identified NF-κB as a key mediator of LCN2 induction. While this study does not provide any information about LCN2 in PCa *per se*, it does provide further evidence that LCN2 is produced in response to acute stress (Mahadevan et al., 2011).

Very recently, a study by Tung et al (2013) provided a more in depth analysis of LCN2 in PCa. Higher LCN2 levels were found to correlate to poorer tumour differentiation and higher Gleason score. Also, using shRNA, the group also suppressed LCN2 expression in DU145 and PC3 cells. Suppressed LCN2 expression resulted in an increase in cells in G0/G1 arrest. This was also associated with a reduction in cell migration. It was also found that cells without LCN2 had higher levels of p21 and phospho and total-p53, reciprocally, Cyclin D1 was reduced in these cells. Finally, a xenograft model in mice showed that when LCN2 knockout cells were injected, tumour weight volume was significantly reduced. This study however did not investigate the effects of LCN2 on hormone receptor regulation, or EMT, and also leaves open some key questions about the global effects of LCN2 (Tung et al., 2013). As such, the role of LCN2 in PCa is a worthwhile area of investigation. Given that steroid receptor expression in PCa is of critical importance, any potential role of LCN2 warrants further study and may provide insight as to exactly what role LCN2 is playing in this disease.

Chapter 2
Materials and Methods

2.1 Cell and Tissue Culture.

The parental cell lines PC3, DU145, LNCaP were all obtained from the European Collection of Cell Cultures (through Sigma-Aldrich, St Louis, MO, USA) and normal prostate epithelial PNT2 cells were
kindly provided by Norman Maitland (University of York). The MCF7 breast cancer cell line was provided by Dr Sahira Khalifa (QMUL) derived from a stock from Cancer Research UK.

Prostate and breast cancer cell lines, particularly those which express oestrogen receptors are known to react strongly to the presence of phenol red, which acts as ER agonist. To eliminate any interference from phenol red, all cells were cultured in phenol red- free RPMI 1640 medium supplemented with 10% (v/v) FBS, L-Glutamine (2 mM), penicillin (50 µg/mL) and streptomycin (50 mg/mL) (all Lonza. Basel Switzerland). All cell lines were cultured in either T-25 or T-75 flasks (Fisher Scientific, Loughborough, UK) and incubated at 37^{o}C in a humidified incubator with 5%CO_2/95% air until they reached 70-80% confluence, with media being changed every 3-4 days depending on cell density.

2.2 Splitting and Counting Cells

To split cells, media was removed, and flasks rinsed lightly with PBS and aspirated. 1X Trypsin-EDTA (PAA, Little Chalfont, UK) was added (3mL for a T-25 flask, 5mL for a T-75), and incubated at 37^{o}C for ~5 minutes, or until all cells were free floating. Trypsin was neutralised through the addition of warm FBS containing media in a 1:1 (v/v) ratio and transferred to 15 mL tubes. Cells were centrifuged for 5 minutes at 1200 RPM, and the supernatant aspirated. The resultant pellet was suspended in

1 mL of FBS containing media and counted using a haemocytometer. Cell counts were assessed using an average of the outer 4 quadrants of the haemocytometer grid and multiplied by 10,000 to obtain a total number of cells per pellet. Under usual circumstances, cells were split 1:10 into new flasks and supplemented with fresh media

2.3 Retroviral transduction

Retroviral transduction provides a powerful method to study the effects of a specific gene in cells. The process utilises the virus' abilities to integrate into chromosomal DNA. Before viral particles can be generated, the coding sequence for the gene of interest is inserted into a bacterially derived plasmid through ligation. The inserted gene is situated between two flanking LTR (long terminal repeat) sequences and a Ψ signalling motif. Plasmids are then transfected into Phoenix cells. Phoenix cells are modified 293T- human embryonic kidney cells which have been inserted with viral packaging proteins GAG, POL and ENV. When the gene-containing plasmid is inserted into the Phoenix line it will generate viral particles which are released into the media (Figure 2.1). Viral particles are then centrifuged into cells and the gene is inserted into the chromosomes and constitutively driven by a Cyclomegalovirus promoter.

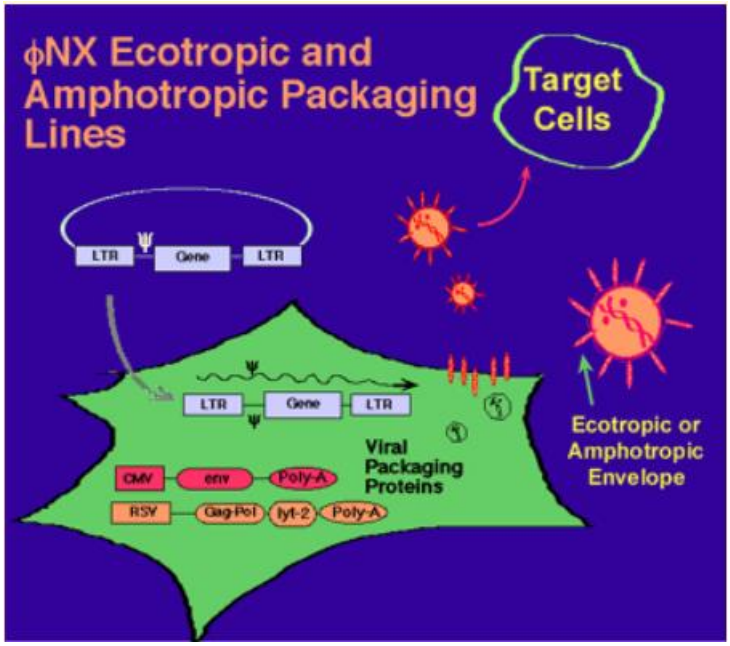

Figure 2.1: Overview of viral transfection. Plasmids containing gene of interest are transfected into Phoenix (ΦNX) cells and combine with viral packaging proteins to produce a virus which can be added to other cell lines.

2.4 Generation of an LCN2 containing plasmid.

Plasmids containing the LCN2 gene were kindly supplied by Dr Zhimin Tong (M.D. Anderson, Texas, USA). However, overall yields were very low. As such, the entire LCN2 coding sequence was amplified directly from plasmids via RT-PCR PLATINUM® Pfx kit (Invitrogen, Carlsbad, CA, USA) using primers with a modified phosphorylated 5' end using the sequences:

Forward- 5'[Phos]GAAATCATGCCCCTAGGTCTCC3', and reverse 5'[Phos] CACTCAGCCGTCGATACACTG 3'. PCR amplification was carried out using reaction: PLATINUM® Pfx DNA polymerase-0.5 µl, 1 µl template DNA, 1.5µl

Primer mix (both Forward and reverse), 1.5 µl 10mM dNTP mix, 1 µl 50nM $MgSO_4$, 5µl Pfx amplification buffer, 39.5µl dH_2O. Reactions were performed using 35 cycles of 95^oC- 15 secs, 60^oC-30 secs, 68^oC-60 secs. Resultant DNA was ~2 µg/µl and was purified by running on a 0.8% (w/v) agarose gel and cut out under UV light and dissolved in QB buffer (supplied with Platinum pfx kit) in a 3:1 ratio at 50^oC for 10 minutes. Dissolving reactions were stopped using a 1:1 volume of 100% isopropanol (v/v) and centrifuged through a DNA collection column for 1 minute. DNA was spun dry and diluted with 50µl elution buffer.

The pBABE-puro plasmid is a constructed circular DNA containing numerous restriction sites (Figure 2.2). Plasmids also contain both ampicillin and puromycin resistance genes. 0.5 µl of pBABE-puro plasmid was cut using the SALI restriction enzyme (New England Bioscience, MA, USA) for 1hr at 37^oC in Buffer 3 and BSA (both from New England Bioscience, Boston, MA, USA) according to the manufacturer's instructions. 1 µl of Antarctic phosphatase (New England Bioscience, Boston, MA, USA) was added to de-phosphorylate the hanging ends and incubated for 30 minutes at 37^oC. Both enzymes were deactivated by heating to 65^oC for 20 minutes. A further restriction enzyme Klenow (New England Bioscience, Boston, MA, USA) was utilized to remove the hanging ends of DNA and create blunt ended DNA fragments. 0.5µ l Klenow, plus 1 µl of dNTPs were added to the reaction and incubated for 15 minutes at 12^oC. All reactions were deactivated by incubated at 75^oC for 20 minutes. Cut pBABE-puro was then isolated in an 0.8% (w/v) agarose gel then dissolved and purified as above.

For the ligation reaction, a fragment to plasmid ratio of 3:1 was utilised according to manufacturer's recommendations and the size of the DNA fragments taken into

consideration (LCN2 gene fragment= 600 base pairs, vector fragment =5100 base pairs). 10 reactions were created each with 5 µl of pBABE-puro (@8 ng/µl) and 2.25 µl of LCN2 gene fragment (@10 ng/µl) were supplemented with T4 ligase, 1 µl of ATP buffer mix (both New England Bioscience, Boston, MA, USA and made up to 10 µl with dH_2O. The reactions were left overnight at room temperature.

Ligated plasmids were transfected into TOP10 OneSHOT competent bacteria (Invitrogen, Carlsbad, CA, USA) using a heat shock method at 42^oC as per manufacturer's instructions and plated onto ampicillin containing agar plates and left overnight at 37^oC as well as control bacteria containing plates. Colonies were then selected for amplification by MINIprep (Qiagen, Venlo, NL) as per manufacturer's instructions. Pelleted bacteria were digested and DNA extracted, then eluted using elution buffer.

As blunt-ended ligation was used for gene insertion, it was necessary to determine whether the DNA fragment was orientated in the correct position. The LCN2 gene was found to contain a SCAI restriction site, as well as being present in pBABE-puro. Thus, a double digest was performed on the plasmids using SCAI and BAMHI, which has one restriction site on the pBABE-puro backbone. Correct orientation was determined based on gene fragment size, with correct orientation displaying bands of ~600bp in length whereas incorrect orientation displayed a 200bp fragment.

2.5 Generation of the LNCaP-LCN2 and LNCaP-pBP cell line.

Phoenix cells were seeded into 6-well plates with 50,000 cells per well, supplemented with 2ml of DMEM media and allowed to attach for 24hrs at 37^oC in a

humidified incubator with 5%CO_2/95% air. For transfection, plasmid was added to transfection reagent Fugene 6 (Roche, Basal, Switzerland) at a ratio of 1:3 in 97 µl of serum free media in a glass tube. For the LCN2 containing plasmid (@335 ng/µl), 3 µl of plasmid was added to 3 µl of Fugene whereas for native vector (@1000 ng/µl) 1µl of plasmid was added to 3 µl of Fugene. Transfections were left to rest for 10 minutes at room temperature with very gentle mixing. 103 µl of the mix was then added drop wise to each well and incubated for 24hrs followed by a media change to remove Fugene toxicity. Cells were incubated for a further 24 hours. In parallel, LNCaP cells were seeded at high density and allowed to seed for 24 hrs.

Media was removed from Phoenix cells and filtered through a 40µm carbonated filter (Fisher, Loughborough, UK) and a 5ml syringe. Resultant media was supplemented with polybrene (5 µg/ml). Filtered media was then added to LNCaP cells in a 6 well plate and centrifuged at 3000 rpm for 60 minutes at 32^{o}C. Virus containing media was then removed and LNCaP cells supplemented with fresh RPMI1640 media and incubated for 24 hrs after which LNCaP cells were supplemented with 1 µg/ml of puromycin. A control plate of LNCaPs was also supplemented with puromycin and selection of clones was carried out until 100% of un-transfected cells had died. The remaining population of cells was henceforth known as LNCaP-LCN2 and LNCaP-pBP (empty vector) cells. (Note, LNCaP-LCN2 was sometimes labelled as LNCaP-NGAL for labelling purposes to aid identification)

Validation of the LNCaP-LCN2 cell line was performed using qPCR for the LCN2 gene as well as ELISA and western blotting.

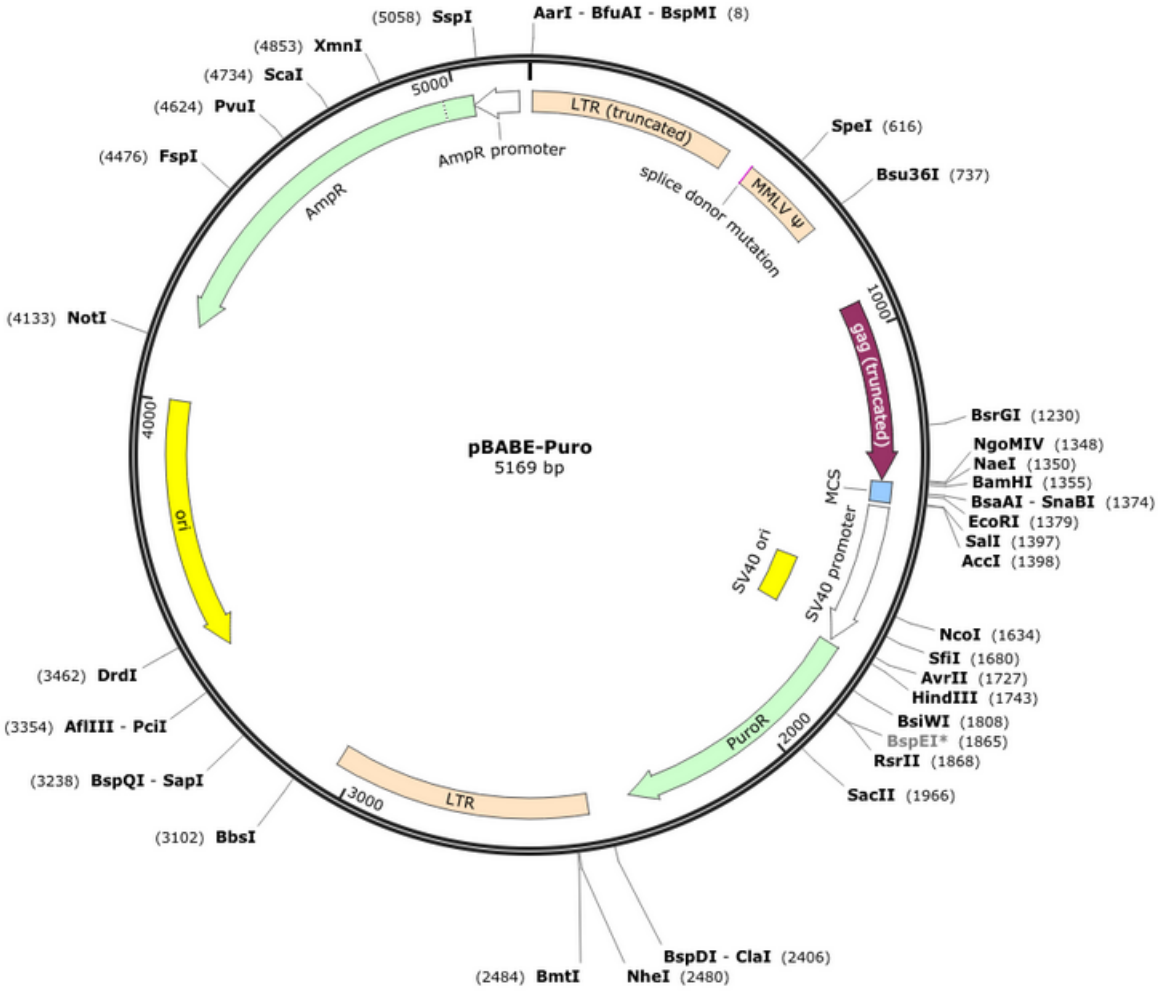

Figure 2.2 Vector map of pBABE-puro. Vector contains numerous restriction sites, an SV40 promoter region, puromycin and ampicillin resistance genes. Inserted genes are flanked by two LTR regions and a Ψ site. For LNCaP-LCN2, the LCN2 gene fragment was inserted at the SAL1 site (1397).

2.6 Synthesis of the LNCaP-GLI1 cell line.

The LNCaP-GLI1 cell line was previously created in our lab by Dr. Sandeep Nadendla. The methods used for the generation of this cell line were identical to LNCaP-LCN2 (section 2.3). Briefly, amphotropic retroviral particles containing either the pBABE-puro (empty vector) or the pBABE-PURO-GLI1 were generated using the Phoenix packaging cell line (Nolan Laboratory, Stanford, USA). Parental LNCaP cells were exposed to the viral particles through centrifugation at 300xg for 1 hour at 32^{o}C and supplemented with polybrene (5µg/ml). After 72 hours, cells were subsequently selected with puromycin to generate the LNCaP-pBP and LNCaP-GLI1 cell lines.

In parallel, Dr Sandeep Nadendla also generated the PC3-GLI1, DU-145 and NEB-1-GLI1 (keratinocyte) cell lines using identical methods, but substituting for LNCaP cells.

2.7 Synthesis of the PC3-shLCN2 cell line.

Short hairpin RNA (shRNA) is a robust and long term method for the silencing of a specific gene. shRNAs are short sequences of RNA (19-21bp) in length. These RNA sequences are bound to an antisense strand and connected with a short hairpin loop. The sequences for these hairpin loops may be contained within a lentiviral vector which is able to integrate into chromosomal DNA. The lentiviral vectors also contain constitutive promoters to drive RNA synthesis in the cell.

Upon transcription, the RNA strands form natural hairpin structures, and are targeted by the protein Drosha which cleaves the pre-microRNA structure so that can be exported from the nucleus by Exportin. Once in the cytoplasm, the hairpin structure is cleaved by Dicer leaving two RNA strands. The antisense strand of RNA is then

targeted by the RISC complex and together these bind the sense strand of mRNA of the target gene which is then targeted for destruction (Figure 2.3).

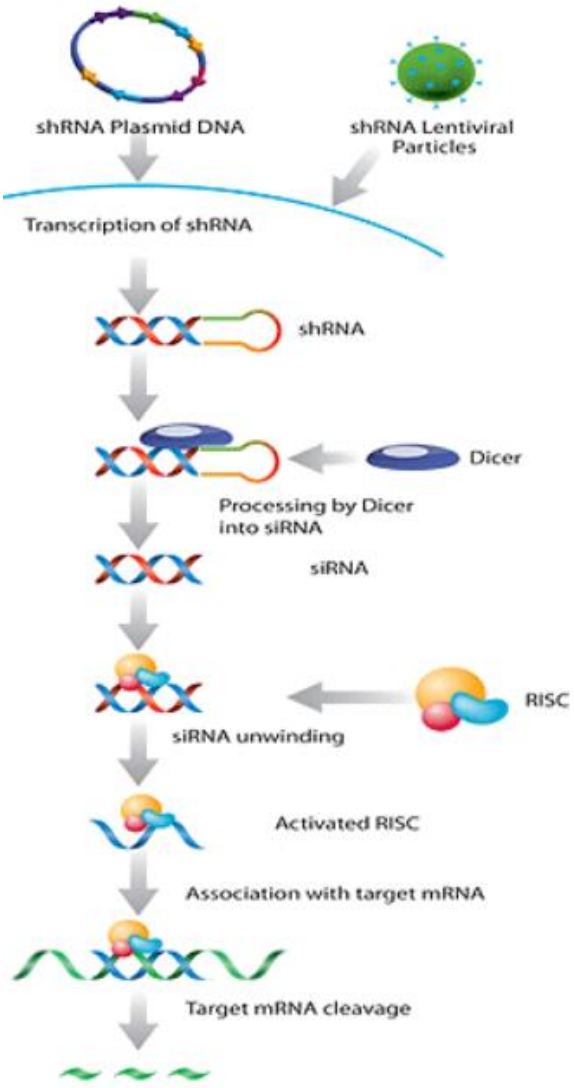

Figure 2.3 shRNA-Mechanisms of action. Plasmids containing shRNA sequence are transfected into cells and inserted into chromosomal DNA. Transcribed shRNA forms a hairpin loop which is cleaved by dicer into siRNA strands. Single strand siRNA is bound by the RISC complex and is able to target corresponding mRNA sequences for degradation. (www.sbct.com)

For the generation of a PC3-shLCN2 cell line, pLenti-L6H vectors containing a short hairpin (sh)RNA sequence were kindly supplied by Dr Zhimin Tong (Tong et al., 2005) (M.D. Anderson, Texas, USA) who in turn received from the Jang-Seong Kim laboratory (Mogam Biotechnology Research Institute, Yongin-city, South Korea) (Lee et al., 2006) targeting LCN2 with the sequence 5' CACCATGCCCCTAGGTCTCCTGTGG-3', with expression under the U6 constitutive promoter. Vectors also contain a blasticidin resistance gene This vector has been used in published papers by both groups. In addition, a control vector containing shRNA with a non-targeting empty vector sequence was provided. These were combined with the viral packaging vectors pCMV (Addgene, MA, USA) containing genes encoding for GAG and POL, and the pMDG-VSVG containing VSVG (Addgene) These vectors were amplified as above using the QIAPrep Spin Maxiprep kit as per the manufacturer's instructions. Plasmid vectors were transfected into OneShot® TOP10 chemically competent bacteria (Invitrogen, Carlsbad, CA, USA) and spread on 1% agar plates containing ampicillin (100µg/ml) and incubated overnight at 37^{o}C. Single colonies were selected and added to 1ml of LB broth to form starter cultures. Starter cultures were added to 200ml of LB broth (15g/l in distilled water and autoclaved) and shaken overnight at 37^{o}C. Bacterial solutions were placed into 50ml plastic tubes and centrifuged at 4000rpm for 15 minutes and supernatants discarded. Pellets were suspended in 10ml of buffer P2 and rested for 5 minutes. 10ml of buffer P3 was added and chilled on ice for 20 minutes. Solutions were centrifuged for1 minute at 10,000 rmp at 4 ^{o}C. Supernatants were decanted into Qiagen-tip 500 columns and allowed to drain through followed by 2x washed by

buffer QC DNA was eluted using 5ml of buffer QF. DNA was precipitated by adding 7ml of isopropanol, then centrifuged for 1 minute at 10,000 rpm. Tubes were rinsed using 5ml of 70% (v/v) ethanol, followed by centrifugation for 1 minute at 10,000 rpm. Remaining ethanol was removed by centrifugation and air-drying. DNA was re-suspended in 1ml of dH2O

293-FT cells (provided by Dr. Cleo Bishop, QMUL, UK) were grown in high glucose DMEM (Lonza) at a density of 50,000 cells/cm^2 in a six well plate and allowed to attach for 24 hrs. 293-FT were then transfected using FuGene (Roche) in serum free media, with a total plasmid to Fugene ratio of 3:2. Lentiviral vectors were supplemented with the vectors pCMV, pMDG which contain the GAG, POL and ENV viral proteins and either pLenti-L6H-shLCN2 or pLenti-L6H-shControl. In parallel, PC3 cells were seeded at 30,000 cells/well in a 6 well plate and allowed to settle for 24hrs.

Viral particles were filtered using a 40nm carbonated filter and supplemented with polybrene (5µg/ml).Virus containing media was then added to parental PC3 cells and underwent centrifugation at 300xg for 1 hour at 32^{o}C. Fresh media was then added. After 72 hours, cells were subsequently selected with blasticidin (1µg/ml) (PAA laboratories, Little Chalfont, UK) until all un-transfected control cells had died after approximately 2 weeks, thereby creating both the PC3-shLCN2 and PC3-shControl cell lines. Using an identical protocol, but using MCF7 cells, the cells lines MCF7-shLCN2 and MCF7-shControl were created.

2.8 Short interfering-RNA targeted gene suppression.

Short interfering RNAs (siRNAs) provide a powerful tool for temporary suppression of a target gene. The method of siRNA suppression is similar to that of shRNA, except that they do not contain a hairpin structure. As such siRNAs can be transfected directly into cells without the need for a viral vector. However, this means that any suppression is temporary and will only last until the siRNAs are used up by the cell or degrade.

siRNA suppression of GLI1:

7000 cells/cm^2 were reverse-transfected with control siGLO (Dharmacon, Lafayette, CO, USA), *Silencer*® Select Negative Control No.1, or siRNA targeting GLI1 (Ambion *Silencer*® Select s5815 or s5816) and/or GLI2 (Ambion *Silencer*® Select s5817) using the Hiperfect (Qiagen) transfection reagent to produce a final concentration of 30 nM; Briefly, siRNA was pipetted onto fresh plates and rested for 2 minutes before being diluted in 100µl of serum free RPMI 1640 media and rested for a further 15 minutes followed by addition of cells and FBS (10% v/v) containing media. Fresh FBS (10% v/v) containing medium was added 24 hr post-seeding. RNA and protein was extracted from samples 96 hours post-seeding. For time course analysis, extracts were taken at 2, 3, 4 and 7 days (including one additional media change)

siRNA suppression of LCN2.

Targeted suppression of LCN2 was carried out using OnTarget® Plus siLCN2 (Thermo Scientific, Waltham, MA, USA) using the protocol listed above at an

optimised concentration of 50nM for 72 hours was determined. For time course analysis, extracts were taken after 2, 4 and 6 days post seeding.

2.9 RNA extraction

Prior to harvesting cells were washed twice with PBS, mRNA extraction was performed using RNEasy Mini Kit (Qiagen, West Sussex, UK) according to the manufacturer's instructions. RLT plus buffer was supplemented with β-mercaptoethanol (1:1000). Genomic DNA was extracted using the gDNA extraction columns provided. RNA was eluted using 50µl of nuclease free H_2O. Samples were quantified using a nanodrop (Thermo Scientific, Waltham, MA, USA) at 260nm, with mRNA quality assessed using 260/240 (260nm detects total nucleic acids, 240nm detects background noise). All mRNA samples were stored at -80^{o}C.

2.10 cDNA synthesis

Complimentary DNA (cDNA) was synthesised using a SuperScript® VILO™ cDNA Synthesis kit (Invitrogen™, Paisley, UK) using 2-2.5 ug of mRNA The reaction was carried out in a PCR machine with the following program: Samples are brought to room temperature of 25^{o}C for 10min, followed by cDNA synthesis at 42^{o}C for 2hrs and a final reverse transcriptase inactivation or reaction termination step at 80^{o}C for 5min. The resultant cDNA was quantified using NanoDrop and stored at -20^{o}C.

2.11 RT-PCR

RT-PCR was performed using REDMIX Mastermix (Thermo Scientific, Waltham, MA, USA) in nuclease free 200 µl tubes containing: 10 µl REDMIX (in kit, containing Taq polymerase) , 6µl dH_2O, 1µl each of forward and reverse primers (1 µM) 1µl $MgCl_2$

(25nM), 2µl cDNA (100ng/µl). All reactions were carried out using the following profile:

5 minutes at 95^{o}C. 15 Seconds at 95^{o}C, 18 seconds at 60^{o}C (or similar annealing temperature). 20 seconds at 72^{o}C. Primer details are listed in Table 2.1.

2.12 QPCR

Quantitative polymerase chain reaction (qPCR) enables a real-time reading of cDNA, and hence mRNA levels of specific genes. qPCR works by attaching dNTPs which have fluorescent tags which are incorporated into double stranded DNA as it is amplified. Fluorescence is detected by lasers within the machine, and readings are taken at each cycle at the extension stage (Fig 2.4). The increasing intensity is recorded as a curve displayed on screen. Thresholds are arbitrary, but placed where curves reach X=Y (in most cases 0.2 fluoro-units. The earlier the curve appears, the more mRNA is present for that gene (Figure 2.4). All values are then normalised to a housekeeping control gene. After the qPCR is run, a melt curve is generated. This can be used to identify the length of the cDNA fragment. In general, most fragments of 15-300bp produce peaks at ~85^{o}C, whereas primer-dimers and other junk material produces peaks at ~75 ^{o}C and hence discarded. Multiple peaks indicate bands of more than one length being present.

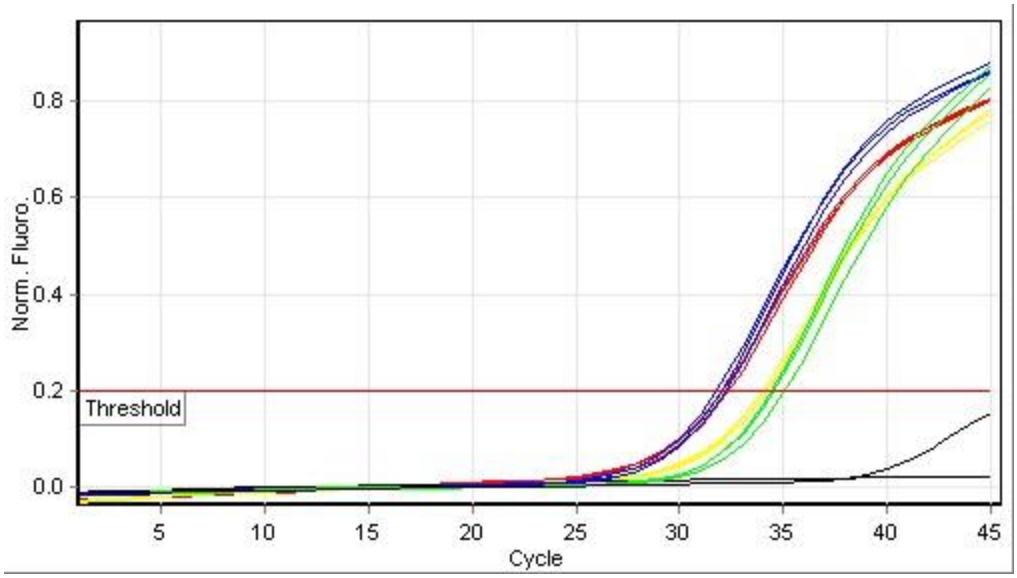

Figure 2.4 qPCR analysis curves Sample figure of a qPCR curve using QIAGEN rotor gene software. Fluorescence is detected on the Y-Axis, with an exponential S-curve generated for each reaction. The further left a curve, the greater the amount of starting cDNA. In this case, the blue and red curves reach the threshold ~1 cycle before yellow and green. 1 cycle= 2x more starting mRNA. I.e. blue and red samples have roughly double the amount this gene expressed.

QPCR analysis was carried out using a Rotor-Gene-Q machine (Qiagen, West Sussex, UK) and associated software. Primers used are listed in table 2.1

qPCR reactions were carried out using Rotor-Gene SYBR Green PCR Kit (Qiagen) containing fluorescent probes and dNTPs. All samples were performed in triplicate. Each sample contained the following components: 10µl SYBR Green, 5 µl dH_2O, 1µl each of forward and reverse primers (1 µM) 1 µl $MgCl_2$ (25 nM), 2 µl cDNA (100 ng/µl). Primers are listed in table 2.1. Samples analysed on the Rotor-Gene-Q with the accompanying software using the following programme:

5 minutes at 95^{o}C 5 seconds at 95^{o}C.

5 seconds at 60^{o}C (or similar annealing temp.) 10 seconds at 60^{o}C x 45 cycles.

15 minutes melt from 50^{o}C to 99^{o}C

Analysis of the melting curve graph of the PCR product indicated that the data generated was from a single product and confirmed by running on a 1% (w/v) agarose gel. Relative induction values (x) were calculated using the formula $x = 2^{-\Delta\Delta CT}$ whereby Ct represents the mean threshold cycle of replicate analyses, ΔCt represents the difference between the Ct values of the target gene and the reference gene GAPDH, and ΔΔCt is the difference between the ΔCt values of the target gene for each sample compared to the ΔCt mean of the reference sample.

To confirm whether cDNA fragment sizes were correct, following the qPCR run, samples for each gene were supplemented with loading buffer (BlueJuice™ Gel Loading Buffer 10X, Invitrogen, Carlsbad, CA, USA) and run on a 1% (w/v) agarose gel. This was then cross-referenced to the melt curve generated by the Rotor-gene software.

Gene	Forward (5’ to 3’)	(Reverse 5’ to 3’)
AGR2	AGCCGCCGACTCACACAAGG	AGGGTCTGGGGCAGTTTGGGT
AR	TACCAGCTCACCAAGCTCCT	GCTTCACTGGGTGTGGAAAT
BOCT	CCAACTTCATTGCCCATGCC	CTCTGTTGGGGTTCCCTTGT
CD44	GTGATCAACAGTGGCAATGG	CCACATTCTGCAGGTTCCTT
E-cadherin	TGCCCCCAATACCCCAGCGT	ACGGTGGCTGTGGAGGTGGT
EGFR	CAGCGCTACCTTGTCATTCA	TGCACTCAGAGAGCTCAGGA
ERBB2 (HER2)	TCCAGCCCTAGTGTCAGGTC	CCAGCAGGGCTTCTTCTGT
ESR1 (ERα)	CCAGCACCCTGAAGTCTCTG	ACTCATGTGCCTGATGTGGG
ESR2 (ERβ)	CGACCACTAAGGACTCTACC	TCGCACTGGTACATGGCTAA
GAPDH	GCCTTCCGTGTCCCCACTGC	GCTCTTGCTGGGGCTGGTGG
GLI1	GAAGACCTCTCCAGCTTGGA	GGCTGACAGTATAGGCAGAG
GLI2	TGCCACTGGGAAGACTGCACC	AAGGGCTTCTGCTCCCGCTG
IL1B	GGGCCTCAAGGAAAAGAATC	TTCTGCTTGAGAGGTGCTGA
KDR	ACGGCGCTTGGACAGCATCA	ATTTCGTGCCGCCAGGTCCC
KLK3 (PSA)	CACAGCCTGTTTCATCCTGA	AGGTCCATGACCTTCACAGC
KLK5	TTTTCAGAGTCCGTCTCGGC	ACACCAAGCACTTTGTCCCA
KLK6	GTGTGCTGGGGATGAGAAGT	CACATGTCAGGGTCACTTGG
LCN2	CCCGTGTTGGGGGCTCTGCATG	GTTGGTGTCACCACTCGGACG
ΔP63	GTCCCAGAGCACACAGACA	GAGGAGCCGTTCTGAATCTG
P-Cadherin	AACCTCCACAGCCACCATAG	GTCTCTCAGGATGCGGTAGC
SPARC	CGCATGCGGGACTGGCTCAA	TGAGGGGAGCACGCAGTGGA
SLUG	CTTTTTCTTGCCCTCACTGC	GCTTCGGAGTGAAGAAATGC
SNAIL	ACCCCACATCCTTCTACTG	TACAAAAACCCACGCAGACA
SPRY1	AGGTCTGAAAGGGCAATCCG	TTCCACCATGCTCTCAGCAG
ST14	CCCAGACCTTCAGGTGTTCC	TCAAGCAGAGCCCATTGAGG
TWIST1	GTCCGCAGTCTTACGAGGAG	CCAGCTTGAGGGTCTGAATC
Vimentin	TGGCCGACGCCATCAACACC	CACCTCGACGCGGGCTTTGT

Table 2.1 List of primers used

2.13 Protein Extraction and quantification from Cell Lines.

Prior to extraction, cells were washed in PBS. Protein extraction was carried out using a 50mM Sodium Hydroxide solution heated to 100^{o} C. 220µl of hot protein lysis buffer (50 mM Tris–HCl, pH 8.0, 2% sodium dodecyl sulphate (SDS)) was added to cells, and removed with a cell scraper. Samples were boiled for 5 minutes before quantification. Protein levels were quantified using the Bio-RadDC Protein Assay detection kit (Bio-Rad, Boston, MA, USA) according to the manufacturer's instructions. 20 µl of protein were added to 1 ml clear plastic cuvettes and supplemented with 98 µl of solution A and 2 µl of solution S, then rested for 3 minutes. 800 µl of solution B was added and mixed gently. Proteins are bound by a copper tartrate solution, which is able to reduce folin, thereby turning the solution blue. The greater the intensity of blue colour, the greater the protein concentration. Values were measured at wavelength of 655 nm in a spectrometer and protein concentration calculated against a standard curve derived from bovine serum albumen (provided in kit).Samples were all stored at -80^{o}C for future use.

2.14 Western Blotting / Gel electrophoresis.

Western blotting was performed using 8-12% (w/v) polyacrylamide-tris gels. Gels were comprised of. distilled water,30% (v/v) acrylamide gel, 1.5 M Tris (pH 8.8), 10% (w/v) SDS, 10% (w/v) ammonium persulphate (APS) and tetramethylethylenediamine (TEMED) (0.2% v/v). TEMED and APS combine with the acrylamide to form long cross-linked chains. SDS interacts with the proteins, giving them a negative charge which enables them to be attracted by an electric current. The varying percentage gel was dependent on the molecular weight of the

relevant protein, with 8% gels used for detection of proteins >150 kDa, 10% gels for proteins 20-150 kDa and 12% gels for proteins <50 kDa.

Prior to protein loading, protein samples were heated to 95^{o}C for 3 minutes before loading dye was added (loading dye is at a 5x concentration, [100mM Tris-HCl (pH 6.8), 200mM dithiothreitol, 4% SDS, 0.2% (w/v) bromophenol blue, 20% (v/v) glycerol]). ColorPlusTM (New England Bioscience, Boston, MA, USA) ladder was used For protein size verification. Biotinylated protein ladder (Cell Signalling) was also used in some experiments as an additional marker. After loading, the gel was subject to a current of ~100v for 1-2 hours until the loading dye had run off the gel. For mixed molecular weight gels, pre-cast 18-well gradient gels (4-15%) were obtained from BioRad (Berkeley, CA, USA).

Protein was transferred to Hybond (Amersham Bioscience, Amersham, UK) nitrocellulose using a Trans-Blot Turbo Semi-dry transfer machine and transferred using the 'mini-gel' setting for 25 minutes. Following transfer, membranes were washed in PBS-T (0.2% v/v) and stained with Ponceau stain (Invitrogen, Carlsbad, CA, USA) to detect correct transfer. Membranes were then blocked in either 5% (w/v) milk or BSA mixed with PBS-T or TBS-T for 1 hour. Antibody (See Table 2.2) was added to fresh blocking solution, and membranes incubated overnight at 4^{o}C. Following incubation, membranes were washed 3 times for 5 minutes in either PBS-T or TBS-T, and incubated with HRP linked secondary antibody in milk for 1 hour at room temperature. Membranes were washed a minimum of 3 times in either PBS-T or TBS-T. Membranes were probed using an ECL Prime ^{TM} western blotting detection kit (GE Healthcare, Little Chalfont, UK).

Antibody	Specificity	Company
Androgen Receptor	Rabbit	Cell signalling (MA, USA)
α-tubulin	Mouse	Santa-Cruz, CA, USA
p-AKT	Rabbit	Cell signalling
Total AKT	Rabbit	Cell signalling
E-cadherin	Rabbit	Cell signalling
EGFR (total)	Rabbit	Cell signalling
p-EGFR	Rabbit	Cell signalling
ERK (Total)	Rabbit	Cell signalling
Estrogen Receptor α	Mouse	R&D systems, MN, USA
Estrogen Receptor β	Mouse	R&D systems
LCN2	Rat	R&D systems
Total mTOR	Rabbit	Cell signalling
p-mTOR, total mTOR	Rabbit	Cell signalling
pS6K	Rabbit	Cell signalling
Vimentin	Mouse	Santa-Cruz
p-4EBP1	Rabbit	Cell signalling

Table 2.2 List of Antibodies used.

2.15 ELISA

Enzyme-Linked Immunosorbent Assay (ELISA) uses enzyme linked antibodies to detect levels of protein. This method is particularly useful for detecting secreted proteins, as in this case the protein can be extracted from media. In sandwich ELISA, antibodies targeting a protein are attached to a plate and bind to the protein of interest. Further antibodies are then added which are bound to an enzyme which is degrades substrates into a colourful solution. The absorbance of this solution can then be measured using a colourimiter.

For the detection of LCN2 protein an R&D systems (Minneapolis, USA) Quantikine ELISA kit DLCN20 was employed. Cells were seeded in T25 flasks (250,000 cells/well) and incubated for 48 hrs (At which point cells are ~70% confluent). 3ml of media extracted directly from the T25 flasks and centrifuged at 2000 RPM for 5 minutes to remove floating cells. Supernatant was transferred to Ultra-spin concentrating columns containing a protein filter (Fisher UK, Loughborough, UK) and centrifuged at 4000 RMP for 15 minutes, thus removing any material less than 10 kDa in size.

75µl of concentrated media was added to 100µl of assay diluent on the ELISA plates and incubated for 2hrs at 4^{o}C. Washing and incubation of LCN2 conjugates were carried out according to the manufacturers' instructions. Enzyme substrate was added at a 1:1 ratio and incubated for 30 minutes at room temperature in the dark. All samples were performed in triplicate.

Plates were read using an Optima plate reader using wavelengths 450nm and 570nm using a 'flat-bottomed plate' setting. Standard curves were generated using recombinant LCN2 protein concentrations as provided in the kit.

2.16 Cell Proliferation assays

Alamar Blue

Resazurin is a blue dye which is reduced by mitochondria to become pink in colour and is an effective assay of cell proliferation. Cells were plated into 12 well dishes at a density of $1x10^5$ cells/cm^2 in triplicate, and supplemented with 1ml of RPMI 1640 media (with 10% v/v FBS). 24h post seeding, 100µl 10x Resazurin (AlamarBlue™ (Invitrogen, Carlsbad, CA, USA)) was added and incubated for 4 hours. 3x 100µl of the resulting media was added to an opaque 96 well plate from each well. Plates were then scanned in a plate reader at 570 nm. Cells were then washed with PBS and replenished with new RPMI 1640 media (with 10% v/v FBS). Readings were taken at either every 24 h or 48 h intervals

2D colony formation Assay

Cells were seeded in 6cm plastic dishes at a low density of 40 cells/cm^2 and cultured for 14 days. Cells were washed with PBS and stained with 1x crystal violet (1% w/v in a 75% water/ 25% Methanol v/v solution) for 5 minutes before rinsing. Colony counting was performed manually using a 1 cm transparent grid (Fisher UK, Loughborough, UK).

3D colony formation in soft agar

To provide a 3D context for cell proliferation, cells may be cultured in an agar matrix so that cells are held in suspension. Six well plates were coated in a 1% (w/v) low melting point agarose gel (Sigma) and allowed to set and solidify. Cells of interest

were split and suspended at 20,000 cell/ml in RPMI 1640 media (with 10% v/v FBS). Media and agarose gel were combined in a 1:1 ratio to generate a 0.5% agarose solution with 10,000 cells/ml. 1 ml of this solution was plated and allowed to set. Agarose layers were supplemented with 1ml of fresh RPMI 1640 media (with 10% v/v FBS) which was changed ever 2-3 days for a total of 14 days. Colonies were counted manually using a $1cm^2$ grid (Fisher UK, Loughborough, UK). Wells were stained with 1x crystal violet (1% w/v in a 75% water/ 25% Methanol v/v solution) for preservation.

Senescence Assays

β-Galactosidase senescence kit # 9869s were purchased from Cell Signalling (Boston, MA, USA) and used according to the manufacturer's instructions. Cells were seeded at at 30,000 cells/well and cultured in 6 well plates for 3 days. Cells were fixed using the fixative solution provided in the kit and rinsed with PBS. 1ml of the β-Galactosidase staining solution containing X-Gal was added to wells and incubated overnight at 37^oC in a CO_2 free chamber. Senescent cells appear break down the X-Gal, creating a blue colour which is visible under a microscope.

DAPI Analysis

4',6-diamidino-2-phenylindole (DAPI) is a fluorescent dye which bind to A-T rich areas of DNA in chromatin. DAPI bound to DNA fluoresces at 460nm which can be detected under the microscope. Cultured cells were washed 3 times for 5 minutes each in PBS and fixed in a 4% (v/v) paraformaldehyde solution for 20 minutes at room temperature. Cells were washed again twice in PBS then were incubated in a 1:5000 DAPI solution (Purchased from Cell signalling) in PBS in the dark for 5

minutes. Cells were rinsed in PBS and imaged using a microscope with a 360nm ultraviolet laser.

2.17 Migration assays

Scratch wound assays

Cells were plated in a 6cm plastic dish at a density of $30x10^5$ cells/cm^2 and incubated for 48h or until cells reached 100% confluence. Prior to the assay, 10 µg/ml mitomycin C was added to cells and mixed thoroughly incubated for a further 4 hours. Using a 200 µl pipette tip, a line was scored through the middle of the dish. The resulting scratch is approximately 2mm wide. Width readings were taken using a Nikon Eclipse microscope, with 6 readings taken per scratch. The edge drawing function of Nikon microscope software (bundled with microscope) was also utilised to determine scratch widths. Scratch width was recorded after 24 hours.

Live cell imaging

To obtain a real-time assessment of cell movement and migration, time lapse imaging was employed.

Cells were seeded into 6-well plates at a range of densities (10000, 20000 and 50000 cells/well) and incubated at 37^oC in a humidified chamber with 5% CO_2 95% air for 24hrs. Plates were then placed in a humidity controlled and 5% CO_2 containing chamber. Bright field images of specific co-ordinates within each well were captured by a Nikon time-lapse microscope (BioStation IM-Q, Nikon Surrey, UK). Images were captured every 15 minutes for 18 hours. Images were collated into .avi format.

2.18 Microarray analysis

Microarrays provide a whole-genome view of mRNA transcription. Microarrays are small chips containing oligonucleotides corresponding to each gene transcript in the human genome. RNA from cells of interest are converted to cDNA, then fragmented and labelled with fluorescent tags. If these fragments bind to oligonucleotide with a corresponding sense strand, they will fluoresce, and this is detected by scanners. Higher fluorescence equals greater amount of mRNA expression.

For this study, GeneChip® Human Gene ST Arrays (Designed by Affymetrix, Santa Clara, CA, USA) were employed for microarray analysis. The GeneChip array contains probes for 36,079 human genes, including a number of microRNA sequences. Each gene is has multiple probes, preventing cases of false-positives.

Microarray profiling was carried out for LNCaP-pBP vs LNCaP-LCN2 cells, and for PC3-shControl vs PC3-shLCN2 cells. With each cell line being performed in triplicate using 3 separate chips. Prior to testing, RNA (extracted using methods detailed in section 2.9) was subjected to quality control. Both quality control and the running of the GeneChip assay were kindly carried out by the Genome Centre at QMUL. Raw data was normalised and noise reduction was applied before being assigned to individual genes using Affymetrix bundled software. To account for background noise and false positives, data was subjected to the multi array average (RMA) method. RMA utilises quantile normalisation that will fit all the chips used from the experiment into the same distribution and also gives them the same mean. This then provides an expression value for each gene. From this, differentially expressed genes **(**DEGs) can be separated based on P-values and fold change using -log values.

PANTHER pathway analysis

PANTHER gene classification software (http://www.pantherdb.org) is an online network analysis tool which works by sorting gene lists into their roles in biological processes. The software is also able to place genes into known signalling pathways based on previous literature. Using raw Log fold expression values, an arbitrary cut off point of either +1.5 fold or -1.5 fold (relative to controls) was taken to select genes which were either up- or down- regulated. The gene symbols for the selected groups were imputed into the PANTHER software and analysed for pathway regulation using the histogram tool. Using the same tool, genes were also divided according to biological function.

MetaCore analysis

MetaCore^{TM} pathway analysis provides a more in-depth analysis of gene ontologies and pathways. Metacore software is able to identify whether genes are transcription factors, kinases or cell membrane proteins etc. The software is also able to integrate genes into more statistically significant DEG pathways based on mathematical algorithms. Noise reduction also filters out many insignificant genes to provide a robust analysis of DEGs.

The raw data was normalised using the MetaCore pathway analysis software (GeneGo, CA, USA) which was kindly done by Dr Joanne Selway and Avijit Guha Roy from The University of Buckingham.

To generate the probabilities of gene expression between the control cell group and the experimental cells, the Wilcoxon's signed rank test was used whereby P-values were used to compare between different groups of genes. Tukey's Biweight which

are then anti-logged to generate fold change values comparing the genes between samples (Gentleman et al., 2005). Genes with a P-value at or below 5% and a fold change greater than +/- 2 fold are considered as DEGs. DEGs were analysed in MetaCore using integrated GeneGo database of process networks and cellular pathways. P-values represent the probability for a set of genes to appear on a network or process map to arise by chance. The smaller the P-value is, the less likely that the result has occurred by chance. The P-value also considers the number of genes from the experimental data versus the number of genes in the network map. The formula for calculating the P-value was:

$$\text{P Value} = \frac{R!\, n!\, (N-R)!\, (N-n)!}{N!} \sum_{i=\max(r,R+n-N)}^{\min(n,R)} \frac{1}{i!\, (R-i)!\, (n-i)!\, (N-R-n+i)!}$$

N = total number of nodes in MetaCore database

R = number of the network's objects corresponding to the genes in microarray data list

n = total number of nodes in each small network generated from the microarray data

r = number of nodes with data in each small network generated from the microarray data

Gene-E analysis

Gene-E software, (developed by the Broad Institute, Harvard, MA, USA) is an analysis tool which is able to generate heat maps of gene expression based on raw data and fluorescence intensities generated from microarray analysis. The Gene-E software is thus able to plot fluorescence values between samples on an X-Y plot.

Raw fluorescence values were paired up with Affymetrix gene probe symbols. All unconfirned genes, pseudogenes genes without official gene symbols, as well as corrupted or blank data were removed from gene lists. Probe intensity comparison was carried out using the '2 way variables plot graph' function.

2.19 Statistical Analyses

Unless otherwise stated, or where it was logistically impossible, all experiments were performed in triplicate, and performed n=3 times at different time periods. For experiments such as qPCR and Alamar blue, standard deviations were calculated using the formula.

$$\text{Standard deviation} = \sqrt{\frac{\Sigma(x - \bar{x})^2}{(n - 1)}}$$

x = score

$\bar{x}$ = mean

n = number of values

Σ = sum of values

From this, the standard error of the mean may be calculated using the formula:

$$\text{Standard error} = \frac{\sigma_x}{\sqrt{N}}$$

Where σ_x = Standard deviation

N = Number of observations

To determine statistical significance between two data sets, Student's t-test was employed using the standard formula of:

$$t = \frac{\bar{x}_1 - \bar{x}_2}{\sqrt{\frac{s_1^2}{N_1} + \frac{s_2^2}{N_2}}}$$

$\bar{x}_1$ = mean of the first data set

$\bar{x}_2$ = mean of the second data set

s_1^2 = standard deviation of the first data set

s_2^2 = standard deviation of the second data set

N_1 = number of elements in the first data set

N_2 = number of elements in the second data set

Final values are shown as a p (probability) value, with $p<0.05$ being considered significant. $P<0.01$ and $P<0.001$ were also used for providing greater levels of significance.

Chapter 3

Results: Suppression of GLI1 in Prostate Cancer Cell Lines

Introduction

3.0 Background of previous work on Gli1 in PCa cell lines.

The work presented in this chapter was follows on from the work carried out by Sandeep Nadendla and other members of the Neill lab (Thesis: Sandeep Nadendla 08/2011). Below is a brief summary of the data obtained prior to the start of the project and which is necessary for the understanding of the following chapters and results.

It has been described in previous studies that GLI1 and GLI2 expression in PCa is predominantly associated with basal cells, which are further associated with an androgen independent phenotype. However, the link between GLI and androgen independence was poorly understood (Chen et al., 2009, Shaw and Prowse, 2008).

To assess the role of GLI in androgen independence in PCa, levels of GLI (both GLI1 and GLI2) were analysed across a wide range of PCa cell lines: LNCaP, PC3, DU145 and PNT2. Luciferase reporter analysis revealed that GLI activity was significantly higher in the androgen independent cell lines PC3 and DU145 than in the androgen dependent LNCaP and PNT2 cell lines. It was thus hypothesised that GLI expression was contributing to the androgen independent phenotype. To further elucidate any role of GLI1 in the regulation of androgen receptor, GLI1 was ectopically expressed via a lentiviral vector in the LNCaP cell line - which had the lowest GLI1 expression- to generate the LNCaP-GLI1cell line. Immediately following drug selection, LNCaP-GLI1 cells exhibited a distinct tightened or cobblestone cell morphology, whereas LNCaP-pBP (empty vector) cells exhibited a more diffuse morphology. This was evidenced by colony formation assays, whereby LNCaP-GLI1 cells formed large and visible colonies, whereas controls did not. This tight

morphology was similar to that found in androgen independent DU145 cells. LNCaP-GLI1 Cells were also rounder and less spindly in appearance. LNCaP-GLI1 cells also proliferated a significantly faster rate than LNCaP-pBP cells as shown by Alamar blue^{TM} cell proliferation assays.

Western blot analysis of LNCaP-GLI1 cells revealed a wide range of changes to protein expression. Overall, LNCaP-GLI1 cells exhibited basal-like characteristics and a trend towards a stem-like phenotype. These characteristics included a change forming tight colonies, a higher rate of proliferation and changes to gene and protein expression. LNCaP-GLI1 cells expressed CD44, a key stem cell marker. Indeed, LNCaP-GLI1 cells exhibited many hallmarks of EMT including a total loss of E-cadherin expression, coupled with an increase in vimentin expression and ΔNp63.

Most notably, LNCaP-GLI1 cells did not express androgen Receptor which was coupled to Bicalutamide resistance, and overall maintained a basal-like phenotype. Microarray analysis of both LNCaP-pBP and LNCaP-GLI1 mRNA further confirmed that LNCaP-GLI1 cells had indeed entered into both an EMT and an androgen independent phenotype, as well as effects to a wide range of other genes (Thesis: Sandeep Nadendla 08/2011) (Nadendla et al., 2011).

Given the previous data, there was a clear correlation between GLI1 and an AI and EMT phenotype. It was not known however whether the effects of GLI1 were direct or indirect. Furthermore, it was also unknown whether any phenotypic or gene expression was reversible, and whether cells could be returned to a luminal-like state through the subsequent suppression of GLI1.

As such, the follow on from the work carried out by Dr Sandeep Nadendla the aims of the experiments in this chapter were as follows:

Determine if androgen receptor expression is restored in LNCaP-GLI1 cells through subsequent suppression of GLI1 through targeted siRNA.

Determine if the expression of EMT, basal and stem markers such as E-cadherin, vimentin and CD44 are reversed following GLI1 suppression in LNCaP-GLI1 cells and observe any changes to morphology.

Results

3.1Targeted suppression of Gli1 via siRNA does not reverse phenotype or gene expression in LNCaP-Gli1 cells.

To determine whether phenotypic (particularly EMT and AI) changes observed in LNCaP-GLI1 cells could be reversed through siRNA targeted suppression. Two separate siRNA sequences were used to target GLI1; namely Ambion Silencer® Select #5815 and Silencer® Select #5816, with each sequence targeting a different section of mRNA transcript. According to the manufacturer's optimal conditions, LNCaP-GLI1 cells were transfected with 30nM siRNA. The intracellular red fluorescent dye siGLO was used as positive transfection control. (Cells were also transfected with 10nM siRNA, however this concentration proved to have no GLI1 expression). mRNA and protein were extracted from samples after 24, 48, 72, 96 and 120 hours post transfection. Visual observation of LNCaP-GLI1 cells following siRNA targeted silencing did not reveal any obvious phenotypic changes, with cells remaining in tight colonies (Figure 3.1 A).

qPCR analysis of GLI1 gene expression revealed that both the 5815 and 5816 siRNAs were effective in silencing GLI1. Silencing increased linearly, peaking at 96h for both siRNAs before showing a slight loss of effect after 120h. Indeed, after 96h, mRNA expression of GLI1 was undetectable (no expression after 45 cycles) (Figure 3.1B).

Following confirmation of GLI1 silencing, RT-PCR was utilised to analyse expression of key GLI1 target genes, specifically the basal marker ΔP63 and androgen receptor. Results showed that despite the total silencing of GLI1 transcription, no changes to expression were observed in any of genes tested (Figure 3.1C).

GLI2

LNCaP-GLI1 cells also express high levels of GLI2 mRNA (Thesis: Sandeep Nadendla 08/2011). GLI2 may therefore be responsible for maintaining the phenotype observed in LNCaP-GLI1. Targeted siRNA silencing was performed on GLI2 using Ambion Silencer® Select #5817. siRNA was transfected into LNCaP-GLI1 cells for 24, 48, 96 and 120h. qPCR analysis revealed that siRNA targeted silencing was successful, with silencing peaking at 96 hours post transfection (230 fold reduction in expression). No phenotypic changes were observed in LNCaP-GLI1 cells (Figure 3.1A). No change in GLI1 expression was observed. qPCR analysis was then employed to observe expression levels of the AR and ΔP63. Despite strong silencing of GLI2 (Figure 3.1B), no significant changes in expression were observed in any gene (Figure 3.1C).

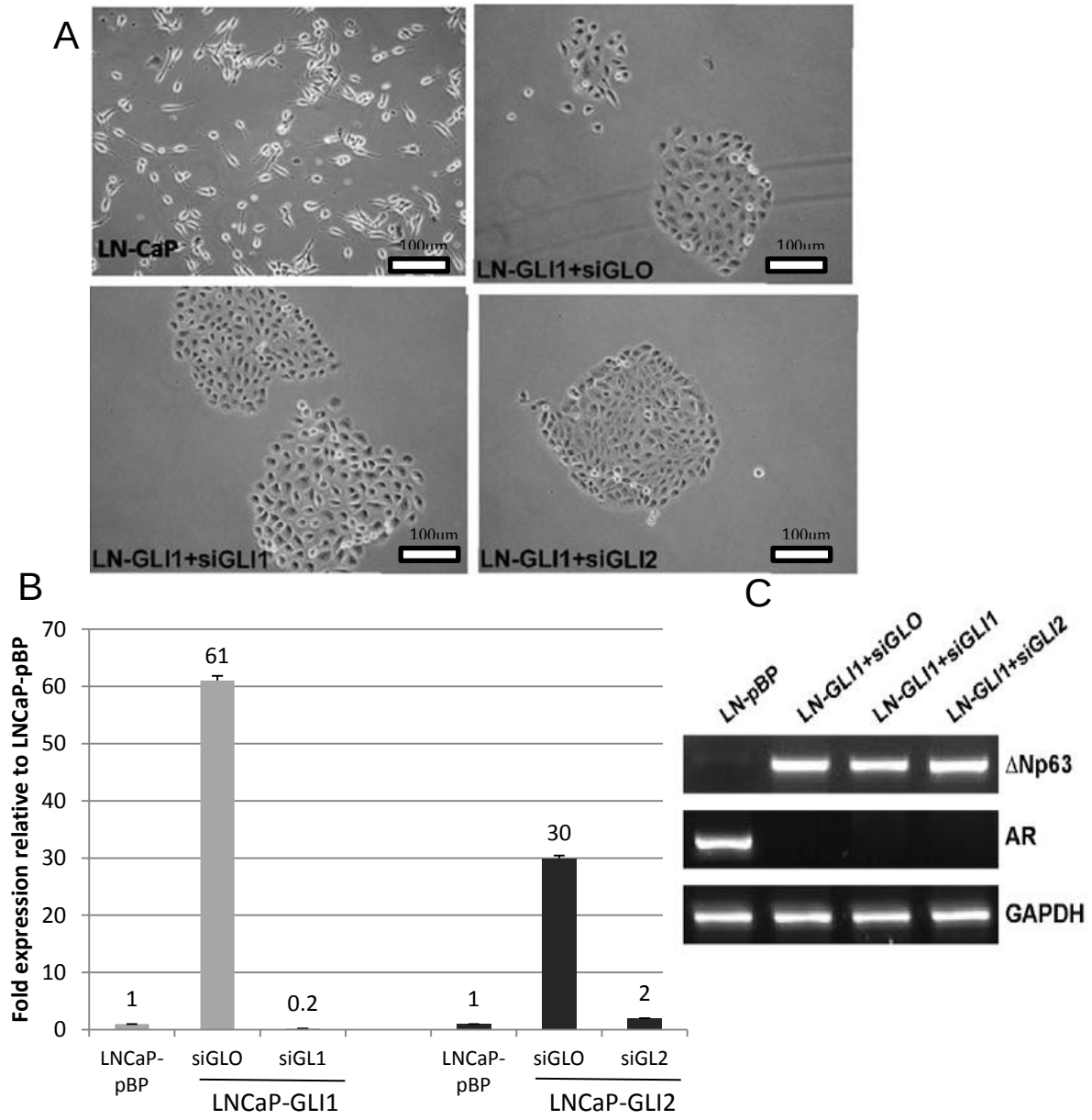

Figure 3.1 Effects of suppression of GLI1 or GLI2 on morphology and gene expression: A Bright field images of LNCaP, LNCaP-GLI1 with siGLO control, and LNCaP-GLI1 cells +siGLI1 or +siGLI2 96hrs post transfection. x20 magnification **B** siRNA knockdown of both GLI1 and GLI2 as analysed by qPCR analysis. Values are fold induction relative to LNCaP-pBP controls after 96 hours post transfection +/- SEM. **C** RT-PCR analysis of AR and ΔNp63 following siGLI1 or siGLI2 transfection (Representative of n=3).

3.2 Double GLI1 & GLI2 silencing

GLI1 and GLI2 operate using positive feedback loops whereby they are able to initiate their own transcription (Regl et al., 2002). GLI1 is able to activate GLI2 transcription and vice-versa. Moreover, GLI1 and GLI2 have been shown to transcribe an overlapping set of genes, and in many cases exhibit redundancy. It was therefore proposed that the targeted silencing of GLI1 may be compensated for by GLI2. Therefore, silencing of a single gene may be ineffective.

To address this issue, a double targeted silencing of both GLI1 and GLI2 was performed by transfecting both Ambion Silencer® Select #5816 and #5817 in LNCaP-GLI1(both siRNAs were transfected at 30nM/ml . As both individual siRNAs were optimised to be most effective after 96h, mRNA and lysates were extracted at that time point only.

96 hours post transfection no obvious changes were observed to cell morphology. LNCaP-GLI1 cells remained compact and highly proliferative (Figure 3.2A). Total GLI activity, as detected by the GLI1 luciferase reporter was reduced by 105 fold. qPCR analysis revealed 26 fold and 30 fold reductions in GLI1 and GLI2 respectively. Despite silencing of both GLI1 and GLI2, target genes were analysed via by both qPCR and RT-PCR showed no statistically significant change to mRNA expression in E-cadherin, vimentin, CD44, ΔP63 or AR (Fig 3.2B)

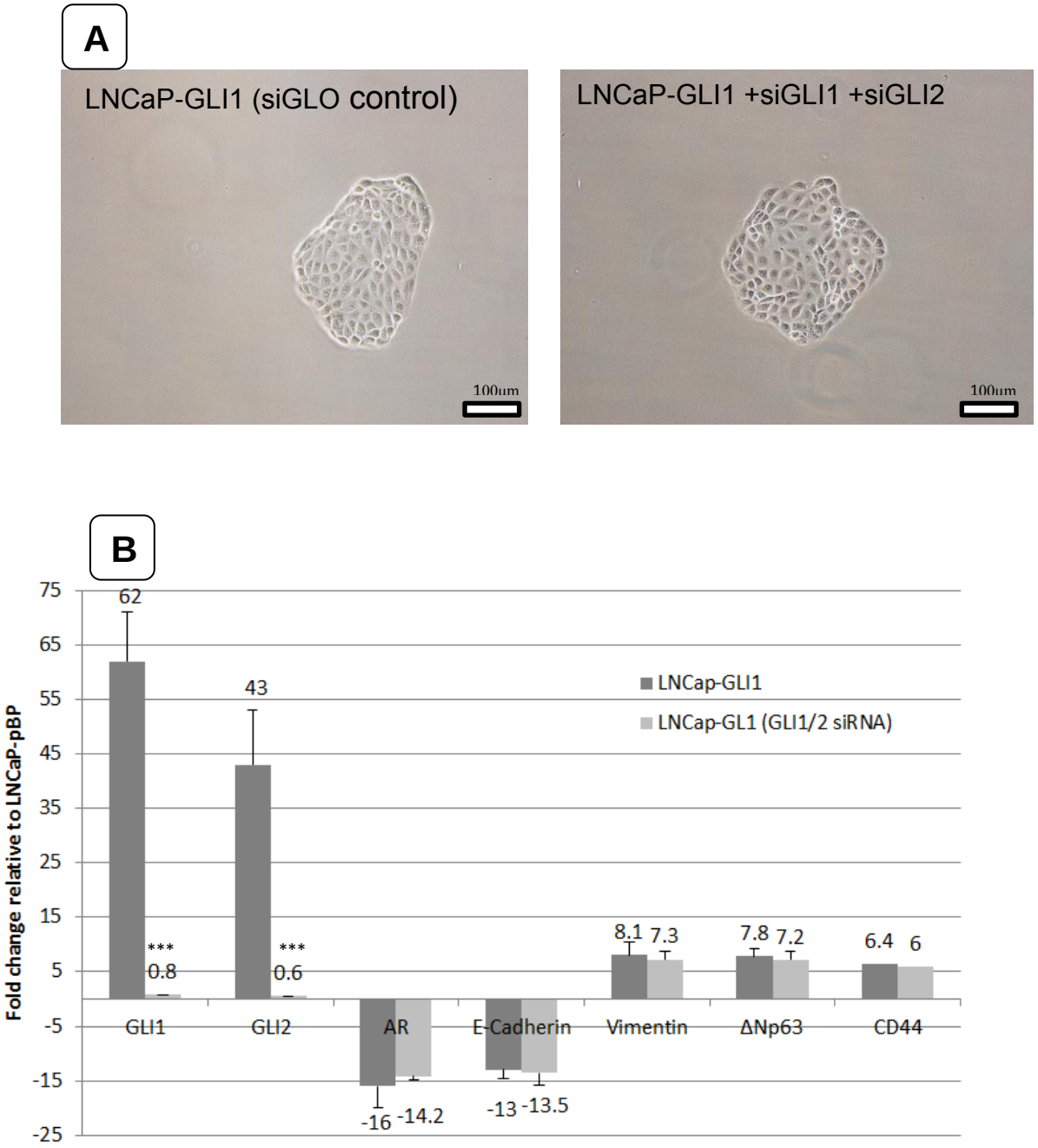

Figure 3.2 Double siRNA knockdown of both GLI1 and GLI2. A-Cells were transfected with siRNA targeting both GLI1 and GLI2 for 96hrs- bright field images x20 magnification. **B** qPCR analysis of AR, EMT and stem markers in siGLI1/iGLI2 LNCaP-GLI1 cells after 96hrs. Values are fold expression relative to LNCaP-pBP. +/- SEM. Statistical analysis was carried out using Student's t-test ***p<0.001.

3.3 Prolonged Exposure to GLI1 and GLI2 siRNA

siRNA targeting both GLI1 and GLI2 were shown to have optimal efficacy after 96 hours. However, although mRNA is suppressed and while GLI1 protein has a short half-life, this may not be a sufficient time period for observable phenotypic change. To address this issue, LNCaP-GLI1, PC3 and DU145 cells were transfected with siRNA targeting both GLI1 and GLI2 (conditions as above) until cells reached ~70-80% confluence whereby cells were split and re-transfected every 72-96 hours for a total of 14 days (i.e. 3 transfections in total). Following 14 days of siRNA exposure, no morphological changes were observed and cells did not revert to a luminal like shape (Figure 3.3A). Moreover, there was no visually obvious change to cell proliferation or cell toxicity. qPCR analysis also indicated GLI silencing similar to that recorded after 96h (Figure 3.3B). The GLI target genes E-cadherin (CDH1), vimenin AR and ΔP63 were analysed via qPCR, however no significant changes to expression were observed in any cell, or in any cell line.

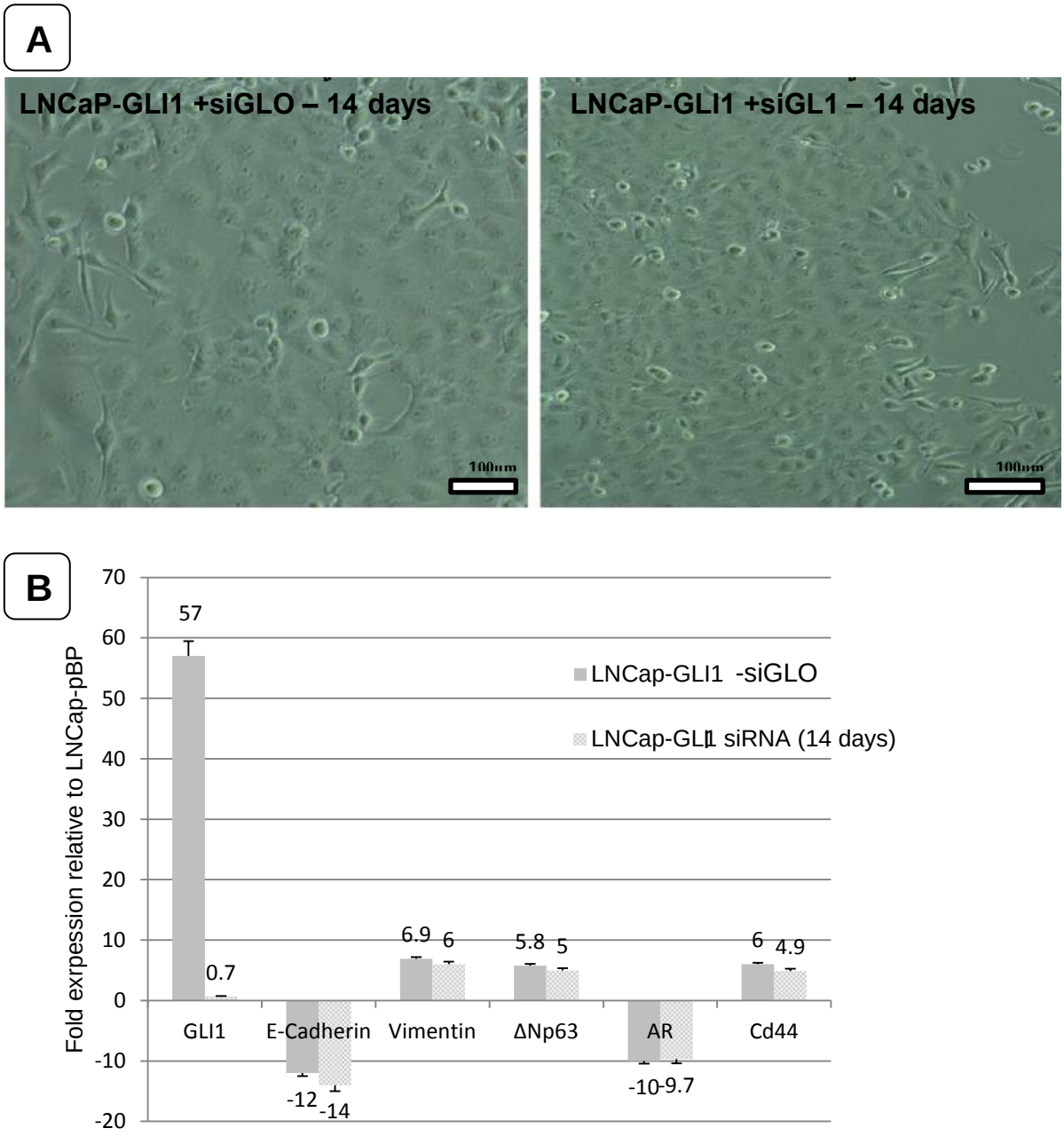

Figure 3.3 Long term siRNA suppression of GLI1. LNCaP-GLI1 cells were transfected for 14 days with siRNA targeting GLI1. A- Bright field images of LNCap-GLI1 transfected with siGLO or siGLI1 for 14 days. **B**- qPCR analysis of GLI1 target genes in control and siRNA treated LNCaP-GLI1 cells. All values are relative to LNCaP-pBP +/- SEM, n=3. Statistical analysis was carried out using Student's t-test.

3.4 siRNA targeting of GLI1 and GLI2 in DU145 and PC3 cells

As Ectopic GLI1 expression may have an exaggerated phenotype due to abnormally high levels of protein, the effect of GLI1 suppression was also performed in PC3 and DU145 cells. Both cell types expressed high levels of GLI1 and are both androgen independent and basal-like. Thus, it was investigated whether suppression of GLI would lead to a more luminal phenotype. Double knockdown of both GLI1 and GLI2 was carried out as previously described to eliminate any redundancy effects. As above, suppression of GLI1 and GLI2 was successful in both cell types. However, following 96hrs of transfection, no change in phenotype was observed. Also, no changes were observed to either AR, or to EMT markers in either cell type (Figure 3.4)

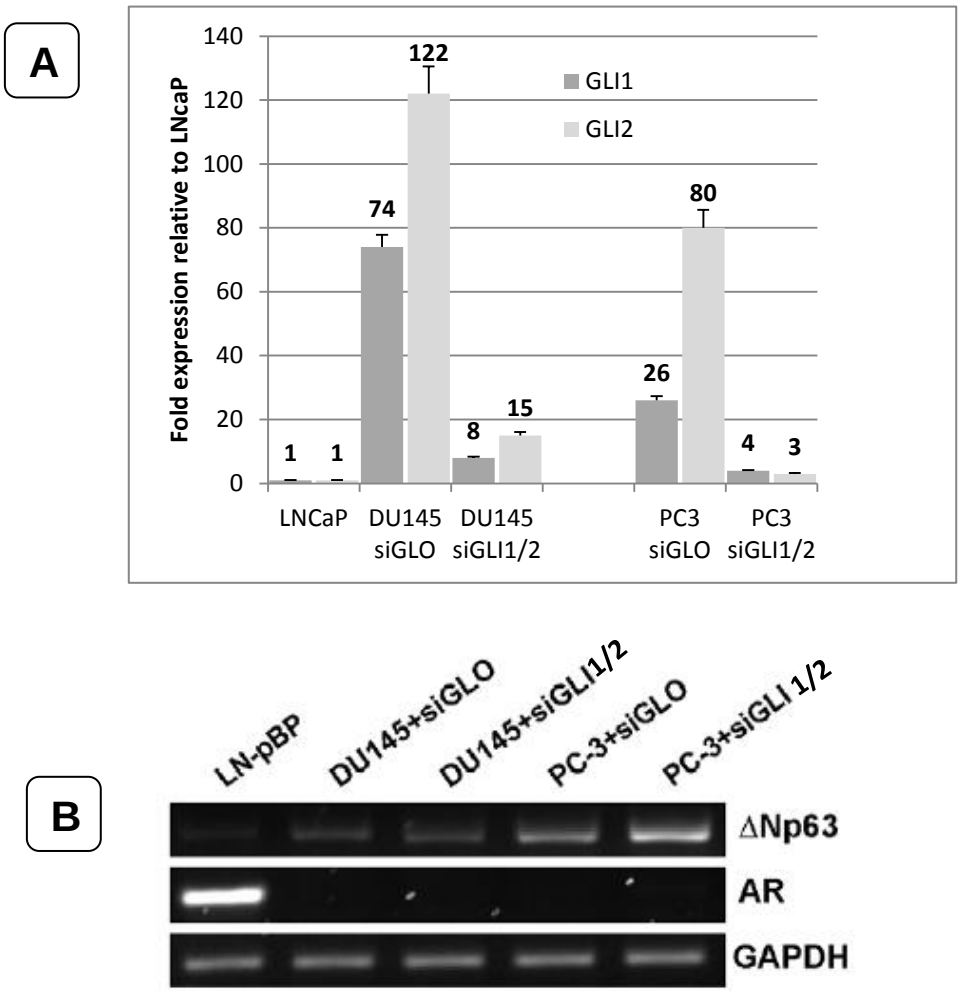

Figure 3.4 siRNA targeting of GLI1 and GLI2 in DU145 and PC3 cells. A-qPCR analysis of GLI1 and GLI2 in DU145 and PC3 cells following siRNA transfection of both siGLI1 and siGLI2, or by siGLO control for 96hrs in DU145 and PC3 cells. Values are fold change relative to LNCaP +/- SEM. **B**- RT-PCR analysis of ΔNP63 and AR following siRNA transfection of both siGLI1 and siGLI2, or by siGLO control for 96hrs

3.5 Pharmacological inhibition of Hedgehog pathway

In addition to siRNA based targeting of GLI1 expression. I also employed the Hedgehog pathway pharmacological inhibitors KAAD-Cyclopamine and SANT1. These drugs target SMO and lead to a loss of GLI1 and GLI2 expression (Rubin and de Sauvage, 2006). Both drugs were added to LNCaP-GLI1 cells to determine if they affected GLI expression and whether there was any effect on downstream targets. Drugs were added for 48hrs before harvesting, however neither KAAD-Cyclopamine or SANT1 was able to able to significantly reduce GLI1 or GLI2 expression. There was also no effect on downstream targets E-cadherin, AR and CD44 (Figure 3.5A). PC3 cells which also express high levels of GLI were used as a positive control for drug efficacy (Figure 3.5B)

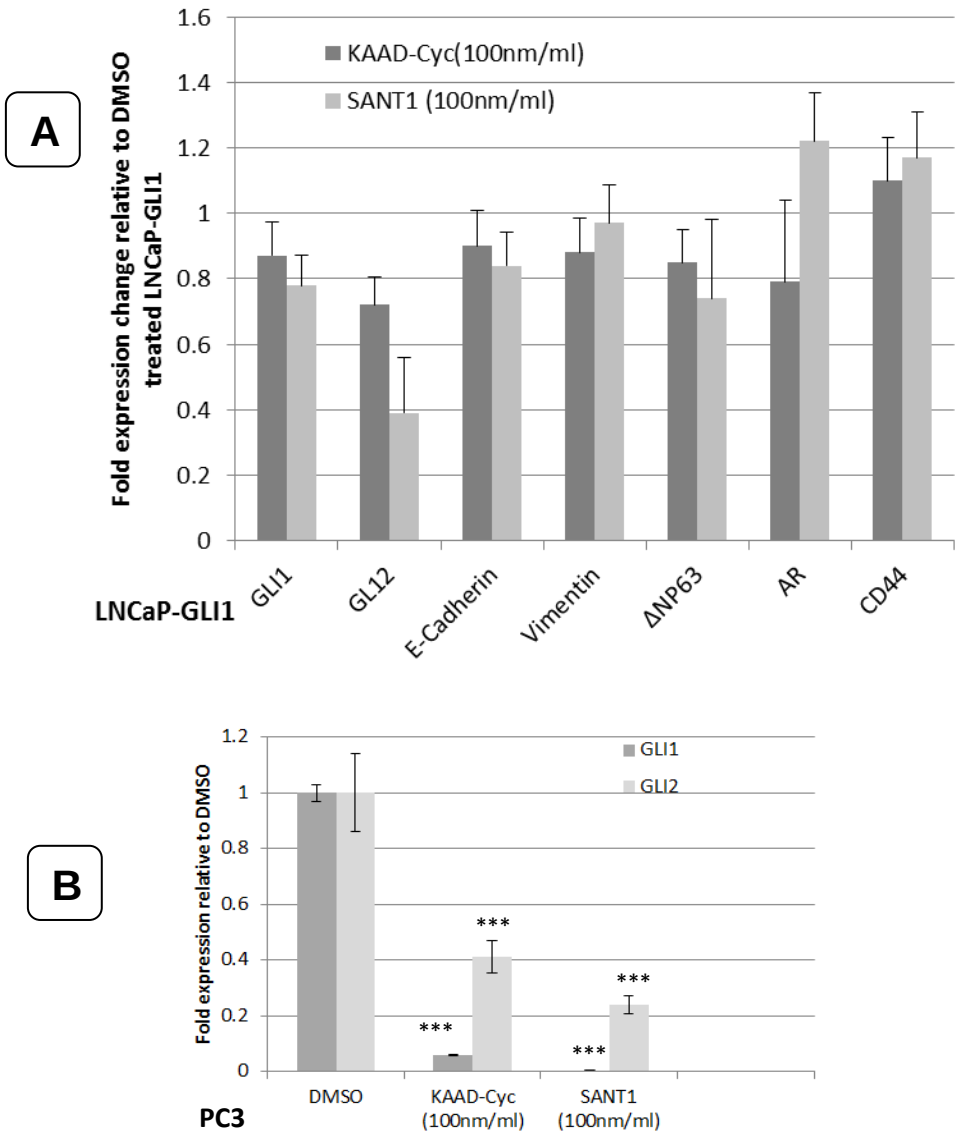

Figure 3.5 Treatment of LNCaP-GLI1 cells pharmacological hedgehog inhibitors A LNCaP-GLI1 cells were treated with KAAD-Cyclopamine or SANT1 for 48hrs. qPCR analysis of GLI1/2 and downstream GLI targets. **B** qPCR analysis of PC3 cells treated with KAAD-Cyclopamine or SANT1. Values are mean of n=3 experiments ± SEM. Statistical analysis performed using t-tests. ***P<0.001

3.6 Discussion and conclusions.

The change from an androgen-dependent to an androgen dependent phenotype is a critical transformation in the advancing of prostate cancer. As such it is necessary to determine the molecular mechanisms behind this shift. It was previously demonstrated by our lab that ectopic GLI1 expression led to an androgen independent phenotype, and this was associated with an EMT. In the data provided here, I have shown that the phenotypes shown were unaffected by subsequent suppression of GLI.

In this study, I employed siRNA to suppress GLI1 expression. While this was successful, I observed no subsequent changes to either morphology or gene expression, even after 14 days of suppression. It should be noted however that only a small range of genes were investigated for differential gene expression, and it is likely that suppression of GLI1 had effects other downstream targets which were not investigated. A method of GLI1 suppression is through pharmacological inhibitors, specifically the SMO inhibitors KAAD-Cyclopamine and SANT1. These drugs were added to LNCaP-GLI1 cells, however, no significant changes were observed to GLI1 levels. This was likely due to the naturally low levels of SMO in LNCaP cells, and ectopic expression of GLI1 may act independently of SMO altogether, or may be being produced at such a high level as to overwhelm the inhibitory effects of SMO. Cyclopamine, and to a lesser extent SANT1 are both used for the treatment of prostate cancer (Rubin and de Sauvage, 2006), and in particular other SMO antagonist drugs have been used to target cancer stem cell formation (Merchant and Matsui, 2010). However, in the results presented in this chapter, SMO inhibitors had little effect on downstream GLI expression in LNCaP-GLI1 cells and to GLI1 target

genes. This therefore suggests that these drugs may be less effective in patients where prostate cancer cells have already acquired a cancer stem cell phenotype, or to PCa cells with already active GLI expression but low SMO levels.

A further pharmacological inhibitor GANT61 has previously been shown to target both GLI1 and GLI2, however in our hands this drug had no effects on GLI expression on any cell lines tested, and at high concentrations was highly toxic, and as such was not investigated further.

The GLI1 gene is expressed at low levels in the normal prostate, but is higher in the basal layer relative to epithelial cells. However it is greatly increased in prostatic hypoplasia. The data generated from LNCaP-GLI1 cells provides an intriguing insight into how GLI1 is functioning and its downstream effects. As such, it was therefore important to fully investigate whether GLI1, a transcription factor was a critical mediator of the AI and EMT like phenotype. The data provided from temporary suppression of GLI1 however suggests that GLI1 is turning genes on and off, but that these changes are mono-directional, and once a gene is turned on, it cannot be turned off and vice versa. However, this hypothesis is somewhat unlikely given the data from 2 week suppression and the general characteristics of transcription factors. It is more likely that GLI1 activates a cascade of other genes or transcription factors which then in turn alter the expression of the downstream genes. While this is the more likely of the two hypotheses, exactly what mechanisms or pathways are being activated is not easily identifiable, as there are likely to be numerous interconnecting pathways. Some potential mechanisms which are activated by GLI1 are the Ras/MEK pathway which has been shown to interact with hedgehog signalling (Stecca et al., 2007). The TGF-β pathway has also been implicated in GLI1 signalling (Javelaud et al., 2012), as has the Wnt/β-Catenin

pathways (Yanai et al., 2008, Mullor et al., 2001). In a study by Nadiminty et al (2011) the group used microarray analysis to identify NF-κB regulated genes in the LNCaP cell line. A comparison of microarrays from our lab and the Nadiminty et al study revealed a degree of overlap. Out of 50 top up-regulated genes, 15 were also highly up-regulated in LNCaP-GLI1 cells including ANAX2, PLAU, TIMP1 and LCN2 It is likely GLI1 is activating more than one pathway, and indeed there may be significant degrees of interconnectivity and feedback. Nevertheless, the data generated by Sandeep Nadendla (Nadendla et al., 2011) and the data in this chapter does indicate that GLI1, or its downstream targets are in part responsible for a shift to an androgen independent and EMT like phenotype, and potentially to the advancement of aggressive PCa.

In conclusion, the data in this chapter suggests that GLI1 over-expression leads to an androgen independent and EMT phenotype which is non-reversible by siRNA based means.

While significant research has been done on the exact mechanisms of the hedgehog pathway, comparatively little has been shown regarding the actual effects of GLI1 activation on a global scale. However, the mechanism by which GLI1 was inducing androgen independence and EMT was still unknown. As such, I sought out genes which were up-regulated by GLI1 which might be driving the effects seen. Using the data already available from both LNCaP-GLI1 microarray data, as well as an extensive literature search, a number of potential candidates emerged as possible effectors of GLI1 and the cause of the phenotypic changes seen. Of these candidates, one gene in particular stood out as being worthwhile for further investigation. This gene was lipocalin 2.

Chapter 4
Ectopic Expression of LCN2 in the LNCaP cell line

As previously mentioned in section 1. Lipocalin 2 was identified from microarray data which showed this gene to be highly upregulated in LNCaP-GLI1 cells, and that LCN2 featured in ontological groupings for both hormone resistance and subsequently chosen for further investigation. However, to date there is no published data on any links between LCN2 and hormone resistance in prostate cancer. As such it was decided to observe the effects of ectopic expression of the LCN2 gene in a prostate cancer cell line. Therefore aims of the work carried out in this chapter were as follows:

Identify the expression levels of LCN2 in a range of prostate cancer cell lines and determine any links to GLI1 signalling

Ectopically express the LCN2 gene in a cell line where there is little native expression; then determine the effects of LCN2 on steroid receptor expression, EMT and proliferation

4.1 Characterisation of LCN2 in LNCaP-GLI1 cells

Lipocalin 2 was previously identified from microarray data in LNCaP-GLI1 cells, where ontological grouping of highly upregulated genes placed it in both EMT and hormone signalling ontology groups. As such, LCN2 was selected for further investigation to determine whether it was at least partially responsible for the phenotypic and signalling changes seen in LNCaP-GLI1 cells, particularly with regards to AR signalling and EMT. Microarray analysis showed a 55 fold increase of LCN2 mRNA between LNCaP-pBP and LNCaP-GLI1 cells. To validate this, more sensitive qPCR analysis was performed (Figure 4.1A) qPCR validation revealed that LCN2 showed a 3400 fold lower expression in LNCaP-pBP compared to LNCaP-GLi1 expression (Figure 4.1B).

A

Symbol	Accession No.	Fold change v LN-pBP	Fold change v DU145	Fold change v PC-3	Functional Group (Figure S2)
ABCC3	NM_003786.2	98.30	13.122	3.669	ATP and glucose metabolism
CLDN1	NM_021101.3	65.57	4.865	15.793	Cell-cell adhesion, EMT
LCN2	NM_005564.3	55.32	287.939	6.102	EMT, Hormone independence
SMOX-4	NM_175842.1	52.23	3.106	4.033	None
TAGLN	NM_003186.3	19.49	9.323	28.077	Cytoskeletal regulation
SMOX-2	NM_175840.1	19.30	3.047	3.529	None
SUSD2	NM_019601.3	15.83	19.827	10.819	None
TUBB2B	NM_178012.3	10.87	6.804	8.643	ATP and glucose metabolism, Rho GTPase signalling
NKD2	NM_033120.2	10.49	7.649	21.551	None
HCP5	NM_006674.2	10.33	3.221	5.446	None
APOE	NM_000041.2	10.04	8.952	4.633	Angiogenesis, Apoptosis regulation, Cytoskeletal regulation
ARMCX2	NM_177949.1	10.01	4.019	5.739	None

B

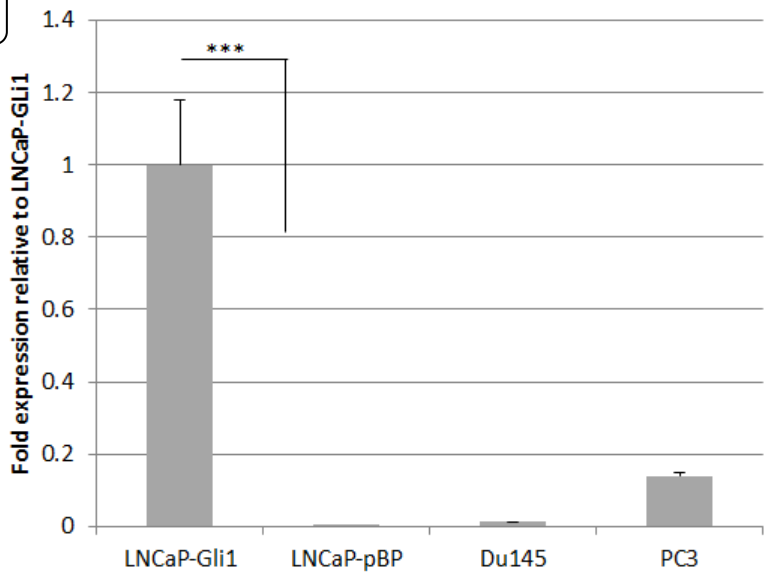

Figure 4.1: LCN2 in PCa cell lines A Table showing the 12 most up-regulated genes in LNCaP-GLI1 cells. Data shows comparison between LNCaP-PBP , DU145, and PC-3 PCa cell lines. **B** qPCR analysis of LCN2 expression in PCa cell lines. Data is presented as the mean +/- SEM for n=3 experiments. Statistical analysis was carried out using Student's t-test to compare changes in LCN2 expression in relation to LnCaP-GLI1 cells. Statistical analysis was carried out using Student's t-test *** P<0.001.

4.2 LCN2 as an intracellular homodimer.

Based on the data shown in section 4.1 which confirmed the up-regulation of LCN2 mRNA expression in LNCaP-GLI1 cells, levels of LCN2 protein were also assessed.

Western blot analysis was used to detect intracellular LCN2 protein expression in LNCaP-GLI1 cell lysates. For comparison, Western blot analysis was also carried out on lysates from DU145 and PC3 cell lines. Surprisingly, LCN2 protein expression was relatively low in some cell lines and did not appear to correlate with LCN2 mRNA. Indeed, as shown in Figure 4.1A LNCaP-GLI1 had the highest mRNA expression of all PCa cell lines; however, LCN2 protein expression was the lowest of all cell lines with the exception of LNCaP-pBP (Figure 4.2A). In contrast PC3 cells, which did have relatively high levels of LCN2 mRNA (over 500 fold compared to LNCaP cells) also showed relatively high levels of LCN2 protein expression. However, it was also observed that the molecular weight of the LCN2 band detected was 45-48 kDa compared to the published molecular weight of 23-25 kDa. The antibody used in these Western blots was the one most commonly cited in the literature, LCN2 antibody MAB1757 (R&D) (Yang et al., 2009, Aberle et al., 1997, Flo et al., 2004, Tong et al., 2005). In all experiments carried out using this antibody rather than the traditionally described molecular weight of 23-25kDA, bands obtained via Western blot were consistently found at 45-48 kDa. This band was observed in every cell line tested including the MCF-7 Breast Cancer (BCa) cell line. Moreover, this band was reduced very significantly when LCN2 was silenced (See Chapter 5 and Chapter 8)

Since the 46 kDa band was approximately double the predicted molecular weight, I hypothesised that the band detected may be an LCN2 homodimer. A literature search revealed that LCN2 had indeed been previously described as a sulphur

linked 46 kDa homodimer by Kdjelsen et. al., (1993) in one of the first ever descriptions of the LCN2 protein. However, this homodimer has not been characterised and in all subsequent publications it is only mentioned in text. It was also noted from the literature search that the vast majority of previous publications measured only secreted LCN2 either by ELISA or Western blot, and not intracellular levels (Yang et al,. 2009).

To further address this issue, alternative antibodies were tested targeting LCN2. The monoclonal NGAL-5G5 antibody (purchased from Santa Cruz) was used to probe whole cell lysates (Figure 4.2B). This antibody did produce bands at 24 kDa. However, expression was relatively weak, and was completely absent in LNCaP-GLI1 cells. Tantalisingly, this antibody also appeared to show a doublet band for PC3 cells (possibly due to glycosylation) (Miyamoto et al., 2011). Unfortunately, the antibody worked only once and in subsequent experiments did not detect any LCN2 bands. A replacement antibody also showed no LCN2 expression under any conditions tested and thus was not used for further research in this thesis.

Over the course of this project, a number of other LCN2 antibodies became available for purchase. A further antibody R&D AF1757 was purchased in 2013. This antibody also detected a band at 23Kda, albeit weakly (Figure 4.2C). Notably however there were also faint bands present at ~45kDA. Again, this antibody appeared to be unstable, and produced only very dirty blots after a couple of uses. Unfortunately this antibody ceased to work before it was possible to test for LCN2 expression in LNCaP-GLI1 cells. Despite the presence of dimers, as it provided the clearest and most stable results, and as it was the most cited, it was decided that all future work would be used using primarily the MAB1757 antibody.

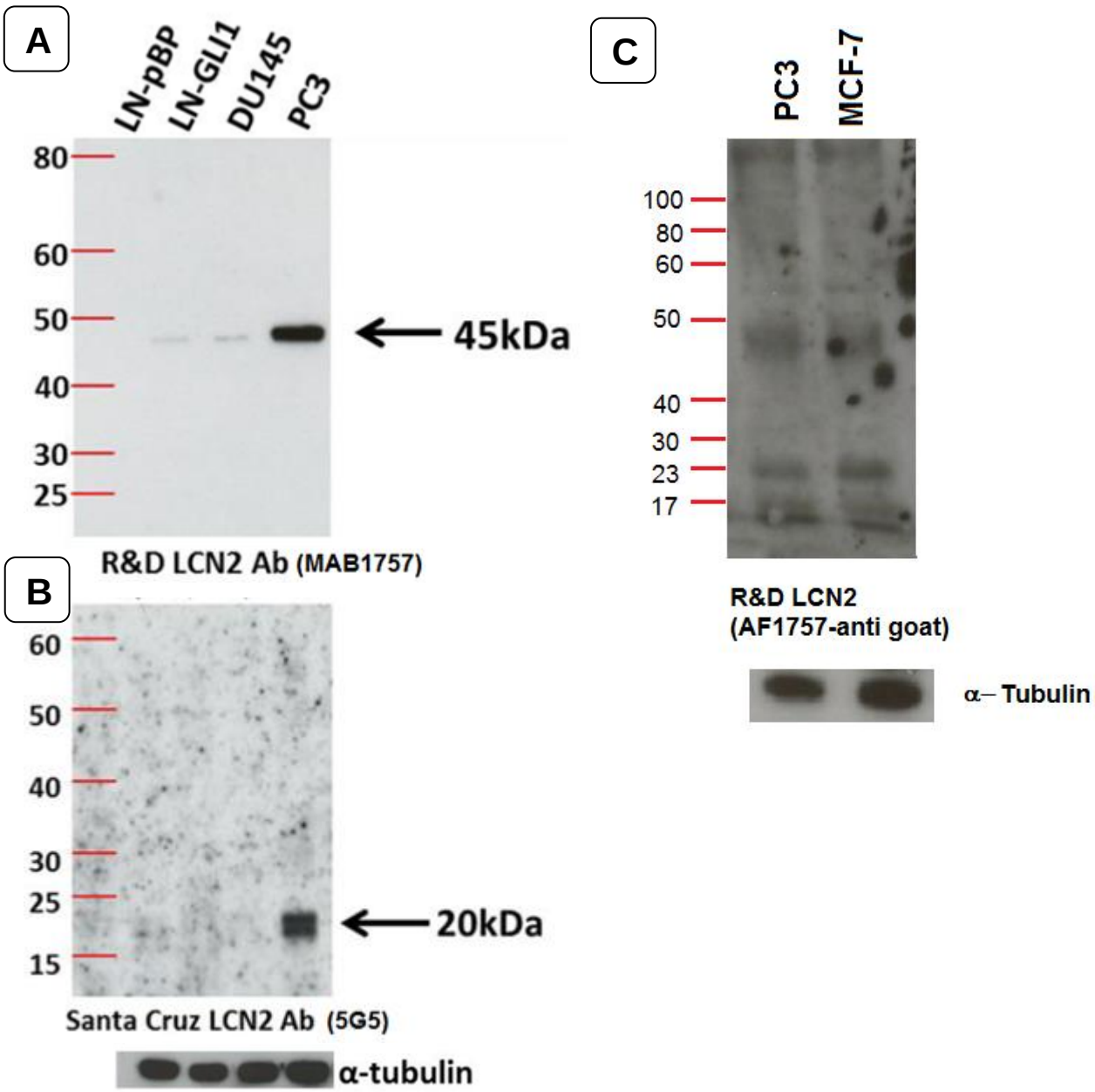

4.2- Western blot analysis of cell lysates for LCN2. Western blot analysis of various antibodies targeting LCN2 showing presence of a 45 kDa band. **A** R&D MAB1757 rat monoclonal, 3 minute exposure. **B** Santa Cruz 5G5, mouse monoclonal 10 minute exposure. **C**- R&D AF1757 goat polyclonal, 10 minute exposure, PC3 and MCF-7 positive controls only. Western blots are representative of n=3 experiments for A, n=1 for B and C as antibodies ceased to work.

As can be seen in figure 4.2A, not only was LCN2 protein being detected at a high molecular weight, but also evident was that LNCaP-GLI1 cells produced relatively little intracellular protein than was expected given that these cells produce much higher levels of LCN2 mRNA than PC3 cells (see Figure 4.6B). One possible reason for this discrepancy could be that LCN2 is more rapidly secreted from LNCaP-GLI1 cells, and is thus not detected. To resolve these issues, cells were cultured for 48 hours, and supernatants harvested under reducing and non-reducing conditions to investigate any sulphide-linked protein (Figure 4.3). PC3 cell lysates were also analysed to provide a positive control for the high molecular weight band.

Also, it was previously found that expression of LCN2 in LNCaP-Gli1 cell lysates was lower than expected based on mRNA expression. However in cell supernatants expression of LCN2 in LNCaP-GLI1 cells was comparable to those found in PC3 cells. Hence it may be seen that the discrepancy between mRNA expression and cell lysate protein expression is likely due to rapid secretion of monomeric protein.

Additionally, it was found that the 20-25 kDa band only was found under both reducing and non-reducing conditions in LNCaP-GLI1 c and DU145 cell supernatants. There was however a faint band at 45 kDa in reduced PC3 cells, this therefore demonstrates that the 45 kDa band is not due to protein extraction methods, but rather that intracellular LCN2 being detected by the MAB1757 antibody is in a homodimeric state, whereas secreted LCN2 is largely monomeric.

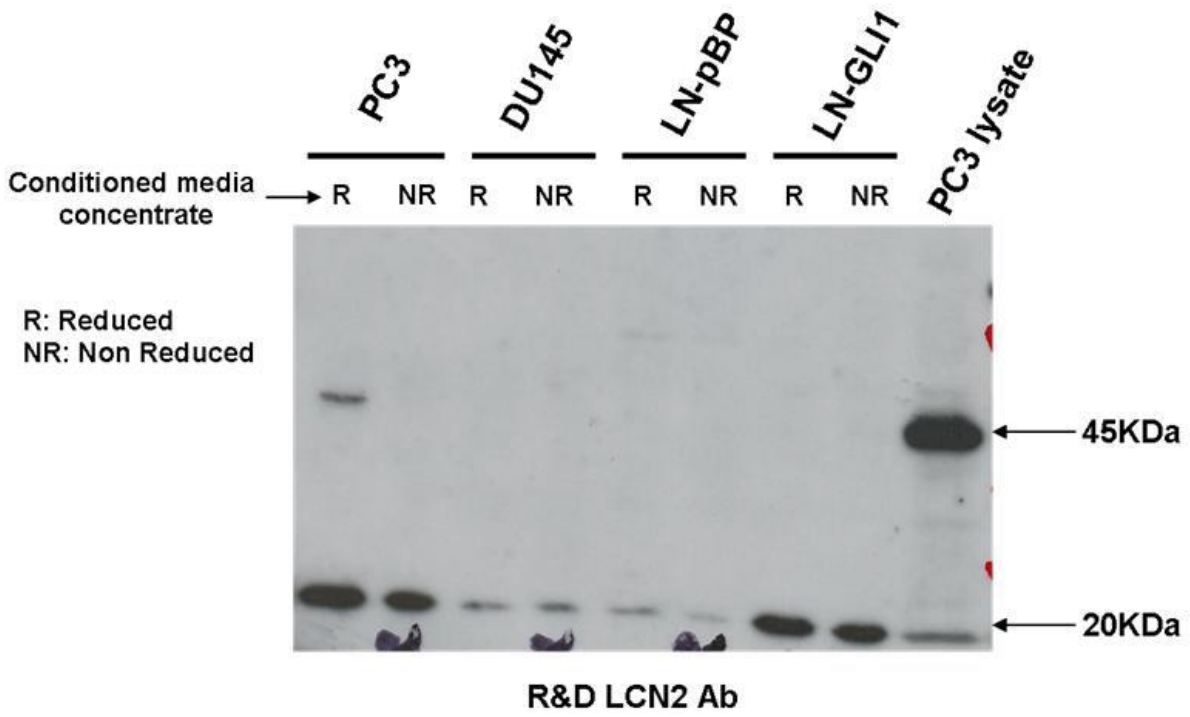

4.3 Western Blot analysis of LCN2 in culture supernatants. Cells were cultured for 48hrs and analysed using reducing and non-reducing conditions. Lysates were analysed using the R&D MAB1757 rat monoclonal antibody. Data shows that LCN2 detected in cell culture supernatants displayed a band at ~20 kDa, whereas cell lysates displayed a band at ~45 kDa. Data is representative of n=3 experiments.

To further investigate the levels of secreted LCN2 protein by PCa cells, a LCN2 specific ELISA was carried out (Figure 4.4A). The ELISA kit purchased from R&D systems contains the same MAB1757 antibody as used previously in Western blots shown above. Results showed high levels of secreted LCN2 protein in LNCaP-GLI1 cells (3.5ng/ml). By comparison, PC3 cells showed the highest secreted LCN2 levels amongst other PCa cell lines (1.75ng/ml).

Combining ELISA and Western blot data, there appears to be wide variability between cells as to whether LCN2 is secreted immediately (as in LNCaP-GLI1 cells) or retained intracellular. I therefore hypothesised that rapid secretion may be due differential levels of lipocalin 2 Receptor (LCN2-R, also known as BOCT). While LCN2-R is very poorly characterised, Devireddy et al., (2005) did show it to be a capable of both secreting and internalising LCN2 protein. qPCR analysis was carried out on LNCaP-pBP, LNCaP-GLI1 and PC3 cells. It was found that LCN2-R expression was 4.4 and 5.2 fold higher respectively relative to LCN2-R expression in PC3 cells (Figure 4.4B). While protein expression analysis was not performed, this result may help explain why secreted and intracellular levels vary between cell lines.

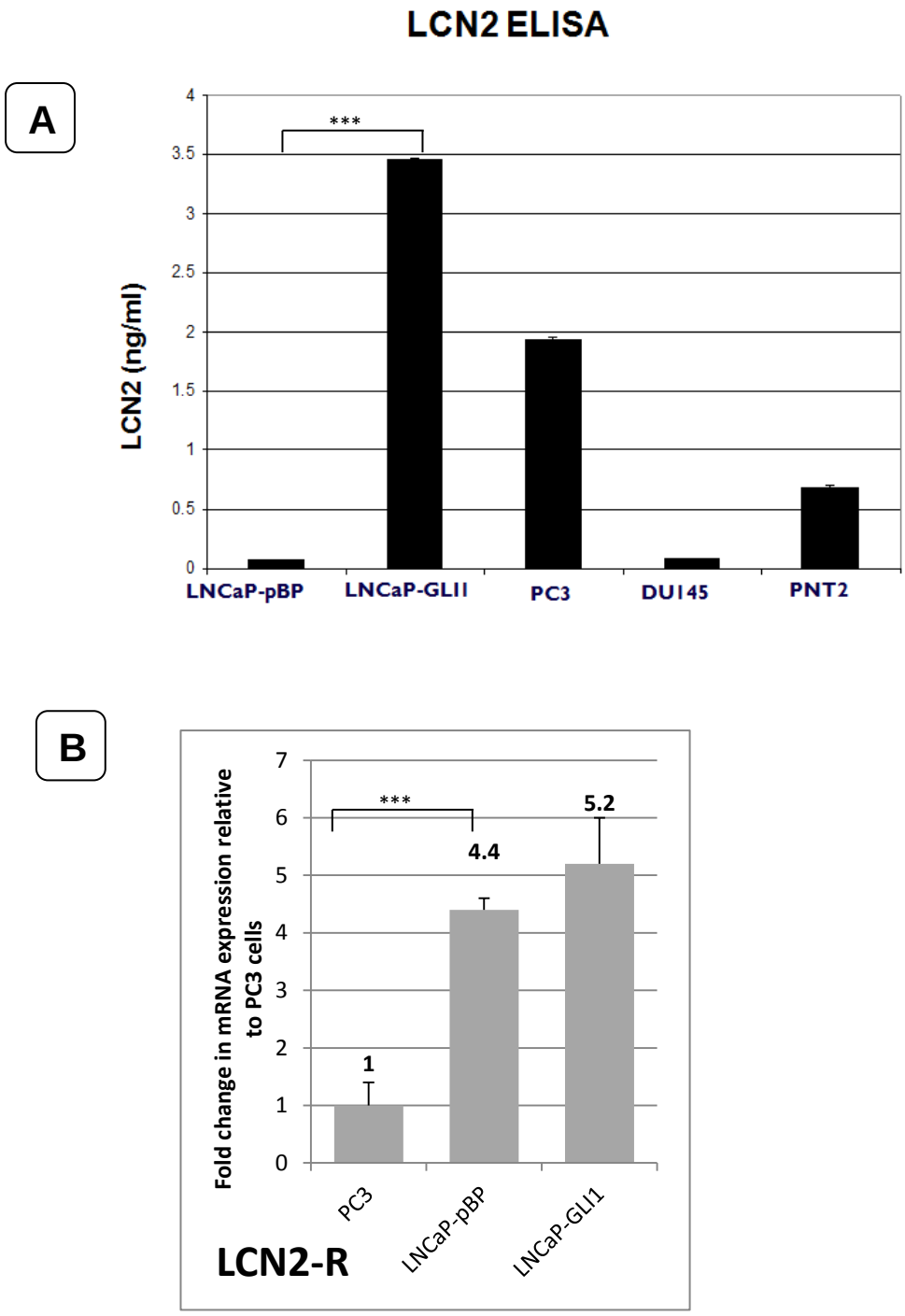

Figure 4.4 Analysis of LCN2 secretion by PCa Cell lines. **A** Cells were cultured for 48hrs prior to harvesting of supernatants. ELISA was carried out on supernatants as described in Chapter 2: Materials and Methods. Results show the mean secreted LCN2 +/- SEM for n=3 experiments. Student's t-test to compare LCN2 secretion against LNCaP-pBP cells. *** P<0.001. **B** qPCR analysis of LNC2-R in prostate cancer cell lines. Values are relative to PC3 +/- SEM, n=3 .Statistical analysis was carried out using Student's t-test.

Overall, results indicated that high a level of LCN2 mRNA does result in increased LCN2 protein levels. However there is a wide difference in the localisation of the protein between cell lines. In LN-CaP-GLI1 cells, it appears that the majority of the protein is secreted rapidly by the cells. Conversely, in PC3 cells, LCN2 protein is retained inside the cell, as well as being secreted. When combined, the data indicates that LCN2 does appear to exist as a homodimer within the cell, but that only the monomer is secreted. Exactly how the LCN2 homodimer is cleaved however is unknown, but is likely to have significant effects on its function within the cell.

4.3 Effects of GLI1 on LCN2 expression in PCa cell lines and NEB=1 keratinocytes

Since GLI1 was seen to lead to elevated levels of LCN2 in LNCaP cells, this was also investigated in a range of other PCa cell lines. Therefore, in parallel to ectopic expression of GLI1 in LNCaP cells, Sandeep Nadendla and other members of the Neill lab ectopically expressed GLI1 the in cell lines DU145, PNT2 and in the immortalised keratinocyte cell line NEB1 to generate DU145-GLI1, PNT2-GLI1 and NEB1-GLI1 stable cell lines respectively which were used for other projects. Subsequently, I probed protein lysates from these cells lines for LCN2 by Western blot. Results showed that ectopic GLI1 expression led to increased LCN2 expression in PNT2 cells. NEB1 cells also showed an elevated level of LCN2 expression relative to controls. However, no change was evident in DU145-GLI1 cells. Additionally, the MCF-7 cell line was utilised as a positive control (Yang et al,. 2009) (Fig 4.5).

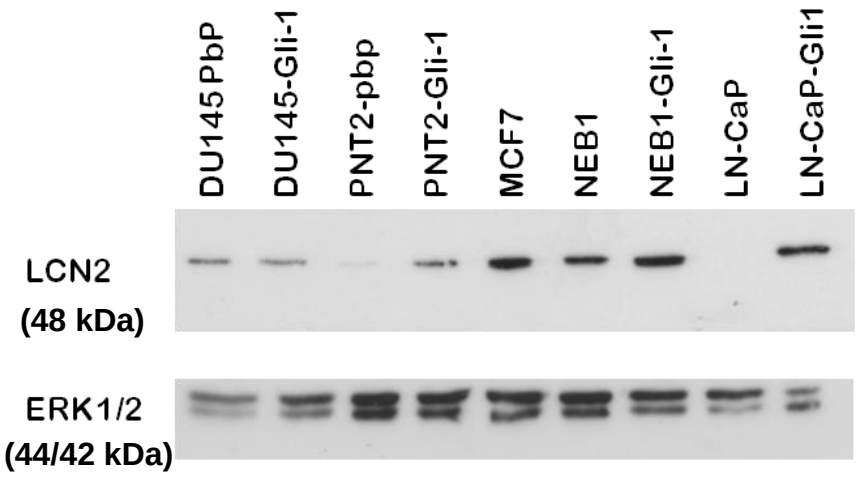

Figure 4.5 Ectopic expression of Gli-1 in a range PCa cell types and in the immortalised keratinocyte cell line NEB-1. Gli-1 was ectopically expressed in DU-145 and PNT-2 PCa cell lines, as well as in the NEB-1 keratinocyte cell line (See Section 2.6).Western blot analysis of LCN2 in cell lysates using the MAB1757 antibody showed up regulation of LCN2 in PNT-Gli-1, NEB1-Gli1 and LNCaP-Gli1 (Representative of n=3 experiments).

4.4 Effects of GLI silencing on LCN2 expression.

Using the same conditions as in section 3.2, targeted siRNA silencing of both GLI1 and GLI2 was carried out using gene specific siRNA's #5816 and #5817 respectively. Silencing was carried out on both LNCaP-GLI1 cells and PC3 cells. PC3 cells were used as they have a high endogenous level of LCN2 and also high levels of GLI1 (Nadendla et al 2011). As previously mentioned, (See section 3.2), a double siRNA silencing (both GLI1 and GLI2) was also carried out to eliminate any redundancy effects. Results showed that despite strong silencing of both GLI1 and GLI2 expression, there was no significant change in LCN2 mRNA expression in either LNCaP-GLI1 or PC3 cells (Fig 4.6A). Also, no change was observed in LCN2 intracellular protein expression by Western blotting in either LNCaP-GLI1 or PC3 cells (Fig 4.11B). Additionally, no change was observed in secreted LCN2, as analysed by ELISA (Figure 4.6C).

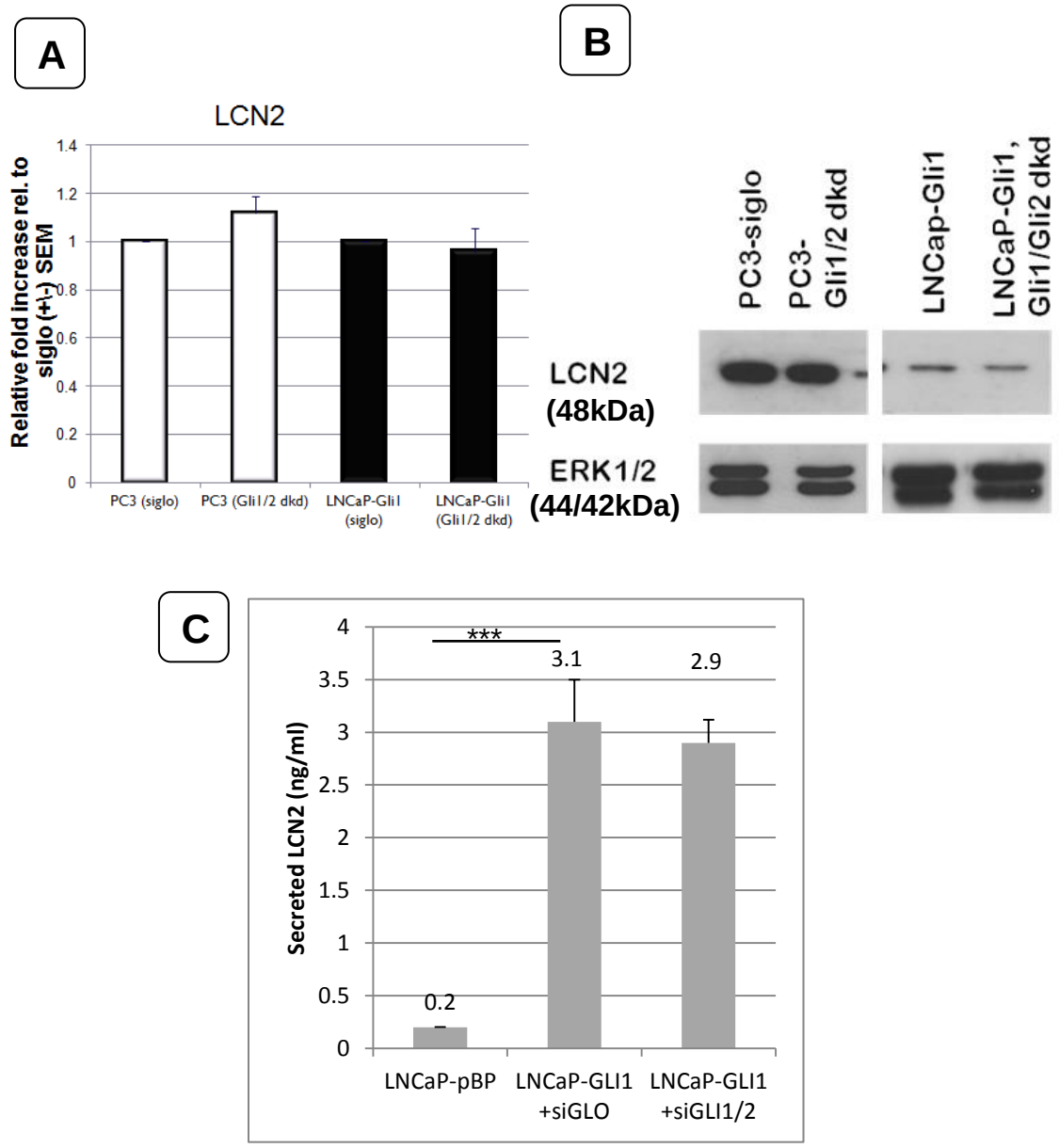

Figure 4.6 Effects of siRNA knockdown of GLI on LCN2 expression: A qPCR analysis of LCN2 expression in PC3 and LNCaP-GLI1 following simultaneous double knockdown (dkd) of GLI1 and GLI2. GLI suppression is identical to Figure 3.4. Data in shows mean +/- SEM for n= 3 experiments. **B** Western blot analysis of PC3 and LNCaP-GLI1 following knockdown. mRNA and protein extraction were carried out at the same time. Data is representative of n=3 experiments. **C** ELISA analysis of secreted LCN2 protein in LNCaP cells 96hrs post transfection +/-SEM.***p<0.001 Statistical analysis was carried out using Student's t-test.

4.5 Generation of an LNCaP-LCN2 cell line: Cloning the LCN2 gene

To further investigate the role of LCN2 in PCa cell lines, it was decided to analyse the effects of ectopically expressing LCN2 in LNCaP cells independently of GLI1 overexpression. Since LNCaP-GLI1 cells showed such a marked change in LCN2 expression and because these cells show marked changes in both AI and EMT, it was decided to address whether LCN2 played an important role in the phenotypic changes (e.g. AI and EMT). Because LNCaP cells have the lowest level of LCN2 mRNA expression of all commonly used PCa cell lines, indeed, LCN2 expression is essentially undetectable via qPCR. Ectopic expression of LCN2 would not interfere with any endogenous protein.

Previously published pLenti-L6H-LCN2 vectors containing the LCN2 gene were obtained from Dr. Zhimin Tong (MD Anderson, Texas), which had previously been used for ectopic expression in pancreatic cells (Tong et al, 2008). However, DNA extraction from the samples sent to us from his laboratory was very low (15ng/ µl). Multiple attempts to increase DNA yield through miniprep and maxiprep cloning techniques were also unsuccessful in obtaining a high enough yield suitable for transfection in part due to a very low uptake of plasmids by TOP10 competent *E.Coli*, with few colonies forming on agar plates (See materials and methods section 2.5).

To combat this issue, it was decided to sub-clone the LCN2 coding fragment from the pLenti-L6H-LCN2 plasmid. The entire fragment (724bp) was amplified by RT-PCR, purified, and sub-cloned into the pBABE-puro vector under the control of the constitutively-on cyclomegalovirus promoter (see materials and methods section 2.5) This new plasmid pBabe-PURO-LCN2 was successfully transfected into LNCaP

cells. As a control, empty pBabe-PURO plasmid was also transfected into LNCaP cells to generate an LNCaP-pBP cell line. (To differentiate between the LNCaP-pBP cell line generated as a control for LNCaP-GLI1, this cell line was also labeled LNCaP-pBP(2)).

4.6 Characterization of the LNCaP-LCN2 cell line.

Following 2 weeks of selection by puromycin, cells were harvested and analyzed for LCN2 expression via qPCR, which confirmed a very large (>250 fold) induction of the LCN2 gene relative to LNCaP-pBP. No change to LCN2 expression was observed in LNCaP-pBP relative to parental LNCaP cells. When LNCaP-LCN2 cells were compared to other cell lines for LCN2 expression, mRNA levels were approximately similar to those found in PC3 and MCF-7 cells (additional positive control shown by Yang et al., 2009 to have high LCN2 levels) (Figure 4.7A)

While mRNA expression was found to be very high in the LNCaP-LCN2 cells; when LCN2 intracellular protein expression via Western blot was examined, it was found to be relatively low in comparison (Figure 4.7B). In this regard, LNCaP-LCN2 cells displayed a similar characteristic to that found in LNCaP-GLI1 cells which also showed low expression of LCN2 intracellular protein. As such, it was theorized that LCN2 was being rapidly secreted from the LNCaP-LCN2 cells. To confirm this, ELISA analysis was performed on secreted LCN2 derived from cell supernatants. Results revealed a strong increase in secretion of LCN2 protein in LNCaP-LCN2 cells (1.8ng/ml) relative to, PC3 cells (2.3ng/ml) (Figure 4.7C) and comparable to levels of LCN2 secreted by LNCaP-GLI1 cells (See Fig 4.4A).

As with LNCaP-GLI1 cells, I hypothesized that rapid secretion may be due to higher LCN2-R expression. qPCR analysis of LCN2-R revealed that LNC2-R expression was 4.6 fold higher than in PC3 cells, although there was no significant difference between LNCaP-pBP and LNCaP-LCN2 cell lines (Figure 4.7D).

Overall, the data indicates that ectopic expression of LCN2 in LNCaP cells was successful, and that in a similar manner to that seen in LNCaP-GLI1 cells the LCN2 protein is rapidly secreted by the cells

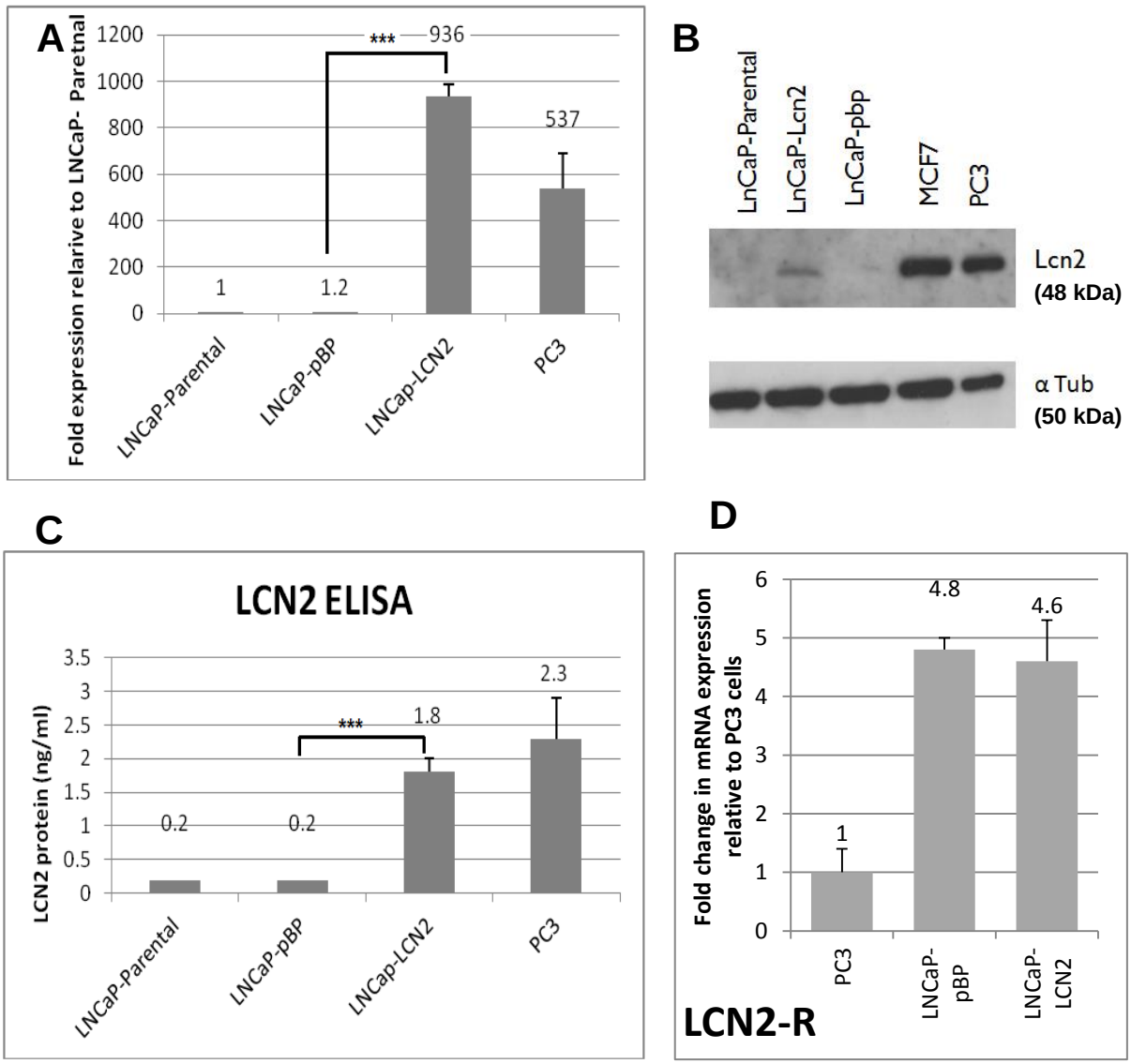

Figure 4.7 Ectopic expression of LCN2 in LNCaP cells. **A** qPCR analysis of LCN2 expression relative to LNCaP-parental cells showing a significant increase in LCN2 mRNA in LNCaP-LCN2 cells with comparison to PC3 cells (mean values +/- SEM for n=3 experiments.) **B** Western blot analysis of LCN2 protein in LNCaP-LCN2 shows only weak bands relative to PC3 and MCF-7 BCa cell lines (representative of n≥3 experiments.) **C** ELISA showing secreted LCN2 in supernatant from LNCaP-LCN2 and PC3 cells. **D-** qPCR analysis of LCN2-R expression in PC3, LNCaP-pBP and LNCaP-LCN2 cells +/- SEM. Statistical analysis was carried out using Student's t-test.

4.7 Effects of LCN2 on morphology of LNCaP cells: Morphology and proliferation

(Note: Both LNCaP-pBP and parental LNCaP cells were used for all experiments unless otherwise stated) LNCaP-LCN2 cells were found to be stable over multiple passages. However, no obvious morphological changes were observed. No changes were observed to colony shape or formation, and cells also retained their spindle-like shape (Figure 4.8A)

LNCaP-pBP and LNCaP-LCN2 cells were analysed for changes to cell proliferation by Propidium Iodide (PI) FACS cell cycle analysis. However, no significant changes in cell cycle were observed in LNCaP cells expressing LCN2 (Figure 4.8B-E). This analysis was carried out n=3 times using cells at different passages, but no significant differences were observed in any instance.

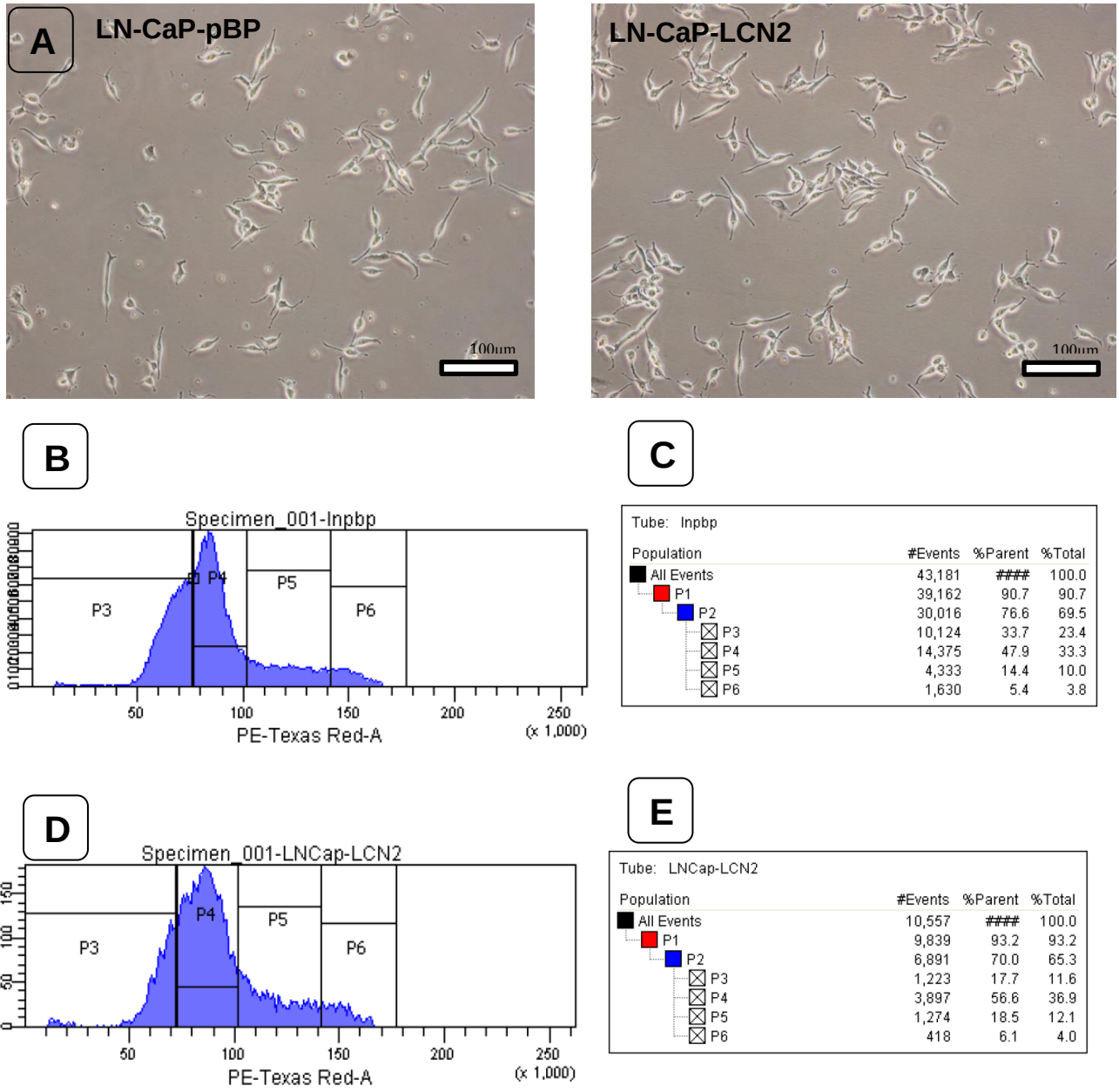

Figure 4.8 Effects of LCN2 expression on cell morphology and cell cycle in LNCaP cells. A- Brightfield image analysis of LNCaP-pBP and LNCaP-LCN2 cells (x20 magnification). **B, D-** FACS cell cycle analysis of LNCaP-pBP and LNCaP-LCN2 respectively using propidium iodide.**C, E**- Breakdown of cell cycle populations: P3- G0 phase, P4- G1 phase P5-S Phase, P6-G2/M phase. Figures are representative of n=3, all experiments performed in triplicate.

4.8 Effect of ectopic expression of LCN2 on hormone receptor protein expression in LNCaP cells.

4.8.1 Androgen Receptor

Because LNCaP-GLI1 cells were androgen independent and expressed high levels of LCN2, it was decided to investigate whether the high levels of LCN2 may be contributing to a loss of AR expression and may be involved in the AI state of these cells. AR expression in LNCaP-LCN2 cells was analysed by qPCR but no significant difference was observed in the levels of mRNA expression (1.11 fold increase relative to LNCaP-pBP) (Figure 4.9A).

When AR protein expression was analysed by Western blot however, contrary to the expected decrease in AR I observed an increase in AR expression in LNCaP-LCN2 cells relative to both LNCaP-pBP and LNCaP(Parental) cells (Figure 4.9B).

To confirm the activity of increased AR expression, qPCR analysis of the AR target gene KLK3 (encoding for PSA) was performed. LNCaP-LCN2 cells showed a 5.4 fold increase in KLK3 expression relative to LNCaP-pBP cells, hence indicating that AR is indeed active and is able to elicit downstream effects (Figure 4.9A).

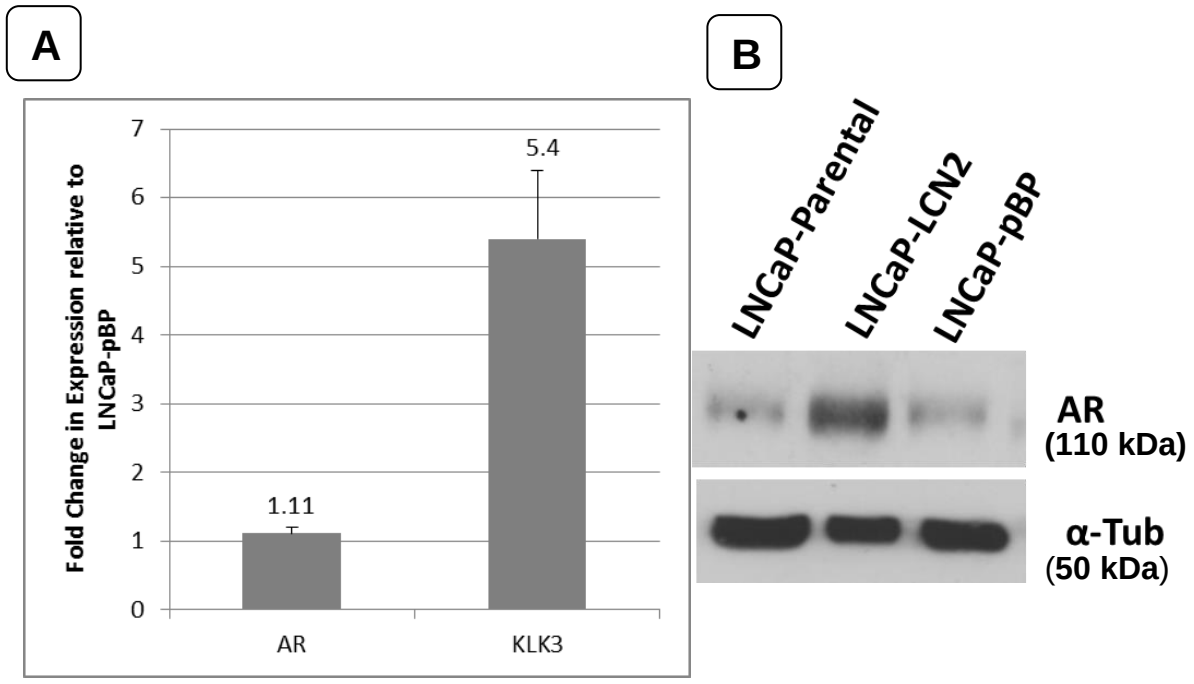

Figure 4.9 Effects of LCN2 on AR and KLK3 (PSA) expression. A- qPCR of AR and KLK3 (PSA) expression in LNCaP-LCN2 cells relative to expression in LNCaP-pBP cells **B**- Western blot of AR expression in LNCaP derived cell lines. Data in panel A represent mean +/- SEM for n=5 experiments. Statistical analysis was carried out using Student's t-test *p<0.05 **p<0.01 ***p<0.001 Western blot analysis is representative of n=4 experiments.

KLK3 expression is known to be affected by cell density and cell confluence (Lilja, 2003). The previous results were obtained from samples at 80% confluence. To eliminate any effects that changes to confluence may be having on AR and PSA expression, both LNCaP-pBP and LNCaP-LCN2 cells were harvested at 50%, 80% and 100% confluence. Cells were also seeded at high density but harvested after 24 hours before they could divide and form colonies and were mostly single cells at 80% confluence. qPCR analysis results showed that, as expected, AR mRNA levels remained constant. There were no significant changes in levels of expression of AR mRNA expression between LNCaP-LCN2 and LNCaP-pBP, and neither were there any significant differences between confluence levels (Figure 4.10A). In contrast, KLK3 levels showed moderate but significant increases to expression based on confluence. In LNCaP-pBP there was a 1.8 fold increase in KLK3 expression in 100% confluent cells relative to 50% confluence. In single cell colonies however KLK3 expression was half that of 50% confluent cells, thus confirming that increased confluence does lead to elevated KLK3 (Figure 4.10B).

At 50% confluence, KLK3 expression was 5.1 fold higher in LNCaP-LCN2 cells relative to LNCaP-pBP (Figure 4.10B). This ~1:5 expression ratio of KLK3 expression (LNCaP-pBP vs LNCaP-LCN2) was also maintained at 80% and 100% confluence. However, in single cells, this ratio was reduced to 1:2 (0.49:1.2 fold relative to 50% confluent LNCaP-pBP cells).

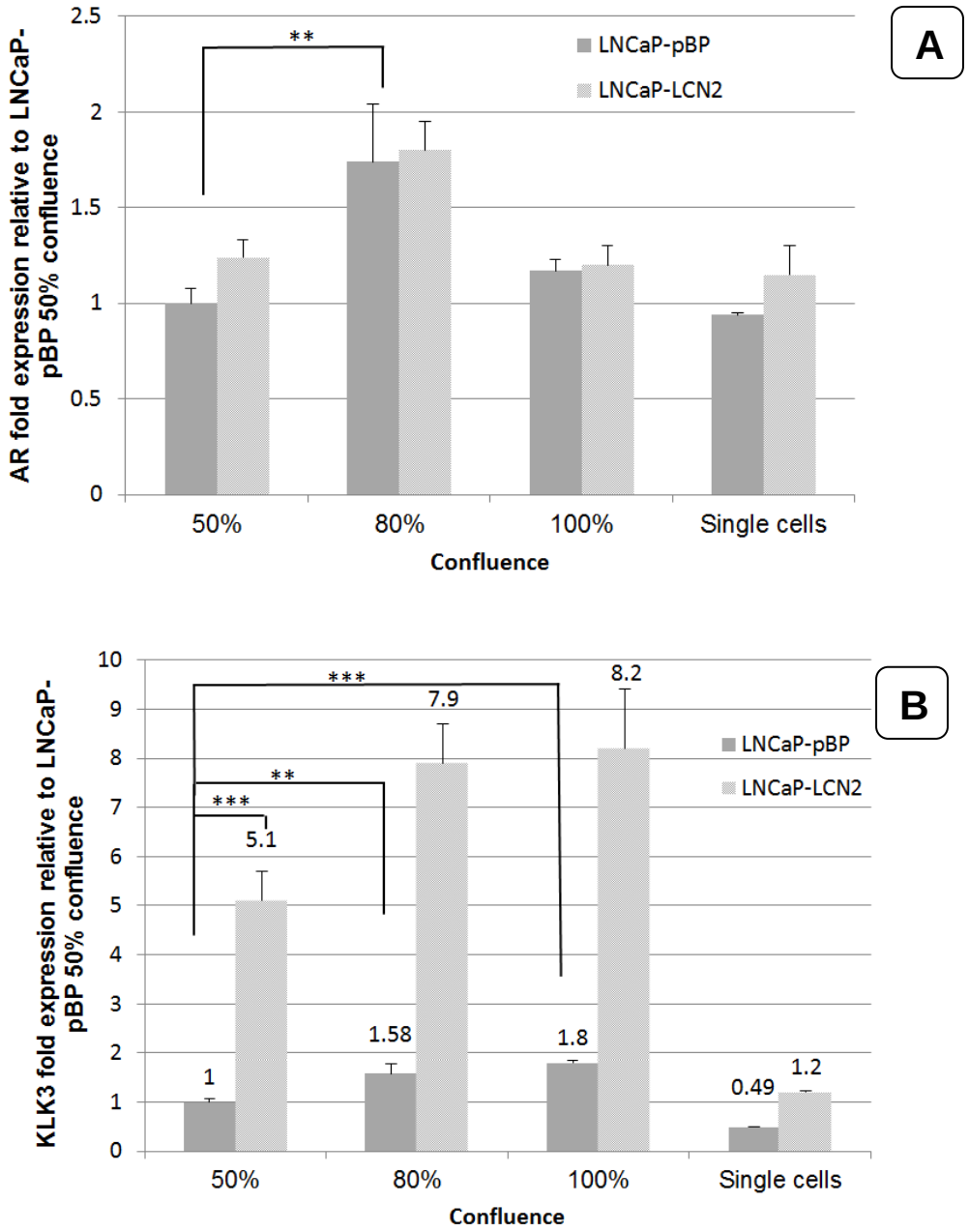

Figure 4.10 Effects of cell confluence on KLK3 and AR expression in LNCaP-LCN2. qPCR analysis. Cells were harvested at a range of confluence levels. **A** shows androgen Receptor mRNA and **B** shows KLK3 mRNA expression in LNCaP-pBP and LNCaP-LCN2 cells at 50, 80 and 100% density as well as cells in single cell colonies at 80% confluence. Values are relative to LNCaP-pBP at 50% confluence. Data represents mean +/- SEM, n=3. *P<0.05, **P<0.01, ***P<0.001. Statistical analysis carried out using Student's t-test .

4.8.2 Estrogen Receptor

Estrogen receptor (ER) is the primary receptor for the steroid estrogen. ER has two commonly expressed isoforms, namely ERα and ERβ. The two proteins share a 90% sequence homology, but are two separate genes on different chromosomes (6 and 14 respectively) and are able to form both homodimers and heterodimers with each other (Reviewed by (Zhao et al., 2008a)). Both proteins are able to activate similar, but non-identical signalling pathways (Zhao et al 2008.). While not true in some cases, increased ERα has been shown to lead to a reduction of ERβ and vice versa. LNCaP cells express both ERα and ERβ protein, with the ratio favouring ERα (King et al., 2006).

LCN2 has previously been shown to regulate ER levels in breast cancer (BCa) by Yang et al (2009). In their study, a negative correlation was found between LCN2 and ERα (ERβ was not mentioned). Because LCN2 expression has been associated with ER levels in BCa I decide to investigate whether a similar correlation occurred in LNCaP cells.

qPCR analysis of LNCaP-LCN2 cells showed no changes in the expression of either ESR1 or ESR2 mRNA (ERα and ERβ respectively) (Figure 4.11A). However, when protein lysates were analysed via Western blot, distinct changes in expression were observed were observed although these did not correlate with mRNA expression, suggesting a post-transcriptional mechanism of regulation. ERα protein was markedly down-regulated in LNCaP-LCN2 whereas protein expression for ERβ was up-regulated, although the level of expression was still relatively much weaker than ERα (Figure 4.11B)

From these data it was apparent that in LNCaP-LCN2 cells there was marked down-regulation of ERα and an increase in expression of ERβ. However, despite the changes in ER ratios, no significant changes were observed to the classical ER target gene ERBB2 (encoding for HER2 protein). However, a further ERβ target- EGFR (Egloff et al., 2009, Zhao et al., 2008a)- did show a 4-fold increase to mRNA expression (Figure 4.11A).

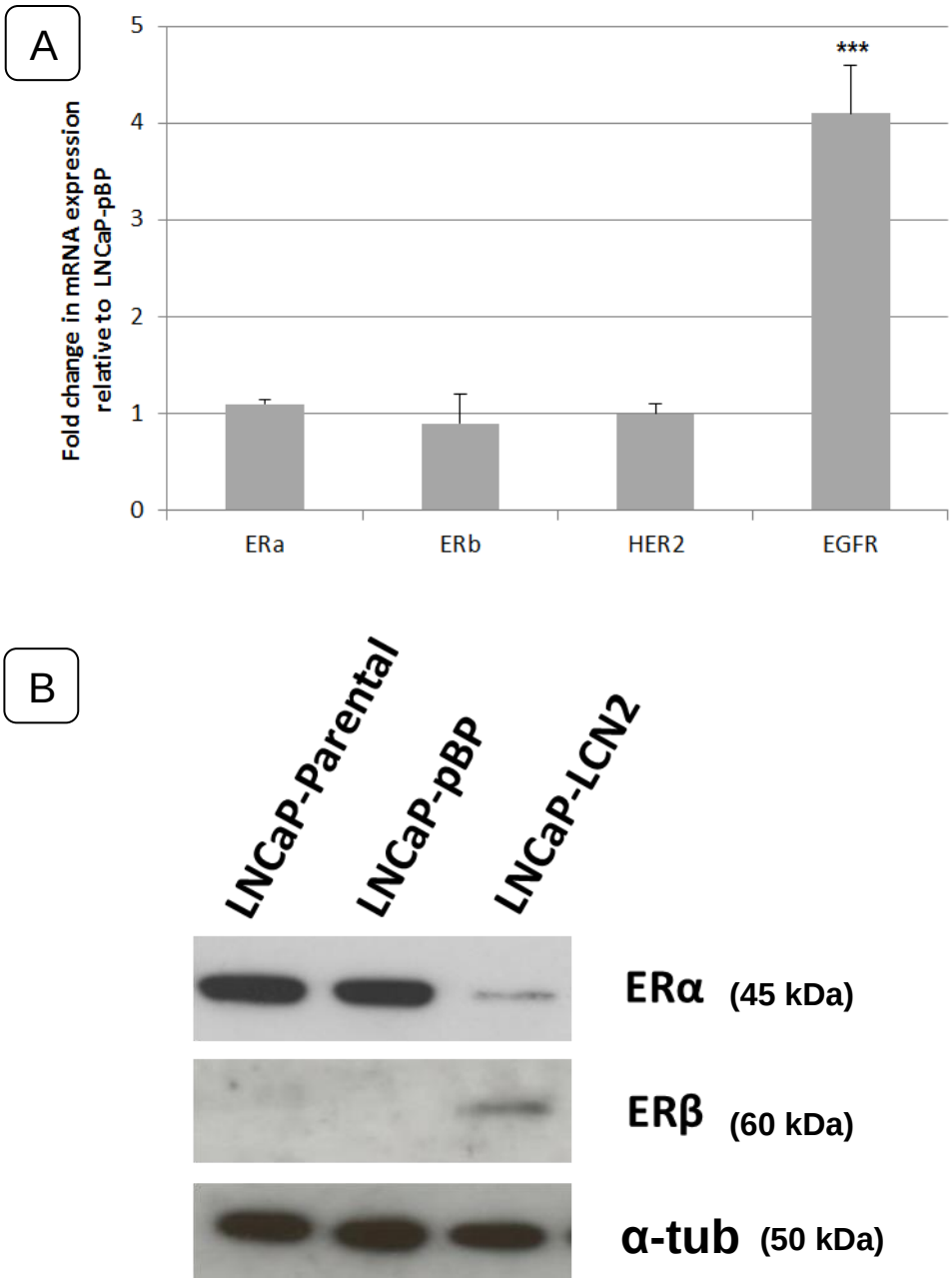

Figure 4.11 Effects of ectopic LCN2 on expression of ERα and ERβ and the ER target genes HER2 and EGFR. A- qPCR analysis of ERα and ERβ and two target genes HER2 and EGFR B: Western blot analysis of ERα and ERβ showed a loss of ERα, and a slight increase in ERβ. Data in panel A shows mean +/- SEM, n=3 experiments. Western Blot in panel B is representative of n= 3. mRNA and protein were extracted simultaneously. Statistical analysis carried out using Student's t-test .***P<0.001

4.9 Functional assessment of AR and ER expression in LNCaP-LCN2 cells

Based on the data shown above in which I showed that LCN2 expression had stimulated an increase in AR expression and a marked down-regulation of ERα and up-regulation of ERβ experiments were performed to determine the functional relevance of these changes in AR and ER expression with regards to cell proliferation and response to receptor agonists and antagonists.

With regards to Androgen receptor functionality; I investigated whether increased AR expression translated to greater sensitivity to the AR antagonist bicalutamide by employing Alamar Blue proliferation assays. LNCaP-LCN2 and, LNCaP-pBP were treated with the AR antagonist bicalutamide for 7 days. Results showed that LNCaP-LCN2 cells were significantly more sensitive to bicalutamide treatment (i.e. had lower proliferation) than LNCaP-pBP controls after 7 days (n=3) (Figure 4.12A). It should be noted however that androgen receptor in LNCaP cells contains a single point mutation in the ligand binding domain and that progestagens, estrogens and several antiandrogens bind the mutated androgen receptor protein which may be mediating any response to either androgen or anti-androgen treatment (Veldshcotte et al, 1992).

Reciprocally, cells were cultured in charcoal-stripped serum (which removes steroid hormones necessary for LNCaP cell viability) and stimulated with the AR agonist dihydro-testosterone (DHT), a more potent form of testosterone. A concentration of 10ng/L in accordance with previous studies (Xu et al., 2006) but this did not enhance proliferation (or enhance cell viability) compared to the control populations (Fig. 4.12B). These results, therefore suggest that while AR may be more highly expressed in LNCaP-LCN2 cells, the protein may not be fully active in the cell.

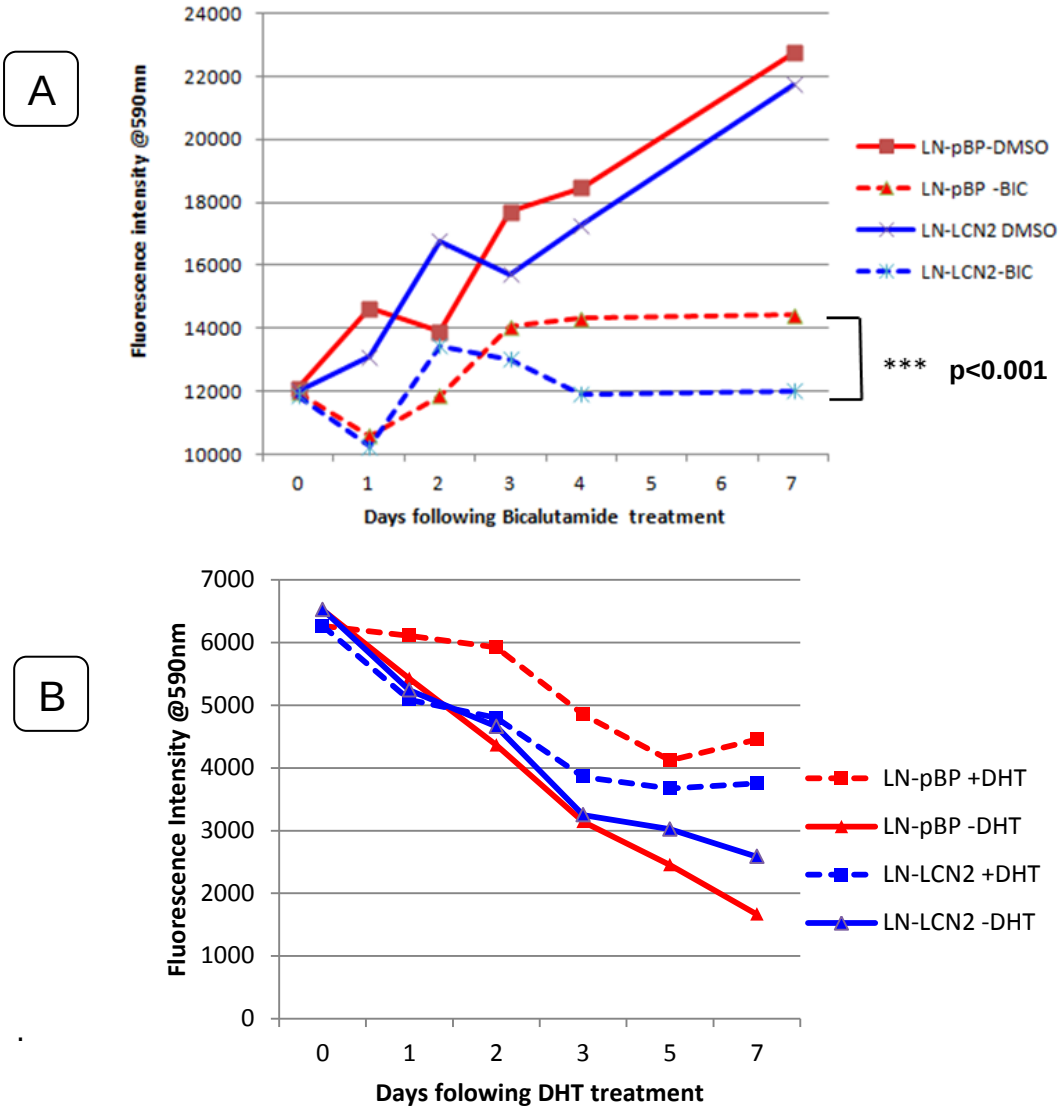

Figure 4.12 LNCaP-LCN2 cells in response to AR agonists and antagonists. Alamar Blue analysis. **A**- LNCaP-pBP and LNCaP-LCN2 cells were treated with AR antagonist bicalutamide (10ng/L), with fluorescence readings taken until untreated cells reached 100% confluence. LNCaP-LCN2 cells had reduced proliferation in the presence of the drug. **B**- Cells were cultured in charcoal stripped media supplemented with DHT (100nmol/ml). All data is the mean of n=3 experiments, with each experiment preformed in triplicate. Error bars for each time point are very small and have been removed for figure clarity. ***P<0.001. Statistical analysis carried out using Student's t-test.

To assess whether loss of ERα expression was functional and whether expression altered response to ER antagonists, I performed Alamar blue proliferation assays (carried out as above). LNCaP-pBP and LNCaP-LCN2 cells were treated with the ER antagonist ICI-182,780 (10μmol/ml). Response to the drug was after observed 4 days of treatment, however there was no significant difference in proliferation rates between LNCaP-pBP and LNCaP-LCN2 cells (Figure 4.13A).

Reciprocally, the effects on proliferation by ER agonists was also investigated. LNCaP-pBP and LNCaP-LCN2 cells were cultured in charcoal-stripped media stimulated with the ER agonist 17β-Estradiol- also known as E2 (100nMol/ml). In both cell types E2 slowed the rate of cell death, however, no significant changes to proliferation were observed. Indeed in all conditions, most cells had died after 6 days (Figure 4.13B).

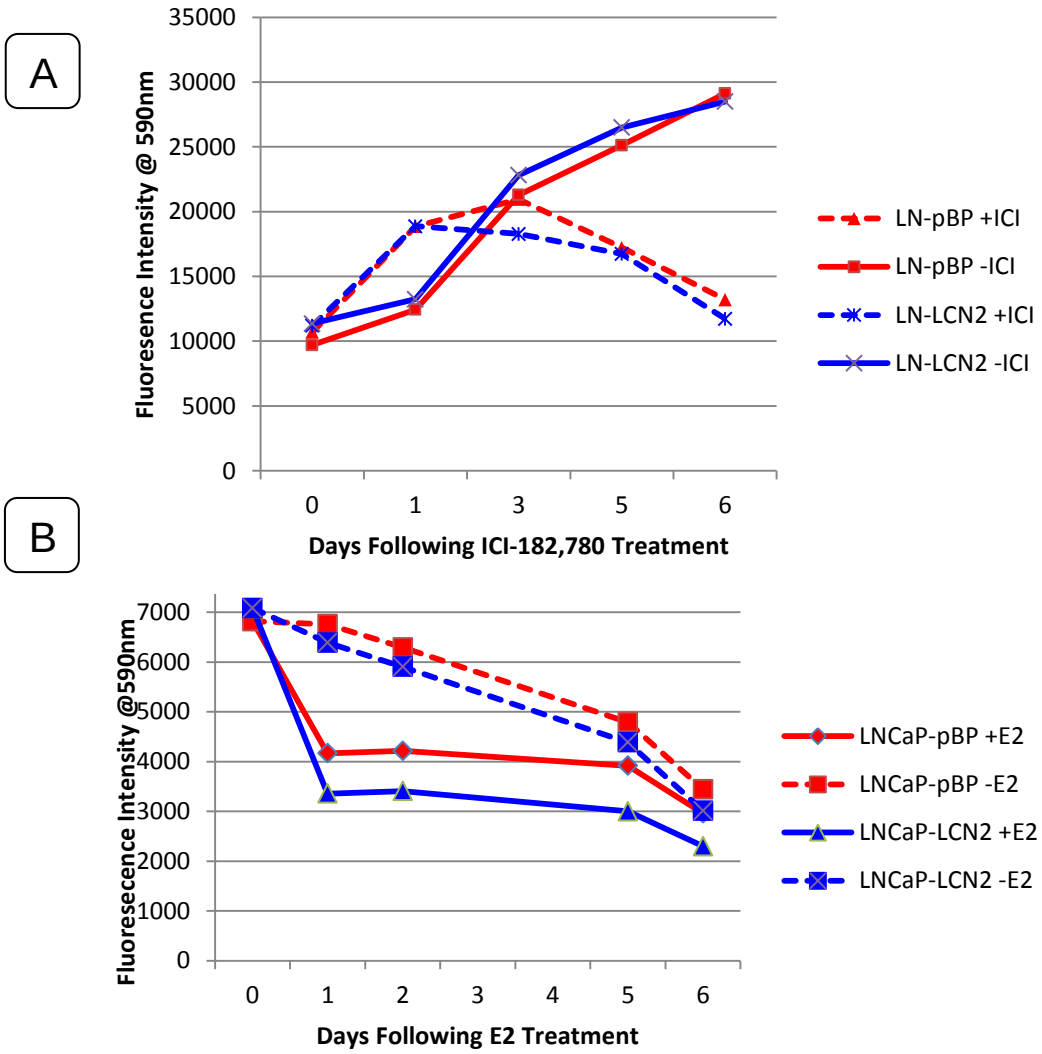

Figure 4.13 LNCaP-LCN2 cells in response to ER agonists and antagonists. Alamar Blue analysis. **A**- LNCaP-pBP and LNCaP-LCN2 cells were treated with ER antagonist ICI-82,780 (10µg/ml), with fluorescence readings taken until untreated cells reached 100% confluence. No significant difference was seen between the cell types in response to the drug. **B**- Cells were cultured in charcoal stripped media supplemented with E2 (100 nmol/ml). All data is the mean of n=3 experiments, with each experiment performed in triplicate. Error bars for each time point are very small and have been removed for figure clarity. Statistical analysis carried out using Student's t-test.

While there was little difference proliferation in response to DHT or E2, I also investigated the effects of this steroid on mRNA expression of downstream targets. LNCaP-pBP and LNCaP-LCN2 cells were cultured in charcoal stripped media and supplemented with 100nMol/ml of DHT or E2 for 48 hours.

To assess the effect of these steroids on AR, mRNA expression analysis was then performed on the AR downstream target PSA (KLK3). In both LNCaP-pBP and LCN2 PSA expression was strongly decreased under charcoal stripped conditions. In both cell types, expression of PSA was rescued following treatment with E2. By contrast, PSA expression was only partially rescued after DHT treatment in LNCaP-LCN2 cells, whereas in DHT treated LNCaP-LCN2 cells expression was rescued to a greater extent (Figure 4.14A).

To assess the effects of ER, in addition to assessing KLK3 expression, I also investigated the expression of the ER target gene EGFR (Filardo, 2002) in cells grown in charcoal stripped media or after stimulation with E2 in LNCaP-LCN2 or LNCaP-pBP cells. In LNCaP-pBP cells, culture in charcoal stripped serum had no significant effects on EGFR expression; addition of either E2 or DHT to this CSS also had no effects (Figure 4.14B). In LNCaP-LCN2 cells however, EGFR expression was significantly reduced in charcoal stripped media grown cells (Figure 4.14B). This expression was however rescued by supplementation of both E2 and DHT. This suggests therefore that LNCaP-LCN2 cells have become more responsive to steroids than LNCaP-pBP cells. It should be noted however that expression of EGFR is regulated by a number of mechanisms, and has a complex association with ER signalling (Egloff et al., 2009). AR has also been shown to up-regulate EGFR, and as such, this may explain an increased response to DHT (Brass et al., 1995).

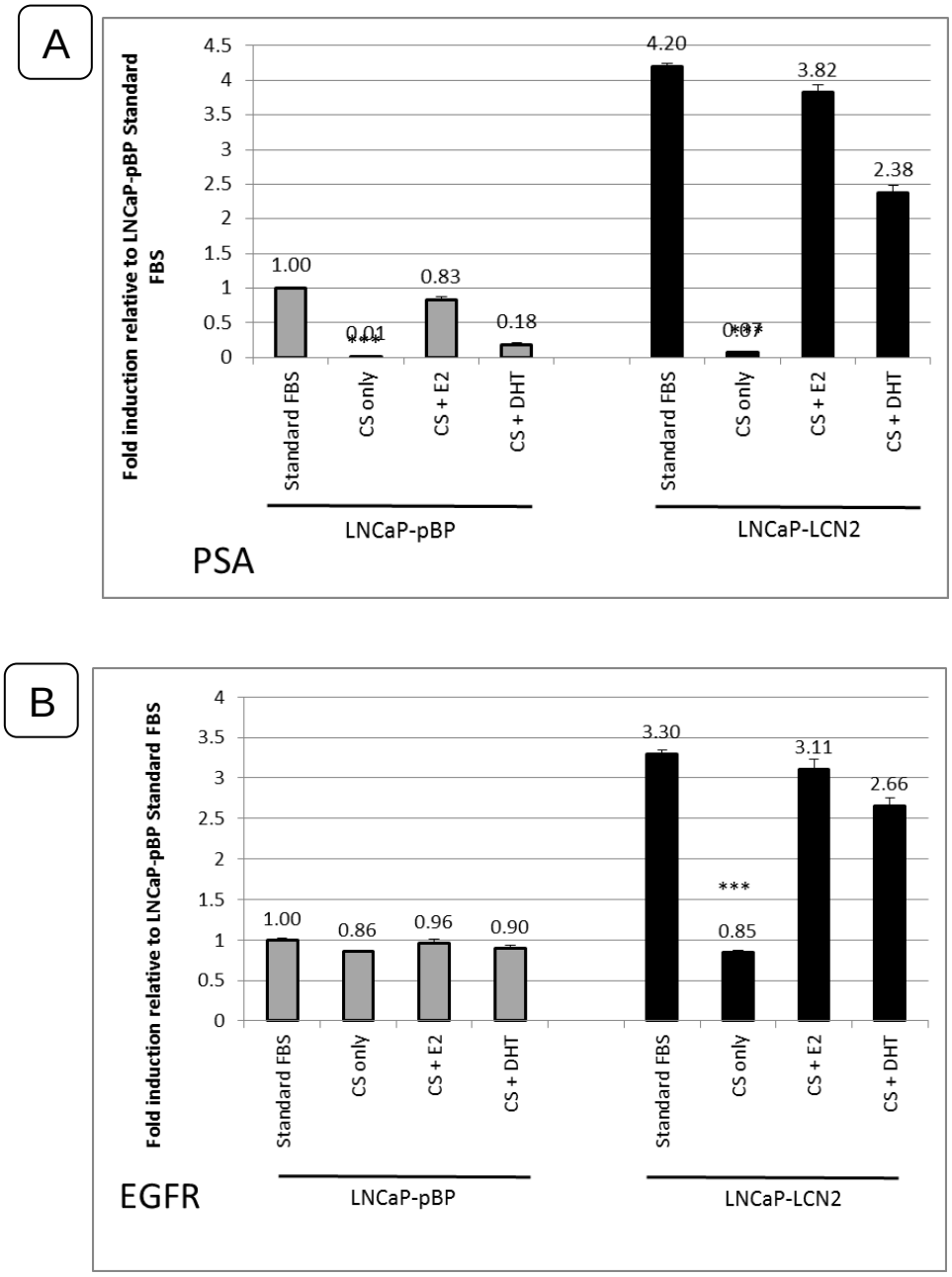

Figure 4.14 Effects of AR and ER agonists on gene expression. LNCaP-pBP and LNCaP-LCN2 cells were cultured for 48hrs in either standard FBS, charcoal stripped (CS) media, or with CS supplemented with the ER agonist E2, or the AR agonist DHT. qPCR analysis of **A**- PSA (KLK3) and **B**-EGFR. All values are relative to LNCaP-pBP cells cultured in standard FBS +/- SEM,n=3 experiments. Statistical analysis was carried out using Student's t-test

4.10 Effects of LCN2 expression on E-cadherin Expression in LNCaP-LCN2 cells.

Aside from androgen independence, one of the key features identified previously in LNCaP-GLI1 cells was that these cells showed many hallmarks of EMT including a loss of E-cadherin, increase in vimentin and increase in ΔP63(See section 3.1). LCN2 was also subsequently identified by microarray analysis in LNCaP-Gli1 as forming part of an EMT signature. Moreover, LCN2 has been identified as inducing EMT in breast cancer cells (Yang et al., 2009). As such, I investigated the effects to EMT markers in LNCaP-LCN2 cells and study the role of LCN2 in regulation of EMT.

qPCR analysis of a range of EMT markers, including E-cadherin, vimentin, CD44, ΔP63 found no significant changes in expression of any of the genes tested. Furthermore, known EMT activators including TWIST1, SLUG and SNAIL also did not show any significant changes in expression (Figure 4.15A). However, the E-cadherin repressor gene ZEB1 (Sanchez-Tillo et al., 2010) showed a 2.3 reduction in expression protein level.

At a protein level LNCaP-LCN2 cells expressed notably higher levels of E-cadherin. Interestingly, there was no reciprocal change in vimentin expression (Figure 4.15B). Here, an increase in E-cadherin was observed in LNCaP-LCN2 cells. No change in expression was seen however for vimentin. It appears therefore, than rather than eliciting complete EMT, the effects of LCN2 seem to be specific to E-cadherin.

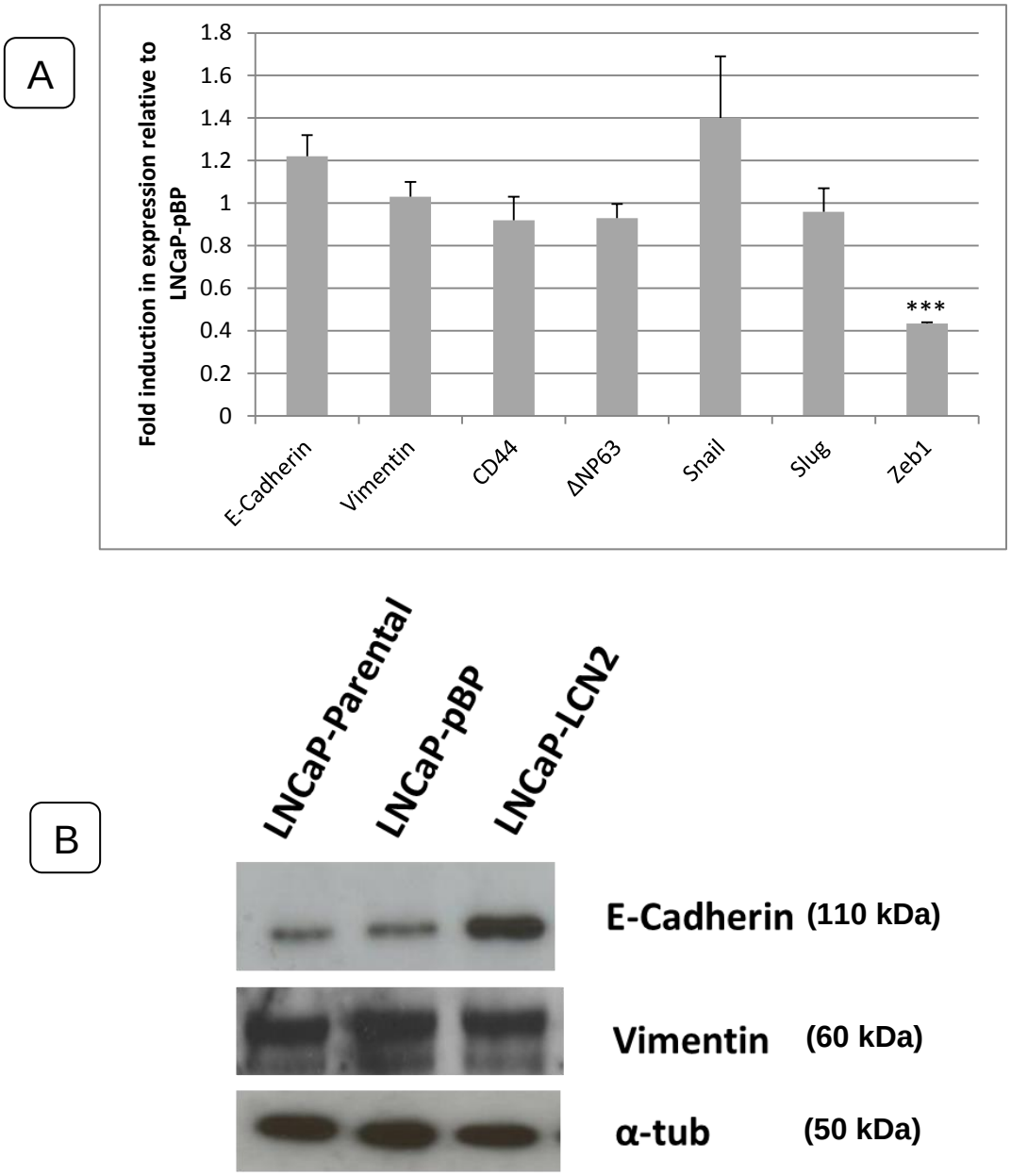

Figure 4.15: Expression of EMT genes in LNCaP-LCN2 cells. A- qPCR analysis of EMT related genes. Values are relative to LNCaP-pBP. Data is mean of n=3 experiments ± SEM. Statistical analysis performed using Student's t-test ***P<0.001 **B-** Western blot analysis of E-cadherin and vimentin in LNCaP-Parental, LNCaP-pBP and LNCaP-LCN2 cells. Note: Membrane is the same as figure 4.16. Results are representative of n=3 experiments.

4.11 Effects of LCN2 on LNCaP cell migration.

To assess the functional relevance of ectopic LCN2 expression and the protein expression changes to E-cadherin in particular, but also AR and ER, LNCaP-LCN2 cells were tested for changes in cell migration and invasion. The role of LCN2 in migration and invasion remains unclear. Previous studies including that by Mir et. al. (2011), have linked increased LCN2 expression to higher rates of both cell migration and invasion (Mir et al., 2012). Conversely, ectopic expression of LCN2 has been linked to reduced migration in liver cells (Lee et al., 2011).

LNCaP (Parental), LNCaP-pBP and LNCaP-LCN2 cells were cultured in 6cm dishes until 100% confluent and treated with Mitomycin C to remove proliferative effects. Scratches approximately 2000 nm wide were created and assessed after 24h. Results showed that LNCaP-LCN2 cells partially lost the ability to migrate into the scratch. After 24h, LNCaP-pBP cells reduced the width of scratches by an average of 751 nm, whereas LNCaP-LCN2 cells reduced the width of scratches by an average of 336 nm ($n=9$, $p<0.05$) (Figure 4.16A-B). This result was also very evident at a visual level. This data also correlates with the higher levels of E-cadherin and ERβ, increased in both of which are associated with reduced migration (Kalluri and Weinberg, 2009, Zhao et al., 2008a) and suggest that in LNCaP cells, LCN2 is an anti-migratory factor.

For invasion analysis, LNCaP-pBP and LNCaP-LCN2 cells were cultured on Matrigel coated inserts and placed under a chemo-attractive FBS gradient. However, results showed that neither LNCaP-pBP nor LNCaP-LCN2 cells were able to invade the Matrigel in sufficient numbers to produce any meaningful results, with only a handful of cells invading for each sample and as a result this area of investigation was abandoned.

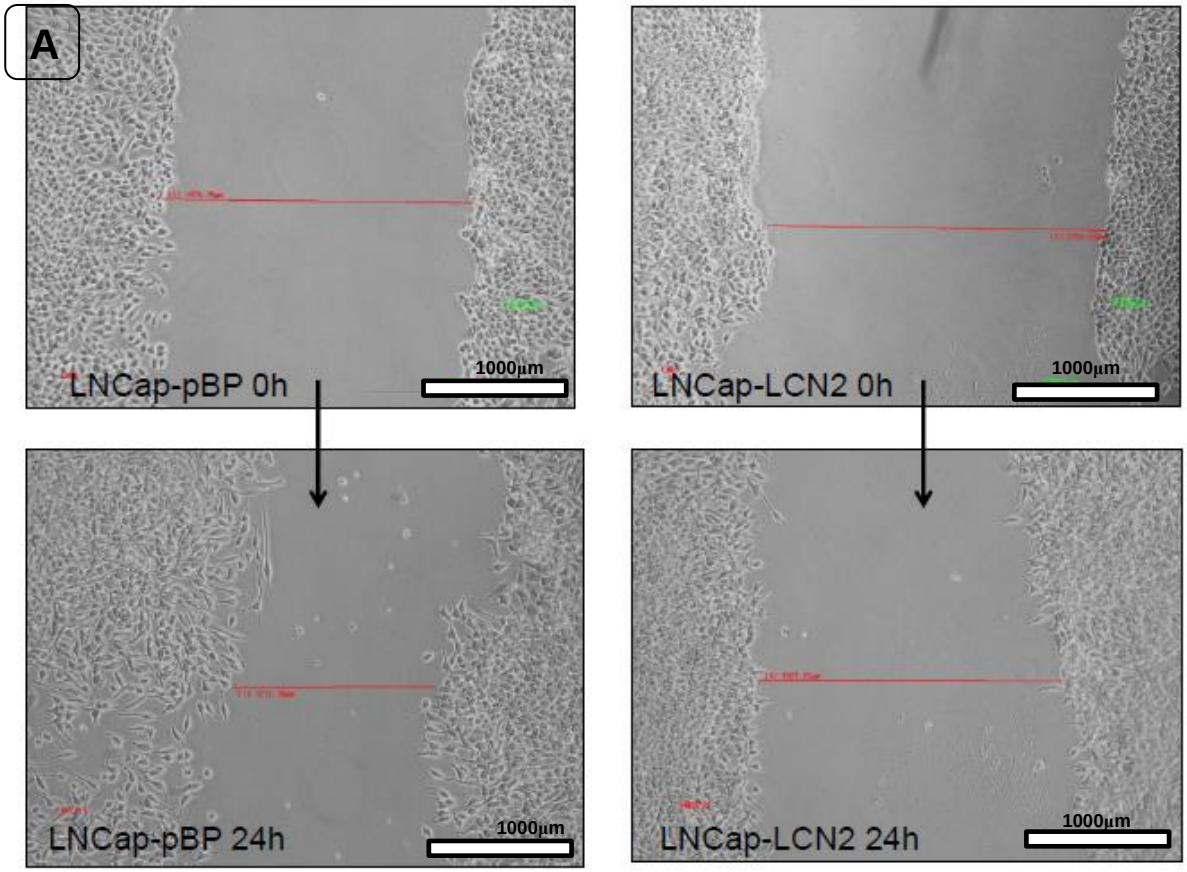

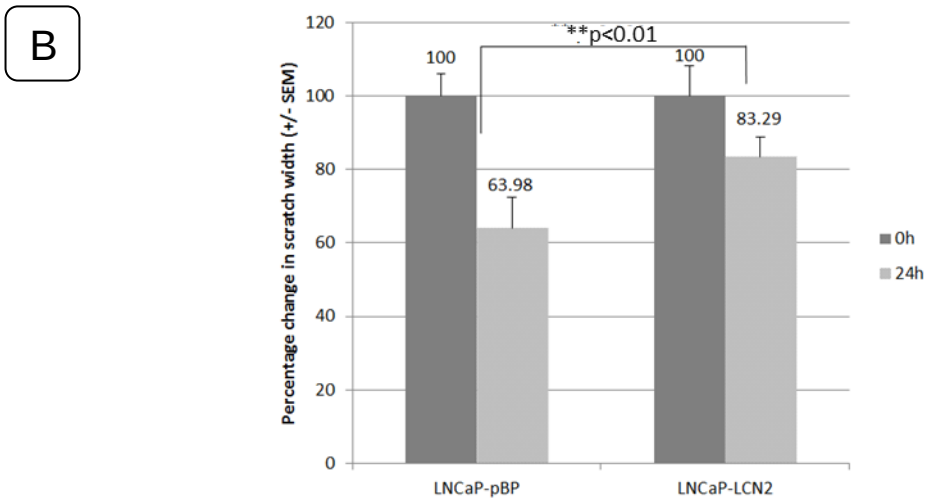

Figure 4.16 Analysis of migration in LNCaP-LCN2 cells. **A** Scratch wound migration assay. 100% confluent cells were treated with Mitomycin C before a scratch was made with a pipette tip. A minimum of 9 width readings taken per sample. A: Bright field image analysis of cells after 0h and 24hrs. **B**- Average width values after 0hrs and 24hrs. All experiments performed in triplicate. Values are mean of n=3 experiments ± SEM. Statistical analysis performed using t-tests. **P<0.01

4.12 mRNA Microarray Analysis of LNCaP-LCN2 cells

As noted above, significant changes were to both mRNA and protein expression were observed in LNCaP-LCN2 cells. However, the genes tested provide only a small fraction of the possible genes being affected by ectopic LCN2. To gain a wide scale overview of the effects of LCN2, mRNA microarray analysis (AFFYMETRIX) was carried out comparing LNCaP-pBP cells to LNCaP-LCN2 cells. The AFFYMETRIX array chip is capable of analysis of ~28500 genes, with each gene having 6-10 probes.

Data from the microarray analysis revealed only minor changes to expression across the genome. As per a wide range of studies, an arbitrary cut of 1.5 fold change was used to differentiate between differential expression or no change. Of the 28500 genes analysed, only 175 genes showed a >1.5 fold change. Of these, 98 showed an decrease to expression in LNCaP-LCN2 and 77 genes showed an increase. A partial list of genes may be seen in Tables 4.2 and 4.3. Of the genes with increased expression, was LCN2 itself. However, raw data showed only an 11-fold increase in LNCaP-LCN2 cells (compared to >250 fold increase as analysed by qPCR). Aside from LCN2, only three genes showed a >2 fold increase, namely CHRNA2 (cholinergic receptor, nicotinic, alpha 2, SERPINB4 (Serpin peptidase inhibitor, clade B (ovalbumin) 4) and OR5B4 (olfactory receptor, family 5B2). A number of key cancer related genes however did show increases of between 1.5 and 2 fold tin expression including SNAI2, MMP7, and IL8. Intriguingly, LCN1, another member of the lipocalin family also showed a 1.7 fold increase in LNCaP-LCN2 cells.

With regards to down-regulated genes, only 5 genes showed a >2 fold decrease in LNCaP-LCN2 relative to LNCaP-pBP cells. GLT8D2, OVOS (Ovostatin) and

FLJ44896 fell into this category, but none of these proteins has been fully described in any literature. A further gene, AXNA1 however, has been extensively studied. AXNA1 (Annexin A1) is a Ca2+ dependent phospho-lipid binding protein which has been associated with a range of cancers. Annexin A1 is associated with NF-κB signalling repression, and has been shown to be up-regulated following ERα activation .

Genes which showed either a >1.5 or <-1.5 fold change were analysed using PANTHER pathway analysis. Biological function analysis revealed 55 genes associated with 'Metabolic processes' and 53 for 'Cellular processes', both categories however are fairly vague and broad. However, categories such as cell communication and immune response scored highly (35 and 27 genes respectively). Genes were also analysed for pathways, however only 31/146 were able to be categorized. Tantalizingly, inflammation and EGF signalling had the highest hits, although the sample is too small to provide any statistical results.

Quite why the microarray data was so minimal is unknown. Indeed, qPCR analysis on the same sample of mRNA showed significant changes to genes such as KLK3. However, these did not appear in the microarray data. Also, an 11 fold increase of LCN2 itself is suspiciously low considering a >250 fold increase seen in qPCR. Nevertheless, results do indicate that LCN2 is able to elicit a genetic effect on LNCaP cells.

Gene Symbol	Gene Description	mRNA Accession	Fold Change LNCaP (Control/LCN2)
LCN2	lipocalin 2	NM_005564	11.0995
CHRNA2	cholinergic receptor, nicotinic, alpha 2 (neuronal)	NM_000742	2.14394
OR5B2	olfactory receptor, family 5, subfamily B, member 2	NM_001005566	2.02382
LOC642947	hypothetical protein LOC642947	AK129705	1.92066
UGT2B28	UDP glucuronosyltransferase 2 family, polypeptide B28	NM_053039	1.9125
CCDC141	coiled-coil domain containing 141	NM_173648	1.87223
GSTM1	glutathione S-transferase mu 1	NM_000561	1.8405
LOC284861	hypothetical LOC284861	AK128837	1.80533
RARRES3	retinoic acid receptor responder (tazarotene induced) 3	NM_004585	1.76682
SNAI2	snail homolog 2 (Drosophila)	NM_003068	1.76363
MMP7	matrix metallopeptidase 7 (matrilysin, uterine)	NM_002423	1.74786
HIST1H2BJ	histone cluster 1, H2bj	NM_021058	1.7427
LCN1	lipocalin 1 (tear prealbumin)	NM_002297	1.73229
CCBE1	collagen and calcium binding EGF domains 1	NM_133459	1.70906
ADH1C	alcohol dehydrogenase 1C (class I), gamma polypeptide	NM_000669	1.68051
SNORD116-28	small nucleolar RNA, C/D box 116-28	NR_003361	1.65406
SOX7	SRY (sex determining region Y)-box 7	NM_031439	1.63084
LOC100128840	hypothetical LOC100128840	AK058065	1.62272
BTC	Betacellulin	NM_001729	1.62111
SPDYE3	speedy homolog E3 (Xenopus laevis)	NM_001004351	1.60832

Table 4.1- List of top 20 genes found to be up-regulated in LNCaP-LCN2 cells relative to LNCaP-pBP. Anti-log fold change in expression generated from Affymetrix GeneChip array data. All values had p-values <0.001

Gene Symbol	Gene Description	Accession No.	Fold Change LNCaP (Control/LCN2
GLT8D2	glycosyltransferase 8 domain containing 2	NM_031302	-2.195173545
OVOS	ovostatin	BX647938	-2.169921723
C8orf73	chromosome 8 open reading frame 73	NM_001100878	-2.094883478
FLJ44896	FLJ44896 protein	AK126844	-2.025739974
ANXA1	annexin A1	NM_000700	-2.011685811
ZNF443	zinc finger protein 443	NM_005815	-1.989329149
FAM99A	family with sequence similarity 99, member A	NR_026643	-1.919784002
CNN3	calponin 3, acidic	NM_001839	-1.870763259
RNU5A	RNA, U5A small nuclear	NR_002756	-1.867190337
FAM129A	family with sequence similarity 129, member A	NM_052966	-1.862801566
XAGE-4	XAGE-4 protein	AJ318895	-1.848473037
NCRNA00116	non-protein coding RNA 116	BC064430	-1.845685829
BICC1	bicaudal C homolog 1 (Drosophila)	NM_001080512	-1.782203402
S100A4	S100 calcium binding protein A4	NM_019554	-1.765239579
LOC255411	hypothetical LOC255411	NR_029449	-1.753571189
PRSS1	protease, serine, 1 (trypsin 1)	NM_002769	-1.744886263
OVOS	ovostatin	BX647938	-1.740736699
OR8H1	olfactory receptor, family 8, subfamily H, member 1	NM_001005199	-1.737468714
LOC644714	hypothetical LOC644714	BC047037	-1.732978793
ND2	MTND2	ENST00000361453	-1.726101139

Table 4.2- List of bottom 20 genes found to be down-regulated in LNCaP-LCN2 cells relative to LNCaP-pBP.

4.13 Chapter Discussion

The aim of ectopically expressing LCN2 in LNCaP cells was to identify whether it was regulating some of the phenotypic and gene expression changes previously seen in LNCaP-Gli1 cells, especially with regards to androgen independence and EMT. However, results showed that rather than promoting AI and EMT, LCN2 instead had the effect of increasing AR and E-cadherin expression.

Lipocalin 2 is a secreted protein with a molecular weight of ~25kDA. However, when I employed the MAB1757 (R&D) antibody on whole cell lysates, Western blot bands were consistently 48 kDa were seen. This band was not the LCN2/MMP9 complex (molecular weight 119kDA). The band was also present using different methods of cell lysis including RIPA buffer. The MAB1757 antibody is the most cited for LCN2 (e.g. Mahadevan et al 2012; Yang et al 2009, Bi et al 2012), and until very recently the only monoclonal antibody for LCN2 commercially available. This antibody has been used previously on both cell supernatants and whole cell lysates, and is also used for ELISA testing. Notably, while molecular weights of 25kDA have been described for secreted LCN2 in previous literature, this data is absent when presented for whole cell lysates (E.g. Tong et al, 2008). LCN2 existing as a sulphur homodimer was first described by Kjeldsen et al in 1994. However in all subsequent literature, this point is mentioned in text only.

In addition, as seen in figure 4.7 and 4.12, when intracellular levels of LCN2 were analysed in both LNCaP-Gli1 and LNCaP-LCN2 cells respectively, protein expression was lower than expected relative to mRNA expression. Analysis of secreted LCN2 however showed that the protein is produced, but is rapidly expelled from these cells, and that the secreted LCN2 is monomeric. It was also found that

expression of LCN2-R was higher in all LNCaP derived cell lines. While only qPCR analysis was carried out, this may provide a partial reason as to why LCN2 is secreted more rapidly than in PC3 cells. However, the precise functions of LCN2-R are very poorly understood, and may not necessarily have a role in LCN2 cleavage. The existence of different states of LCN2 within and outside the cell has also not been reported before, and exactly how or why this state occurs is unknown but may require cleavage of sulphur bonds. It would therefore be interesting to investigate the 3D structure via either mass-spectrometry or crystallography and whether homodimeric LCN2 binds differently to substrates. Given that this antibody is also the most commonly used form for tissue immunohistochemistry, this has a potential impact on these types of results.

Aside from the MAB1757 antibody, the 5G5 (Santa Cruz) and AF1757(R&D) antibodies mentioned in section 4.10 other antibodies were assessed including a polyclonal rabbit antibody from Abcam and an anti-rabbit polyclonal from Millipore (AB2267) However, in both cases antibodies were did not work or produced blots which were too dirty to use. Other antibodies are now very recently available for LCN2, although there was insufficient time to analyse these sufficiently.

In this study, contrary to predictions, I observed a novel positive correlation between LCN2 expression and Androgen receptor protein expression. mRNA expression of AR did not change however, and regulation appears to be post-transcriptional. Post-transcriptional or post-translational regulation has been reported at a number of levels including by targeting to E3 ligases (Yeap et al., 1999). Alternatively, AR mRNA is targeted by EBP1 for degradation (Lonergan and Tindall, 2011) . AR has also been shown to be regulated by a number of miRNAs including miR-221 and miR-31 (Sun et al., 2013, Lin et al., 2013). Both AR and LCN2 are also known to be

regulated to some level by NF-κB and this acts as a potential mediator of LCN2 signalling.

LNCaP-LCN2 cells were more sensitive to bicalutamide, however they did not show increased response to DHT. A higher concentration of DHT (1μM) was also attempted (n=1) but also showed no difference between the two cell types and was subsequently abandoned. It is therefore likely that even with increased AR expression, the addition of DHT alone is insufficient to rescue the LNCaP cells in charcoal stripped media.

In addition to AR expression, a decrease in ERα, but increase in ERβ was observed. This data therefore correlates with previous data, particularly Yang et al 2009 which also showed a negative correlation between ERα and LNC2. However, other studies such as Yang et al., 2009 do not mention ERβ expression. ERα : ERβ ratios are not always opposing, but ERβ expression is known to repress ERα expression and vice versa (Matthews and Gustafsson, 2003). Despite a change in ERα: ERβ ratio, no significant changes were observed in LNCaP-LCN2 cells in response to either the ER agonist E2 or the antagonist ICI-082,780. As with DHT, it is likely that supplementation with E2 alone is insufficient to promote growth in charcoal stripped media over many days. With regards to ICI-082,780, no resistance was observed in LNCaP-LCN2 cells. This may be due to ICI-082,780 binding to both ERα and ERβ, inhibiting the protein binding to estrogen (Matthews and Gustafsson, 2003). It is possible that the increased ERβ in LNCaP-LCN2 cells is counteracting loss of ERα. Alternatively, ERα expression did not totally disappear, and the low levels of ERα may be sufficient to confer sensitivity to the drug.

One of the aims of this chapter was to determine whether LCN2 affected EMT. Previously LCN2 was identified as being a member of the EMT ontological grouping in LNCaP-GLI1 cells (See Chapter 3 and Nadendla et al. 2011). Moreover, Yang et al., 2009 showed an inverse correlation between LCN2 and E-cadherin Results shown here (Figure 4.20) showed that LNCaP-LCN2 cells increased E-cadherin and induced an EMT phenotype. As such it was originally hypothesised that E-cadherin expression would be suppressed in LNCaP-LCN2 cells and cells would enter into an EMT phenotype. However, the results in this chapter suggest that LCN2 positively correlates to E-cadherin expression. Results also showed that rather than affecting all EMT related genes, specifically only E-cadherin expression was altered, and this was associated with a loss of the E-cadherin repressor ZEB1 (Graham et al., 2008).

It is also possible that the changes to ERα and E-cadherin are linked. It is currently generally regarded that ERα acts as an inhibitor of E-cadherin expression (Park et al., 2008, Oesterreich et al., 2003). Additionally, ERβ has been shown to act as an E-cadherin promoter, particularly in prostate cells (Park et al., 2008). ERβ activation of E-cadherin was also independent of vimentin. Interestingly however, regulation of ERα, ERβ and E-cadherin by LCN2 was post-transcriptional. Both ER isoforms are known to be regulated at multiple levels. ER is targeted to proteasomes by E2 ligases (Le Romancer et al., 2011). As with AR, ER mRNA is also targeted by mIR-221 for translational control (Zhao et al., 2008b). It is hence possible that LCN2 may be associated with this mRNA.

In this study, microarray analysis was employed to obtain a more global analysis of LCN2's effects. Although experiments were performed in triplicate, analysis was carried out at the same time. As noted in section 4.16, the gene expression profile was much lower than was expected given the changes to protein expression, and

genes such as KLK3 and ZEB1 did not show any significant difference in analysis. This may be attributable to a faulty or less sensitive chip. Alternatively it may that as microarray analysis often less sensitive that qPCR is and may be that changes to expression were not great enough to be detected the array. In this case data may show that the effect of LCN2 ectopic expression has relatively little effect on LNCaP cells, possibly due to its high rate of secretion from cells.

In conclusion, a number of points may be seen from the data in this chapter:

1. LCN2 exists as a dimer inside the cell, but is secreted as a monomer and that secretion rates differ between cell lines.
2. Ectopic LNC2 expression leads to a positive correlation to androgen Receptor and PSA expression
3. Conversely, that LCN2 shows a negative correlation to ERα expression and changes the ERα:ERβ ratio
4. Ectopic LCN2 expression shows a positive correlation to E-cadherin and to a loss of migratory potential.

As ectopic expression of LCN2 in LNCaP cells introduced a gene where it was not previously present, to further investigate the role of LCN2 in PCa cells, it was decided to investigate the effects of suppressing expression in a cell line where LCN2 was naturally present, namely PC3 cells.

Chapter 5: The effect of Suppressing LCN2 in the PC3 cell Line

Introduction

The cell line PC3 is a commonly used PCa cell line (Sobel and Sadar, 2005). This line is derived from a PCa bone marrow metastasis. PC3 cells have high metastatic potential and are p53 null. PC3 cells are androgen insensitive, and do not express AR (van Bokhoven et al., 2003). As mentioned in section 4.10, PC3 cells were identified as having the highest levels of LCN2 at the intracellular protein level amongst a range of PCa cell lines. This was further confirmed by qPCR data. Furthermore, PC3 cells were identified as having the highest levels of secreted LCN2 as determined by ELISA (2ng/ml). In addition, using the Gene Expression Atlas (http://www.ebi.ac.uk), PC3 was identified as having highest level of LCN2 mRNA among all frequently cited PCa cell lines and was indeed had the highest level of LCN2 expression of all non-pancreatic cancer cell lines (Leung et al., 2012).

Given that both PC3 and LNCaP-GLI1 cell lines expressed high levels of LCN2, and are both androgen independent. It was originally hypothesised that LCN2 may be driving AI in PCa, and that suppression of LCN2 may re-instate the androgen dependent phenotype. However, given that ectopic LCN2 in LNCaP cells led to increased AR, this is unlikely to be the case. However, as LCN2 is expressed at such high levels in PC3 cells, it was decided to investigate changes upon its suppression, particularly towards hormone receptor regulation. As ectopic LCN2 led to reduced ERα expression in LNCaP cells, any mirroring of this in PC3 cells would also provide a more concrete data on the precise role of LCN2 in PCa cell lines.

Results

5.1 LCN2 expression in PC3 cells is not affected by SMO inhibitors

LCN2 was the gene with one of the highest fold changes in LNCaP-GLI1 cells (See section 4.9), and PC3 cells also display high levels of Hedgehog signalling (Nadendla et al., 2011). As such, I aimed to determine whether inactivation of the hedgehog pathway and GLI1/2 in PC3 cells had any effect on LCN2 expression. Suppression of the hedgehog pathway was first attempted using the pharmacological hedgehog pathway antagonists KAAD-Cyclopamine and SANT1, which have been shown to inhibit GLI1/2 expression (Karhadkar et al., 2004). PC3 cells were treated with the SMO KAAD-Cyclopamine and SANT1 (both at 50 and 100 nmol/ml) for 72h. The direct GLI inhibitor GANT61 (50 nmol/ml) was also used (Pan et al., 2012), however this was found to be toxic to cells and hence abandoned. Both KAAD-Cyclopamine and SANT1 suppressed the expression of GLI1 (Figure 5.1A) However, no significant changes were seen to LCN2 expression (Figure 5.1B), suggesting that LCN2 is either not a direct GLI1 target, or that any activation by GLI1 is irreversible. Despite this, it was noted that although GLI1 was suppressed by inhibitors, GLI2 expression was not as affected. It is therefore possible that LCN2 is activated by GLI2 as well.

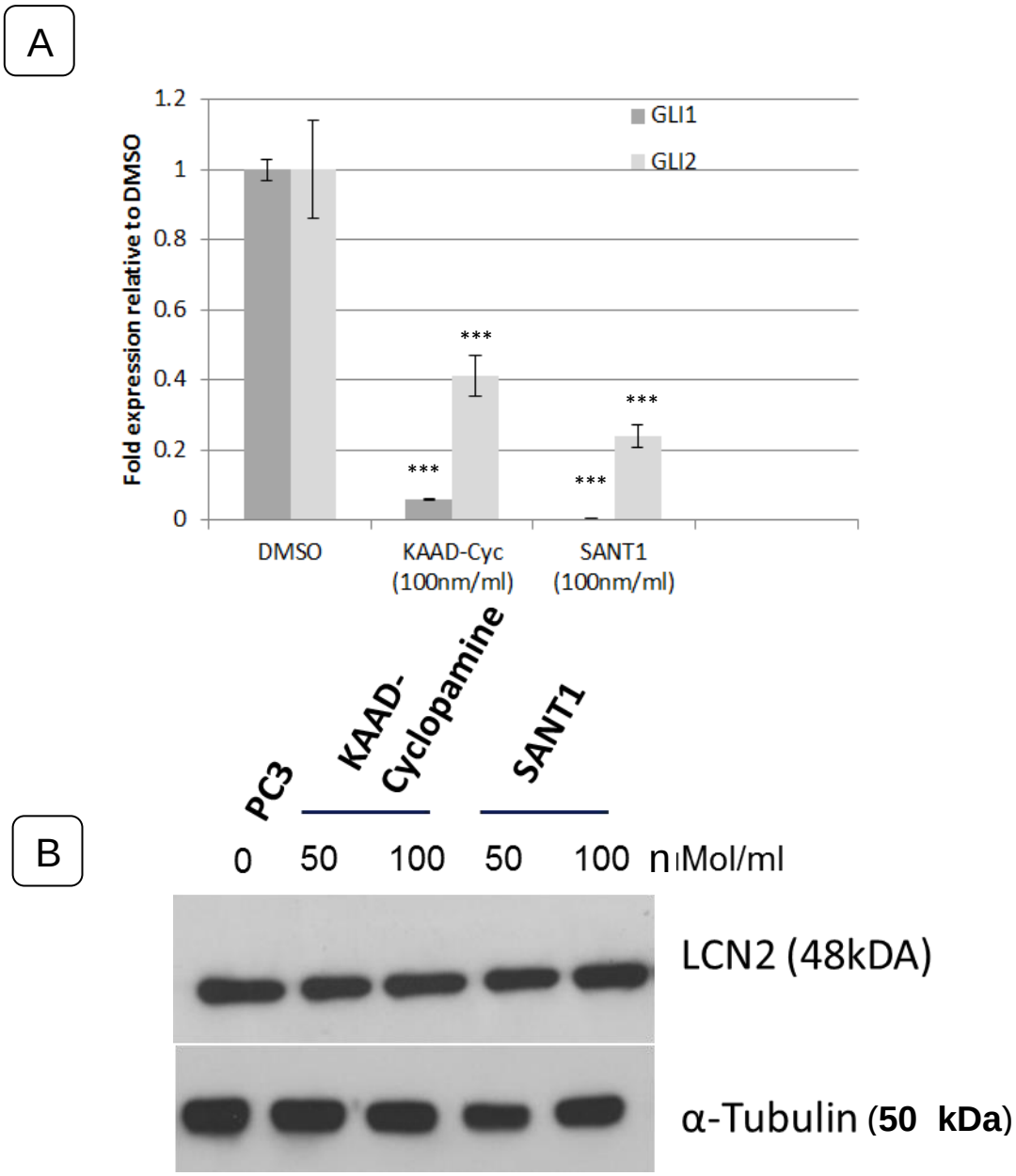

Figure 5.1 Effect of Hedgehog suppression on LCN2 by pharmacological inhibitors. **A** PC3 cells were treated either KAAD-Cyclopamine or SANT1 for 72hrs. qPCR analysis of GLI1 and GLI2 expression relative to DMSO treated cells +/- SEM ***p<0.001(n=3). (Figure is using the same data as figure 3.5) **B** Western blot analysis of LCN2 protein in PC3 cells treated with drugs at either 50 or 100 nMol/ml for 72 hours. Representative of n=3 experiments.

5.2 Suppression of both GLI1 and GLI2 does not affect LCN2 expression

To further investigate the role of GLI1 in LCN2 regulation, and to also uncover any role of GLI2 as well, siRNA was employed to suppress both of these genes. Double knock-down of GL1 and GLI2 was performed simultaneously using the siRNAs 5816 and 5817, both at concentrations of 20 nmol/ml. Suppression of GLI1 and GLI2 was confirmed by qPCR (See figure 3.4). Expression of LCN2 however was unaffected at either the mRNA level (Fig 5.2A) or by Western Blot (Figure 5.2B).

Combined with the data from SMO inhibitors therefore, it appears that LCN2 is unaffected by subsequent inhibition of GLI or the HH pathway. As seen with LNCaP cells, expression of GLI1 does lead to significantly higher levels of LCN2, however, in both the case of LNCaP-GLI1 and in PC3 cells, subsequent inhibition of GLI had no effect on LCN2. As such, it was subsequently decided to investigate the effect of suppressing other signal transduction pathways associated with LCN2 regulation.

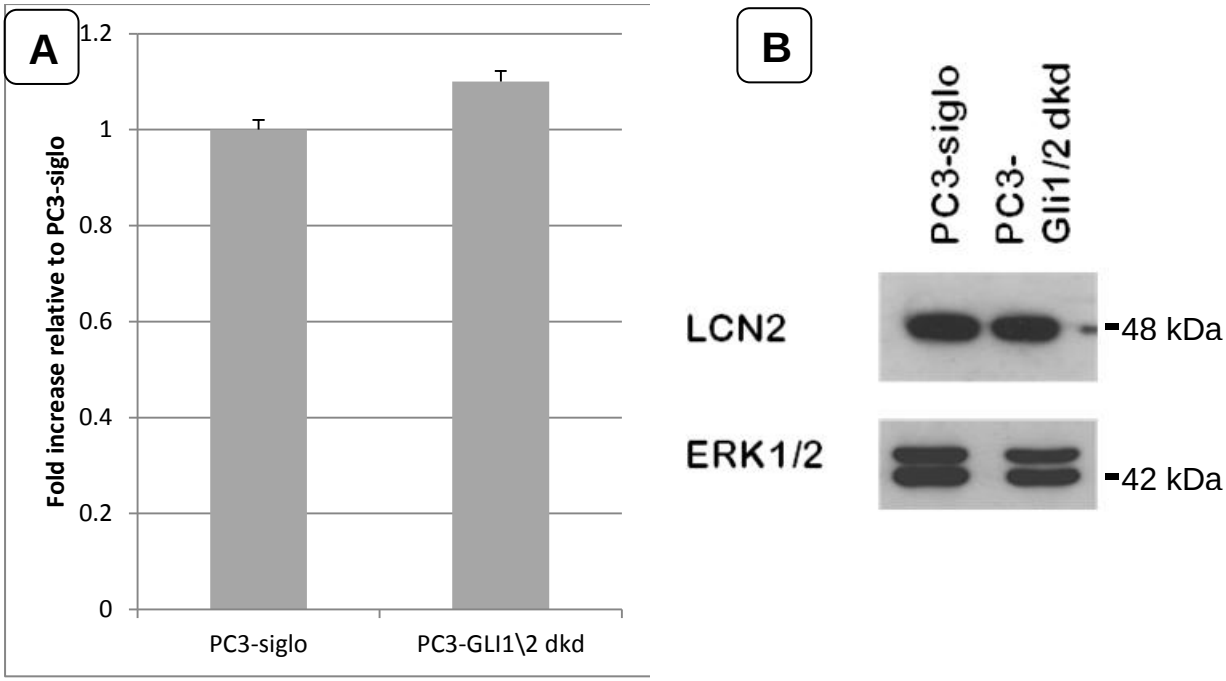

Figure 5.2- Effect of GLI1/2 suppression by siRNA on LCN2 expression. PC3 cells were transfected with siRNA targeting both GLI1 and GLI2. GLI suppression was previously confirmed in PC3 cells (see Figure 3.4). **A** qPCR analysis of LCN2 expression in PC3 cells transfected for 72hrs with both siGLI1 and siGLI2, or with siGLO control (+/- SEM, n=3). **B** Western blot of whole cell lysates using the same conditions (mRNA and protein extracted in parallel). Representative of n=3 experiments.

5.3 LCN2 expression is unaffected by NF-κB inhibition.

Given that inhibition of GLI did not affect LCN2; it was decided to investigate other potential factors were able to affect its expression. Of the numerous potential candidates, the transcription factor NF-κB has been previously shown in the literature to be a key regulator of LCN2 expression. There are known to be NF-κB binding sites at the LCN2 promoter(Karlsen et al., 2010, Li et al., 2009) and a number of studies have linked the two genes. Notably, Li et al (2009). used the NF-κB inhibitor BAY-11-7082 to suppress LCN2 expression in murine breast cancer cells (Li et al., 2009). A similar approach was also used by Leng et. al., (2009) also in breast. However, significant changes were only observed above 50μM/L Also, Mahadevan et al. (2011) successfully employed BAY-11-7082 to reduce LCN2 expression in the prostate cell line TC1 which had been subject to endoplasmic reticulum stress. BAY-11-7082 is not a direct NF-κB inhibitor per se, rather it inhibits the Iκκ complex which in turn binds to NF-κB, and sequesters it in the cytoplasm (Lee et al., 2012). Phosphorylated IKK is chaperoned to proteasomal degradation sites, freeing the NF-κB complex. BAY-11-7082 acts to permanently inhibit the phosphorylation of Iκκ, and thereby NF-κB (Lee et al., 2012).

In order to investigate the role of NF-κB in the regulation of LCN2, a strategy similar to that used by Li. Et al (2009) was used. PC3 cells were treated for 6 hours with the drug, then were supplemented with fresh media for a further 24 hours. A range of concentrations from 0-30nMol were used. It was discovered that BAY-11-7082 was highly toxic to cells. Indeed, all concentrations above 5μmol/ml killed virtually all cells within 24 hours. Cells were therefore harvested only at concentrations of 1μM, and 2μM. A 5μM/mL concentration was also used although it should be noted that approximately 50% of cells died before harvesting.

Inhibition of NF-κB was confirmed by a reduction in IL-1B expression (Jiang et al., 2004). This was strongest at 5μM (-8.5 fold). A -4.1 fold was seen at 2μM and 1.95 fold for 1μM. When LCN2 was analysed via qPCR however, no significant changes were observed under any condition (Figure 5.3). In addition, experiments were attempted whereby PC3 cells were treated for 24hours with BAY-11-7082 with no media change, however this proved to be too toxic, and cells either died or looked unhealthy. Contrary to previous studies therefore (Mahadevan et al., 2011, in murine prostate and Li et al., 2009 in 231BR murine breast cell lines), NF-κB inhibition did not show any affect in LCN2 expression at concentrations used. It is possible however that the toxic effects of BAY-11-7082 are stronger than the effects on LCN2 expression, and that cells died before any change to LCN2 could be observed.

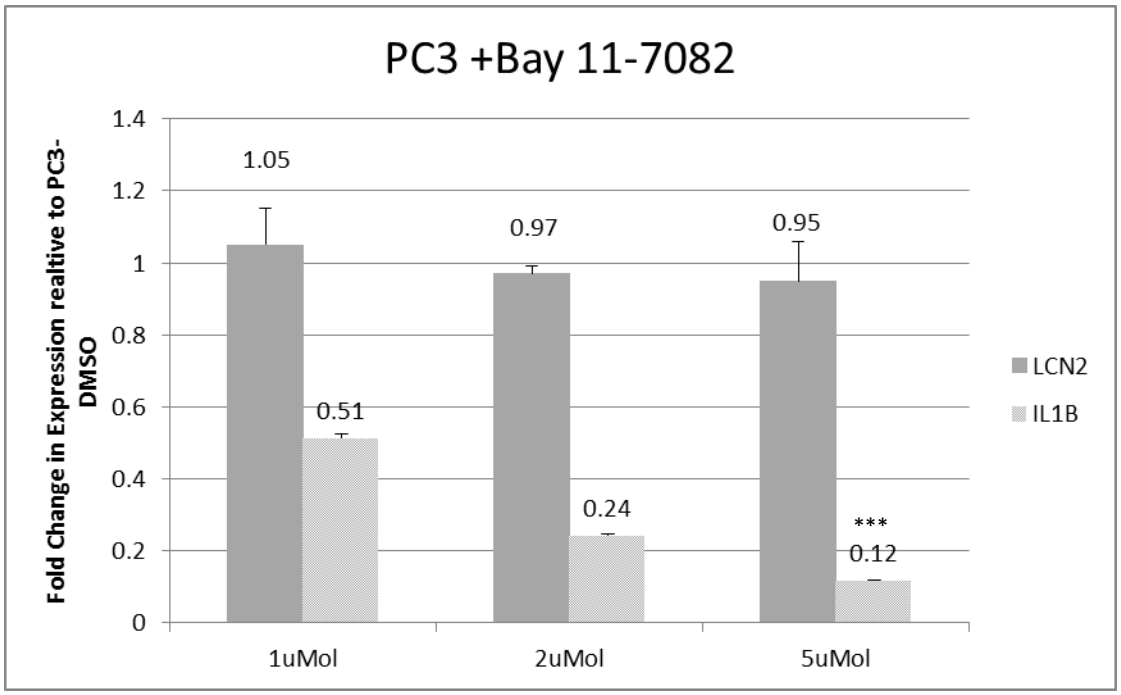

Figure 5.3 LCN2 expression is not affected by BAY 11-7082 qPCR analysis of LCN2 and known target gene IL1B in response to BAY11-7082Cells were treated for 6 hours, followed by 24hrs in fresh media. All data is relative to PC3 cells treated with DMSO only. Data is mean of n=3 experiments +/- SEM ***p<0.001. Statistical analysis was carried out using Student's t-test

5.4 Effect of a range of Pharmacological Inhibitors on LCN2 expression.

Since NF-κB inhibition had no effect on LCN2 expression, a range of pharmacological inhibitors were tested to observe they effect LCN2 expression. For this, inhibitors targeting previously proposed LCN2 regulatory pathways were used namely the PI3 Kinase (Lee et. al. 2011), the MEK/ERK pathway (Yang et. al. 2009) AKT pathway and the EGFR signalling pathway (Mir et. al. 2012) The inhibitors used were U0126 (MEK/ERK), Wortmannin (PI3K), API2 (AKT) and AG1478 (EGFR). PC3 cells were treated with each of the drugs for 48 hrs before harvesting.

qPCR analysis for LCN2 in treated cells revealed that the drugs Wortmanin, U0126 and API2 had no significant effect on LCN2 expression, although the EGFR inhibitor AG1478 did reveal a 4 fold decrease in expression of LCN2 (Figure 5.4A). [It should be noted that for all previous experiments the housekeeping gene GAPDH was used as a loading control. However, both Wortmanin and AG1478 gave rise to a >2 fold decrease in GAPDH expression relative to DMSO treatment alone, therefore in terms of LCN2 values, AG1478 treatment showed an 7 fold decrease in expression and wortmanin a 2 fold decrease. Despite this, when LCN2 protein was analysed via Western blot there was only minor reduction in expression suggesting that the LCN2 protein is fairly stable within PC3 cells.

The reduction of LCN2 in response to AG1478 was similar to the results found by Mir et al. (2011) who also noted a loss of expression in treated A549 adenocarcinoma cells. In this paper however, the authors only noted notable loss of expression at 30μM. Moreover, they also presented protein based data, not mRNA analysis. To further analyse the efficacy of AG1478 in reducing LCN2 expression, and in an attempt to confirm Mir et. al.'s 2012 results. PC3 cells were treated with the drug at

concentrations of 1µM, 5µM, 10µM, 30µM and 100µM. The 100µM concentration proved to be highly toxic to the cells and therefore discarded. qPCR analysis showed that 1µM and 5µM did not result in any notable effect on LCN2 expression, whereas 10µM and 30µM both resulted in a 4.2 fold and 4.0 fold reduction. This shows that the effect of AG1478 on LCN2 is not linear, or as potent in PC3 cells as A549 (Human alveolar adenocarcinoma) cells, although it should be noted that at 30µM, there was notable cell death, and many of the cells looked unhealthy before harvesting (visual observation only).

For positive controls, as p-ERK (the traditional U0126 target) and p-AKT (wortmanin and API2 targets (Carnero et al., 2008)) were relatively low in PC3cellls, the keratinocyte cell line NEB1 which have higher levels of these proteins was employed to determine the efficacy drugs. P-EGFR was used to determine AG1478 activity, also in NEB1 cells (Figure 5.4B)

When taken together, it appears that in PC3 cells at least regulation of LCN2 is unaffected by a range of pharmacological inhibitors with the exception of the EGFR inhibitor AG1478. These drugs included those targeting pathways already shown to interact with LCN2 expression. This suggests that regulation of LCN2 is likely to be fairly robust, and possibly not controlled by a single pathway alone.

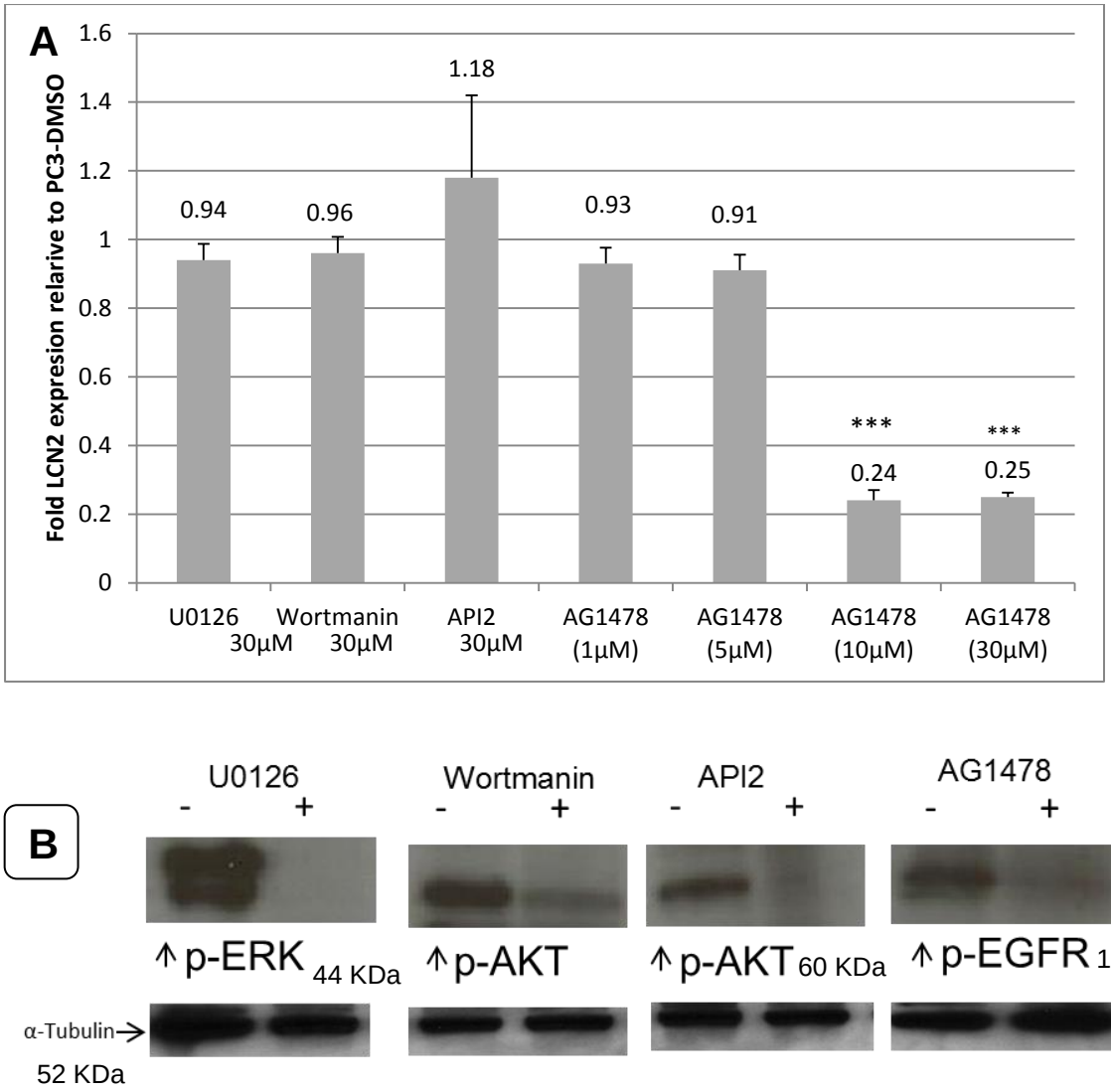

Figure 5.4: LCN2 expression in response to a range of pharmacological inhibitors. A PC3 cells were exposed to a range of pharmacological inhibitors- U1026 (Targeting MEK/ERK); Wortmanin (MAPK pathway) API2 (Targeting AKT) and AG1478 (Targeting EGFR) at a range of concentrations. Data are mean of n=3 experiments +/- SEM. Statistical analysis was carried out using Student's t-test ***p<0.001. **B** Western blots for positive controls. NEB1 cells were treated with U0126, Wortmanin API2 and AG1478 (All at 30μM/ml for 48hrs). Representative of n=3 experiments.

5.5 shRNA based suppression of LCN2 in PC3 cells

Since pharmacological inhibitors were not successful in suppressing LCN2, in order to fully suppress expression, alternative methods were required. For this, it was decided to utilise shRNA technology. While a number of commercial vectors exist, none of these at the time had been proven in any previous publication. Therefore, vectors were obtained from Zhimin Tong's laboratory (M.D Anderson, Texas) as used in their 2009 study (Tong et al., 2009) which were originally developed by Lee et. al., (2007). The shRNA was contained within a pLL-317 plasmid vector. This plasmid also contains a blasticidin resistance gene. Alternatively, vectors containing no shRNA insert were used. This was transfected into FT293 to generate viral particles (see Materials and methods section 2.6). Viral particles were transfected into PC3 cells and selected for 2 weeks with blasticidin. This resulted in the creation of 2 cell lines namely PC3-shLCN2 and PC3-shControl (hereafter shCon).

5.6 Confirmation of LCN2 suppression in PC3-shLCN2 cells

Following 2 weeks of selection, cells were grown until 80% confluent, then split, and grown in a T25 flask before being split again, this time with samples taken for mRNA and protein extraction. qPCR analysis of PC3-shLCN2 cells showed a >1000 fold reduction in LCN2 expression (Figure 5.5A). There was no significant difference in expression between PC3-shCon and PC3-Parental cells. Furthermore, protein expression of LCN2 from protein lysates was also reduced significantly when analysed via Western blot (Figure 5.5B). Again, there was no notable difference between PC3-shCon and PC3-Parental cells.

Subsequently, media conditioned on PC3-shLCN2 cells was analysed for secreted protein expression. Both PC3-shCon and PC3-shLCN2 samples contained 1.8-

2.0ng/ml. PC3-shLCN2 cells on the other hand recorded <0.01ng/ml (Figure 5.6C). All of the above experiments were repeated at numerous passages with similar results and suppression was found to persist even after 15 passages.

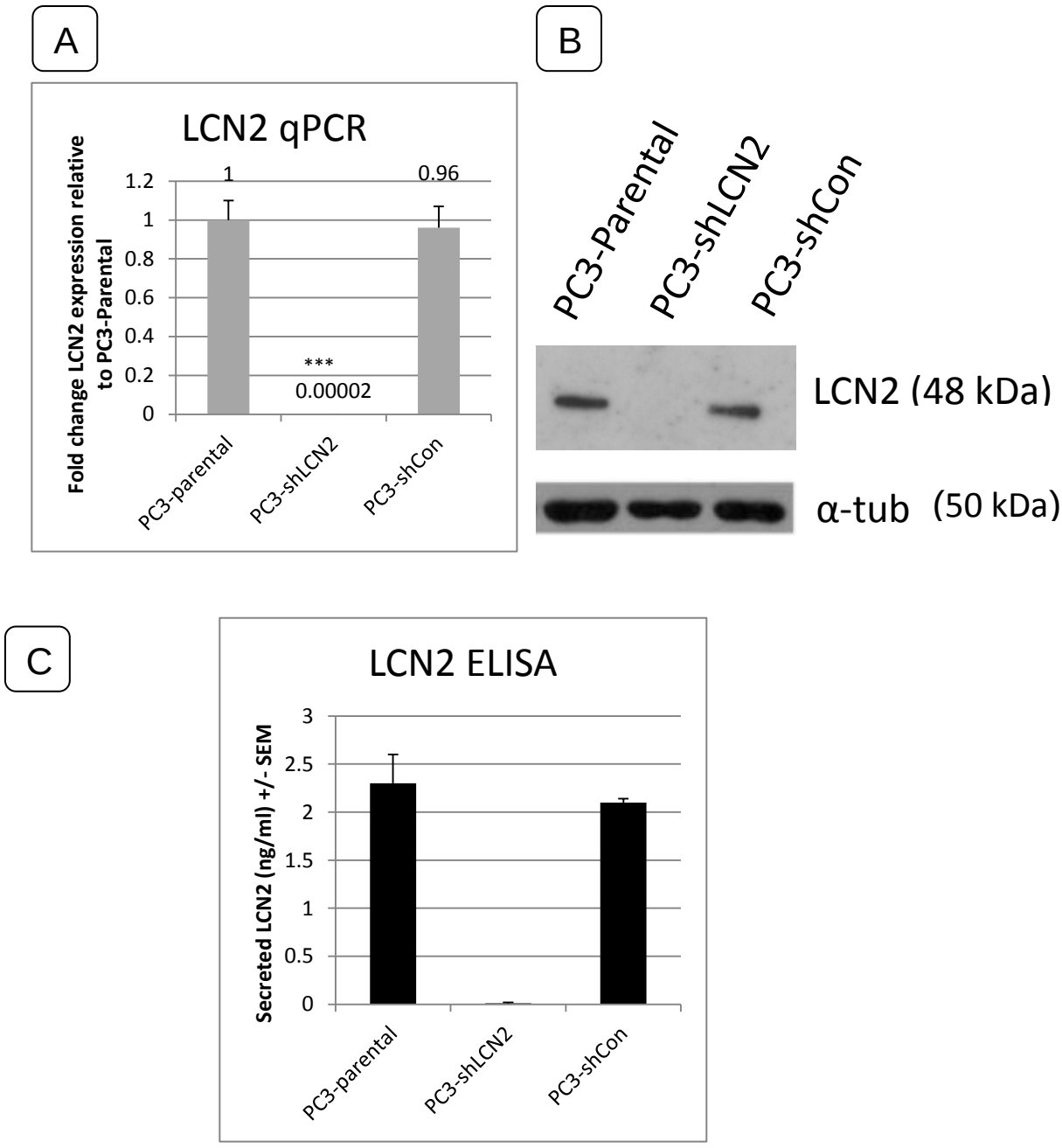

Figure 5.5: Suppression of LCN2 in PC3 cells. A- qPCR analysis of LCN2 mRNA expression in PC3-shLCN2 and PC3-shLCN2 cells relative to parental. Data is mean of n=4 experiments +/- SEM ***p<0.001. PC3. **B**- Western blot analysis of whole cell lysates (MAB1757 antibody) representative of 4 blots (mRNA and protein extracted in parallel). **C**- ELISA analysis of secreted LCN2 in ng/ml +/- SEM Statistical analysis was carried out using Student's t-test ***p<0.001 (n=3).

5.7 PC3-shLCN2 cells exhibit a distinct morphology

Parental PC3 cells are an average of ~15-20μm in size (Li et al., 2008) While there is a fair degree of variability between cells, the majority maintain a polarised structure, with a roughly ovoid shape, and are visually similar to fibroblastic cells. The majority of PC3 cells contain cellular protrusions, lamellipodia and filopodia which are used for migration and cell movement. PC3 cells do form colonies, but cells are not tightly packed, and cells may migrate from the original colony (Figure 5.6 A and B (Sobel and Sadar, 2005).

PC3-shLCN2 underwent selection for 2 weeks, followed by a further 4 days until cells reached 80% confluence. At this point, no visual changes were evident, although at this stage, there were not enough cells to extract mRNA or protein. However, following 2 further passages significant changes were observed to PC3-shLCN2 cells. Most notable was that cells were much larger in surface area relative to controls. Cells appeared to have a loss of cell polarity and overall shape. There was considerable loss of a defined cell edge, and colonies were less compact. There was considerable variation in morphology between cells. As can be seen in Figure 5.6C-D some cells were more spheroid than others, and lost fillapodia. Others on the other hand did not completely lose this function. Interestingly, there was a subset of cells which had an even more radical morphology. These cells were extremely large and flat and have no protrusions and had numerous vacuoles Figure 5.6, arrows).Under a phase light microscope, it was notable that these large cells appeared to lose some phase contrast, and had a dramatic loss of a defined cell edge. Visually, approximately 10% of the PC3-shLCN2 population were of this cell type, but were more evident a few days post seeding. Also, visually, there appeared to be a higher number of apoptosing or dead cells in the media.

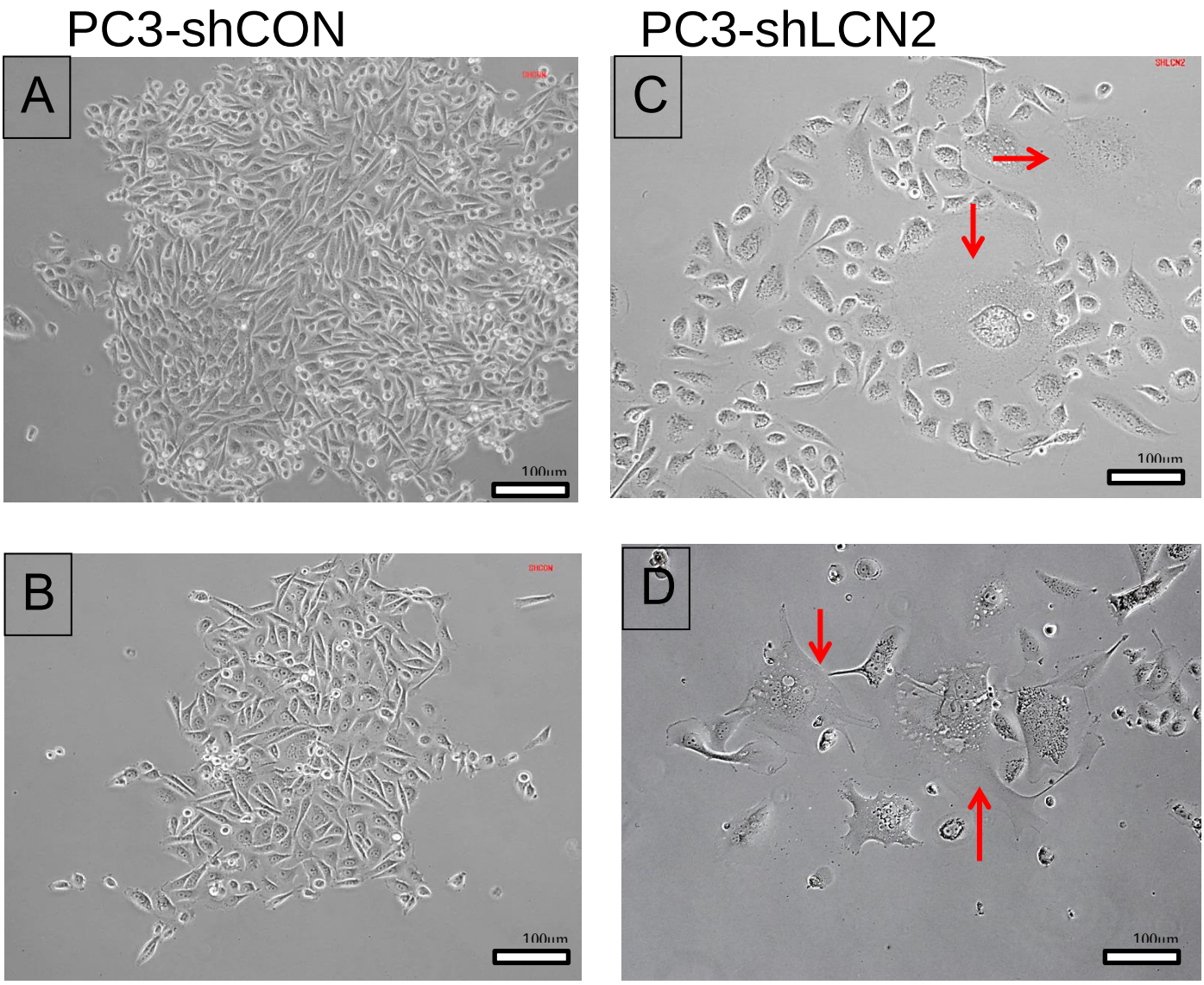

Figure 5.6 PC3-shLCN2 cells exhibit a marked change in morphology: Left panel- PC3-shCon cells in larger (A) or smaller colonies (B). Right panel. PC3-shLCN2 cells in a larger colony (C), enlarged cells are labelled with red arrows. Note- this is how the majority of colonies appear (D) Colony of PC3-shLCN2 cells with particularly pronounced morphological changes with the loss of defined cell edge (arrows). Note- pictures have been sharpened and contrast enhanced for printing purposes only. X20 magnification.

5.8 PC3-shLCN2 cells are not senescent

The drastic morphological changes observed in PC3-shLCN2 cells suggested that a number of cellular processes were involved with LCN2 suppression. One of these processes was senescence. The large, flattened cells seen in PC3-shLCN2 cells were very reminiscent of the typical 'fried egg' like morphology of a central nucleus surrounded by a flattened cytoplasm classically associated with a senescent phenotype (Goldstein, 1990, Shin et al., 2011). It was therefore hypothesised that PC3-shLCN2 cells were entering a senescent state.

To test this theory, PC3-shLCN2 and controls were tested for markers of senescence. Senescent cells are known to produce β-Galactosidase which is able to cleave X-Gal, leaving a blue precipitate. PC3-shLCN2 cells and controls were tested for β-Galactosidase activity through a commercial kit (Goldstein, 1990). H_2O_2 treated PC3 cells were used as a positive control. Results showed that contrary to expectations, PC3-shLCN2 cells did not show any β-Galactosidase activity (Figure 5.7A). PC3-shCon cells did also not show any activity.

To investigate senescence further, PC3-shLCN2 cells were tested for the expression of known senescence induced genes DEC, DEC2 and SHP1 (Xu et al., 2012b) by qPCR (Figure 5.7B). However, no change to expression was observed in any of these markers. Overall therefore, it may be seen that PC3-shLCN2 are likely not to be in a senescent state and that morphological changes observed are not part of this mechanism,

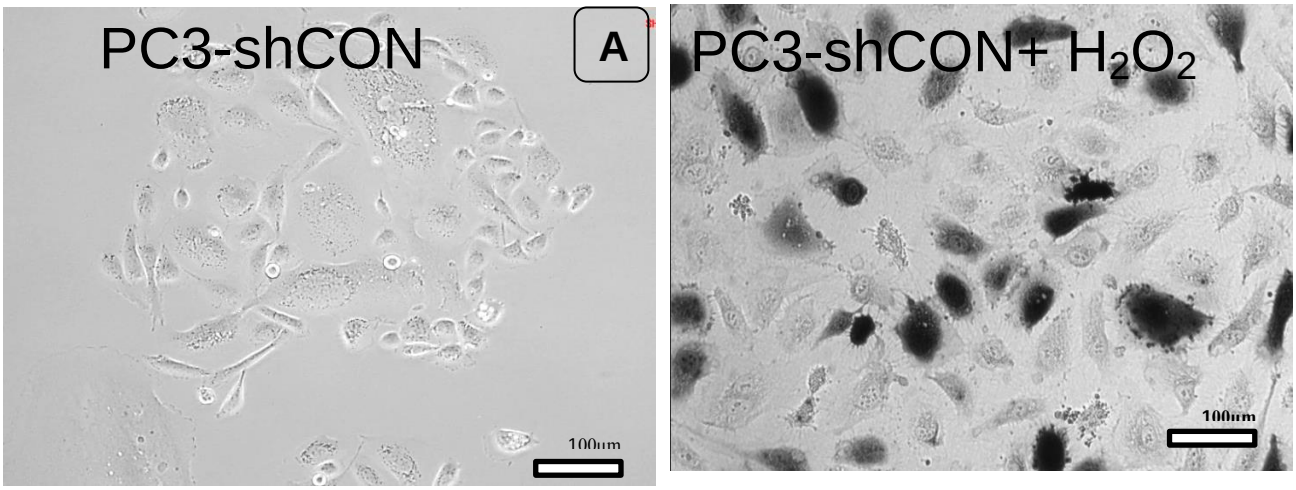

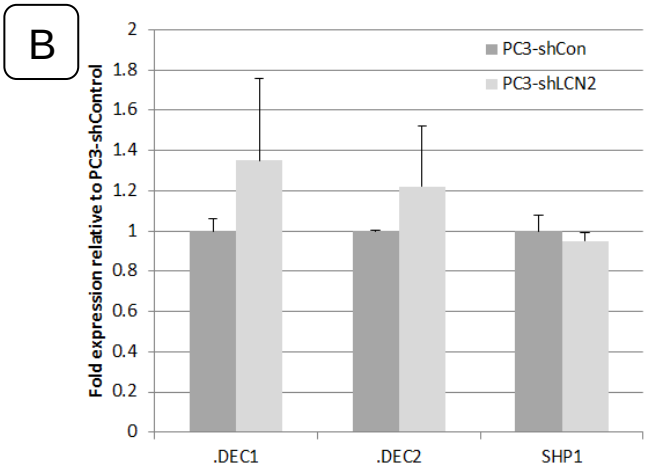

Figure 5.7 PC3-shLCN2 cells are not senescent. A Left- PC3-shLCN2 cells were treated with β-Galactosidase. Right- Positive control, PC3-shCon cells were treated with H_2O_2 for 48hrs before β-Galactosidase testing. Black spots indicate positive staining. Images have been modified for extra contrast for printing purposes only (Representative of n=4 experiments) x20 magnification. **B** qPCR analysis of senescence related genes DEC1, DEC2 and SHP1. Values are relative to PC3-shConl +/- SEM

5.9 PC3-shLCN2 cells exhibit a multi-nucleated phenotype and shifts on cell cycle.

Since PC3-shLCN2 cells were found not to be senescent, the cause of the phenotypic changes was unclear. Therefore, FACS analysis using propidium iodide (PI) was performed on cells to determine any changes to cell cycle. Figure 5.8A shows the FACS cell cycle profile for PC3-shCon cells. Unlike a normal cell line, PC3 cells shows an highly proliferative phenotype, with a large proportion of cells in S and G2 phase, indicative of fast proliferation. 31% of cells were in S phase, and a further 19% of cells were found to be in G2 phase (Figure 5.8B)

PC3-shLCN2 cells showed a markedly different FACS cell cycle profile which was highly skewed. Firstly, (as seen in Figure 5.8C-D) there were a high percentage of apoptotic or dead cells (labelled P3) comprising 11.8% of the population analysed, and which therefore backed up the visual observations. 57% cells of cells were in the G1 (P6) phase. 22% of cells were found to be in S phase (P5), which is relatively high for a cell line. However, 16.3% of cells were in G2 (P5), which is far lower than found in PC3-shCon cells indicating a loss of aggression in these cells. Most interestingly however was the observation that 3% (+/-2) of cells were in a >G2 state, suggesting that are these cells are in a state of polyploidy or have multiple nuclei. Indeed, the data showed cells with up to 16N. This unexpected result suggests that the suppression of LCN2 leads major disruption of the cell cycle or cell division process which may also be leading to cell death. To help confirm the results observed via FACS, cells were stained with the nuclear dye DAPI. As can be seen in Figure 5.9, the majority of PC3-shCon cells contain only a single or dividing nucleus. Although a small minority of cells do contain more than one nucleus, these cells are rare and many were undergoing apoptosis.

A

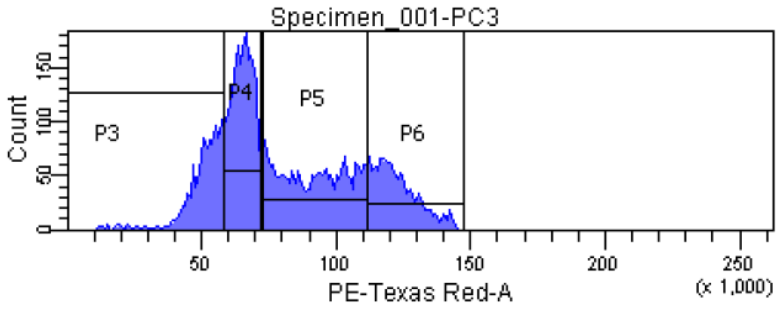

B

Tube: PC3

Population	#Events	%Parent	%Total
All Events	140,263	####	100.0
P1	45,346	32.3	32.3
P2	6,107	13.5	4.4
P3	1,051	17.2	0.7
P4	1,934	31.7	1.4
P5	2,004	32.8	1.4
P6	1,165	19.1	0.8

C

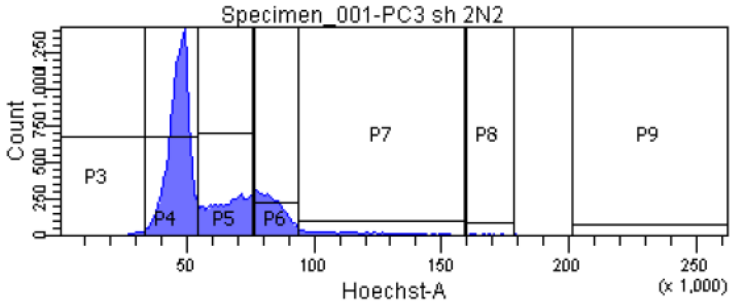

D

Tube: PC3 sh 2N2

Population	#Events	%Parent	%Total
All Events	30,000	####	100.0
P1	26,526	88.4	88.4
P2	21,099	79.5	70.3
P3	78	0.4	0.3
P4	12,008	56.9	40.0
P5	4,595	21.8	15.3
P6	3,443	16.3	11.5
P7	639	3.0	2.1
P8	10	0.0	0.0
P9	0	0.0	0.0

Figure 5.8 FACS cell cycle analysis using propidium iodide. Left panel, whole population graph. **A**- FACS profilePC3-shCon cells. **B** Breakdown of cell cycle populations: P3-G0 phase, P4- G1 phase P5-S Phase, P6-G2/M phase. **C**- PC3-shLCN2 cells FACS analysis. **D** P3- G0 phase, P4- G1 phase P5-S Phase, P6-G2/M phase. P7-9 >G2 phase. Representative of n=3 experiments taken at different passages.

By contrast, PC3-shLCN2 cells had a very different nuclear morphology which supports the FACS data. Approximately 85-90% of cells had single nuclei. These corresponded to cells which were smaller and rounder. However, in the cells which were highly enlarged and flattened, ~10-15% contained multiple nuclei. There was significant variation between cells. Some cells contained 3-4 nuclei, whereas others contained many more, indeed, some cells had upwards of 40 nuclei. Notably, many of these nuclei were small or incomplete and fragmented which may be indicative of mitotic checkpoint dysregulation (Figure 5.9). Also, within these cells, there appeared to a loss of nuclear structure, with nuclei appearing near the cell surface and dispersed apparently randomly. In the vast majority of cases, the multi-nucleated phenotype corresponded to flattened and unorganised cell morphology. Indeed, the more abnormal the morphology tended to correspond to a higher level of dysregulation in the nucleus. The presence of a multi-nucleated phenotype suggests that PC3-shLCN2 cells had lost a critical component of their cell-cycle mechanism or nuclear organisation. There are a number of reasons why this phenotype may be occurring, and it was unclear whether this was due to a loss of LCN2, or an off-target effect remained unclear. Indeed, it raises a number of questions, for instance: are the multi-nucleated cells viable? Are they able to divide? Also, why does this particular phenotype occur only in 10-15% of cells?

PC3-shCon

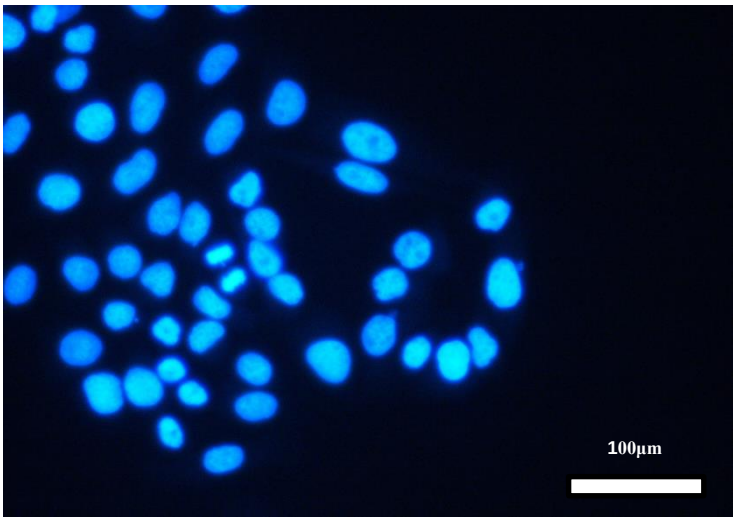

PC3-shLCN2

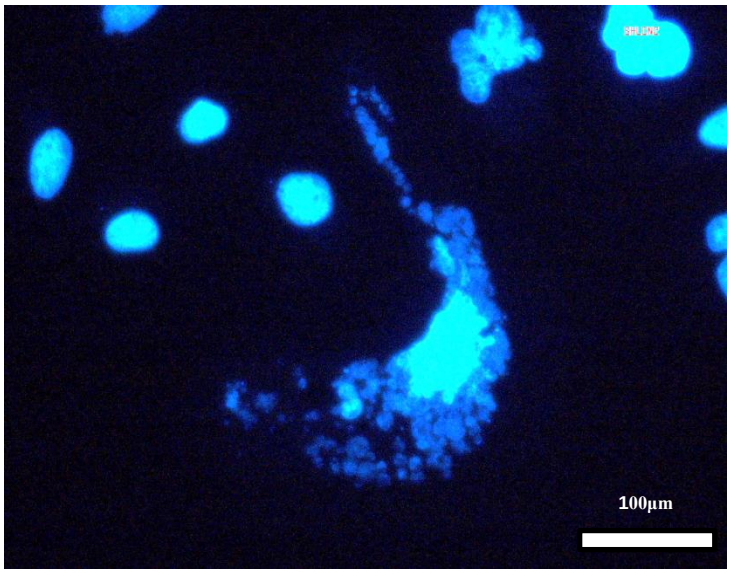

PC3-shLCN2

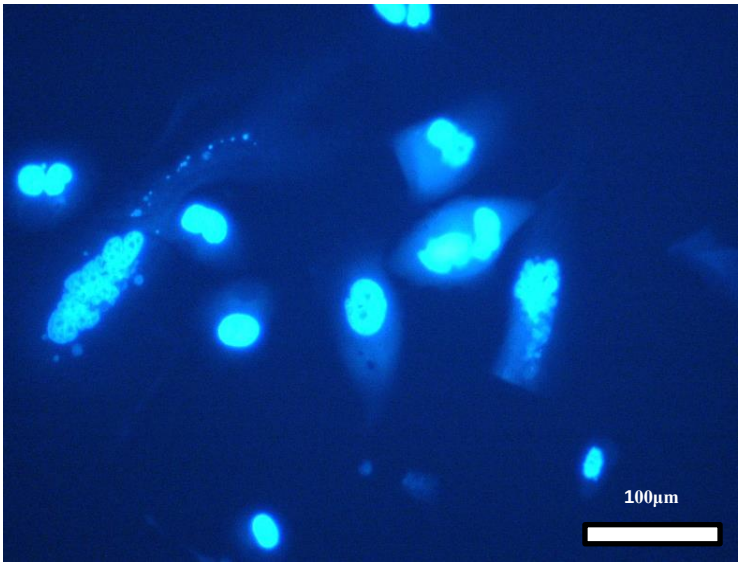

Figure 5.9 DAPI image analysis of PC3-shCon andPC3-shLCN2 cells. PC3-shCon and PC3-shLCN2 cells were fixed in paraformaldehyde and stained with DAPI. x40 magnification of cells . Scale bars- 100µm

5.10 Generation of a PC3-shLCN2 clonal cell line.

While PC3-shLCN2 cells virtually a complete loss of LCN2 expression as assessed by qPCR and Western blotting, in order to fully eliminate any chance of residual PC3-parental cells interfering with subsequent results, single cell colonies were derived from PC3-shLCN2. This process would also help determine whether all PC3-shLCN2 cells all had the capability to divide, particularly with regards to the multi-nucleated sub-population.

PC3-shLCN2 cells were diluted manually to a concentration of ~1cell/100 µl and plated on a 96 well plate. Following 24 hours, 57/96 wells contained 1 cell, 16 contained 2 or more cells and 23 contained no cells and were therefore discounted. 9/55 single cell colonies were determined to have the more enlarged and flattened morphology associated with the multi-nucleated phenotype. Following 7 days of culture, only 49 wells still contained cells. Of these, 35 had only a single cell, or had divided once only. Of the flattened and enlarged cells, none of the 9 formed colonies (1 cell had died). The remaining 14 wells contained colonies of at least 20 cells, but of varying cell number. 6 of these colonies were selected for further culturing representing a range of different colony sizes. These colonies were labelled A7, B4, B7 E5, F1 and F3 according to their position on the plate Figure 5.10A).

All 6 colonies were cultured in T25 flasks until 80% confluent. However, while none of the colonies derived from larger/flat cells. In all 6 cases, larger and flattened cells were present (Fig 5.11A). Moreover, in every sub-colony, the percentage of these enlarged cells was 10-20% (Fig 5.10B). LCN2 suppression was confirmed for each clone by qPCR which showed virtual total knockdown as per the heterogeneous population.

The results from single cell colony formation reveal that it is likely that the enlarged and multi-nucleated cells were not capable of forming colonies. However, there were only 9 of these cells in the sample; therefore this result is not conclusive. Additionally, not all PC3-shLCN2 cells were capable of colony formation, indeed only 25% of cells divided more than once, indicating that PC3-shLCN2 cells do not have stem-like characteristics. Most notably, in each clonal line, the ratio of multi-nucleated cells remained constant suggesting that this characteristic is not spontaneous, but rather is part of the overall PC3-shLCN2 phenotype is inherent to the cell line and not an artefact of the transfection.

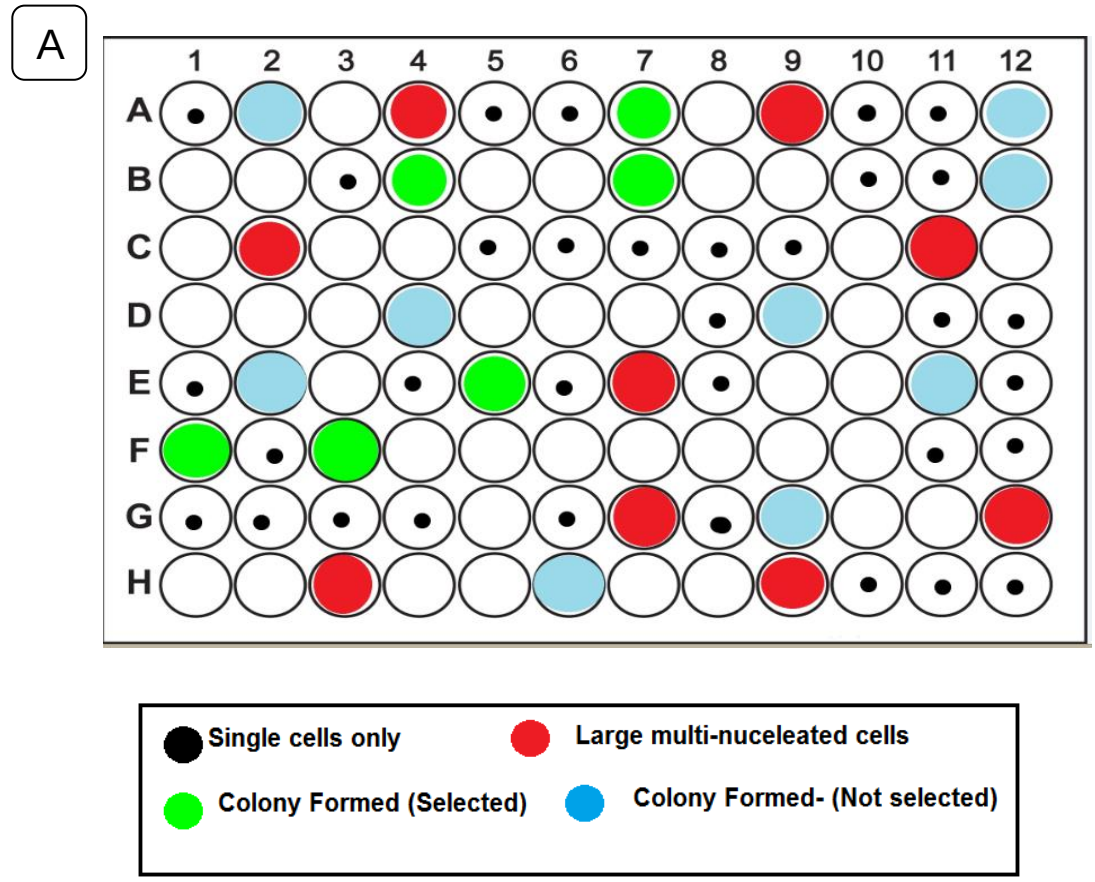

Figure 5.10 Generation of PC3-shLCN2 clones. A Single cells were seeded and grown for 10 days in a 96 well plate- layout shown. No large cells formed colonies. **B** Bright field images of sub-colonies B4 and F7 after 20 days of culture. x20 magnification.

5.11 Aberrant PC3-shLCN2 cells are migratory and motile

PC3-shLCN2 wells were found not to be senescent, however whether cells, especially the highly enlarged cells were capable of movement was unknown. To address these issues, 10000 PC3-shCon and PC3-shLCN2 cells were seeded in 6 well plates (3 wells for each cell line) and cultured for 48 hours to enable cells to settle. Plates were imaged using time-lapse photography, with images taken every 15 minutes for 12 hours. Unfortunately, due to issues with CO_2 leakage, cells started to die after 9 hours. Nevertheless,. Images were then collated into videos. Figure 5.11 displays sample images from PC3-shCon cells over 12 hours. Considerable variation existed within the population with some cells maintaining their morphology throughout, whereas others showed changes over time. As would be expected, PC3-shCon cells migrate through the use of lamellipodia.

By contrast, PC3-shLCN2 cells revealed a remarkably different behaviour. The population of relatively smaller cells migrated in a similar manner to PC3-shCon cells. Notably, cells showed evidence of lamellipodia when migrating, but with apparently less directionality than PC3-shCon. Also, morphology was relatively stable over the time period.

The most obvious feature of the PC3-shLCN2 population was the highly enlarged and flattened cells. As seen in figure 5.11, these cells did not remain in this state continuously. Rather, these cells contracted and expanded rapidly. The cells were also migratory, however rather than following thin or protruding lamellipodia, the cells followed a broader edge, or appeared to move at random. This data suggests that these aberrant cells are not senescent, and are indeed highly active. It also shows

that there are significant regulatory pathways being activated or deactivated rapidly. However, this data may also indicate that the cells are under stress and have lost some form of internal regulation.

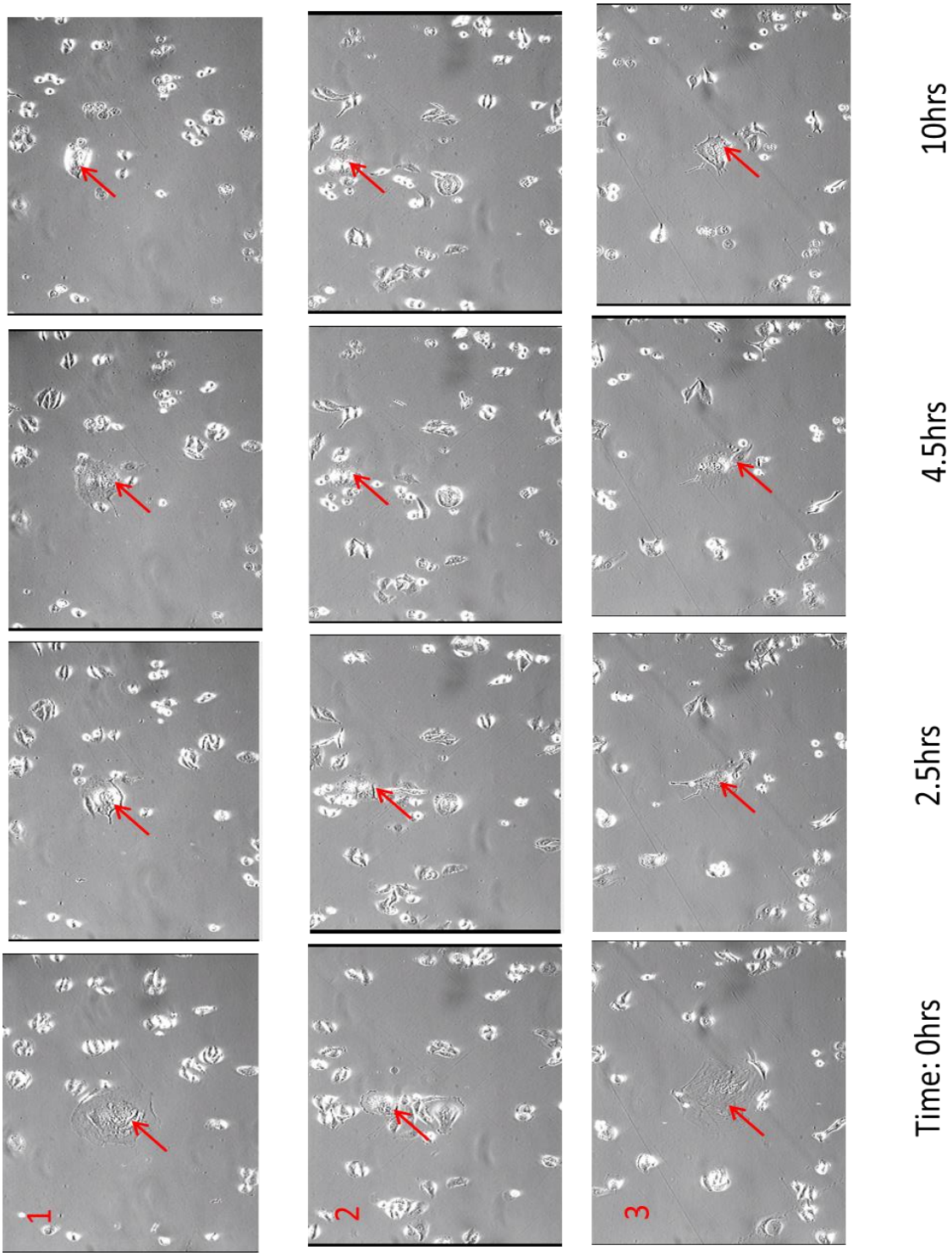

Figure 5.11 Time lapse imagery of PC3-shLCN2 cells. PC3-shLCN2 cells were cultured at low density before being analysed via a time lapse microscope. Images were every 14-15 minutes. Cells of interest are labelled with arrows. Each group of images is from a different well. x20 magnification

5.12 PC3-shLCN2 cells display reduced proliferation in 2D and 3D cultures.

Since PC3-shLCN2 cells showed such a notable shift in cell cycle. This was likely to be affecting cell proliferation rates. Alamar Blue was employed to analyse proliferation rates. Results confirmed that over 7 days, PC3-shLCN2 cells proliferated on average 0.61x the rate of PC3-shCon (Figure 5.14). No statistically significant difference was observed between PC3-shCon and PC3-Parental cells. (Figure 5.12)

All of the above experiments involving PC3-shLCN2 were performed on a 2D plastic substrate. However, this method of culture does not accurately mimic the conditions within a tissue whereby cells grow in three dimensions and are able to grow into a soft matrix rather than impervious plastic. To overcome this issue, PC3-shCon, PC3-shLCN2 and PC3-Parental cells were grown in a soft agar suspension consisting of 3 layers: 1% agar 0.6% Agar and cells and media. Cells were cultured for 14 days with media changed every 3 days.

PC3-shCon and PC3-Parental cells both formed 3D colonies in culture (Figure 5.13). These colonies ranged in size from a 10's of cells to colonies 1000-2000μM in diameter. These colonies in most cases were either compact spherical or ovoid in shape. From ~1000 cells seeded, colony density was 6 colonies/cm^2 whereby a colony was defined as >50 cells. By contrast, PC3-shLCN2 cells did not form any colonies whatsoever in soft agar (Figure 5.13), and no cells in the matrix were able to divide more than twice to form colonies >50 cells (i.e. 0 colonies/cm^2), although notably some single divisions were common. Indeed, it appeared that the majority of cells had died indicating that PC3-shLCN2 cells are incapable of growth within a 3D substrate.

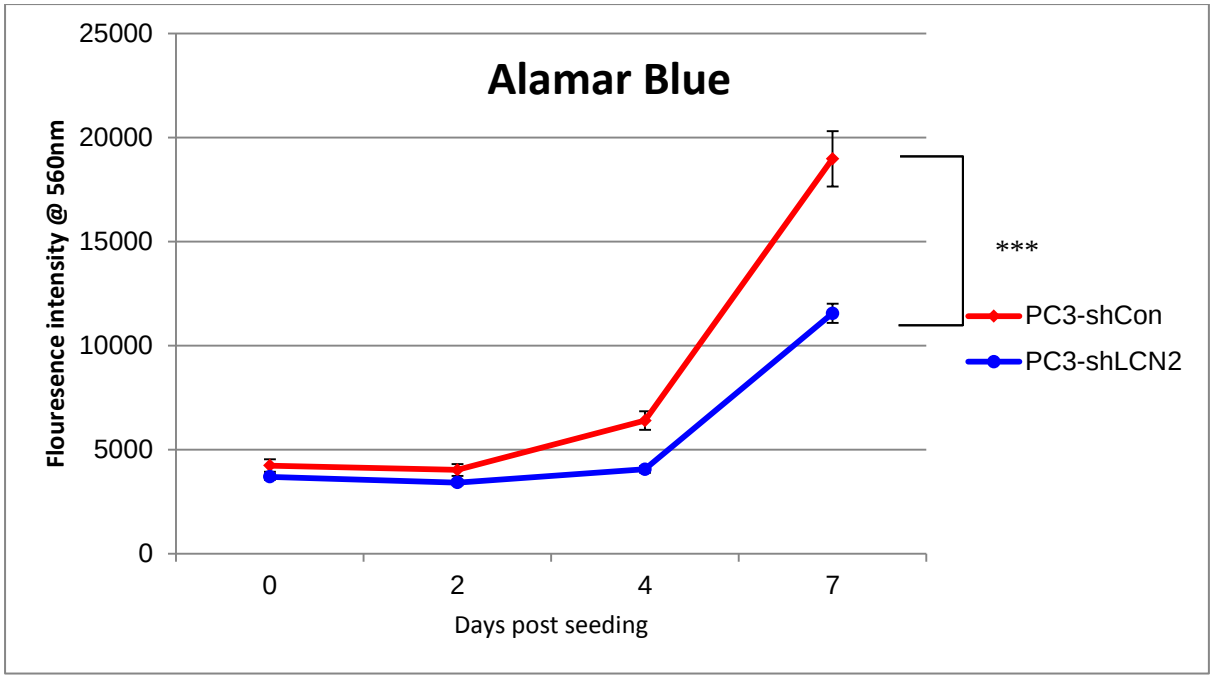

5.12 PC3-shLCN2 proliferation in 2D culture Alamar Blue proliferation assay- cells were cultured for 7 days until PC3-shLCN2 cells obtained 100% confluence. Values are mean of n=3 experiments +/- SEM for each data point. Statistical analysis was carried out using Student's t-test.. ***p<0.001

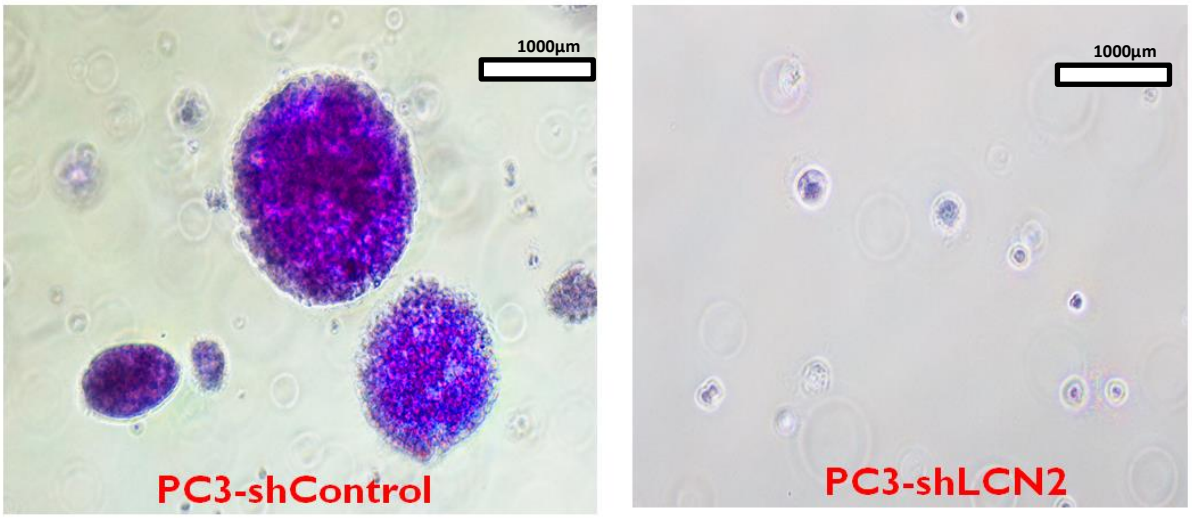

5.13 PC3-sLCN2 colony formation in 3D culture. Soft agar colony formation assay. x10 magnification. Cells were cultured 14 days in a 0.6% Soft agar/ media mixture layered on a 1% soft agar solution and supplemented with media and stained with crystal violet. (n=3). Images are representative of n=3 experiments. All conditions performed in triplicate.

5.13 Hormone receptor regulation PC3-shLCN2 cells.

PC3 cells are an androgen independent PCa cell line which do not express the AR protein, and mRNA expression of AR is very low (Alimirah et al., 2006). However, PC3 cells are not totally hormone independent and have been shown previously to still express both ERα and ERβ. Indeed, at a protein level, ERβ is expressed at a relatively higher level than ERα (Mak et al., 2010). ERβ expression has also been shown to inhibit EMT in PC3 cells (Mak et al., 2010). Given that LNCaP-LCN2 cells showed significant changes to both ER and AR expression, it was hypothesised that suppression of LCN2 in PC3 cells would also be affecting their expression as well.

Previously, I found that LNCaP-LCN2 cells had increased levels of AR protein (but not mRNA) expression (See section 4.16.1). I subsequently investigated AR expression in PC3-shLCN2 cells to determine any changes to expression. AR mRNA is expressed very weakly in PC3 cells, and mRNA expression also did not change PC3-shLCN2 cells (Figure 5.14A). However PC3 cells do not express AR protein; this was unchanged in PC3-shLCN2 cells (Figure 5.14B). As such, these results indicate that LCN2 has little effect on AR in PC3 cells, or that due to low initial expression in control cells, any changes were undetectable. The role of AR signalling in PC3-shLCN2 therefore was not explored further.

Previously, I found that LNCaP-LCN2 cells had reduced ERα expression, but increased ERβ expression (See section 4.16.2). Therefore, I aimed to see if and changes to ERα/β expression occurred when LCN2 was suppressed in PC3-shLCN2 cells. qPCR analysis of both the ESR1 and ESR2 genes (which encode ERα and ERβ respectively) did not show any change in expression relative to PC3-shCon cells (Figure 5.14A).

With regards to ER protein expression. ERβ was also found to be expressed at a higher level than ERα in PC3-shCon cells. Thus agreeing with previous studies in PC3 cells (Mak et al., 2010). In PC3-shLCN2 cells however, ERα expression was markedly increased (Figure 5.14B). This was mirrored by a loss of ERβ expression. This therefore, was the opposite effect seen in LNCaP-LCN2 cells (See section 4.16.2).

To test the functional relevance of the change in ER expression, Downstream ERα targets were analysed. The classical ER target HER2 (Li et al., 2009) however was unchanged in PC3-shLCN2 cells relative to controls and remained only weakly expressed suggesting that classical ER signalling had not been activated. Alternatively, this may be due to fairly weak mRNA signals in both PC3-shLCN2 and control cells. However, a further ER target, EGFR did display a decrease in expression mRNA level (reduced 2.3 fold) (Figure 5.14A). At the protein level, PC3-shLCN2 cells also showed a reduction both phospho-EGFR and to total EGFR (Figure 5.14B. Loss of EGFR expression therefore was in direct contrast to LNCaP-LCN2 cells which showed increased EGFR mRNA expression (See figure 4.16A)

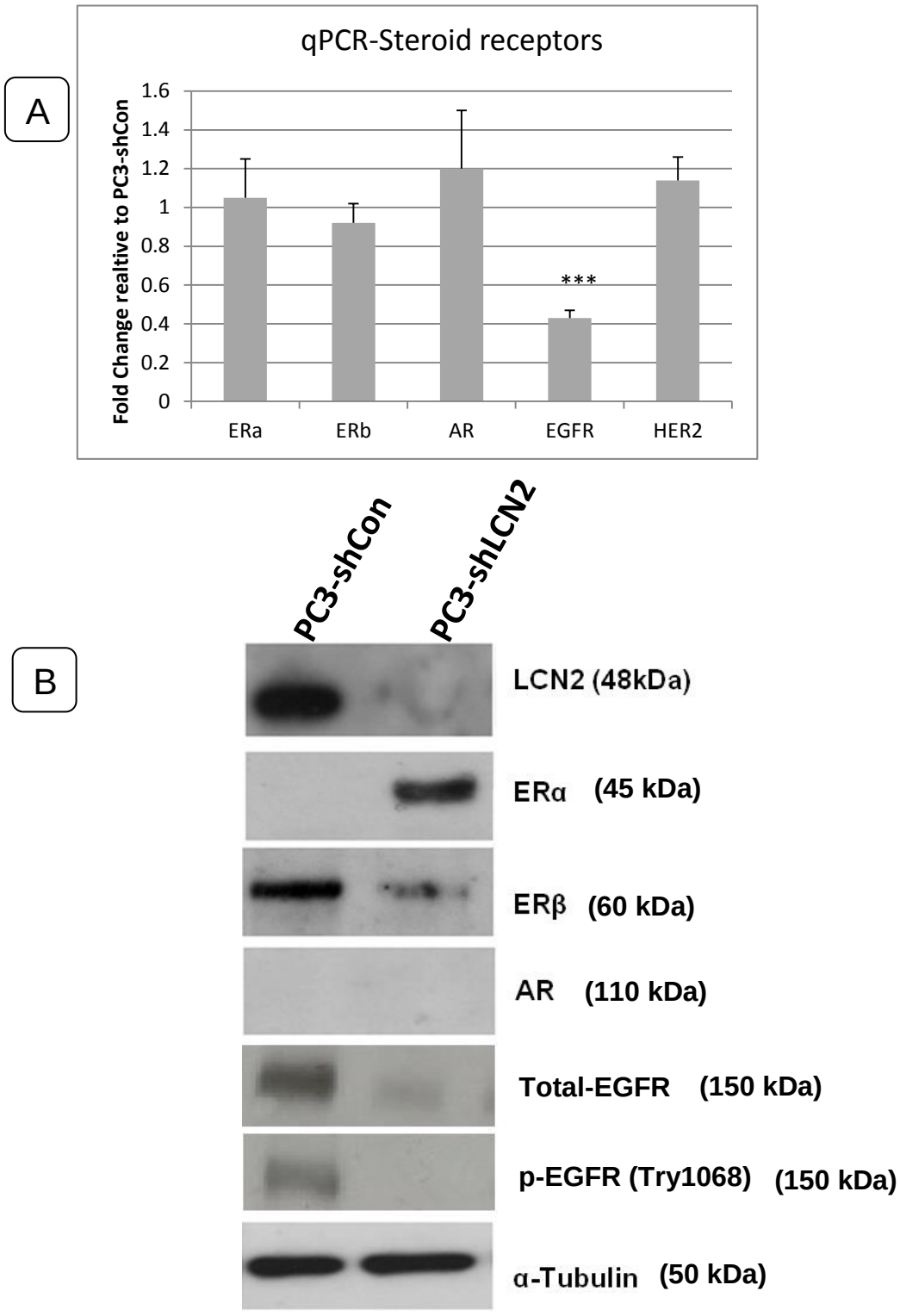

Figure 5.14 PC3-shLCN2 cells display altered ER protein expression. A- qPCR analysis of ERα, ERβ, and the target genes HER2 and EGFR IN PC3-shLCN2 cells relative to PC3-shCon. Values are mean of n=3 experiments taken at different passages.+/- SEM ***p<0.01 B- Western blot analysis of ERα, ERβ, AR EGFR and p-EGFR. Representative of n=3 blots. Protein and mRNA extracted in parallel.

5.14 PC3-shLCN2 cells are responsive to Estradiol.

To assess the functional relevance of the shift in ERα to ERβ ratio, PC3-shCon and PC3-shLCN2 cells were supplemented with both the ER agonist Estradiol (E2) and the ER antagonist ICI-182-780. Since normal culture media with FBS contains a range of endogenous steroids, both PC3-shCon and PC3-shLCN2 cells were first cultured in charcoal stripped (CS) serum for 7 days to assess the effect on proliferation via Alamar blue assays. CSS had a small anti-proliferative effect on both sets of cells. Following 7 days of culture in CS serum, PC3-shCon cells proliferated at 0.86x rate of those grown in normal serum. PC3-shLCN2 cells proliferated at 0.80x of rate of those grown in normal serum (Figure 5.15). Therefore, the ratio between proliferation between PC3-shLCN2and PC3-shCon and remained relatively stable at 68%. This data also shows that PC3-shLCN2 cells have not become hormone dependent, and are able to proliferate, at least for 7 days, without the presence of steroids.

75,000 cells/ well PC3-shCon and PC3-shLCN2 cells were seeded in CS serum containing media, and treated with either E2 (5nM/ml) or ICI-182-780 (10μM/ml). In addition, cells were also treated with a combination of both E2 and ICI-182-780. Cells were cultured for 5 days, at which point PC3-shCon cells were >90% confluent.

PC3-shCon cells were slightly, but still significantly responsive to E2, and proliferated 14% more than rate of untreated cells ($p<0.01$). In contrast, PC3-shCon cells were unresponsive to ICI-182-780 and showed no statistically significant change to proliferation. Unexpectedly however, cells treated with both E2 and ICI-182-780 showed a notable reduction in proliferation after 5 days (85% of untreated cells,

p<0.01) which may be indicative of a synergistic, albeit counter-intuitive effect between the two compounds.

PC3-shLCN2 cells on the other hand were strongly responsive to E2, with a 45% increase in proliferation relative to untreated cells (p<0.001. Indeed after 5 days of culture, proliferation increased to a similar level of that found in untreated PC3-shCon cells, suggesting that ERα is active in these cells and able to drive growth. However, ICI-182-780 had no statistically significant effect on proliferation. As with PC3-shLCN2 cells, a combination of both ICI-182-780 and E2 had a highly significant inhibitory effect, reducing proliferation by 47.8% relative to untreated cells (p<0.01). There are a number of reasons why this may be the case. Firstly, ICI-182-780 has been shown to promote ERα degradation by localising the protein to the nuclear matrix (Long et. al, 2006). ICI-182-780 is also known to prevent dimerization of ERα, and undimerized protein has been shown to have anti-proliferative effects which may be exaggerated by additional E2.

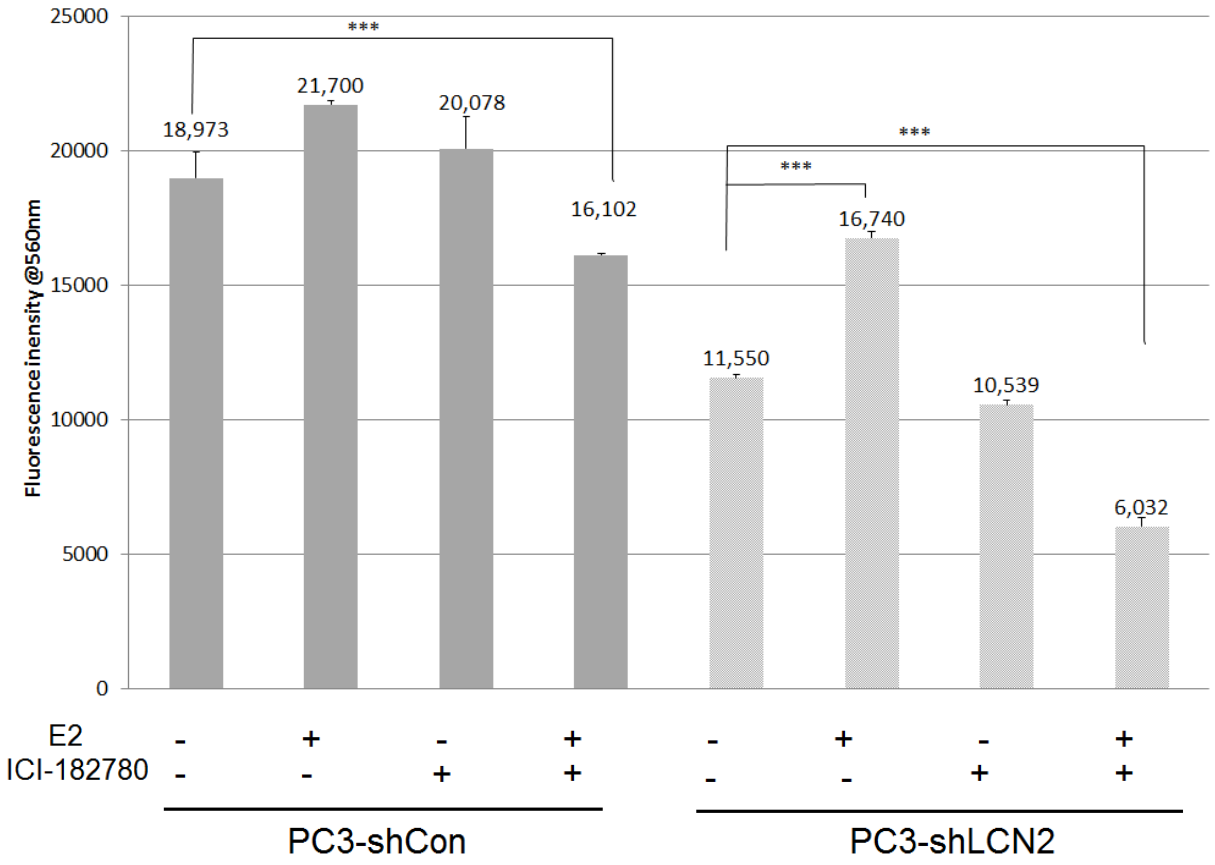

5.15 PC3-shLCN2 cells in response to ER agonists and antagonists. Alamar blue assay. Cells were treated with either the ER agonist E2, or antagonist ICI-182,780 with readings taken at 0, 1, 2 and 5 days at which point PC3-shCon cells attained near confluence. Graph represents readings after 5 days only. Values are mean of n=3 +/- SEM. ***p<0.001

5.15 E-cadherin Expression in PC3-shLCN2 cells

As well as steroid receptor expression, the effects of LCN2 were also investigated with regards to EMT. LCN2 has been previously been shown to down-regulate E-cadherin (Yang et. al, 2009; Leng et. al. 2009), and this was also associated with an increased vimentin expression. However, in LNCaP-LCN2 cells, I observed the opposite effect of E-cadherin expression being increased. Also, PC3-shLCN2 cells exhibited visible changes to cell membranes, (such as loss of phase contrast and defined edges) and size which may be indicative to changes to structural proteins such as E-cadherin. Therefore, I aimed to investigate the effects of LCN2 suppression on E-cadherin, as well as a range of classical EMT markers in PC3-shLCN2 cells.

PC3 cells display signs of a partial EMT signature, with high expression of vimentin and CD44 (Tai et. al,. 2009). However, PC3 cells still express low levels of E-cadherin. In my experiments, E-cadherin protein was detected at identical low levels in PC3-Parental cells and PC3-shCon cells. However in PC3-shLCN2 cells, E-cadherin protein expression was completely lost. vimentin and CD44 however did not show any change to protein expression in PC3-shLCN2 cells (Figure 5.16A).

With regard to mRNA expression, E-cadherin (gene name CDH1) was strongly repressed in PC3-shLCN2 cells. Initial results revealed a 10.1 fold reduction (Figure 5.16B) subsequent qPCR analysis consistently showed between an 8-12 fold reductions in CHD1. When other EMT markers were tested however, no change to mRNA expression was observed for vimentin (VIM), CD44 or ΔNP63. Combined with protein expression, the therefore suggests that the loss of LCN2 (as with ectopic

expression) is not influencing EMT as a whole, but rather appears to acting specifically on E-cadherin.

E-cadherin (CHD1) mRNA expression is known to be regulated by a range of transcription factors. Of these, TWIST1, SNAI1 (a.k.a Snail), SNAI2 (a.k.a Slug) and ZEB1 have been implicated with controlling E-cadherin's role in EMT. While there is some debate to the precise roles of these transcription factors, TWIST1, Snail and Slug have been shown to positively regulate E-cadherin, whilst ZEB1 has been shown to repress its transcription. qPCR analysis was therefore carried out on these genes to observe if any changes in expression were observed in PC3-shLCN2 cells.

Results revealed that there were indeed changes to transcription factor expression (Figure 5.16B). TWIST1 displayed a modest but consistent increase in expression of 1.33 fold in PC3-shLCN2 relative to PC3-shCon ($p=0.021$). SNAI2 (Slug) did not show any significant change. SNAI1(Snail) however did show a 4.2 fold decrease in expression ($p<0.01$). Conversely, ZEB1 showed a 4.31 fold increase in PC3-shLCN2. While no protein analysis on these genes was performed. It appears therefore that observed changes to expression are in accordance with previous literature and give an insight into the mechanisms by which E-cadherin is being repressed in PC3-shLCN2 cells.

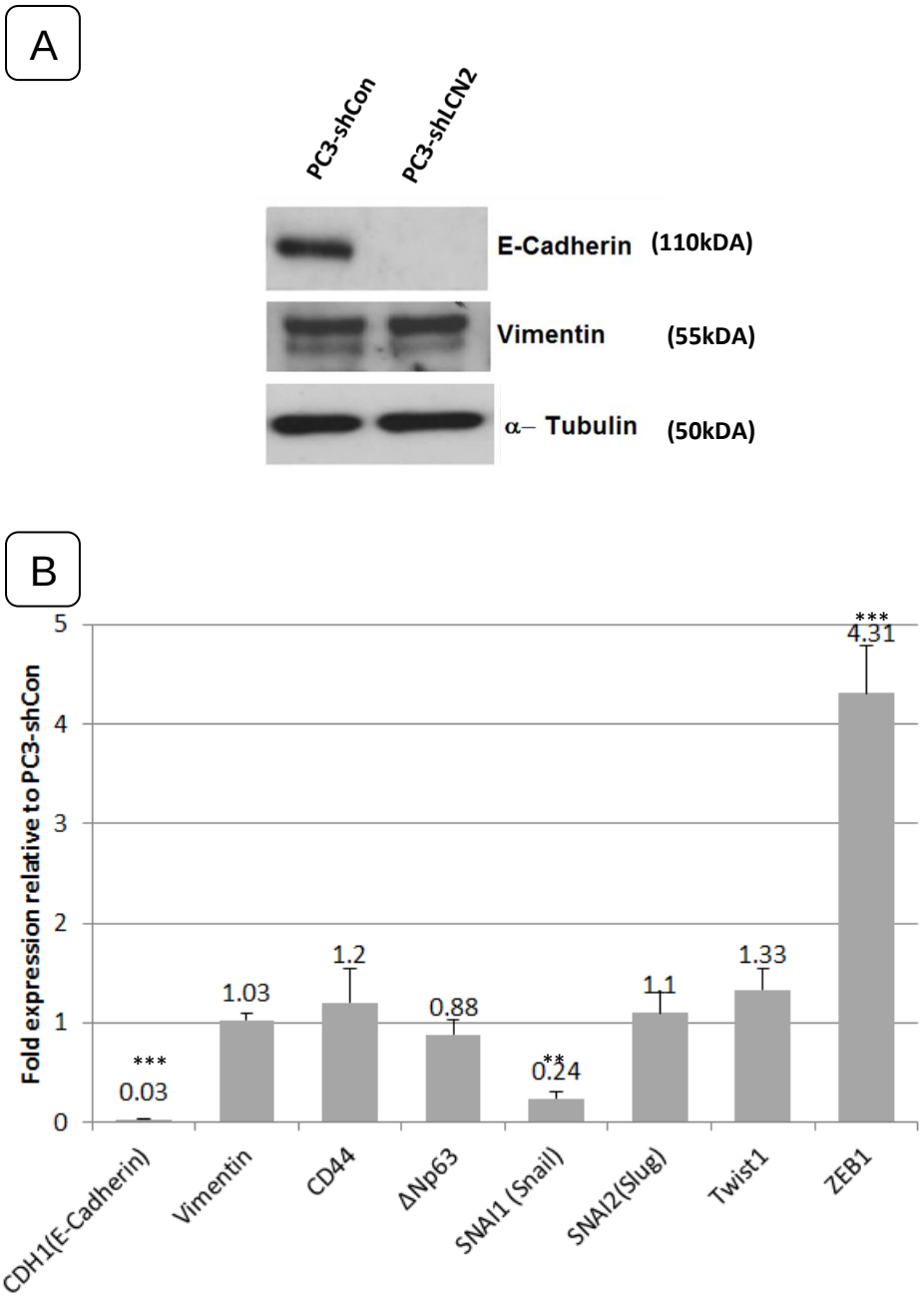

Figure 5.16 EMT marker expression inPC3-shLCN2 cells: A- Western Blot analysis of E-cadherin and vimentin. Representative of 3 blots **B**-qPCR analysis of EMT linked genes. Values are relative to expression in PC3-shLCN2 cells +/- SEM Statistical analysis was carried out using Student's t-test. **p<0.01 ***p<0.001. Average of n=3.

5.16 Discussion

In this chapter I have demonstrated that suppression of LCN2 in PC3 cells results in changes in cell morphology coupled with changes to both ER and E-cadherin expression.

LCN2 was investigated in PC3 cells as it was hypothesised that LCN2 may be a target gene of the hedgehog pathway or GLI1 based on previous data from microarray analysis of LNCaP-GLI1 cells. However, no change to LCN2 expression was observed upon suppression of GLI1. It may be the case that GLI may activate LCN2 in a non-reversible method, as was seen for ΔNP63 and CD44 (See section 3.4). However, since GLI is such a widely expressed gene this is unlikely given that having a non-reversible switch would have major implications for all cells. More likely is that GLI interacts with other pathways which are not turned off when GLI is inhibited. For instance, GLI may be activating the NF-κB pathway (Riobo et al., 2006) which is known to bind to the LCN2 promoter (Karlsen et al., 2010). .As GLI interacts with a wide range of pathways, it is difficult to identify exactly which factors these may be, and may involve more than one pathway. Alternatively, LCN2 expression may by symptomatic of an unrelated pathway which does not interact with GLI directly. GLI1 is known to confer morphological changes and changes to cell cycle, and LCN2 expression may be a result of these.

NF-κB has been shown to be one of the key regulators of LCN2 expression and has been shown as a promoter of LCN2 mRNA expression (Li et al., 2009, Tung et al., 2013). The NF-κB inhibitor BAY-11-7082 had a strong toxic effect on PC3 cells, however, unexpectedly; it did not affect LCN2 expression at all. It may be that NF-κB acts only as an initiator of transcription, or that other factors are involved as well.

Alternatively, it may be that in PC3 cells, the toxic effects of the drug simply occur before any inhibition of LCN2 can occur or be detected. NF-κB is known to interact with a range of apoptotic factors including BCL2 and BCLxL (Chen et al., 2000, Viatour et al., 2003). Therefore apoptosis may be occurring before any interaction with LCN2 can take effect.

Aside from NF-κB, I observed that EGFR inhibition led to partial suppression of LCN2, correlating with other studies which have shown similar results (Mir et al., 2012, Viau et al., 2010). PC3-shLCN2 cells showed decreased expression of both total and phosphor-EGFR. This may therefore be indicative of a feedback mechanism between the EGFR and LCN2 whereby the expression of one activates the other. Indeed, a study by Lim at al. showed that LCN2 expression was positively correlated to EGFR expression in ovarian cells (Lim et al., 2007). Both positive and negative feedback loops exist for EGFR (Avraham and Yarden, 2011), and involve numerous interconnected mechanisms including estrogen receptor (Filardo, 2002). Therefore, in PC3-shLCN2 cells the data suggests that suppression of LCN2 leads to increased ERα, which in turn inhibits EGFR.

Following suppression of LCN2 I observed marked morphological changes in PC3-shLCN2 cells. These included a loss of cellular protrusions and increased cell size. A notable effect was the presence of a sub-population of multi-nucleated cells comprising ~12% of total cells. Moreover, this population was maintained in clonally derived cell lines. However, the multi-nucleated cells themselves were incapable of cell division themselves. This may be indicative of LCN2 disrupting cell division and nuclear assembly and this was backed up by subsequent microarray analysis. During the course of the project, it emerged that Tung et al (2013) also used suppression. LCN2 in PC3 using shRNA. In this study, the authors also noted a large

reduction in proliferation of PC3-LCN2 knockdown cells of 480% after 3 days, although those statistics are somewhat misleading as they are a measurement relative to cell number at day 0. The group also noted an increase in LCN2 knockdown cells in G0/G1 phase, which is also consistent results obtained in this study. The Tung et al. study did not however mention any phenotypic change or changes to nuclear organisation. Notably, the study also showed PC3 LCN2 knockdown cells having increased p53 and p21 levels coupled with a loss of cyclin D1.It appears therefore that the highly enlarged cells may be as a result of key cell cycle checkpoint proteins being dis-regulated, which over time may build up, resulting in catastrophic loss of cellular and nuclear organisation. This may also be why these effects were not noted until a few weeks post viral transfection.

In these results I have demonstrated that PC3-shLCN2 cells showed increased ERα expression, coupled with a loss of both ERβ and E-cadherin. This directly mirrored data from LNCaP-LCN2 (See chapter 4) and confirmed a negative correlation between LCN2 and ERα. With regards EMT expression however, a positive correlation was observed between E-cadherin and LCN2 (also directly mirroring LNCaP-LCN2 data). This correlation was the opposite of what was previously described in breast cancer cells (Yang et al, 2009) with ERα traditionally being described as suppressing E-cadherin expression (Oesterreich et al, 2003). As well as E-cadherin, opposing expression was also seen for the E-cadherin transcriptional repressor ZEB1. As to why there are differences between my study and the Yang et al. 2009 study; it may be that breast cells also express an unknown co-activator or co-repressor which does not occur in PC3-shLCN2 cells. The methylation activity of repressors such SNAIL is also variable between cell type. Also, estrogen receptor itself has been shown to directly interact with E-cadherin expression and can act as

either a activator or repressor depending on whether it is bound to a ligand or not (Cardamone et al., 2009). The data suggests therefore, that unlike in breast cancer cells, in prostate PC3-shLCN2 cells, ER is inhibiting E-cadherin and that differences to breast cancer cells are due to another factor which is different in the parental populations between PC3 and breast cancer cells.

A number of studies have indicated that LCN2 expression contributes to an EMT phenotype (Liao et al., 2013, Yang et al., 2009). Conversely, a recent study by Wang et al. showed LCN2 inhibition of an EMT phenotype in hepatocarcinoma cells (Wang et al., 2013a). In my study, I observed that LCN2 expression was positively correlated to E-cadherin expression, and this may be mediated through ZEB1 repressor activity. However, contrary to previous studies mentioned, the effects of LCN2 appeared to affect only E-cadherin and did not affect other EMT markers such as vimentin. This therefore suggests that LCN2 is interacting with more specific signalling pathways. Indeed, the expression of E-cadherin and vimentin are often independent of other each other and to other EMT markers, and E-cadherin expression does not necessarily lead to loss of vimentin and vice versa (Micalizzi et al., 2010, Kalluri and Weinberg, 2009).

In conclusion, a few key points emerge from the data presented in this study:

1. LCN2 suppression in PC3 cells has a marked effect on cell morphology, proliferation and nuclear stability
2. Further confirmation of a negative correlation between LCN2 and ERα, but a positive correlation to E-cadherin expression

Chapter 6
Global analysis of gene expression in PC3-shLCN2 cells.

Results

6.1 Microarray Analysis of PC3-shLCN2 cells.

LCN2 has been implicated in a wide range of signalling pathways as previously mentioned, including NF-κB (Mahadevan et al., 2011), steroid receptor signalling (Guo et al., 2012), IL1β (Cowland et al., 2006)and angiogenesis (Yang et al., 2013)pathways among others. Studies on these pathways have tended to be focussed on just one of pathway or mechanism. To date however, no comprehensive study has been performed which has looked at global expression patterns in response to either suppressed or ectopic LCN2, and no microarrays have been performed. As LCN2 is still a relatively under-studied protein, there are still many gaps in our understanding of the downstream effects of LCN2. As such many potential LCN2 targets and pathways may have been overlooked or simply not considered in the first instance. As LCN2 is now being proposed as a therapeutic agent and biomarker (Xu et al., 2012a) it is therefore necessary to obtain a fuller picture of what the effects of LCN2 suppression are.

The gap in knowledge of LCN2 function, combined with the numerous phenotypic changes observed in PC3-shLCN2 cells therefore provides a good opportunity to elucidate exactly what influence LCN2 has in cells. mRNA microarray analysis was carried out comparing PC3-shCon cells with PC3-shLCN2. Arrays were carried out in triplicate using AFFYMETRIX arrays. This system contains on average 6-10 mRNA binding sites for approximately 19500 genes. The array also includes data for a sample of 180 microRNAs. The raw data was then analysed by the Robust Multi-array Average (RMA) technique which adjusts for background noise. Statistically corrected values were then anti-logged to provide fold change values.

The results of the microarray revealed numerous changes in expression. Using an arbitrary cut off point of 1.5 fold, 842 genes were up-regulated in PC3-shLCN2 relative to PC3-shControl. Conversely, 808 genes were down regulated < -1.5 fold in PC3-shLCN2, in total 8.04% of all genes were differentially regulated at least 1.5 fold. Using more stringent criteria of 2 fold change, 255 genes were up-regulated, whereas 191 were down-regulated, representing 2.28% of all genes. While tending towards slightly higher numbers of up-regulated genes, overall the numbers of genes either up or down was approximately equal. Tables 6.1A-B list the top 20 up and down genes respectively in PC3-shLCN2 cells relative to PC3-shCon cells. From this list, a number of interesting genes emerge including (up-regulated)VEGFR and SPARC and IL1B as well as (down-regulated) CHD1/E-cadherin, ACTG2 and KLK6. Also notable was in increase in expression of HSD17B12 which is involved with the steroid synthesis pathway.

A: PC3-shLCN2Up-regulated genes

Symbol	Description	Accession No.	Fold Change v PC3-shControl
KDR	Kinase insert domain receptor (a type III receptor tyrosine kinase)	NM_002253	10.056107
SPARC	Secreted protein, acidic, cysteine-rich (osteonectin)	NM_003118	9.426137111
TFPI	Tissue factor pathway inhibitor	NM_006287	9.126109727
CADM2	Cell adhesion molecule 2	NM_001167674	8.594021184
AGR2	Anterior gradient homolog 2 (Xenopus laevis)	NM_006408	8.0556444
HSD17B2	hydroxysteroid (17-beta) dehydrogenase 2	NM_002153	6.558351987
TBXAS1	thromboxane A synthase 1 (platelet)	NM_001130966	6.119158774
SPRY1	sprouty homolog 1, antagonist of FGF signaling (Drosophila)	NM_005841	5.869889452
B3GALT1	UDP-Gal:betaGlcNAc beta 1,3-galactosyltransferase, polypeptide 1	NM_020981	5.630774336
GABBR2	gamma-aminobutyric acid (GABA) B receptor, 2	NM_005458	5.0396842
SPTLC3	serine palmitoyltransferase, long chain base subunit 3	NM_018327	4.637455164
HPGD	hydroxyprostaglandin dehydrogenase 15-(NAD)	NM_000860	4.428035126
HIST2H2BF	histone cluster 2, H2bf	NM_001024599	4.267328972
SLC2A12	solute carrier family 2 (facilitated glucose transporter), member 12	NM_145176	4.218314518
FAM131B	family with sequence similarity 131, member B	NM_001031690	4.218314518
IL1B	interleukin 1, beta	NM_000576	4.189176491
TMPRSS2	transmembrane protease, serine 2	NM_001135099	3.908639874

B: PC3-shLCN2 down-regulated genes

Symbol	Description	Accession No.	Fold Change v PC3-shControl
ACTG2	actin, gamma 2, smooth muscle, enteric	NM_001615	-36.42019311
ESRP1	epithelial splicing regulatory protein 1	NM_017697	-29.10778861
PRND	prion protein 2 (dublet)	NM_012409	-18.98340216
KLK6	kallikrein-related peptidase 6	NM_002774	-14.6213032
ST14	suppression of tumorigenicity 14 (colon carcinoma)	NM_021978	-13.86459273
LAD1	ladinin 1	NM_005558	-13.8325957
IL13RA2	interleukin 13 receptor, alpha 2	NM_000640	-13.547925
CDH1	cadherin 1, type 1, E-cadherin (epithelial)	NM_004360	-11.36610991
CALB1	calbindin 1, 28kDa	NM_004929	-10.17295333
LCN2	lipocalin 2	NM_005564	-10.03289928
CST1	cystatin SN	NM_001898	-9.849155307
CDH3	cadherin 3, type 1, P-cadherin (placental)	NM_001793	-9.713559075
NNMT	nicotinamide N-methyltransferase	NM_006169	-9.232150014
KLK5	kallikrein-related peptidase 5	NM_012427	-8.243936163
LPAR4	lysophosphatidic acid receptor 4	NM_005296	-5.856342784
TNS4	tensin 4	NM_032865	-5.683054957
MAL	mal, T-cell differentiation protein	NM_002371	-5.656854249
ANKRD1	ankyrin repeat domain 1 (cardiac muscle)	NM_014391	-5.553253802
GRHL2	grainyhead-like 2 (Drosophila)	NM_024915	-5.476800516
VCAN	versican	NM_004385	-5.438969491

Table 6.1: List of top 20 up and down regulated genes in PC3-shLCN2 cells. All values on these lists were all found to be statistically significant. A- Top up-regulated genes in PC3-shLCN2 vs PC3-shCon. B- Top 20 down regulated genes. Values are the inverse log2values of fluorescence intensity ratios. Due to multiples probes per gene, all genes presented had p values of at least $p<1x10^{-5}$

6.2 Functional grouping of gene expression in PC3-shLCN2 by PANTHER

In order to determine precisely what pathways and biological functions are associated with LCN2 suppression, raw microarray data may be analysed by a range of different software. PANTHER gene classification software (http://www.pantherdb.org) sorts gene lists into their roles in biological processes. The software is also able to place genes into known signalling pathways based on previous literature. For analysis, all genes with at least a 1.5 fold increase or decrease in PC3-shLCN2 were used as input values. It should be noted that many genes do not appear in any category due to insufficient information, whereas others appear multiple categories.

Genes were categorised into gene ontology (GO) broad biological processes. Of the 842 up-regulated genes, 722 are maintained on the PANTHER database. This generated 1741 hits, due to significant overlap in function, specifically with grouping ‘cellular processes’ which comprised entirely of other groups. Excluding this group, the GO grouping with the highest number of hits was ‘metabolic processes’ with 369 hits. Within this group, 347 are classified as ‘primary metabolic pathways’. This is a somewhat broad term containing a range of different cellular mechanisms. Notably, within this list, the grouping nucleic based metabolic processes and protein metabolic processes had the highest number of hits (142 and 136 hits respectively), whereas the carbohydrate had far fewer hits (50) indicating that there appear to be significant changes to both DNA/RNA and protein regulation based processes rather than affecting energy generation (Figure 6.1A)

Excluding ‘cellular processes’ other groupings with large number of genes were ‘cell communication’ (217 hits); ‘developmental processes’ and ‘immune response’ (both

with 134 hits). 122 hits were also recorded for ‘Transport’, within which 70 were involved with protein transport.

With regards to down-regulated genes, 773 genes were listed in the PANTHER database. Genes were categorised into GO groupings as above. Notably, the percentage of genes in each category was extremely similar to that found with up-regulated genes, with the categories metabolic processes, developmental processes, and immune response all having the largest number of hits (347,161,109 and 104 hits respectively). Ratios within the groups were also highly similar. A slight exception was in metabolic processes, where there were a larger percentage of genes involved with nucleotide metabolism, and fewer genes associated with both carbohydrate and lipid metabolism (Figure 6.1B).This shows therefore that there is not a single GO classification which was differentially regulated in either up or down-regulated gene. It also reveals that that LCN2 suppression is having a major effect on a wide range of cellular processes. These processes also correlate to phenotypic changes seen, such as changes to cellular proliferation In particular, the GO grouping of metabolic processes contains many genes associated with cell division and growth.

A

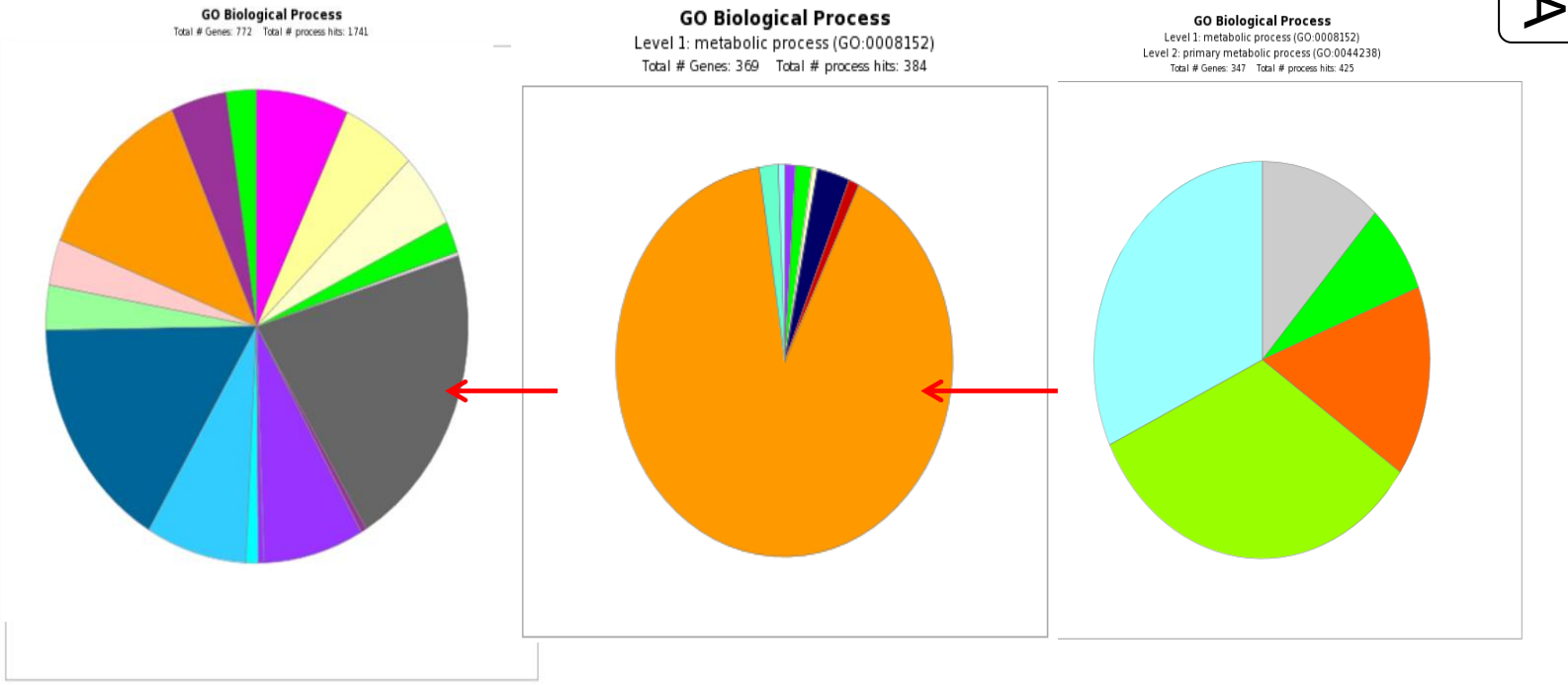

PC3-shLCN2 Up-regulated genes (legend on next page)

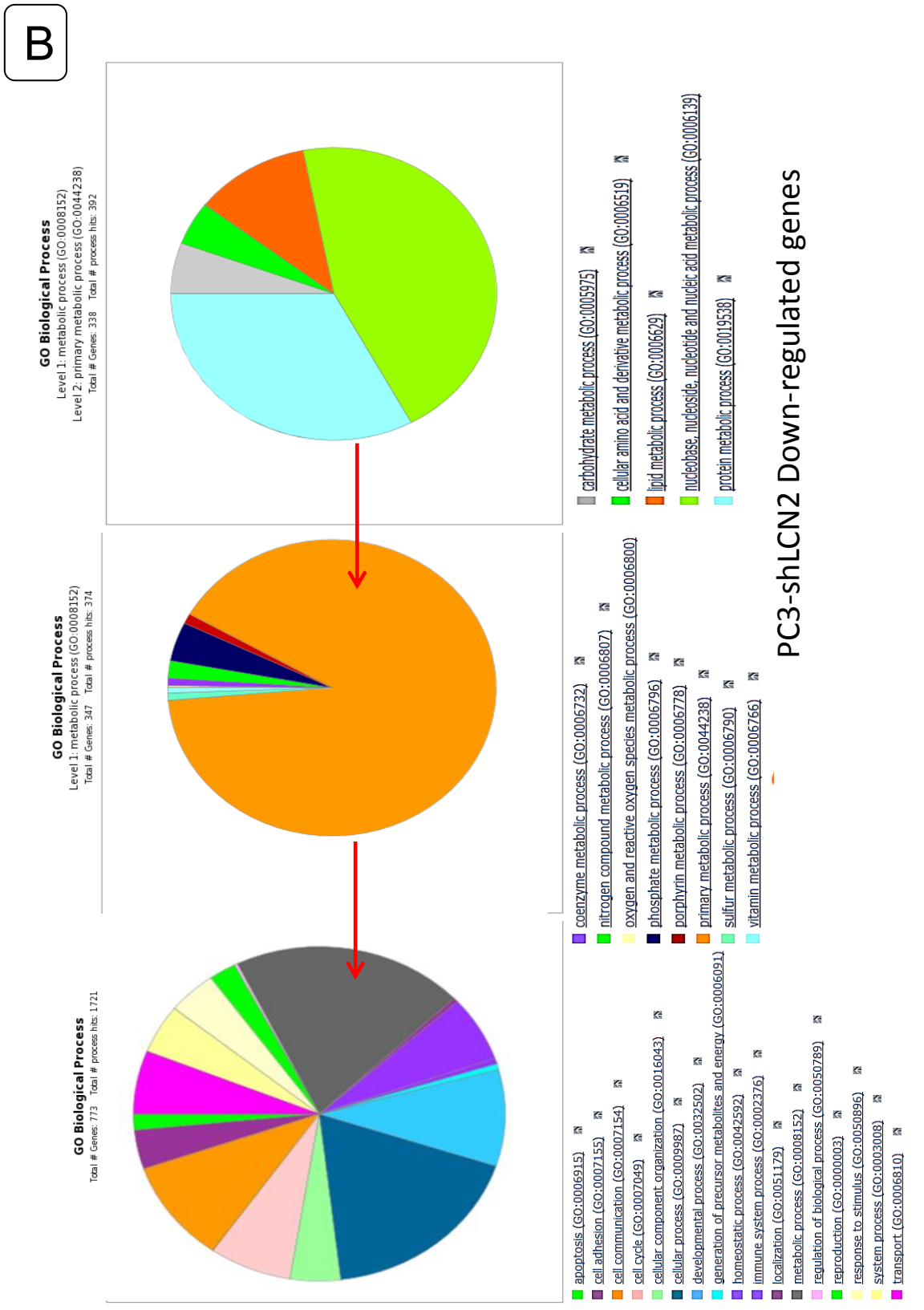

Figure 6.1: PANTHER GO processes. Genes which had a minimum 1.5 fold difference in expression between PC3-shCon and PC3-shLCN2 were grouped by PANTHER according to biological process. Sub-categories of 'metabolic processes' are detailed in the middle and right pie charts. **A**- Up-regulated genes **B**-Down regulated genes.

While GO groupings show the overall function of genes, PANTHER software also enables genes to be categorised according to known signalling pathways. Out of 722 up-regulated genes on the PANTHER database, 344 were included in pathway analysis (Figure 6.2A). Hits were recorded for over 100 signalling pathways. Of these, the grouping with the highest number of hits was 'inflammation mediated by chemokine and cytokine signalling pathway' with 18 hits. This pathway contains genes regulated by interleukins and some NF-κB targets.The category with the second highest number of hits (16) was 'Gonadotropin releasing hormonal receptor pathway'. This pathway covers the ER, AR and progesterone receptor pathways. The WNT pathway also scored 16 hits. Other pathways with high numbers of hits were 'hererotrimeric G-protein signalling pathway' (13 hits) 'Integrin signalling' (12) and angiogenesis (10 hits).

Of the 730 down-regulated genes in the database, only 217 were included in pathway analysis (Figure 6.2B). The pathway with the highest number of hits in this case was the WNT pathway (14), followed by integrin signalling (12). Gonadotropin releasing signalling, inflammation and angiogenesis all had 9 hits. Unlike the up-regulated genes, cadherin signalling and the p53 pathway were both strongly represented with 10 hits each. Also, hererotrimeric G-protein signalling had only 2 genes represented.

When combined, the WNT signalling pathway shows the strongest overall representation with a total of 48 hits, followed by inflammation, gonadotropin releasing, integrin and angiogenesis pathways. From this data, it may therefore concluded that while LCN2 suppression is affecting a wide range of pathways, WNT signalling significantly over-represented.

A

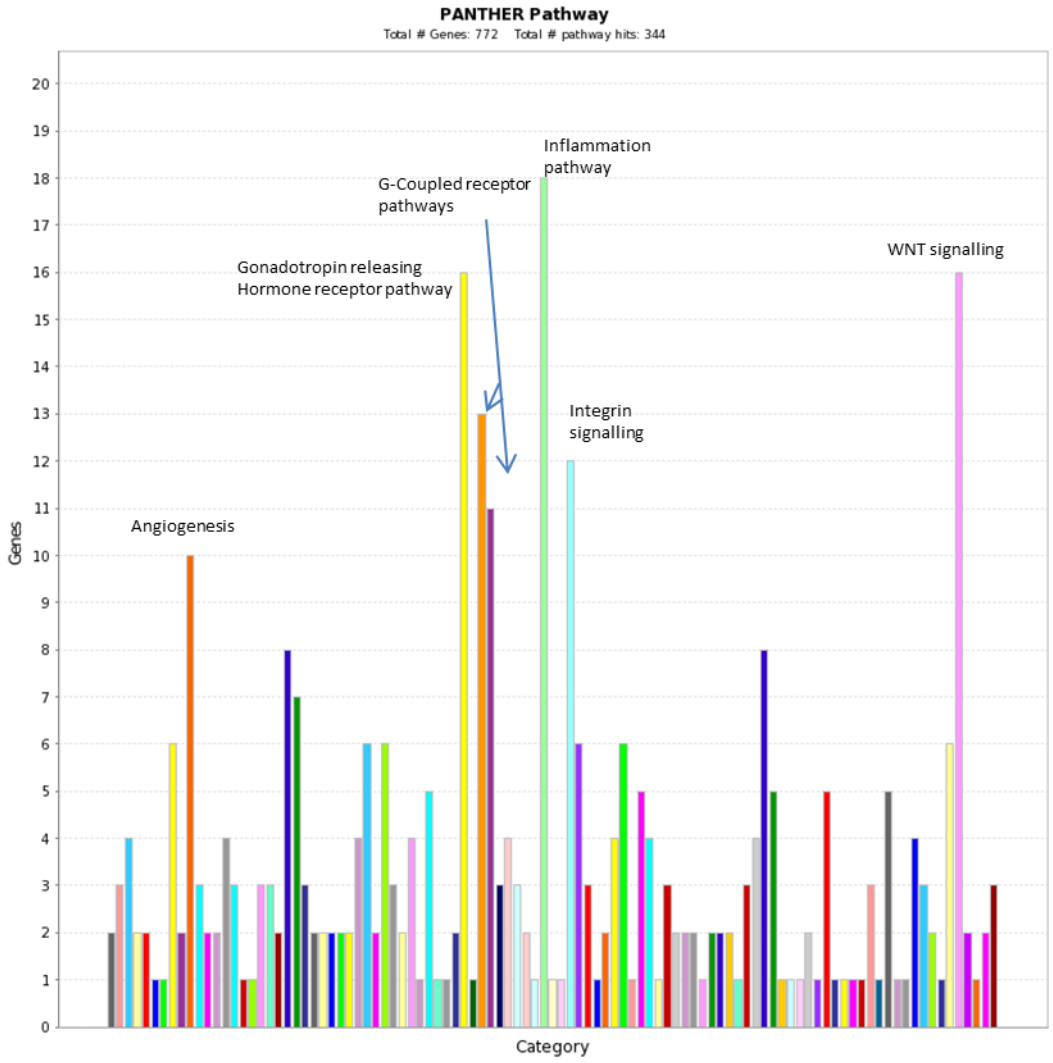

Figure 6.2 (Legend on next page)

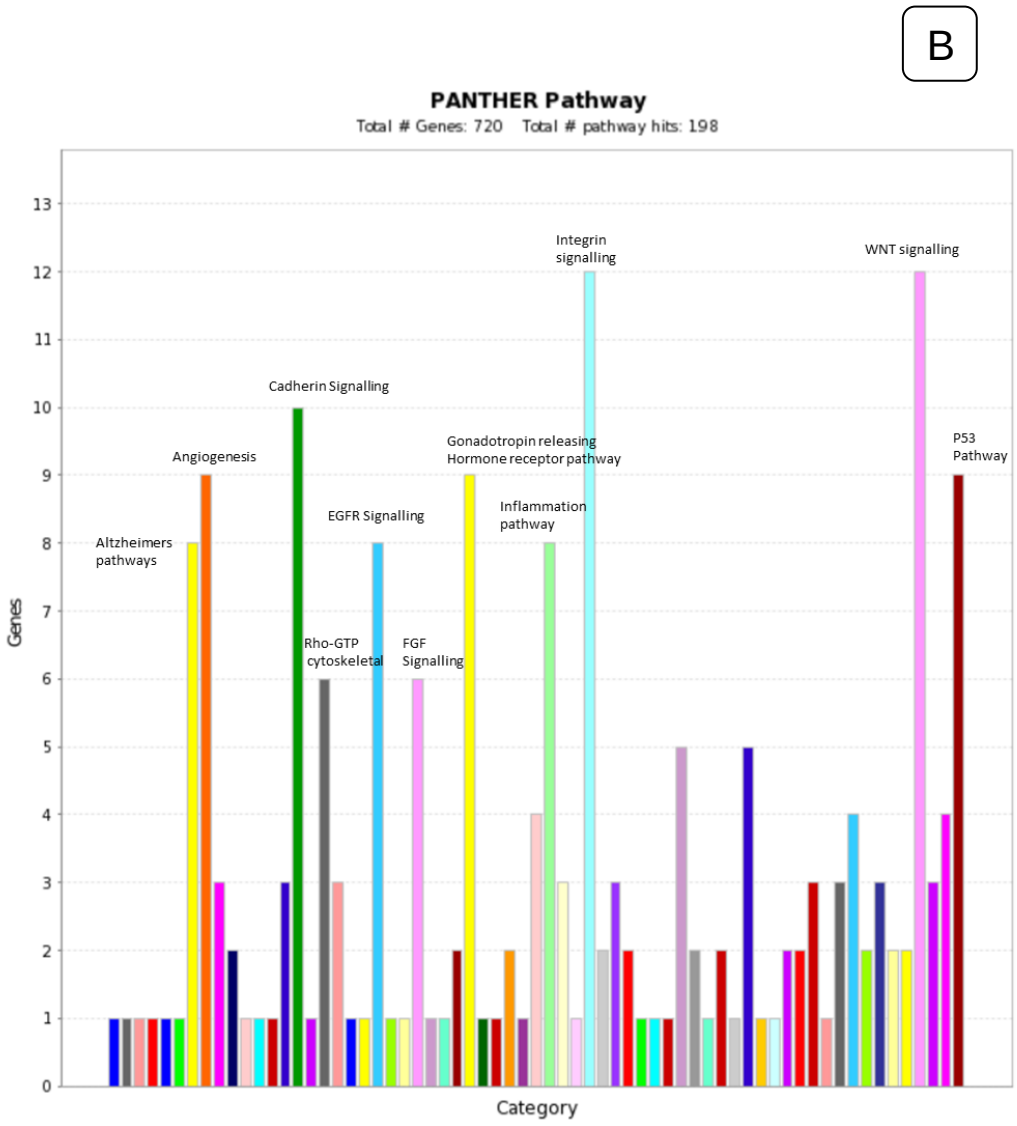

Figure 6.2 continued: PANTHER pathway analysis: Genes which had at least 1.5 fold change in PC3-shLCN2 were categorised into to pathways according to pre-defined algorithms. For brevity, only top ranked pathways are listed. **A**- Up-regulated genes. **B**- Down regulated genes.

6.3 Functional and pathway analysis by METACORE.

PANTHER analysis is useful in generating crude pathway analysis and associations. However this is done simply by inputting gene symbols into the database thereby providing a yes or no answer to whether a particular gene is in a pre-determined grouping or not. PANTHER software therefore does take into account the rank of the gene, the fold change and fluorescence intensity. It also excludes all genes which are not inputted (i.e. those with less than 1.5 fold change in this instance). METACORE analysis on the other hand includes all these factors. METACORE analysis was carried out by Tracy Chaplin at the QMUL Genome centre using dedicated software Ontological and pathway analysis of DEGs (FC>2, $p<0.05$) was completed using Metacore and its GeneGo database. Differentially expressed genes were compared to known cellular pathways and process networks and P values and FDR were calculated for each pathway. Only pathways with a P value and FDR below threshold (0.05) were considered.

Networks were established for the DEGs using the 'analyse network' tool. Briefly this involved using the DEGs (fold change>2 and $p<0.05$) as a seed list, then expanding the network using direct interactions annotated within the GeneGo database and classified according to Z-score and canonical pathway involvement.

Table 6.2A-C demonstrates the biological pathways that were impacted the most significantly. Table 6.2A demonstrates the pathways affected by the up regulated DEGs in PC3-shLCN2 cells. Table 6.23B by the down-regulated DEGs and Table 6.2C by total DEGs. Amongst the highest ranked pathways up-regulated in PC3-shLCN2 cells, the top ranked pathway was TGF, WNT and cytoskeletal remodelling (Table 6.2A). This correlated well to PANTHER data. Other top ranked pathways

were and Chromosome condensation in prometaphase and Regulation of actin cytoskeleton by Rho GTPases. With regards to the highest scoring down-regulated pathways (Table 6.2B), the most represented pathways were ATP/ITP metabolism, Spindle assembly and chromosome separation, Nucleotide excision repair and Spindle assembly and chromosome separation. This therefore appears to fit in well with the morphological changes observed including a low rate of proliferation, aberrant cell division and a multi-nucleated phenotype. Overall (Table 6.2C), the pathway with the highest level of dis-regulation was the clathrin-coated vesicle cycle. This pathway is associated with vesicle assembly and the shuttling of proteins between the golgi and the cell surface membrane. This therefore may help explain why PC3-shLCN2 cells have such an abundance of vesicle-like structures present within the cell.

A Up-regulated DEGs, pathway analysis

#	Pathway Maps	p-value
1	TGF, WNT and cytoskeletal remodeling	1.88E-06
2	Chromosome condensation in prometaphase	2.30E-06
3	Tricarbonic acid cycle	3.39E-06
4	Regulation of actin cytoskeleton by Rho GTPases	4.60E-06
5	Ligand-Dependent Transcription of Retinoid-Target genes	6.22E-06
6	LRRK2 in neurons in Parkinson's disease	6.22E-06
7	Ras family GTPases in kinase cascades (scheme)	1.14E-05
8	Regulation of CFTR activity (norm and CF)	1.14E-05
9	Antigen presentation by MHC class I	1.94E-05
10	Function of MEF2 in T lymphocytes	2.20E-05

B Down-regulated DEGs, pathway analysis

#	Pathway Maps	p-value
1	ATP/ITP metabolism	7.26E-12
2	Spindle assembly and chromosome separation	9.49E-12
3	Nucleotide excision repair	4.44E-11
4	Clathrin-coated vesicle cycle	1.10E-10
5	Transition and termination of DNA replication	1.71E-10
6	Regulation of translation initiation	1.65E-09
7	Mismatch repair	9.47E-09
8	Ligand-Dependent Transcription of Retinoid-Target genes	2.57E-08
9	CTP/UTP metabolism	2.61E-07
10	GTP-XTP metabolism	3.14E-07

C Total DEGs-pathway analysis

#	Pathway Maps	p-value
1	Clathrin-coated vesicle cycle	4.55E-13
2	Transition and termination of DNA replication	1.38E-11
3	ATP/ITP metabolism	2.02E-11
4	Nucleotide excision repair	1.74E-10
5	Spindle assembly and chromosome separation	3.68E-10
6	Mismatch repair	2.47E-09
7	Regulation of translation initiation	1.91E-08
8	Ligand-Dependent Transcription of Retinoid-Target genes	4.05E-08
9	GTP-XTP metabolism	1.56E-07
10	LRRK2 in neurons in Parkinson's disease	3.55E-07

Table 6.3 List of up and down regulated pathways in PC3-shLCN2 cells via METACORE analysis. A- list of top 10 up-regulated pathways in PC3-shLCN2 cells.B-Down regulated pathways C-Overall pathway analysis.

6.4 Analysis of gene expression by GENE-E software

While there were many genes which showed a high level of fold increase, the fold increase alone does show how important such a change would be. If a gene was only very weakly expressed, or mRNA expression is close to zero in PC3-shCon cells, a 2 or 3 fold increase may have little real impact, as the gene is still only expressed at a very low level. By contrast, if a gene is already highly expressed, even a small fold change may result in a much larger amount of extra mRNA being transcribed by the cell. As it would logistically difficult to pursue all up or down-regulated genes, it is necessary therefore to exclude those genes which had very low levels of total mRNA in either sample. Using GENE-E software, a graph was generated which plots total levels of gene expression in PC3-shCon vs PC3-shLCN2 cells based on the average intensity of gene tags in the array. Figure 6.3A shows the expression of all 19500 genes in both cell lines. Each gene is represented by a single dot. The lower the value, the lower the gene expression. The lowest possible value is 2.4 which corresponds to the background intensity or noise. The highest values were approximately 14.2, at which point signal saturation occurs. By using a comparison with genes already tested (EGFR, GAPDH-both highly expressed, PSA-AR (not expressed in PC3 etc.), it was observed that genes with intensity scores of <5 were undetectable by qPCR, or had detectable expression only after 40 cycles and can therefore be excluded from any genes to be pursued Gene expression between genes overall was found to be linear, although fewer genes had either very low or very high expression. Hence, when deciding what genes to explore further. Ideal candidates would preferably be have at least a 2-fold change in expression and have high total intensity readings (Fig 6.3A Circled in red for up-regulated genes, blue for down-regulated genes).

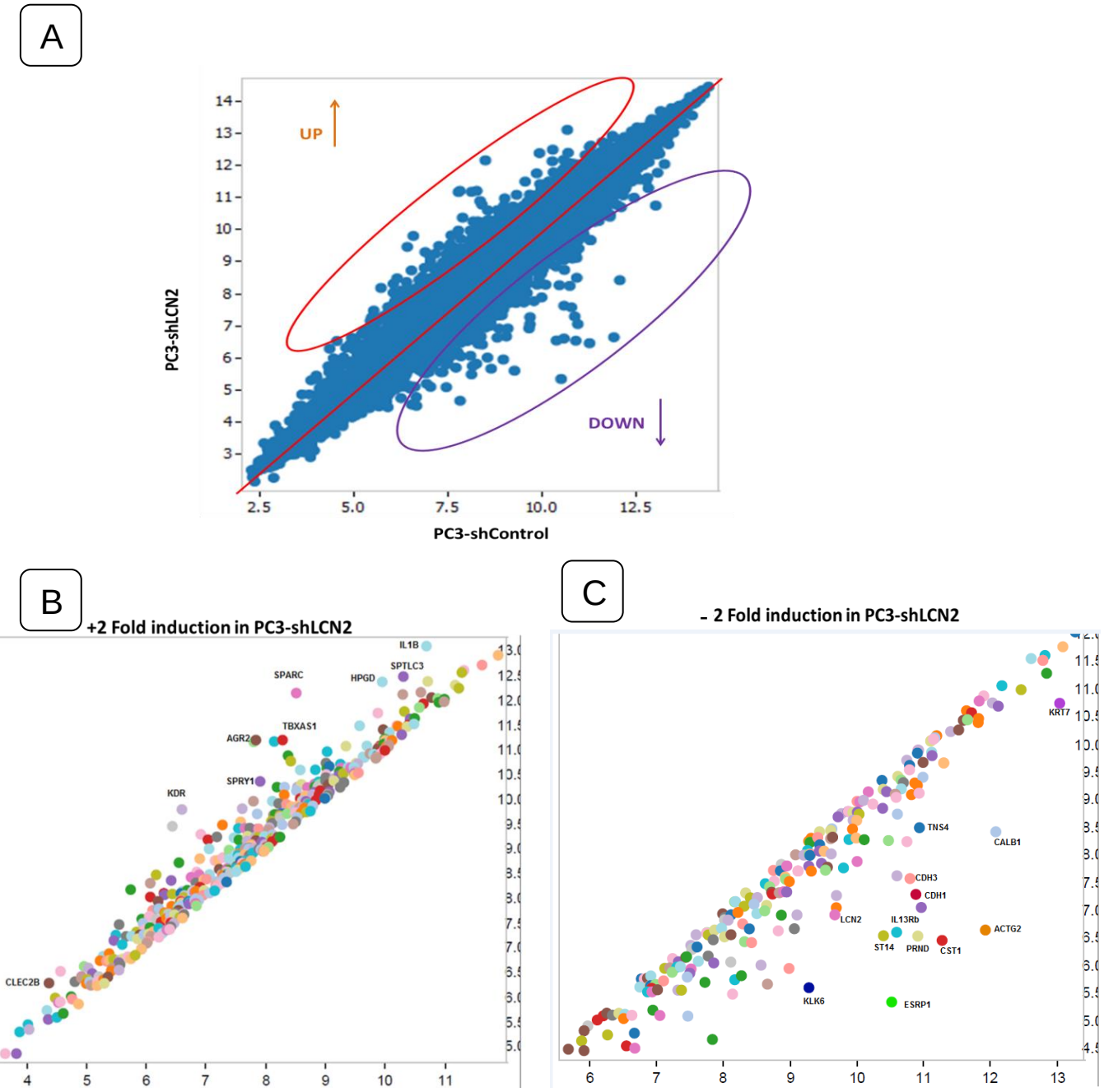

Figure 6.3: Total gene expression values in PC3-shLCN2 **A**: Scatter plot of all 17000 genes from the microarray analysis showing the fluorescence intensity in PC3-shCon vs PC3-shLCN2. Genes of interest are labelled in circles. **B**: Scatter plot containing only genes with a >2 fold increase in PC3-shLCN2. **C**- <-2 fold decrease in PC3-shLCN2. Colours are for identification only.

Figure 6.3B displays only the genes which were up-regulated by at least 2 fold in PC3-shLCN2. Genes which have a higher fold in increase in PC3-shLCN2 are higher on the X-axis. Utilising this data, it is possible to select targets for further research and which may be excluded. For instance, the gene CLEC2B showed a high fold increase in expression. However since both values are below 5, the actual effect on the cell is likely to be negligible. By contrast the genes IL1B, TBAXS1 and HPGD have high expression profiles in PC3-shLCN2 and are hence of more interest as they are likely to have a far greater influence on the cell overall and to signalling mechanisms. From this set of genes, SPARC, IL1B, KDR and AGR2 were selected for further investigation based on both the high fold change, but also the volume of literature and importance of these genes, as genes such as HPDG and SPTLC3 have only scant information regarding their role etc.

SPARC encodes for the protein osteonectin. SPARC is associated with extracellular matrix remodelling and calcium binding (Reviewed by Arnold & Brecken 2009). SPARC has been linked to the progression of a range of cancers. Specifically, in prostate, high levels of SPARC are associated with increased metastatic potential (Derosa et al., 2012). However, SPARC also has some anti-tumorigenic properties which may be dependent on its methylation status (e.g in ovarian cancer) (Arnold and Brekken, 2009).

IL1B (Encoding for IL-1β protein) is a key mediator of inflammation and immune response. It is also initiates the IL1B pathway which is associated with MAPK signalling activation, as well as NF-κB signalling mechanisms. In terms of cancer, IL1B is often associated with tumour progression and in particular inflammation in tumour sites. IL1B is particularly intriguing as it has previously been shown to induce

LCN2 expression in murine adipocytes (Sommer et al., 2009).In human tissue too, IL-1β has been shown to specifically up-regulate LCN2 expression via the NF-κB pathway (Cowland et al., 2006).

KDR, encoding for the protein VEGFR is the receptor for the chemokine VEGF, which is a critical mediator of angiogenesis (Holmes et al., 2007). Notably, KDR itself has not been previously associated with LCN2 expression, however its ligand VEGF has been shown to be induced upon ectopic LCN2 expression in breast cancer (Yang et al., 2009).

AGR2 (Anterior Gradient homologue 2) (Reviewed by Brychtova et al., 2011) is associated with development and differentiation. AGR2 has also been linked to cancer, although whether it acts as a tumour promoter or suppressor is still uncertain and may be tissue specific or dependent on other factors. Most notably however, is that AGR2 has been shown to be transcriptionally activated by estrogen via direct binding of ER to the AGR2 promoter and shows a positive correlation to ER+ BCa tumours.

Figure 6.3C displays all genes which had a >2 fold reduction in expression in PC3-shLCN2 relative to PC3-shCon. In contrast to up-regulated genes, there were a larger number of genes which show a very significant decrease in expression, indeed a number of genes were further from the line of best fit than LCN2 itself. From these, genes were selected for further characterisations based on overall fold change, expression in original PC3-shCON cells, and potential importance of these genes based on literature searches. Genes selected were: CDH1, CDH3, ST14, ESRP1, ACTG2 and KLK6.

CDH1 and CDH3 encode for E-cadherin and P-Cadherin respectively. P-Cadherin is not as studied as E-cadherin, but also plays a role in BCa progression. In contrast to E-cadherin however, it is often cited as a marker of tumour progression (Albergaria et al., 2011).

ST14 (Suppressor of tumorigenicity 14) encodes for the protein matriptase which functions as a serine protease. Contrary to its name, ST14 has been shown to be up-regulated in a number of cancers where it associated with metastasis, particularly BCa progression (Uhland, 2006).

ACTG2 (Actin Gamma 2) is a cytoskeletal protein which is a member of the actin family. While this particular gene is very poorly studied, ACTG2 is a known mediator of internal cell motility (Yonemoto et al., 2006). The ACTG2 showed the highest fold decrease in expression in PC3-shLCN2 cells and is therefore a good candidate for more detailed analysis given then structural changes seen in cells.

ESRP1 (Epithelial splicing regulatory protein 1) has recently been shown to regulate the splicing of different variants of EMT related genes, in particular CD44 and Snail (Yae et al., 2012).

KLK6 is also a serine protease which is up-regulated in a number of cancers, in particular ovarian and BCa (Ghosh et al., 2004). KLK is also of interest in PCa due to its structural similarity with KLK3/PSA (Bayani and Diamandis, 2012).

6.5 Validation of selected microarray based genes via qPCR

Using the genes selected above, validation of results was carried out using qPCR analysis which is more sensitive and accurate. Microarray data is also constrained by the minimum and maximum fluorescence of tags which is not the case in qPCR.

With regards to genes which were up-regulated in PC3-shLCN2 cells. The genes KDR, SPARC, ARG2 and IL1B were validated (Figure 6.4A). Microarray analysis provided KDR with a 10.05 fold increase in PC3-shLCN2 cells relative to PC3-shCon cells. When analysed by qPCR however, this was raised to a 119 fold increase. SPARC had a 9.42 fold increase via microarray, qPCR validation increased this greatly to 133 fold. AGR had a 8.06 fold increase via qPCR, whereas a 19 fold increase was recorded via qPCR. IL1B (4.19 fold increase from microarray) showed an 11.8 fold increase by qPCR analysis.

For validation of down-regulated genes, CDH1, CDH3, KLK6, ESRP1 and ACTG2 were selected (Figure 6.4B). When analysed by qPCR. Both CDH1 and CDH3 showed similar decreases in expression to microarray data (11.3 vs 14 fold for CDH1, 9.7 vs 10.8 fold for CDH3). KLK, ESRP1 and ACTG2 on the other hand, when analysed by qPCR all showed >150 fold decrease in expression. Indeed, in these three genes, expression was effectively nil, and undetectable by qPCR at 40 cycles. In these cases therefore, the data suggests that transcription of these genes has been turned off almost completely. It may also be hypothesised that other genes from the microarray have also been turned off, but were not analysed.

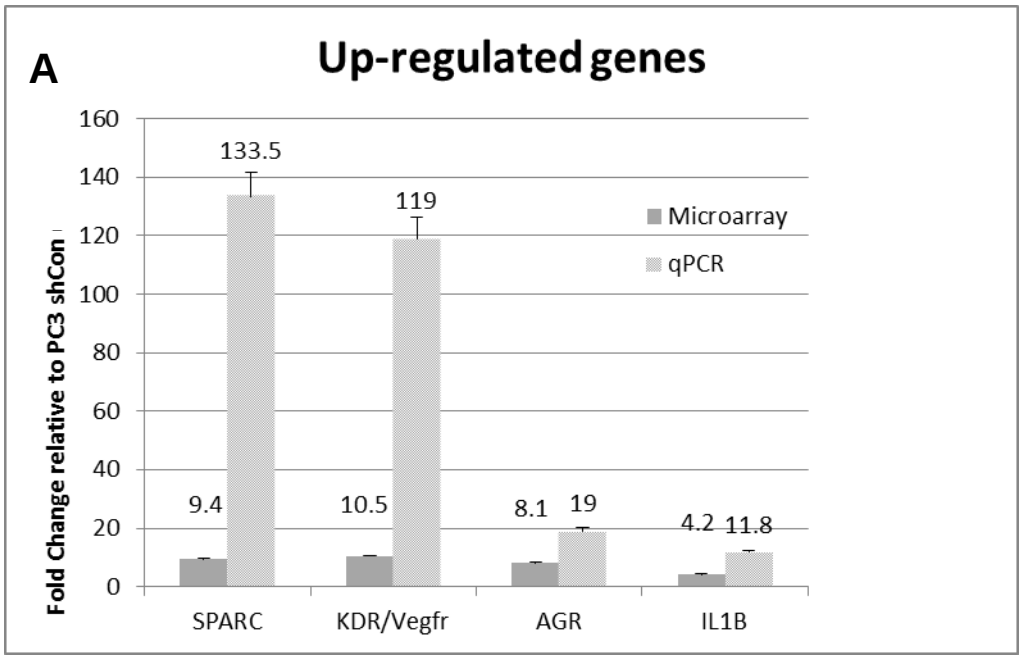

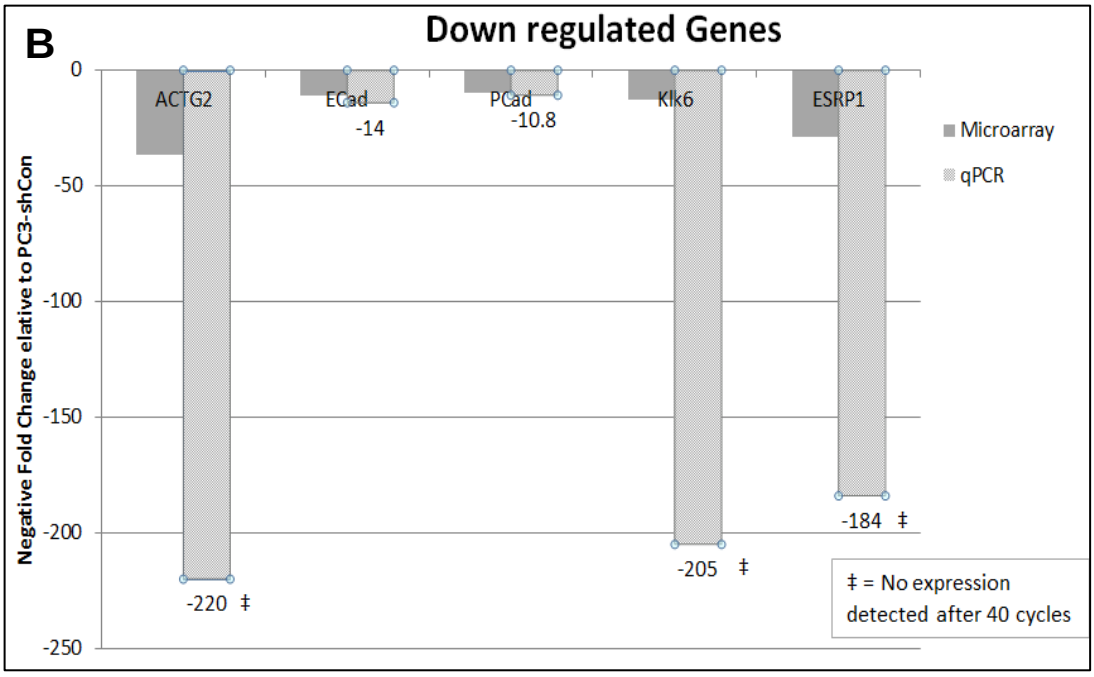

Figure 6.4: Validation of Microarray genes. Fold expression relative to PC3-shLCN2 as detected by either microarray or by qPCR analysis **A**- Up regulated genes **B**- Down regulated genes. Values are fold change relative to PC3-shCon

cells. qPCR data: n=3 +/- SEM. All qPCR values had p values of $p<0.01$ relative to PC3-shCon cells Statistical analysis was carried out using Student's t-test.

6.6 Rescue of gene expression in PC3-shLCN2 cells by conditioned media.

LCN2 is a secreted protein, however its roles in terms of paracrine or autocrine signalling are currently poorly understood, and there is little data regarding how LCN2 precisely functions with regards to pathways. While microarray analysis provides important information, it does not reflect which genes are directly influenced by LCN2 itself, or which are indirectly linked. To help elucidate this further, two approaches were taken. Firstly- rescue of gene expression by supplementary LCN2 protein. Secondly by employing temporary suppression of LCN2 by siRNA.

The stability of LCN2 protein has not previously been described, nor is it known whether LCN2 is targeted for degradation either inside or outside of the cell. However, LCN2 protein was previously shown to be secreted by PC3-shCon cells at high levels, where it was present in cell supernatants as analysed by ELISA. To analyse whether this secreted LCN2 was able ellicit an effect on PC3-shLCN2 cells, PC3-shCon cells were seeded and cultured for 48 hours. Conditioned media (CM) was then filtered and added on PC3-shLCN2 cells for a further 24 hours before harvest (Figure 6.5A).

qPCR analysis carried out on the LCN2 gene revealed that conditioned media had no influence on expression and that the gene remained repressed under the influence of shLCN2. Analysis was then carried out on genes identified from the microarray, namely SPARC, KDR, AGR, IL1B (all up-regulated in PC3-shLCN2) as well as, ST14, CDH1 ESRP1, KLK6 and ACTG2 (down-regulated).

Highly significant reductions in the expression of all up-regulated genes was observed, although in no case did expression levels return fully to those found in PC3-shCon cells. SPARC expression was reduced from a 185 fold increase relative to PC3-shCon to a 21.4 fold increase in cells cultured in CM (i.e there was a 21.1 decrease relative to non CM media). KDR also showed a reduction in expression from 107 fold to 24. AGR2 was reduced from a 19 fold increase relative to PC3-shCon to only a 4.0 fold increase. IL1B on the other hand showed no significant change in expression (Figure 6.5B).

Notably, there were also changes observed in these genes between PC3-shCon cells grown in CM for the full 72 hours compared to those which had media changed after 48 hours. While SPARC had no statistically significant change, KDR expression was increased 6.3 fold in PC3-shCon cells cultured for 72 hours in CM relative to those that underwent media change. Similarly, a 3.2 fold increase was seen in AGR2 CM grown PC3-shCon cells relative to PC3-shCon cells grown in fresh media, thus showing that the expression of these genes is rapidly sensitive to changes to media and environment, and as such may also be a factor when considering the results above.

A different pattern emerged when down-regulated genes were analysed under CM conditions. ST14 showed increased expression (3.2 fold) in PC3-shLCN2 cells cultured in CM compared to those grown in non CM. The genes KLK6, ESRP1 and ACTG2 did not show any response to CM media, and remained effectively non-transcribed. By contrast, CDH1 expression was suppressed even further under CM conditions than non-CM. Under non CM conditions, CDH1expression was found to be 7.5 fold lower than in PC3-shCon. Under CM conditions however, this was decreased further still to 31.15 fold (I.e there was an 8 fold decrease from CM+

compared to CM- conditions). Overall, CM appeared to affect up-regulated genes more significantly that down-regulated genes. It may be the case that the silencing of these genes is irreversible by CM alone.

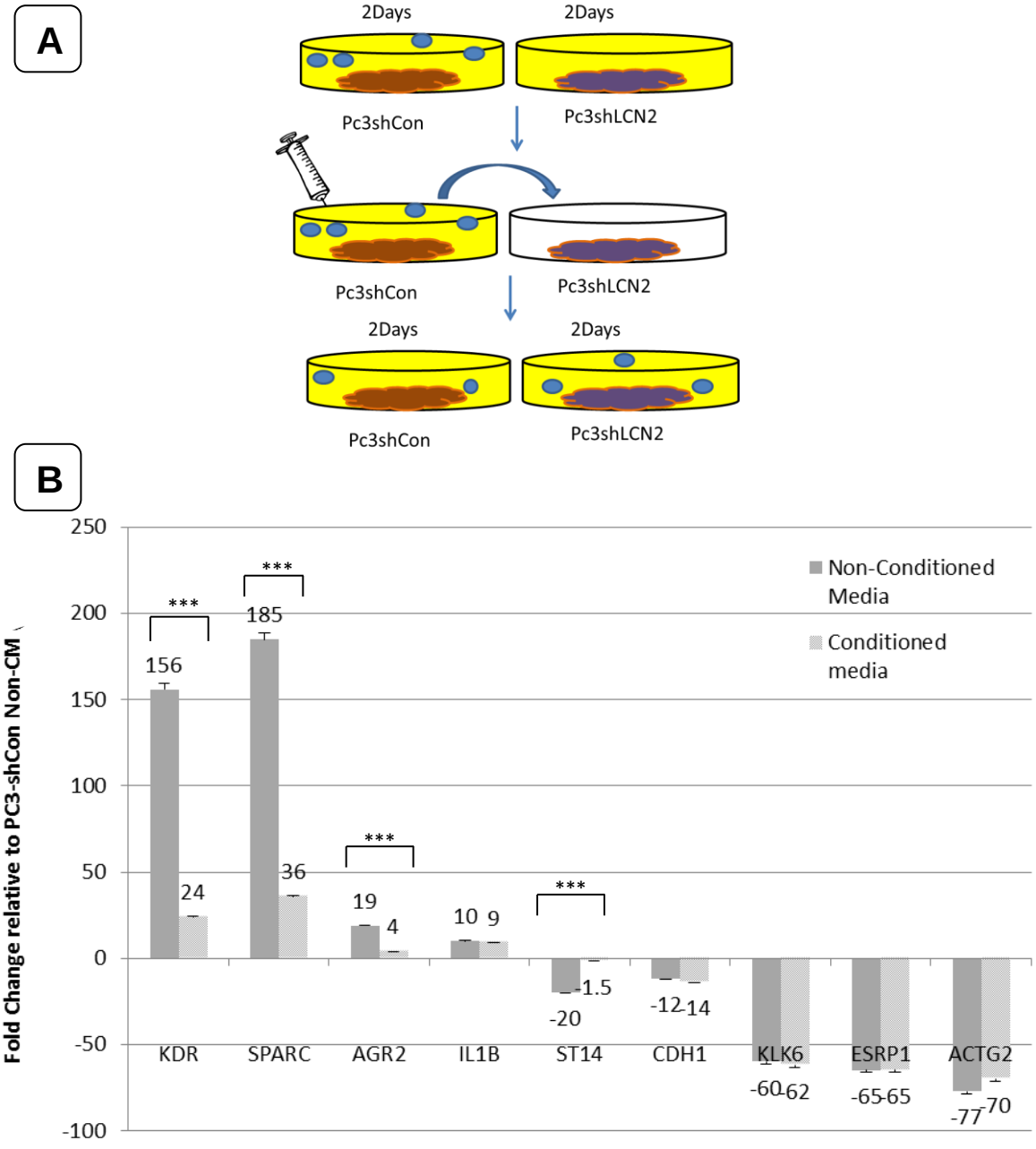

Figure 6.5: PC3-shLCN2 gene expression in response to conditioned media: A- Diagram of experimental procedure. PC3-shCON cells were cultured for 48hrs, supernatant was then removed and filtered, then added to PC3-shLCN2 cells for a

further 24hrs. **B** qPCR analysis of LCN2 target genes. Gene expression is relative to levels in PC3-shCon cells with fresh media +/- SEM, n=3 Statistical analysis was carried out using Student's t-test. ***p<0.001

Protein Expression

In addition to gene expression, the effect of CM on protein expression in PC3-shLCN2 cells was also observed. Using identical conditions to above, protein samples were harvested simultaneously with mRNA samples. ERα was previously shown to be strongly up-regulated in PC3-shLCN2 cells. This was confirmed in PC3-shLCN2 cells grown under normal conditions. However, when PC3-shLCN2 cells were cultured under CM conditions, ERα protein expression was markedly reduced (Figure 6.6). ERβ was also found to be reduced in PC3-shLCN2 cells. However, there was little change to expression in PC3-shLCN2 cells grown under CM. Expression of E-cadherin was absent in PC3-shLCN2 cells under non CM conditions, and there was no change observed under CM conditions, thus correlating with qPCR data.

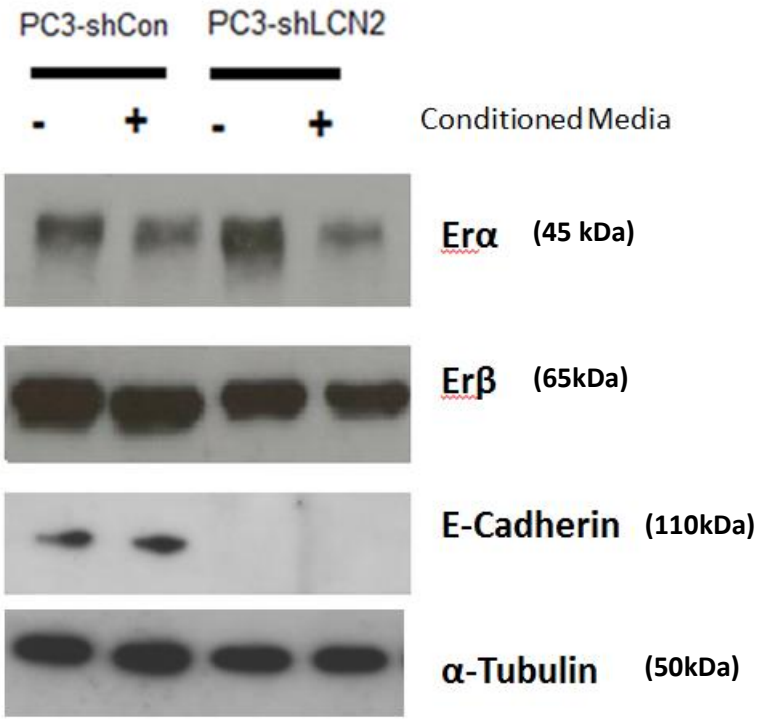

Figure 6.6: PC3-shLCN2 cells protein response to conditioned media: Culture conditions same as above- Western blot analysis. PC3-shCON cells were cultured for 48hrs, supernatant was then removed and filtered, then added to PC3-shLCN2 cells for a further 24hrs. Data is representative of 3 experiments. Protein was extracted in parallel to mRNA (Figure 6.5).

6.7 Rescue of gene expression by recombinant LCN2 protein

While conditioned media significantly changed the expression of both genes and proteins in PC3-shLCN2 cells, these effects cannot be attributed to LCN2 alone. Indeed, while only LCN2 has been suppressed in PC3-shLCN2 cells, there are likely to be many other secreted factors, including other proteins, steroids etc., which may be influencing expression of the genes previously analysed. Therefore, to more precisely identify which genes are influenced by LCN2, and exclude other factors cells were supplemented with commercially available recombinant LCN2 protein produced from *E.Coli* bacteria. Recombinant LCN2 has previously been shown by Yang et al. (2009) to reduce E-cadherin protein expression in modified MCF7 cells, however in the Yang et al. study'effects were only observed at concentrations of 100µg/ml, which are clearly far in excess of what would naturally be found physiologically. Indeed, recombinant protein in the 2009 Yang et al. study was obtained from the same source as X-ray crystallography studies. Hence, to obtain a more accurate qualification of LCN2's effects, PC3-shLCN2 cells were supplemented by the same level as detected in PC3-shCon cells via ELISA of 2ng/ml (See Section 4.10).

PC3-shLCN2, as well as PC3-shCon cells were incubated for 24hrs and with recombinant LCN2 before mRNA and protein harvesting to mimic CM culture conditions. No changes to cell morphology were observed in any case. Cells remained healthy, and there was no visually obvious change in cell death as analysed by the number of floating or dead cells in the media.

qPCR analysis of genes selected from the microarray showed a similar trend to that found with conditioned media, but with less effect. Of the up-regulated genes,

SPARC, KDR, AGR2 and IL1B were analysed. SPARC, KDR and AGR2 all showed a reduction in expression in PC3-shLCN2 cells treated with recombinant LCN2 protein of 2.17, 2.46 and 2.21 fold respectively (corresponding to a 72, 74 and 21 fold increase relative to PC3-shCon cells). IL1B on the other hand did not show any response in expression (Figure 6.7). With regards to genes down-regulated in PC3-shLCN2 cells, no change in expression was observed for CDH1, ESRP1 or to ACTG2. However, an increase in expression was noted for ST14 (as was also seen with conditioned media). In addition, the LCN2 gene itself was also unaffected in PC3-shCon cells, potentially ruling out any feedback mechanisms. It appears therefore that LCN2 is indeed able to partially reverse the changes in gene expression in some but not all genes. The response also correlates well with CM media suggesting that LCN2 is involved, but that other factors are also likely to be acting on PC3-shLCN2 cells as well. As with CM conditions, the genes which were up-regulated in PC3-shLCN2 cells appeared to be more responsive than those down-regulated.

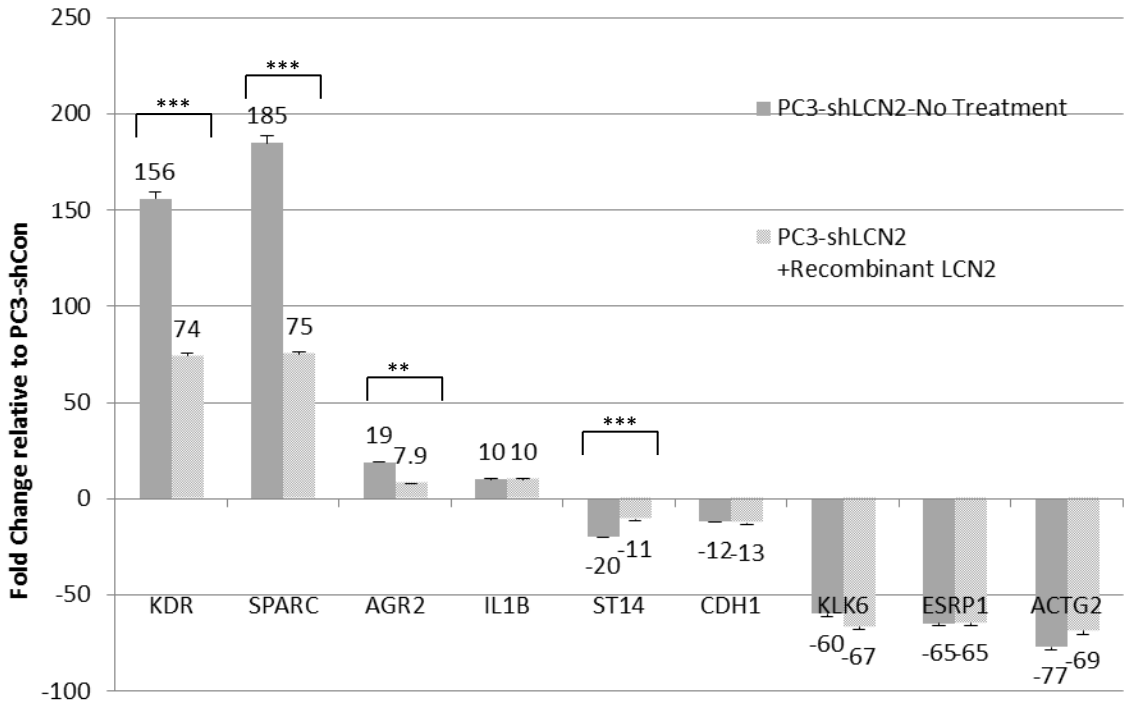

Figure 6.7 PC3-shLCN2 cells in response to recombinant lipocalin 2 protein. PC3-shLCN2 cells were cultured for 48hrs with 2ng/ml recombinant LCN2 (qPCR analysis).Values are relative to untreated PC3-shCon cells Untreated PC3-shLCN2 values are the same as in figure 6.6. Average of n=3 experiments values +/- SEM. Statistical analysis was carried out using Student's t-test. **p<0.01 ***p<0.001

Protein Expression

In addition to gene expression, the effects of recombinant LCN2 were simultaneously assessed on protein expression. As before, ERα was found to be strongly up-regulated in PC3-shLCN2 cells. However, after only 24 hours exposure to 2ng/ml recombinant LCN2, expression was highly reduced (Figure 6.8). Expression for ERβ however was relatively unchanged. In both these cases, mRNA expression was found to be unchanged, and was identical between PC3-shLCN2 and PC3-shCon, thus further reinforcing a post-transcriptional regulation of this ERα by LCN2. EGFR, previously found to be down-regulated in PC3-shLCN2 cells also showed moderate signs of an increase in expression. E-cadherin also did not show any response to recombinant LCN2 and remained unexpressed. In every case, recombinant LCN2 had no effect on the expression of any protein tested in PC3-shCon cells.

To determine exactly what concentrations were necessary for the changes to protein expression to be observed, PC3-shLCN2 and PC3-shCon cells were subjected to treatment of recombinant LCN2 at a range of dosages (0, 1.5 , 5 and 15ng/ml) for 48 hours.

Expression of ERα in PC3-shLCN2 cells was reduced by of LCN2 protein, and showed reductions at both 1.5ng/ml and showed most response at 5ng/ml. Interestingly, reduction was not as high with 15ng/ml LCN2 protein. No change was observed to E-cadherin expression under any dosage.

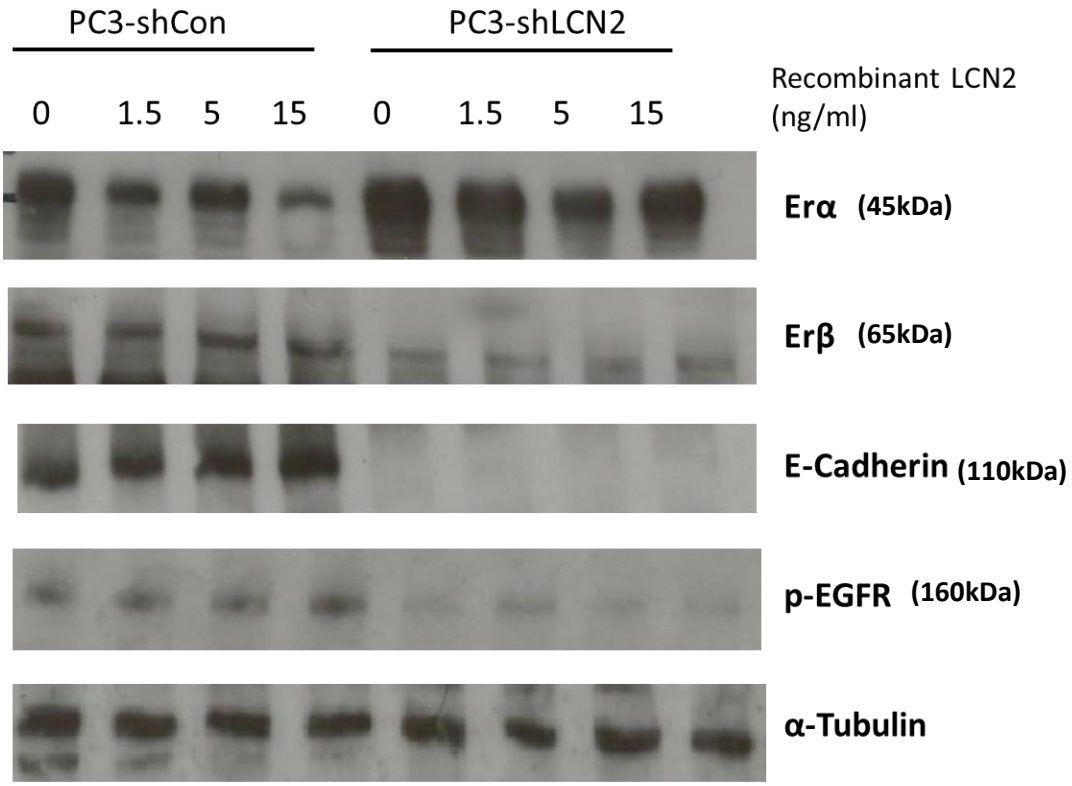

Figure 6.8: PC3-shLCN2 protein expression in response to recombinant lipocalin 2 protein. Western blot analysis of ERα, ERβ, E-cadherin and p-EGFR in PC3-shCon and PC3-shLCN2 cells in response to 48hrs treatment with recombinant LCN2 protein. Representative of n=3 blots.

Effect of Recombinant LCN2 on cell proliferation

Concurrent with analysis of mRNA and protein expression, recombinant LCN2 protein was employed to observe if there were any effects of LCN2 on cell proliferation using Alamar Blue assays. Both PC3-shCon and PC3-shLCN2 cells were supplemented with 2ng/ml of recombinant LCN2 for 7 days until confluence was reached. Results showed that while after 6 days there was a slight increase in proliferation in treated PC3-shLCN2, there was no statistically significant change in proliferation to either cell type (Figure 6.9)

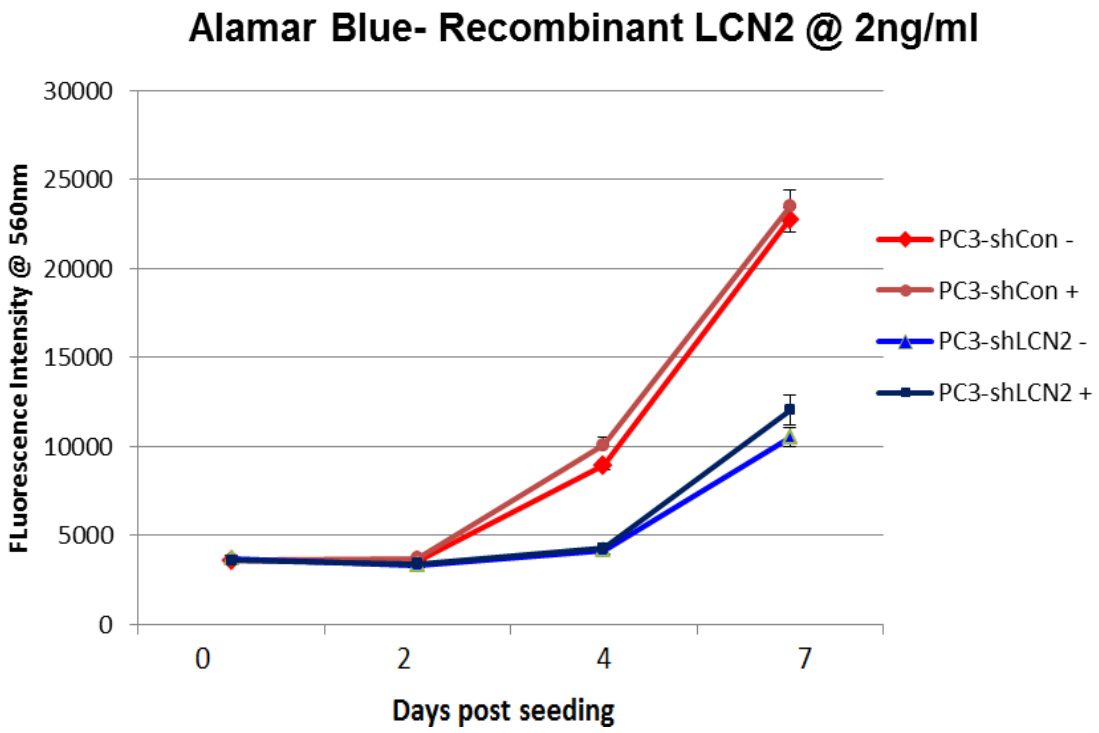

Figure 6.9: Recombinant LCN2 does not affect PC3-shLCN2 proliferation

Alamar blue assay. Cells were cultured with or without 2ng/ml recombinant LCN2 protein for 7 days until PC3-shCon cells were confluent. Fluorescence intensity measured @590 nm +/- SEM, n=3

6.8 Targeted siRNA suppression of LCN2

shRNA is able to provide long term suppression of a target gene, however shRNA may not give a true representation of which pathways are directly associated with LCN2 and which are indirect effects of suppression as other signalling pathways are likely to activated over time. Two siRNA sequences targeting the LCN2 gene were transfected into PC3 cells (Labelled 5G and 5U based on their sequences.) at 100 nmol/ml concentration for 72hrs (according to the manufacturer's optimal specifications). Transfection was validated by siGLO fluorescence in control cells. Analysis by qPCR showed that transfection was highly effective. The 5U sequence reduced LCN2 expression by 178 fold, whereas the 5G sequence reduced LCN2 expression by 235 fold. As the 5G sequence was determined by qPCR to be the more effective of the two siRNA sequences, it was selected for further analysis on gene expression. PC3-Parental cells were transfected with 100nMol/ml siLCN2 and harvested after 2, 4 and 6 days. No morphological changes were evident at any time period. qPCR analysis showed that suppression of LCN2 siRNA was effective at all three time points displaying a 68, 158 and 191 fold decrease in expression respectively (Figure 6.10A). However, analysis by Western blot showed that there whilst there was a slight reduction over time, intracellular protein expression of LCN2 remained strong (Figure 6.10B). Based on these results, data therefore appears to show that LCN2 is relatively stable within the cell, and may have a low rate of turnover. It also suggests that the effects of the siRNA are likely to be minimal due to LCN2 protein still being present over the time scale observed. This may also help explain why morphological changes in PC3-shLCN2 cells were observed only after 2 weeks of growth and selection, and why relatively little changes were seen in LCN2

expression when PC3 cells were treated with pharmacological inhibitors despite knockdown of mRNA.

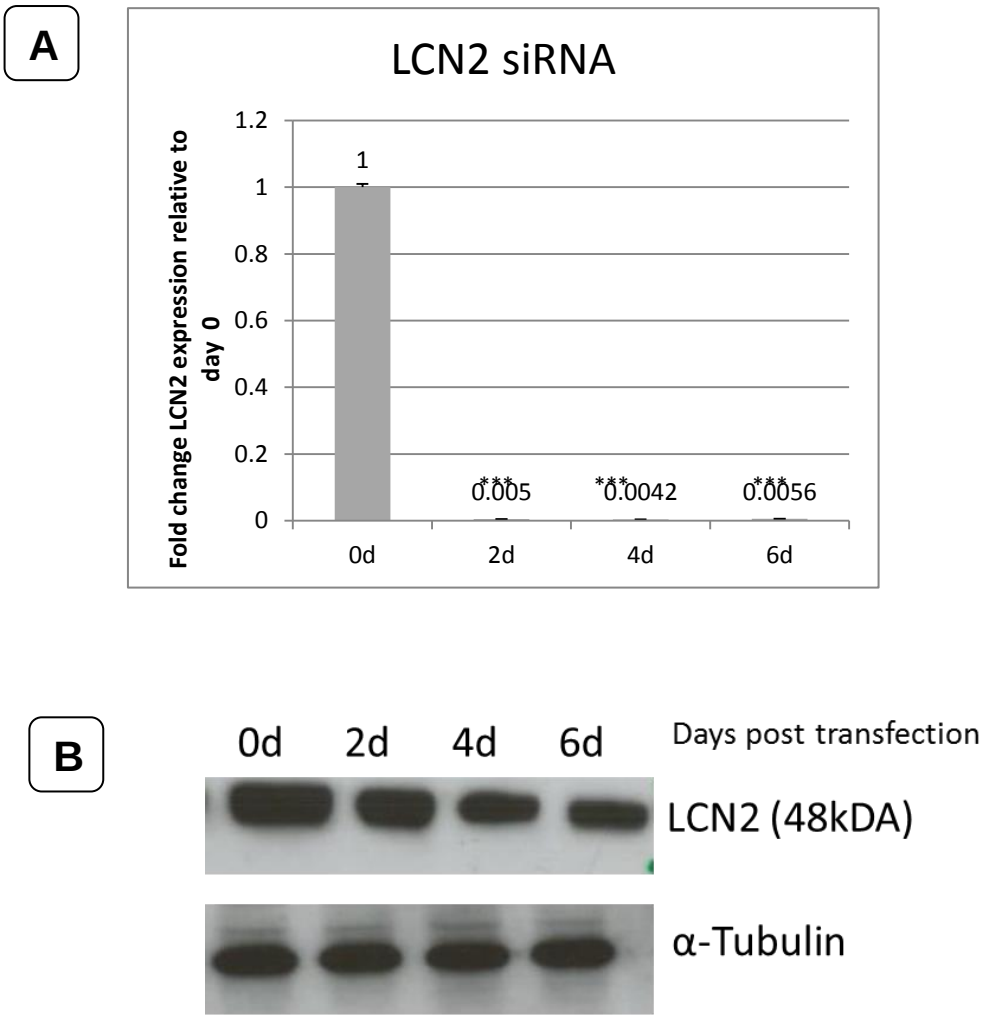

Figure 6.10: siRNA targeted suppression of LCN2 A- qPCR analysis of LCN2 following siRNA targeted suppression. Parental PC3 cells were transfected with siLCN2 for 2, 4 or 6 days. Values are relative to expression at day 0 +/- SEM, n=3 Statistical analysis was carried out using Student's t-test.. **B**- Western blot analysis of LCN2 protein after 2, 4 and 6 days post transfection. Protein was taken in parallel to mRNA samples. Data is representative of 3 experiments.

qPCR analysis of target genes siRNA transfection.

Whilst total suppression of LCN2 protein was not achieved by siRNA, nevertheless, the effects of partial suppression was analysed. Effects were assessed both on genes identified by microarray.

It was previously found that KDR, AGR2 and SPARC were up-regulated in PC3-shLCN2 cells (See section 6.4). I therefore investigated whether these genes were up-regulated by siLCN2. PC3-parental cells were treated with siLCN2 for 2, 4 and 6 days and mRNA expression analysed by PCR.

Results showed that even after 6 days of expression of KDR was unchanged at any time point (Figure. AGR2 expression showed no change in expression after 2 or 4 days, but did show a 2.1 fold increase after 6 days (Figure 6.11). SPARC expression was unchanged after 2 days, but showed a 2.4 fold increase after 4 days and similarly a 2.5 fold increase after 6 days. Indeed, overall down-regulated genes showed a greater overall response than for the up-regulated genes such as KDR.

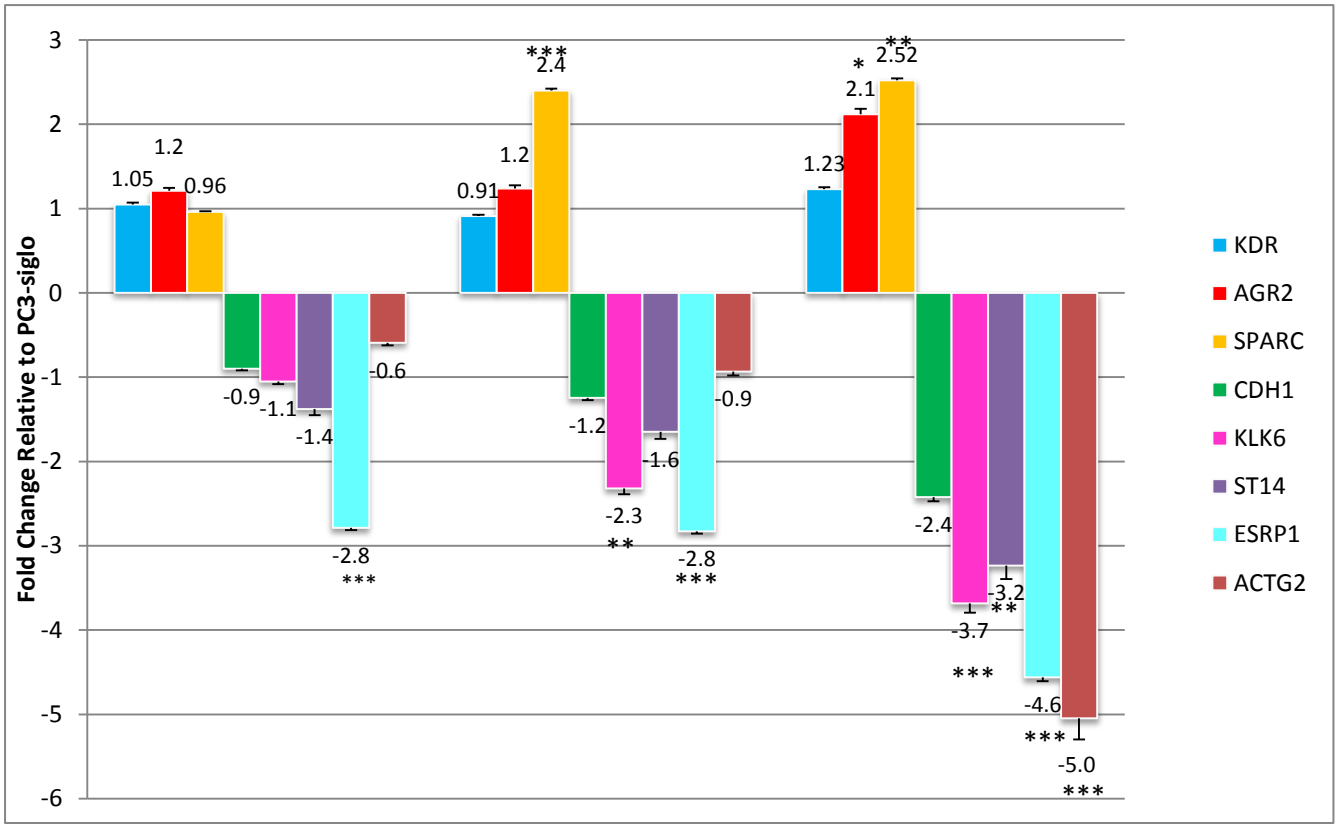

Figure 6.11: Expression of target genes after siLCN2 transfection: qPCR analysis of LCN2 target genes following 2, 4 and 6 days siRNA transfection. Values are relative to expression in PC3-siGLO controls +/- SEM Statistical analysis was carried out using Student's t-test. *p<0.05, **p<0.01, ***p<0.001, n=3.

Previously (See section 5.13), it was observed that ERα protein expression was increased in PC3-shLCN2 cells, coupled with a loss of both ERβ and E-cadherin. Therefore, to determine whether these effects were observable in short term suppression of LCN2, siLCN2 was used in PC3-parental cells (as in figure 6.13) hence assessed the effect of siLCN2 on the protein expression of ERα, ERβ and E-cadherin following 2, 4 and 6 days of targeted suppression.

Following siLCN2 transfection, expression of ERα showed a slight increase after 24 and 48 hours however following 6 days of treatment, there was a marked increase in ERα expression. However there was no apparent change to either ERβ or E-cadherin expression (Fig 6.12). This data therefore indicates that even though LCN2 protein was still present, a small reduction in LCN2 is able to elicit an effect on ERα expression and hence ERα is likely to be a bona-fide LCN2 target protein.

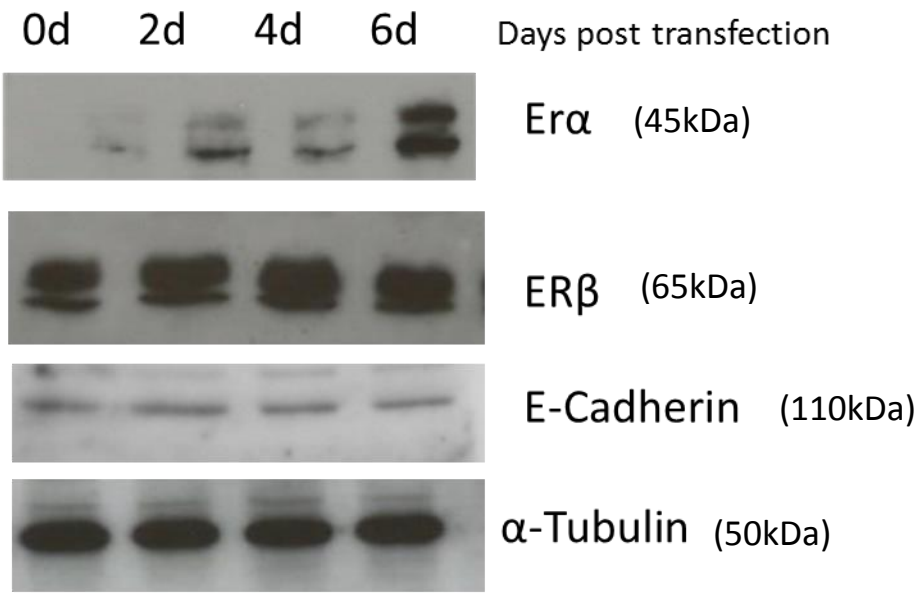

Figure 6.12 Expression of LCN2 target proteins after siLCN2 transfection: Western blot analysis of ERα, ERβ and E-cadherin in response to siLN2 after 0,2,4 and 6 days. Data is representative of n=3 experiments.

6.9 Discussion

While some of the mechanisms of LCN2 regulation have been studied, there is relatively less data regarding its downstream effects .

Microarray analysis of PC3-shLCN2 cells provided a more global analysis of the pathways and genes associated with LCN2. As well as pathways which have already been linked to LCN2 such as Wnt (Ziegler et al., 2007), other pathways such as integrin signalling and gonadotropin-linked signalling have not yet been described and demonstrate that LCN2 has a much wider range of effects than seen previously. Microarray analysis also strengthens LCN2's links to angiogenesis and the p53 pathway in greater detail (Mahadevan et al., 2013). As the effects of LCN2 suppression were fairly wide-ranging, it is therefore difficult to determine precisely which pathways are directly linked to LCN2 and which are downstream effects. Indeed, while some common factors such as NF-κB were implicated in LCN2 signalling, there was no single pathway which stood out as being prominent. Even with regards to Wnt signalling (which had many hits via microarray), defining whether canonical or non-canonical signalling was activated more was unclear. There is significant interplay and interaction between different pathways (Nelson and Nusse, 2004, Gordon and Nusse, 2006).

One of unknown factors with regards to LCN2 is whether the protein has differing intracellular function compared to extracellular function. Here, I have noted that in PC3 LCN2 has high intracellular expression, and that within the cell, LCN2 potentially exists as a dimer. Moreover, by employing both conditioned media and recombinant LCN2 protein I demonstrated that some genes or proteins are activated by secreted LCN2, whereas others such as E-cadherin are not. Recombinant LCN2

protein was used by Yang et al (2009) to induce a reduction of E-cadherin, but only saw a minor reduction after 100µg/ml of treatment, which is over 1000 times physiological levels. Other studies, using recombinant LCN2 have shown it leading to translocation of the pro-apoptotic protein BAX, and have been shown to partially restore growth in LCN2 knockdown thyroid FRO cells (Ianetti et al, 2008).

While the crystal structure of LCN2 is now well known (Goetz et al., 2000), there is virtually no data regarding its post-translational stability. It is not known whether LCN2 is targeted for proteasome degradation and its rate of turnover is also unknown. In this study I noted that pharmacological inhibitors, had relatively less effect than was expected, especially the NF-κB inhibitor BAY-11-7082. Also, siRNA targeted suppression of LCN2 was able to completely inhibit mRNA expression, but had far less effect on protein expression even after 6 days post transfection. Previous studies using siRNA targeting human LCN2 are notably absent. Tong et al. (2008) used siRNA targeting LCN2 in pancreatic cell lines. However, they noted only partial protein suppression in the DLD1 cell line and only minor change in the HCT116 cells. Ianetti et al. (2008) also used siRNA to demonstrate a knockdown of LCN2 protein. However in the Ianetti et al. study, the siRNA construct was constitutively transfected in a plasmid vector. This data therefore seems to suggest that LCN2 protein is actually relatively stable and has a low turnover rate If LCN2 is indeed stable, this may have implications if it is to be used as a drug target.

In conclusion, a number of key points may be derived from the data in this chapter.

1. LCN2 influences the expression of a wide range of genes and signalling pathways including many genes such as SPARC which have not previously been associated with LCN2.
2. That LCN2 acts in a paracrine manner, but that recombinant LCN2 protein was not able to affect expression of genes such as E-cadherin suggesting a further intracellular role for LCN2.
3. Extracellular LCN2 is able to influence ERα expression.

Chapter 7: Defining Network Pathways associated with LCN2 suppression

7.1 Defining network pathways associated with LCN2 suppression

In summary of previous results (See section 6.1), I observed suppression of LCN2 in PC3 cells led to significant changes to the expression of numerous genes. Microarray analysis of PC3-shLCN2 cells also suggested that rather than affecting a single signalling pathway, LCN2 is able to interact with a wide range of networks (See section 6.2). siRNA suppression of LCN2 further confirmed that although some genes are likely to be indirectly affected, expression of genes such as KLK6, and proteins such as ERα show a more rapid response to LCN2 levels.

Combining the data from microarray analysis, drug treatment, shRNA and siRNA it appears that LCN2 is able to regulate a number of separate pathways See sections 5.2, 6.2, 6.8), in particular, LCN2 appears to most significantly influence steroid receptor pathways, EGFR signalling, and WNT signalling. However, how exactly LCN2 is eliciting these effects is unknown given that it has no known phosphorylation activity, and is not known to bind to any other proteins aside from MMP9 (Chakraborty et al., 2013). Indeed, while functional groupings were listed (section 6.2), exactly how LCN2 is interacting with these networks and pathways remains unknown. Hence a range of potential pathways were investigated to observe if they were affected by LCN2 suppression, namely ERK signalling, AKT signalling and mTOR signalling.

ERK is a member, and one of the classical effectors of the MAPK pathway, and has been shown to act directly downstream of a wide range pathways, in particular EGFR and ERα (Filardo et al. 2000). ERK is also of interest as G-coupled receptor (critical mediators of the receptor-tyrosine-kinase to RAS bridge signalling) was highlighted as being up-regulated by PANTHER analysis (Section 6.2). As ERK is a

kinase, total levels of the protein are generally consistent, however p-ERK levels are subject to rapid change. Links between LCN2 and ERK have been previously been linked to LCN2 by Tong et al, 2009 and by Yang et al., 2013 who suggest ERK acts as a mediator of LCN2 activity. However, previously, the MEK (upstream of ERK) inhibitor U0126 was found to have no influence on LCN2 (Section 5.4). To investigate further, levels of ERK were therefore investigated in PC3-shLCN2 cells. It was found that in PC3-shCon cells, p-ERK was found only at very low levels. LNCaP cells by contrast have high expression and used for positive control purposes. There was also no change to p-ERK expression in PC3-shLCN2 cells (Figure 7.1). It was therefore concluded that p-ERK signalling is not a suitable candidate, in PC3 cells at least for acting as a mediator of LCN2 expression.

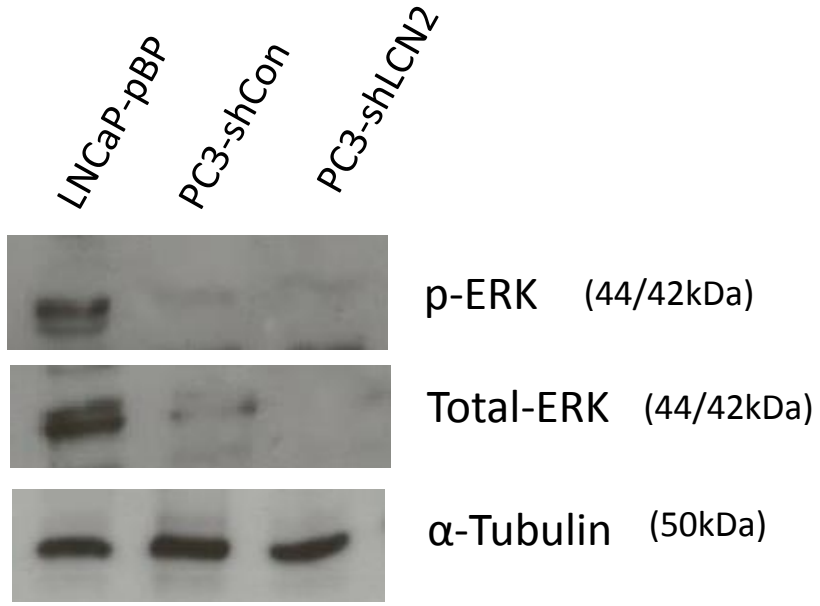

Figure 7.1 ERK expression in PC3-shLCN2 cells. Western blot of phospho-ERK and total ERK in PC3-shCon and PC3-shLCN2 cells. LNCaP-pBP used as a positive control.

7.2 LCN2 and mTOR signalling

mTOR is a protein kinase which is associated with a range of cell functions including cell growth, autophagy and angiogenesis (Sarbassov et al., 2005, Laplante and Sabatini, 2012). mTOR is associated with either of two complexes known as mTOR1 and mTOR2. The mTOR1 complex consists primarily of Raptor, DEPTOR mLST8, in addition to mTOR itself. mTOR2 comprises primarily of mTOR, as well as Rictor and mLST8 (Laplante and Sabatini, 2009). mTOR1 is particularly associated with autophagy inhibition through its activation of ATG13 (Lapnte and Sabatini, 2009). mTOR1 also plays a significant role in transcription and mitochondrial based metabolism (Groenewoud and Zwartkruis, 2013). mTOR2 on the other hand is strongly associated with cytoskeletal remodelling (O'Reilly et al., 2006). Both mTOR1 and mTOR2 complexes are regulated in part by ATK phosphorylation. The two complexes are interdependent, with mTOR1 able to activate mTOR2 and vice-versa (Sarbassov et al., 2005). The primary downstream targets of the mTOR1 complex are p-70S6Kinase (a.k.a p-S6K) and p-4EBP1, which are both phosphorylated and which lead to changes to post-transcriptional regulation of genes (Tabatabaian et al., 2010, Laplante and Sabatini, 2009).

mTOR signalling emerges as a potential candidate in LCN2 signalling for a number of reasons. Firstly, while mTOR signalling itself did not emerge as a significant pathway from microarray analysis via PANTHER, the biological functions designated by METACORE analysis point towards some of the processes traditionally linked to mTOR including pentose phosphate pathways angiogenesis and cytoskeletal remodelling (Sarbassov et al., 2004). The extreme phenotypic changes observed in PC3-shLCN2 cells may also be indicative of autophagy dis-regulation whereby dysfunctional cellular components are degraded.

Previous results demonstrated that ERα and ERβ levels appear to be regulated in PC3-shLCN2 cells by post-transcriptional or post translational mechanisms. mTOR signalling is a key component of post-translational regulation within the cell. Indeed, mTOR signalling has been proposed as an estrogen receptor regulator (O'Reilly et al., 2006) it was therefore hypothesised that LCN2 suppression was affecting mTOR signalling either directly or indirectly.

The mTOR pathway acts primarily through phosphorylation, and has effects more often associated with post-transcriptional regulation rather than direct mRNA changes (Hay & Sonenburg, 2004).The effects of mTOR therefore are unlikely to be readily obvious from Microarray analysis as most of mTOR's effects are only seen post-transnationally. Indeed there was no significant difference in the mRNA transcription levels of mTOR, P70S6K (encoded by the RPS6KB1gene) or 4EBP1. To assay for mTOR activity, Western blot analysis was performed on PC3-shCon and PC3-shLCN2 cells. These populations were also treated with 100 nmol/ml of Rapamycin (the traditional inhibitor of mTOR) for 48hrs.

Regarding p-mTOR expression, under normal conditions, expression was found to be moderately lower in PC3-shLCN2 compared to PC3-shCon cells (Figure 7.2A). However, when cells were treated with rapamycin, PC3-shCon cells were found to unresponsive, and expression of p-mTOR did not change (Figure 7.2A). By contrast, PC3-shLCN2 cells were responsive to rapamycin treatment, and p-mTOR expression was reduced. Levels of total-mTOR were unchanged between both cell types, and between treated and untreated cells. Expression of the classical mTOR target p-S6K was assessed by two antibodies targeting the pSer371 and pThr37/46 phosphorylation sites however no expression for either cell type was observed for pThr37/46. Using the pSer371-pS6K antibody, expression was found to be

significantly reduced, but still present in PC3-shLCN2 cells compared to PC3-shCon cells. In both cell types, treatment with rapamycin totally abolished expression. With regards to p4E-BP1, expression was also found to be similar in PC3-shLCN2 cells compared to PC3-shLCN2 cells. Rapamycin treatment was effective in reducing p4E-BP1 levels in both cell types, but did not totally abolish expression. In addition, levels of p-AKT were assessed in PC3-shLCN2 cells, however levels were found to be similar to PC3-shCon cells and in both cell types p-AKT signals were strong (Figure 7.2B). These results therefore appear to show a notable down-regulation of the mTOR pathway which also fits with the phenotypic changes observed, especially cytoskeletal changes, and post-transcriptional changes observed to genes such as ERα/β.

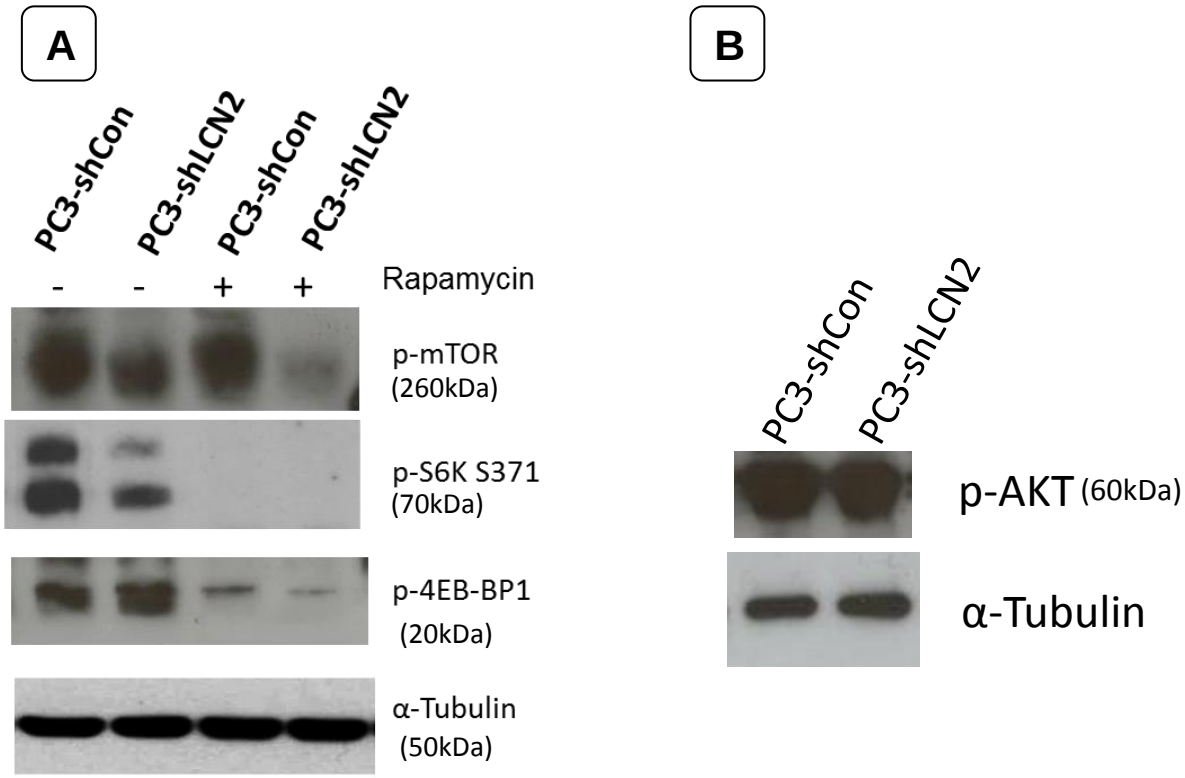

Figure 7.2 mTOR signalling in PC3-shLCN2 cells: **A**-Western blot analysis of p-mTOR and substrates p-S6K and p-4EB-BP1. PC3-shCon and PC3-shLCN2 cells were treated with 10μmol rapamycin. Note shown is p-S6K (Thr378) which showed no expression in either cell type. **B-** Western blot of p-AKT. All data is representative of n=3.

7.3 Effects of recombinant LCN2 and siLCN2 on mTOR signalling in PC3-shLCN2 cells

To further investigate the effects of LCN2 on mTOR signalling, recombinant LCN2 protein was employed to examine if it would affect mTOR and its downstream proteins. Using the same conditions as before (See section 6.7), PC3-shCon and PC3-LCN2 cells were supplemented with 0.5, 1.5, 5 and 15ng of LCN2 protein for 24hrs. p-mTOR expression showed little change following LCN2 treatment. p-S6K(SER371) expression on the other hand did show a positive response to recombinant LCN2. As before, p-S6K expression was higher in PC3-shCon cells, however expression which increased with dosage, with the highest expression at 15ng/ml of treatment. PC3-shLCN2 cells also showed increased expression in response to treatment. With regards to p-4E-BP, the effect of recombinant LCN2 was less obvious; however minor increases in expression were seen in both PC3-shCON and PC3-shLCN2 cells at 15ng/ml of treatment (Figure 7.3)

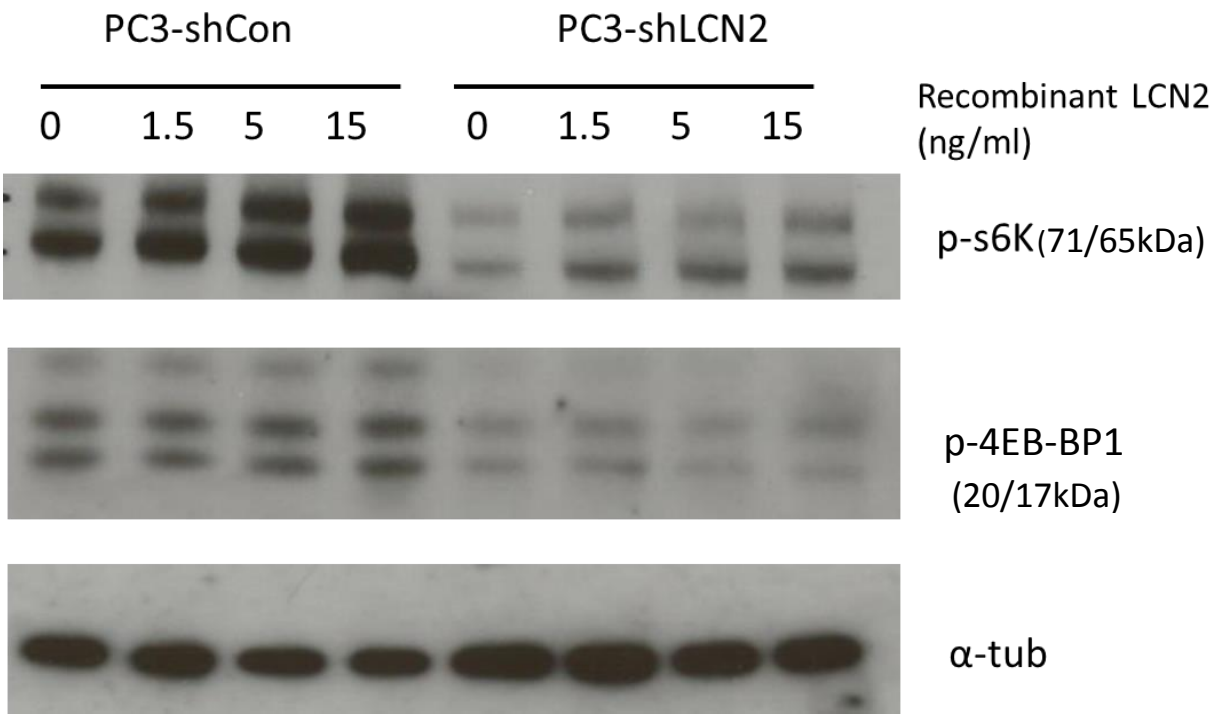

Figure 7.3 mTOR substrates in response to recombinant LCN2 protein. Using identical conditions to figure 6.8, PC3-shCon and PC3-shLCN2 cells were treated with recombinant LCN2 for 48hrs.Data is representative of n=3 experiments.

7.4 Effects of siRNA suppression of LCN2 on mTOR signalling

In order to observe whether temporary suppression of LCN2 affected mTOR associated protein expression, siRNA targeting LCN2 was employed.

Using the same conditions as section 6.8 above, the effects of temporary siRNA mediated LCN2 knockdown was investigated on mTOR linked proteins. Suppression of LCN2 mRNA expression is was already confirmed for previous experiments (See Section 6.8, figure 6.10A) although expression of LCN2 protein remained strong despite the loss of mRNA (See figure 6.10B above). Under these conditions, no observable change was noted to either p-S6K or p-4E-BP1 expression in PC3-Parental cells (Figure 7.4), thus indicating that a more substantial or long term loss of LCN2 may be required to illicit an effect.

When combining all the data therefore, there is evidence for LCN2 affecting mTOR signalling, although effects appear to be dependent on protein levels. Quite how LCN2 is able to influence mTOR phosphorylation remains unknown as p-AKT, which is the primary kinase upstream of mTOR remained unchanged in PC3-shLCN2 cells. However, a large caveat is that AKT is phosphorylated at multiple sites and it may simply be that the antibody used does not detect the correct phosphorylation site. Indeed, the mTOR complex is known to be phosphorylated via the T246 site, whereas the antibody used detected only the S473 site. mTOR signalling is activated by a wide range of kinases. mTOR has been linked to AMPK which is associated with energy production and stress, and is strongly associated with the TSC1/2 complex. Hence, it is possible that LCN2 is able to influence one or more of these signalling mechanisms

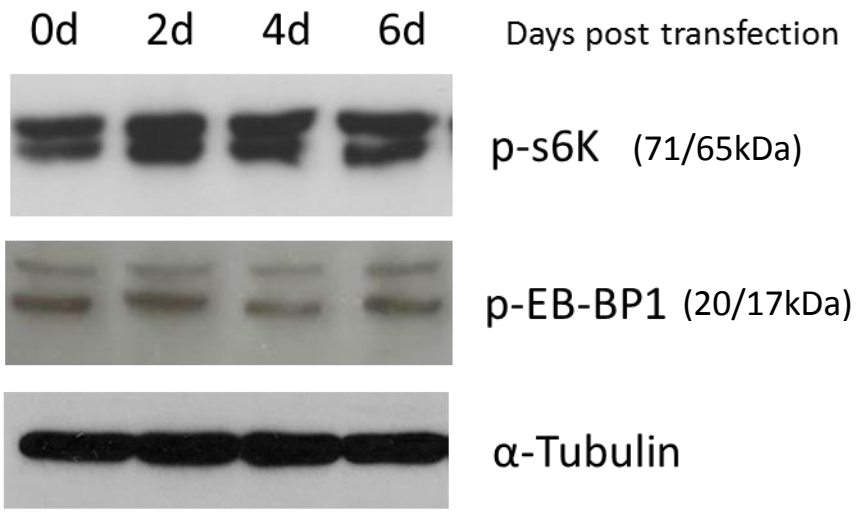

Figure 7.4 Expression of mTOR substrate proteins after siLCN2 transfection: siRNA suppression of LCN2 mRNA was previously confirmed (Figure 6.10). Western blot analysis of p-S6k and p4EB-BP1 -in in response to siLCN2 after 0,2,4 and 6 days. Blot is representative of n=3 experiments.

7.5 LCN2 signalling and iron homeostasis.

The effects of LCN2 suppression on such a wide range of genes, proteins and pathways is somewhat surprising given the small size of the protein itself, and its lack of any phosphorylation site, or indeed of any other conserved enzymatic domain aside from the lipocalin domain itself (Flower, 2000). LCN2 was first described as an iron chelator (Kjeldsen et al., 1994). This function has been linked to immunity against bacteria, but is believed to play a role in the overall homeostasis of the Fe3+ ion within the cell (Torti and Torti, 2011). However, the effects of LCN2 shuttling in and out of the cell are poorly understood. It was therefore hypothesised that the effects and signalling seen previously may be a result of LCN2 altering intracellular iron levels. Within this hypothesis however, there are two possible outcomes of LCN2 suppression: Firstly, LCN2 suppression may lead to the inability of cells to import Fe3+ from their surroundings, leading to iron starvation, conversely, LCN2 suppression may result in cells being unable to export iron, thus leading to iron overload.

LCN2 does not bind to Fe3+ directly, but rather to iron bound to siderophores (Flo et al., 2004). Deferoxamine (a.k.a Desferrioxamine; DFOX) is a commercially available siderophore derived from Streptomyces pilosus bacteria. DFOX functions by binding to free iron within the media, thus preventing its use by cells. Hence, DFOX acts as a model for iron depletion. As DFOX is a long chain siderophores, it is unable to be bound by LCN2 (Gomez-Casado et al., 2013).

PC3-shCon and PC3-shLCN2 cells were treated with 10µg/ml of DFOX (as previously described by Ndong et. al., 2009 for 48 hrs. Following treatment, distinct morphological changes were observed in both cell types. PC3-shCon cells treated

with DFOX were noticeably flattened and larger than untreated cells (Fig 7.5). Under bright field lighting, cells also appeared to lose phase contrast, with a notable loss of cytoskeletal structure. Indeed, treated PC3-shCon cells displayed a phenotype that was strikingly similar of that found in PC3-shLCN2 cells. Cells also looked unhealthy, and higher numbers of dead cells were observed. When PC3-shLCN2 cells were treated with DFOX, cells presented an even more extreme phenotype. In these cells, there was a dramatic loss of phase contrast, cells also became highly flattened. A distinct loss of cell edge definition and in particular of cell-cell edges was observed. Cells appeared to have a dramatic loss of cell shape integrity, and also contained numerous vacuoles. The evidence therefore appears to suggest that preventing PC3 cells from obtaining iron is able to induce a PC3-shLCN2 like phenotype, and can lead to cytoskeletal disruption and loss of cell polarity.

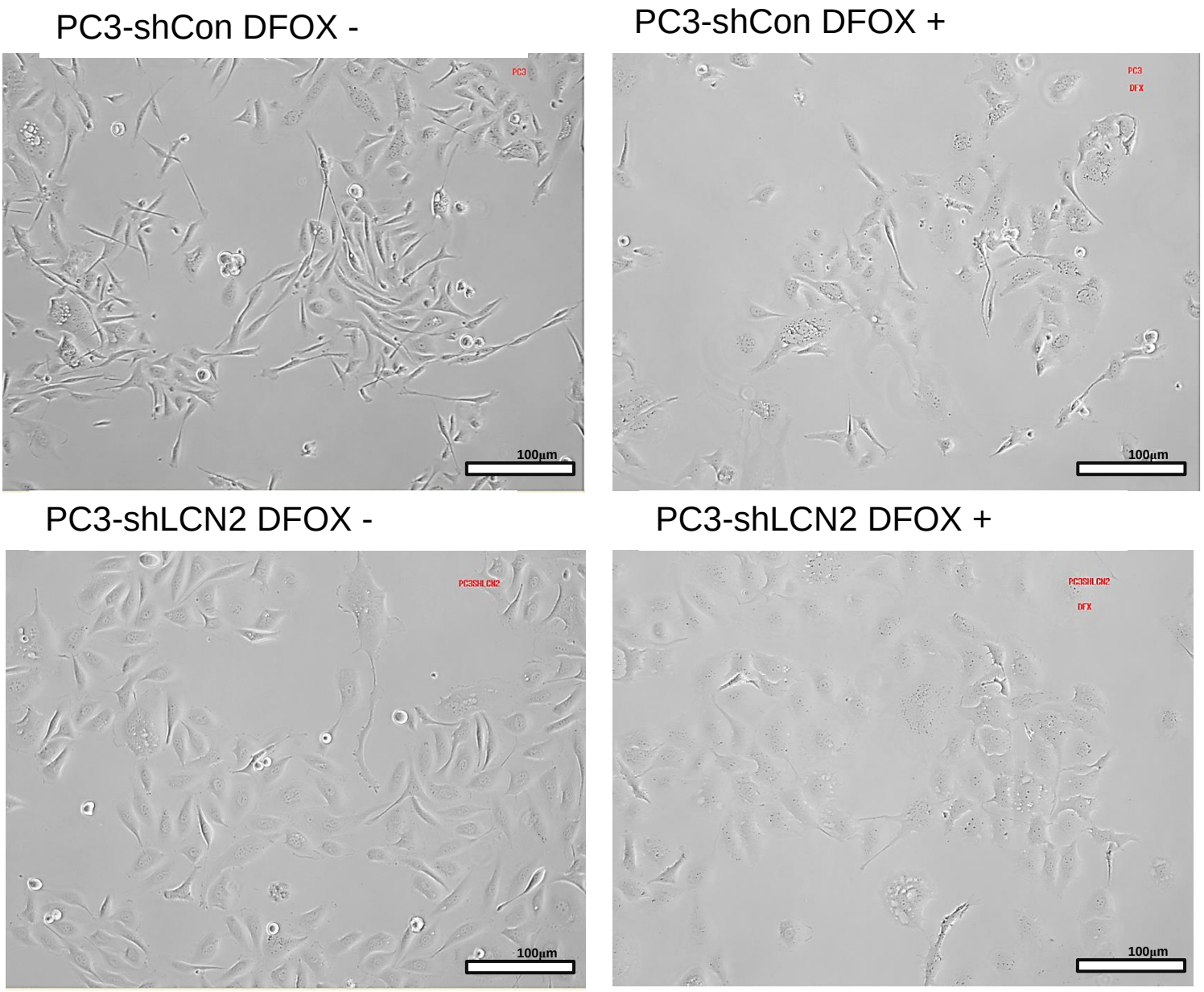

Figure 7.5: Deferoxamine treatment of PC3 cells. PC3-shCon and PC3-shLCN2 cells were treated with 10µM Deferoxamine (DFOX) for 48 hours. Following treatment, PC3-shCon cells showed phenotypic change similar to PC3-shLCN2. DFOX treated PC3-shLCN2 cells showed a further loss of phase contrast and defined cell edges. Images are representative of n=3 experiments. x20 magnification.

7.6 qPCR analysis of DFOX treated PC3 cells shows effects opposite to those found in PC3-shLCN2 cells.

qPCR analysis was carried out on DFOX treated cells to determine effects on mRNA expression (Figure 7.6). Firstly, LCN2 expression itself in PC3-shCon cells was found to be decreased slightly, but significantly, by 1.7 fold . Significant changes were observed a range of other tested genes previously identified from Microarray data. It was found that in DFOX treated cells, in many cases, expression was the opposite of what was previously found in PC3-shLCN2 cells. With regards to genes which were previously found to be upregulated in PC3-shLCN2 cells. A 3.2 fold reduction in SPARC expression was also recorded in treated PC3-shCon cells it was found that PC3-shLCN2 cells treated with DFOX showed a 12 fold reduction in SPARC expression relative to untreated cells (Figure 7.6). A 2.5 relative fold reduction was also observed in KDR expression in both PC3-shCon and PC3-shLCN2. Expression of AGR2 was also reduced in both treated PC3-shCon and PC3-shLCN2 cells.

Changes to mRNA expression were also observed to genes previously found to be down-regulated in PC3-shLCN2 cells. ACTG2 expression in DFOX treated PC3-shCon cells was found to be increased 1.9 fold relative to untreated cells. Also, ACTG2 expression in PC3-shLCN2 cells (which was ~62 fold lower than PC3-shCon cells) was increased by 2 fold when treated with DFOX (Figure 7.6). A similar pattern emerged with CDH1; expression was increased in treated PC3-shCon cells (2.8 fold), whereas expression increased 4.5 fold in PC3-shLCN2 cells (2.2 fold). However, this pattern was not universal. KRT7 expression was reduced in both PC3-shCon and PC3-shLCN2 cells; although there was a greater effect seen in PC3-

shLCN2 (2.4 and 6.6 fold reductions respectively). Expression of KLK6 was unchanged.

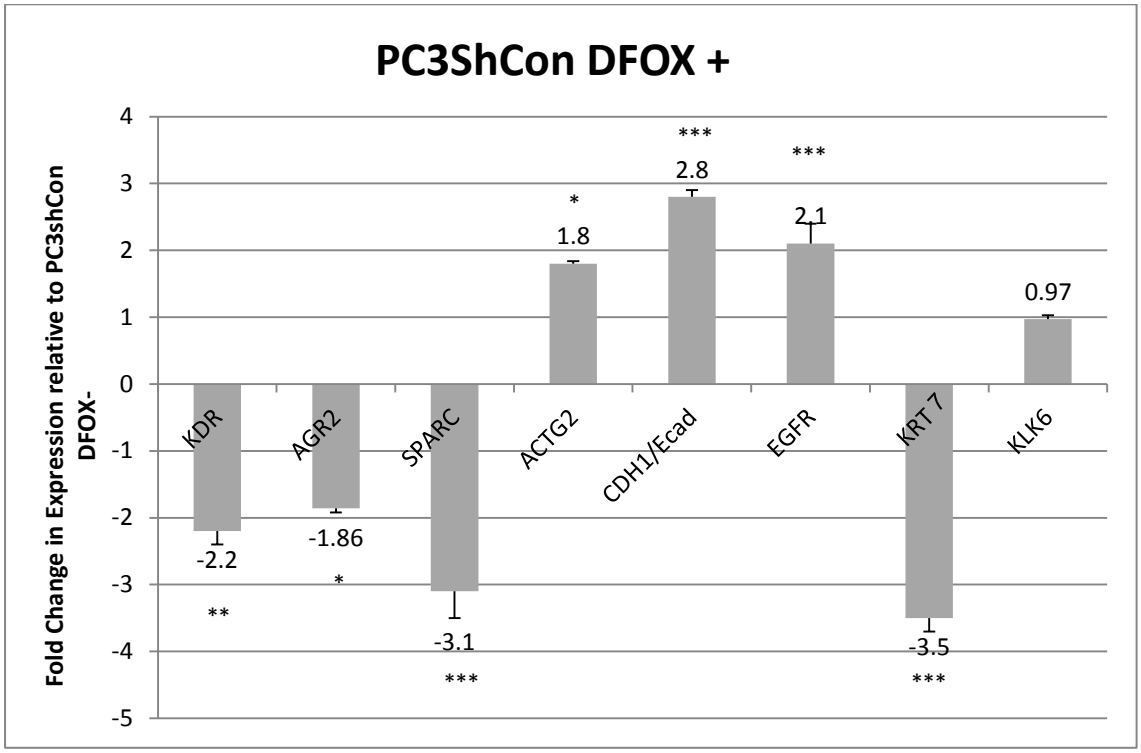

Figure 7.6 PC3 gene expression in response to Deferoxamine. PC3-shCon cells were treated with 10μM Deferoxamine (DFOX) for 48 hours. qPCR analysis of a selection of genes previously identified from microarray analysis as being strongly up or down regulated in PC3-shLCN2 cells (See section 6.2). Values are relative to untreated PC3-shCon cells +/-SEM Statistical analysis was carried out using Student's t-test. *p<0.05 ***p<0.001, n=3.

7.7 Effects of DFOX treatment on protein Expression

In addition to mRNA expression, the expression of key proteins was assessed, in particular those associated with steroid metabolism, or to mTOR signalling.

As with mRNA expression, LCN2 protein was found to be unchanged upon DFOX treatment. With regards to ER expression, Expression of ERα was increased slightly in treated PC3-shCon cells, and also a possible increase in treated in PC3-shLCN2 cells (Figure 7.7A). There was slight reduction in E-cadherin expression in treated PC3-shCon. However, no change was observed in PC3-shLCN2 cells and E-cadherin remained unexpressed.

Protein expression analysis was also carried out on the mTOR pathway. The primary reason for investigating this is due to the interaction of HIF1α and mTOR (Hudson et al., 2002). HIF1α is susceptible to changes in iron levels (Maxwell and Salnikow, 2004), and thus may provide a link to LCN2. HIF1α was very weakly expressed in both PC3-shCon and PC3-shLCN2 cells. When treated with DFOX however, expression was up slightly in DFOX treated PC3-shCon and in PC3-shLCN2 cells, although the level of increase was higher in PC3-shCon than the other(Figure 7.7B) . It should be noted that in all cases, strong bands were seen at ~48 kDa and ~ 52 kDa which may be representative of HIF1α breakdown in normoxic conditions. As such, despite the changes observed, HIF1α is unlikely to be a mediator for LCN2 under these conditions.

With regards to other members of the mTOR signalling pathway, p-mTOR itself was found to be unchanged under DFOX conditions. On the other hand, p-S6k expression was found to be reduced in treated PC3-shCon cells, however, in PC3-shLCN2 cells, this reduction appeared to be greater (Figure 7.7B).

Overall therefore, when combining the data from phenotypic change, qPCR and protein expression, the data suggests that iron chelation is able to induce a PC3-shLCN2 like phenotype, but that this does not correlate to similar gene expression patterns. What the data does show however, is that genes which were associated with LCN2 either from the microarray or otherwise do show a response to DFOX.

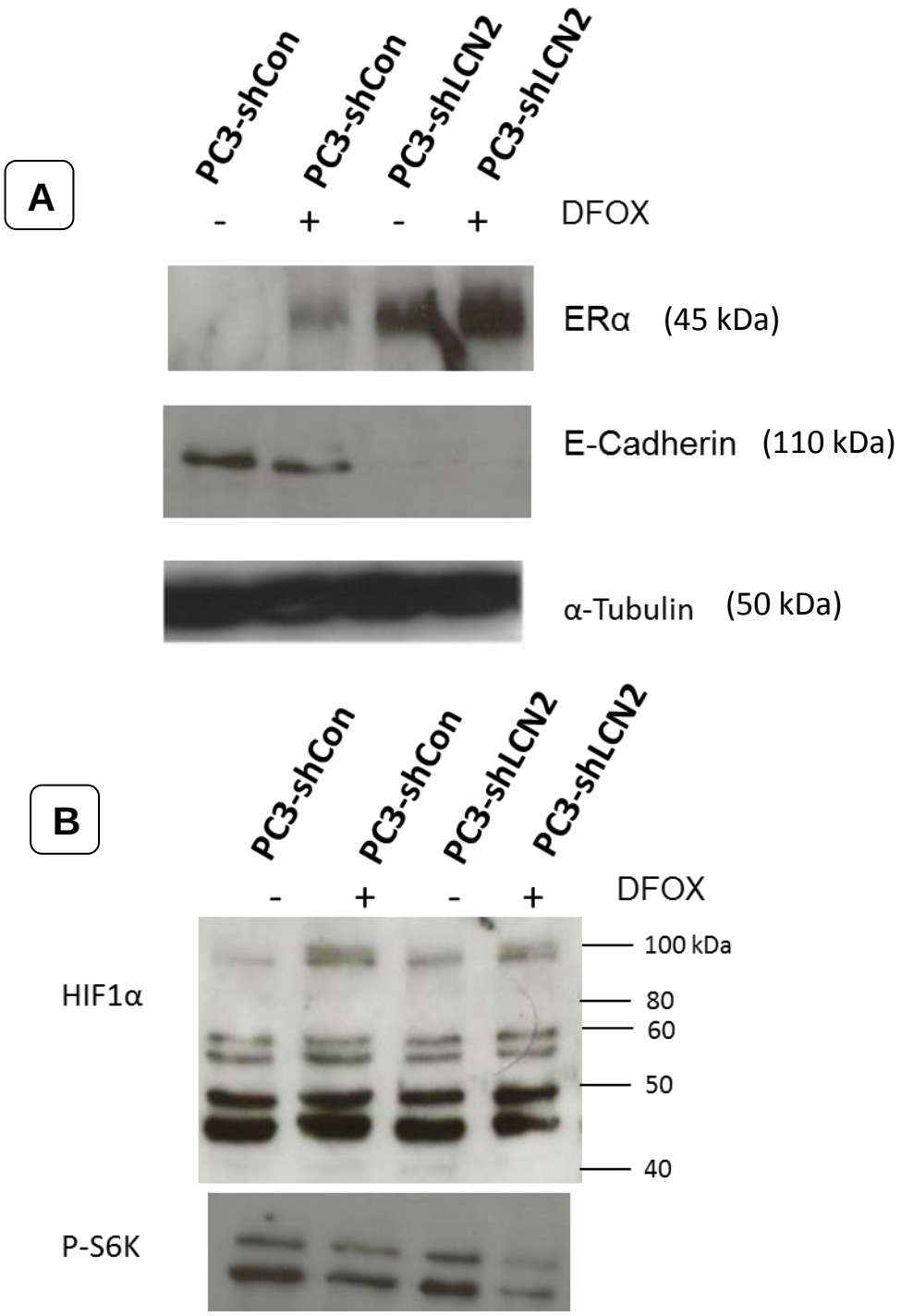

Figure 7.7 PC3 protein expression in response to Deferoxamine: A Western blot analysis of ERα, E-cadherin in PC3-shCOn and PC3-shLCN2 cells in response to deferoxamine treatment. **B** mTOR linked proteins HIF1α and p-S6K in response to Deferoxamine (Note, loading controls were the same for both A and B). Data is representative of n=3 experiments)

7.8 Discussion

Despite research into the effects of LCN2, and its suitability as a biomarker, relatively little is known about its methods of action and exactly how it gives rise to downstream effects. Given that LCN2 lacks any kinase domains, and has no transcriptional activity, the wide ranging effects of LCN2 suppression are likely to be due either to an unknown binding protein, or more likely due the effect LCN2 has on intracellular iron levels .

A number of signalling pathways have previously been proposed for LCN2, including ERK (Mir et al., 2012). However, I found that in PC3 cells at least, ERK is unlikely to be a target of LCN2, although this may be due ERK being only weakly expressed in PC3 cells. Weak ERK expression in PC3 cells may also explain why the ERK inhibitor U0126 had no effect on LCN2 cells (See section 5.2).

In this chapter, I demonstrated that PC3-shLCN2 cells have reduced expression of the mTOR pathway including p-s6K. Moreover, expression of p-s6k was partially restored upon addition of recombinant LCN2 protein. To date, no studies have reported any link between the mTOR pathway and LCN2. The data in this chapter however does suggest that LCN2 is able to directly interact with this signalling mechanism. The mTOR pathway is associated with a number of cellular functions, but particularly autophagy and post-transcriptional regulation. PC3-shLCN2 cells were enlarged and contain a sub-population of cells with a high degree of nuclear aberration. This phenotype may be suggestive of reduced autophagy in the cell which allows the build-up of dysfunctional cellular components (Pattingre et al., 2008). Also, it was previously noted that ERα:β ratios in PC3-shLCN2 cells was

changed (See section 5.13) and that this change was post-transcriptional which may be explained in part by changes to mTOR activity.

In the results shown here, I demonstrated that treatment of PC3 cells with the iron chelator deferoxamine led a phenotype similar to that of LCN2 knockdown cells, coupled with a slight increase in ERα expression. This would seem to suggest that LCN2 is acting to increase the labile iron pool. However, although the morphology of DFOX treated cells was similar to PC3-shLCN2 cells, this did not correlate with gene expression patterns seen in PC3-shLCN2 cells. The role of LCN2 in regulating the intracellular labile iron pool is still unclear. Current hypotheses state that LCN2 binds to siderophores, trafficking iron into the cell where is released. Iron is critical for cell growth, however if there is too much intracellular iron, Fe^{3+} in the cell leads to reduced pH which can lead to activation of mechanisms such as cell cycle arrest (Torti and Torti, 2011).

As LCN2 has no phosphorylation activity, it is probable that LCN2 functions through regulating iron levels, and this may be affecting mTOR expression as well as other phenotypic changes observed. Reduced iron levels in cells has been shown down-regulate the TSC1/2-mTOR pathway (Ndong et al., 2009). Moreover, uptake of nutrients such as iron have also been shown modulate cell size via the AKT/mTOR pathway (Edinger and Thompson, 2002).

High Fe^{3+} levels are also known to activate HIF-1α (Maxwell and Salnikow, 2004). HIF-1α is a known activator of the mTOR pathway (Agani and Jiang, 2013),. As such it appears that suppression of LCN2 leads to the reduction of the labile iron pool. This in turn may be deactivating pathways such as mTOR, and hence leading to the extreme phenotype seen in PC3-shLCN2 cells.

In this chapter, I demonstrated that while Deferoxamine treatment of PC3 cells led to these cells acquiring a PC3-shLCN2 like phenotype, mRNA expression patterns of target genes such as SPARC and E-cadherin were the opposite of those found in PC3-shLCN2 cells. However, expression of ERα was elevated in Deferoxamine treated PC3 cells. The data suggests therefore that although LCN2 may be acting in regulating intracellular iron levels, the precise effects of iron withdrawal are likely to somewhat complex, and effects are also likely to be influenced by other factors such as DNA methylation status, interaction between different cellular pathways and the expression of other iron-related factors such as transferrin (Torti and Torti, 2011).

One issue with LCN2 is that it has been shown to have either pro- or anti- apoptotic effects depending on whether it is bound to iron or not (Devireddy et al., 2005). Hence, removal of iron by deferoxamine may not be having the same effect as suppressing LCN2 completely. Whether iron bound LCN2 affects signalling is very poorly understood, and it therefore possible that iron-free LCN2 is responsible some of the mRNA expression changes observed. A further issue is that LCN2 has been shown not to bind directly to iron, but rather only to siderophores. (Although deferoxamine is a sub-class of siderophore it has been shown not to bind to LCN2 by Correnti et al., 2012). While some siderophores are produced endogenously by human tissue (Raffatellu et al., 2009), there are likely to be fewer siderophres in culture media compared to *in vivo* and thus may influencing results.

In conclusion, the data in the chapter suggests the following:

1) Suppression of LCN2 expression in PC3 cells leads to down-regulation of the mTOR pathway which is partially restorable upon supplementation of recombinant LCN2 protein
2) That treatment of PC3 cells with the iron chelator Deferoxamine results in a phenotype similar to that of PC3-shLCN2, including elevated ERα levels, but opposing effects to expression of some LCN2 target genes.

Chapter 8
Suppression of LCN2 in the MCF7 breast cancer cell line.

8.1 Generation of an MCF7-shLCN2 cell line

To identify whether the effects seen in PC3-shLCN2 cells were characteristic of LCN2 expression in general, or specific to PC3 cells, LCN2 suppression was also performed in a further cell line. Ideally, a further prostate cancer cell line would be preferable in this instance, however out of all the commonly used PCa cell lines, only PC3 shows LCN2 expression at sufficient levels. GEO profiling, which included rarer PCa cell lines such as SV-1 further confirmed PC3 cells as having the strongest LCN2 expression amongst PCa cell lines. Breast cancer cell lines share a number of properties which provide a useful comparison to PCa. Firstly, BCa cell lines are primarily derived from epithelial tissue. Secondly, BCa cell lines are strongly associated with hormone receptor signalling, particularly ERα/β (Alderton, 2012).

In their 2009 study, Yang et al. used the MCF-7 cell line to demonstrate a negative correlation between ERα and LCN2 expression. The MCF-7 cell also line provides a highly suitable model for LCN2 suppression: MCF-7 cells are epithelial and express ERα and E-cadherin (Ye et al., 2010).

LCN2 levels were assessed in MCF-7 cells by qPCR, and ELISA. When analysed by qPCR, MCF-7 showed LCN2 mRNA levels comparable to those found in PC3 cells (Figure 8.1A). ELISA showed that MCF-7 secreted 1.8ng/ml LCN2 protein, slightly less than in PC3 cells, but significantly higher than other PCa cell lines (Figure 8.1B)

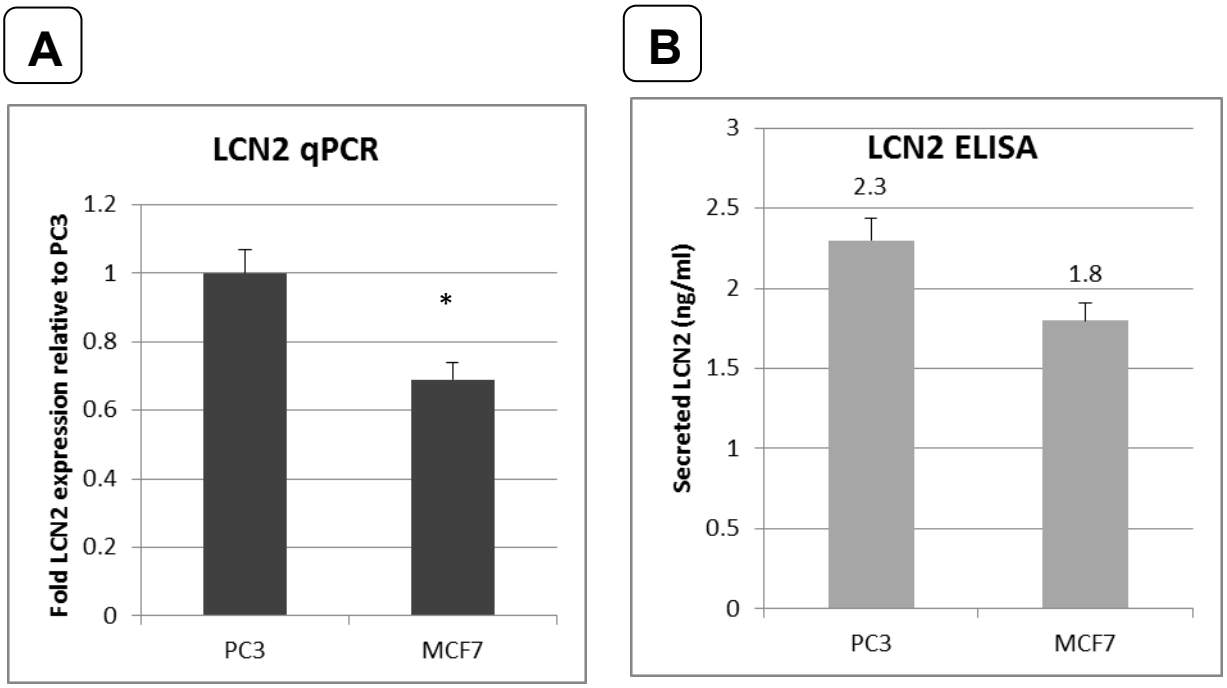

Figure 8.1. LCN2 expression in MCF7 cells. A qPCR analysis of LCN2 expression in MCF7 cells relative to PC3 cells (+/- SEM) Statistical analysis was carried out using Student's t-test.*$p<0.05$ **B** ELISA analysis of secreted LCN2 protein in MCF7 and PC3 cells. Data is mean of n=3.

The MCF-7-shLCN2 cell line was generated using identical methods and vectors as previously described for PC3-shLCN2 (See Materials and methods section 2.7). Empty vector controls were simultaneously used to create an MCF-7-shCon cell line. Cells were selected for 2 weeks under blasticidin treatment. Following a further 10 days of growth and splitting, mRNA and protein extraction was performed. qPCR analysis showed that suppression was successful, showing 22 fold decrease in LCN2 expression relative to both MCF-7-parental and MCF-7-shCon (Figure 8.2A). No difference in LCN2 expression was recorded between MCF-7-parental and MCF-7-shCon cells. Protein analysis via Western blot also showed a significant reduction in expression, although expression was not as total as seen with PC3-shLCN2 cells (Figure 8.2B). Suppression of LCN2 was confirmed using both the MAB1757 antibody (showing a 48 kDa band) and ELISA analysis confirmed a reduction in secreted protein, with MCF-7-shLCN2 cells secreting 0.55ng/ml of LCN2 (Figure 8.2C).

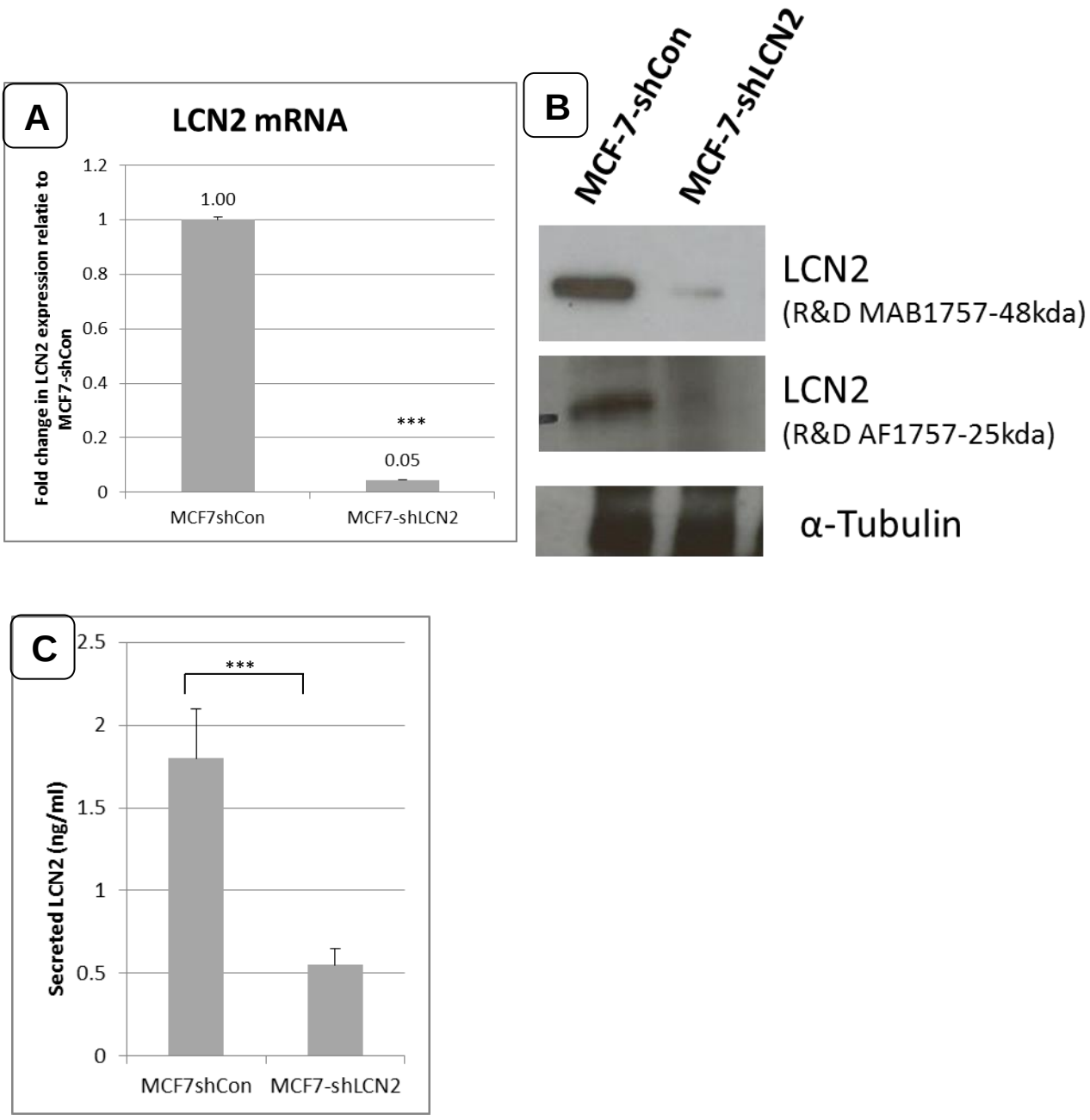

Figure 8.2: Characterisation of the MCF-7-shLCN2 cell line: A- qPCR analysis of LCN2 gene expression in MCF7-shCon and MCF7-shLCN2 cells. Values are relative to MCF7-shCon +/- SEM n=3 **B**- Western blot of LCN2 in MCF7-shCon and MCF7-shLCN2 suppression using both the MAB1757 antibody which detects bands at ~and the AF1747 antibody which detected bands at 25 kDa. Represenative of n=3. Protein and mRNA were extracted in parallel C- ELISA analysis of secreted LCN2 protein following 48 hrs of culture.(+/- SEM, n=3. ***p<0.001)

8.2 MCF-7-shLCN2 cells exhibit morphological changes.

Following 3 weeks of selection, MCF-7-shLCN2 cells were investigated for morphological changes. Under normal conditions MCF-7 cells are non-polar and roughly rounded but irregular in overall shape. Cell protrusions are present, but not prominent. MCF-7 cells form colonies which are moderately tight, but not notably dense. When MCF7-shLCN2 cells were observed however, a distinct morphological change was observed. Cells became flattened, and significantly larger in terms of cell surface area (Figure 8.3). This was combined with a loss of phase contrast under. Cells also showed signs of a loss of cell shape. A number of cells also contained large vacuoles. Indeed, overall, MCF-7-shLCN2 cells displayed a roughly similar phenotype to that found in PC3-shLCN2 cells (See section 5.7).

MCF-7-shCon

MCF-7-shLCN2

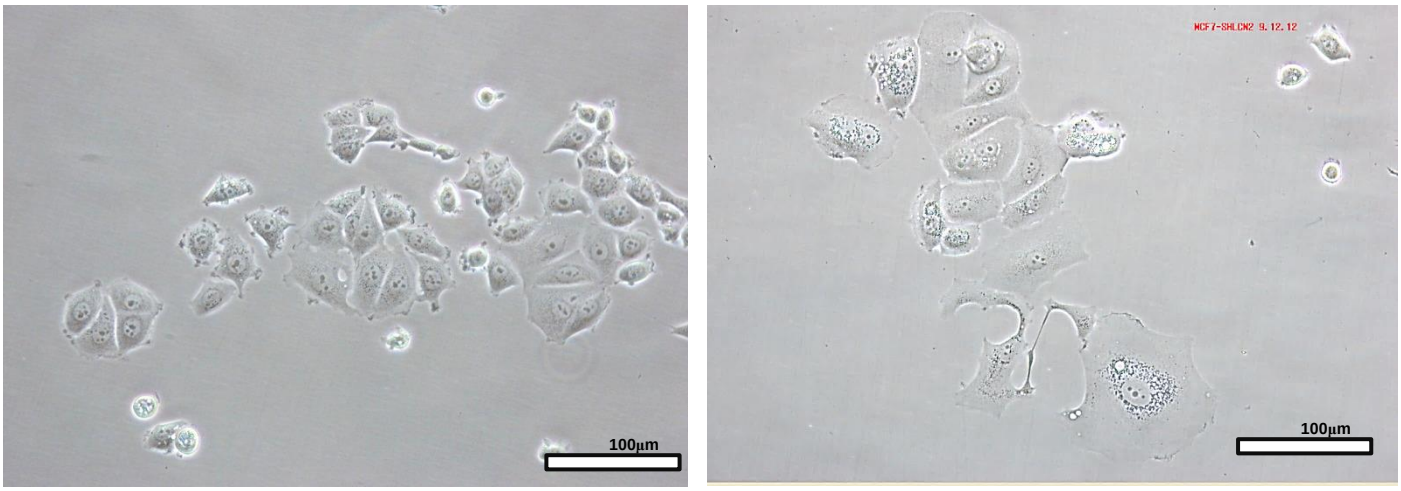

Figure 8.3: Morphology of MCF-7-shLCN2 cells. Bright field image analysis of MCF-7-shCon cells and MCF-7-shLCN2 cells following 3 weeks of selection. MCF-7-shLCN2 cells were notably flatter and displayed a loss of phase contrast. Images have been sharpened for printing purposes only. X20 magnification.

8.3 Gene expression in MCF-7-shLCN2 cells

To determine whether MCF-7-shLCN2 cells displayed similar characteristics in terms of gene or protein expression to PC3-shLCN2 cells, qPCR and Western blot analysis was carried out respectively using genes previously identified as possible LCN2 targets.

qPCR analysis was carried out on a range of genes identified from the PC3-shLCN2 microarray to be either highly up regulated or down regulated (See section 6.1), namely : SPARC, KDR, AGR2 (all up-regulated in PC3-shLCN2), AGTG2, KLK6, KLK5, ESRP1 and ST14 (all down regulated in PC3-shLCN2).

With regards to SPARC, no statistically significant difference in expression was observed. Both KDR and AGR2 on the other hand showed slight but consistent decreases in mRNA expression of 1.58 and 1.48 fold respectively (Figure 8.4A).

While the SPARC and KDR showed little change, genes that were previously found to be down-regulated in PC3-shLCN2 cells (See section 6.1) showed a generally greater level of response. ACTG2 was found to have a 13 fold increase in MCF-7-shLCN2 cells relative to MCF-7-shCon cells. A 7.3 fold increase was also observed for KLK5 in MCF-7-shLCN2 relative to MCF7-shLCN2. Increased expression was also observed for ESRP1 (2.1 fold), and for KLK6 (2.6 fold) (Figure 8.4B).

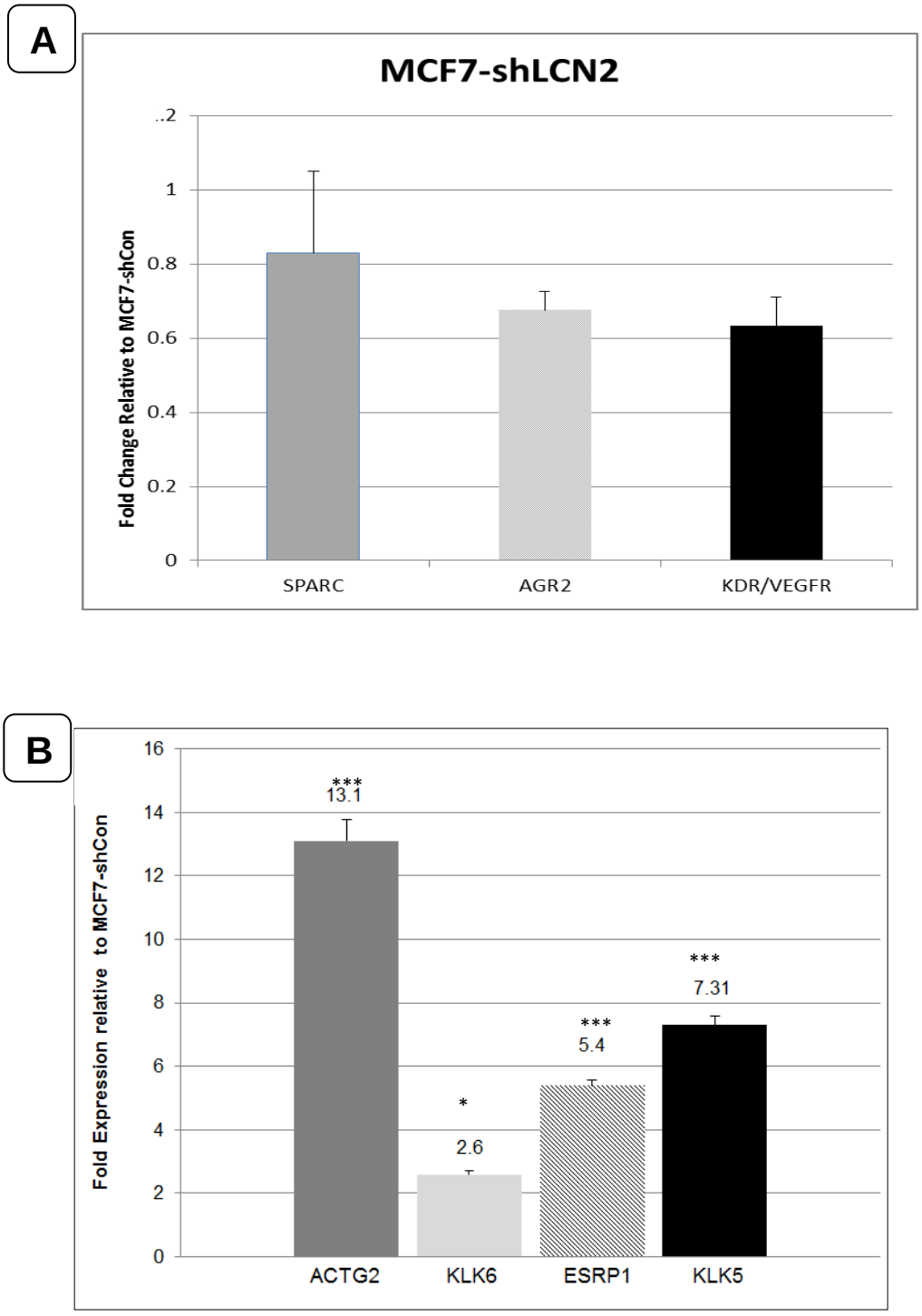

Figure 8.4: Analysis of LCN2 target genes in MCF-7-shLCN2 cells. qPCR analysis **A**- Analysis of SPARC, AGR2 and KDR, all of which were previously up-regulated in PC3-shLCN2 cells (Section 6.2). **B**- Analysis of ACTG2, KLK6, ESRP1 and KLK5 which were all down-regulated in PC3-shLCN2. All values +/- SEM. *p<0.05 ***p<0.001, Statistical analysis was carried out using Student's t-test. n=3)

8.4 ERα and E-cadherin expression in MCF7-shLCN2 cells.

In addition to qPCR analysis, the effects of LCN2 suppression on protein expression were also investigated with regards to steroid receptor EMT marker expression. In a previous study, Yang et. al. (2009) described a negative correlation between LCN2 expression and ERα levels, thus agreeing with data derived from PC3-shLCN2 cells (See figure 5.15). However, the group also described a negative correlation between LCN2 and E-cadherin in contrast to PC3-shLCN2 cells (See Figure 5.18). However, the Yang et al. study used only siRNA targeting LCN2 and did not utilise longer term suppression.

To identify if MCF7-shLCN2 cells agreed with the Yang et al. 2009 study, ERα, ERβ and E-cadherin protein expression was investigated. ERα protein expression was found to be increased in MCF-7-shLCN2 cells relative to MCF-7-shCon cells (Figure 8.5A), thus agreeing with both PC3-shLCN2 cells (See Figure 5.16) and with the Yang et. al. study. ERβ expression was relatively unchanged in MCF-7-shLCN2 cells. E-cadherin expression was also found to be increased in MCF-7-shLCN2 cells (Figure 8.5A), thus agreeing with the Yang et. al. study, but is the converse of PC3-shLCN2 cells (See Fig 5.18). In addition, qPCR analysis was carried out for both ESR1 (ERα) and ESR2 (ERβ) (Figure 8.5B). No significant change in expression was observed for either gene in MCF-7-shLCN2 cells, therefore implying that as with both LNCaP-LCN2 cells and PC3-shLCN2 cells, regulation of estrogen receptor by LCN2 is post-transcriptional.

To assess the activity of ERα activity, expression of downstream markers was assessed. HER2, the traditional marker of ER expression was found to be reduced 5.2 fold relative to controls. This was mirrored by EGFR which had a 5.8 fold

increase. Overall therefore, the data shows that LCN2 had an direct effect on ER expression. Unlike previous genes discussed however, the negative correlation between ERα and LCN2 appears to be same as that found in PC3-shLCN2 cells.. The influence on HER2 was not seen in PC3-shLCN2 cells however, although it should be noted that HER2 mRNA expression in PC3 cells is very low and as such was not pursued.

In PC3-shLCN2 cells, I previously found that these cells had reduced levels of E-cadherin, which was associated with an increase in expression of the E-cadherin repressor ZEB1 (See section 5.15), but that vimentin expression was unchanged. To assess whether any EMT related genes were being differentially regulated in MCF-7-shLCN2 cells, qPCR analysis was performed on E-cadherin, vimentin, SNAI1, SNAI2 ZEB1 and TWIST.

E-cadherin mRNA expression was increased 2.2 fold in MCF7-shLCN2 cells relative to MCF7-shCon (Figure 8.5B). This was coupled with deceases in expression for both ZEB1 and TWIST1 (-2.1 fold and -8.3 fold respectively), both of which are regarded as E-cadherin suppressors (Montserrat et al., 2011). No changes were observed for vimentin or SNAI2 expression. This therefore shows that LCN2 suppression is affecting E-cadherin expression, and this may be regulated through TWIST1 and ZEB1, but that its effects are opposite to that found in PC3-shLCN2 cells (See Section 5.15). The lack of change to vimentin expression also further confirms that LCN2 is affecting E-cadherin specifically rather than all EMT related genes (Fig 8.5B).

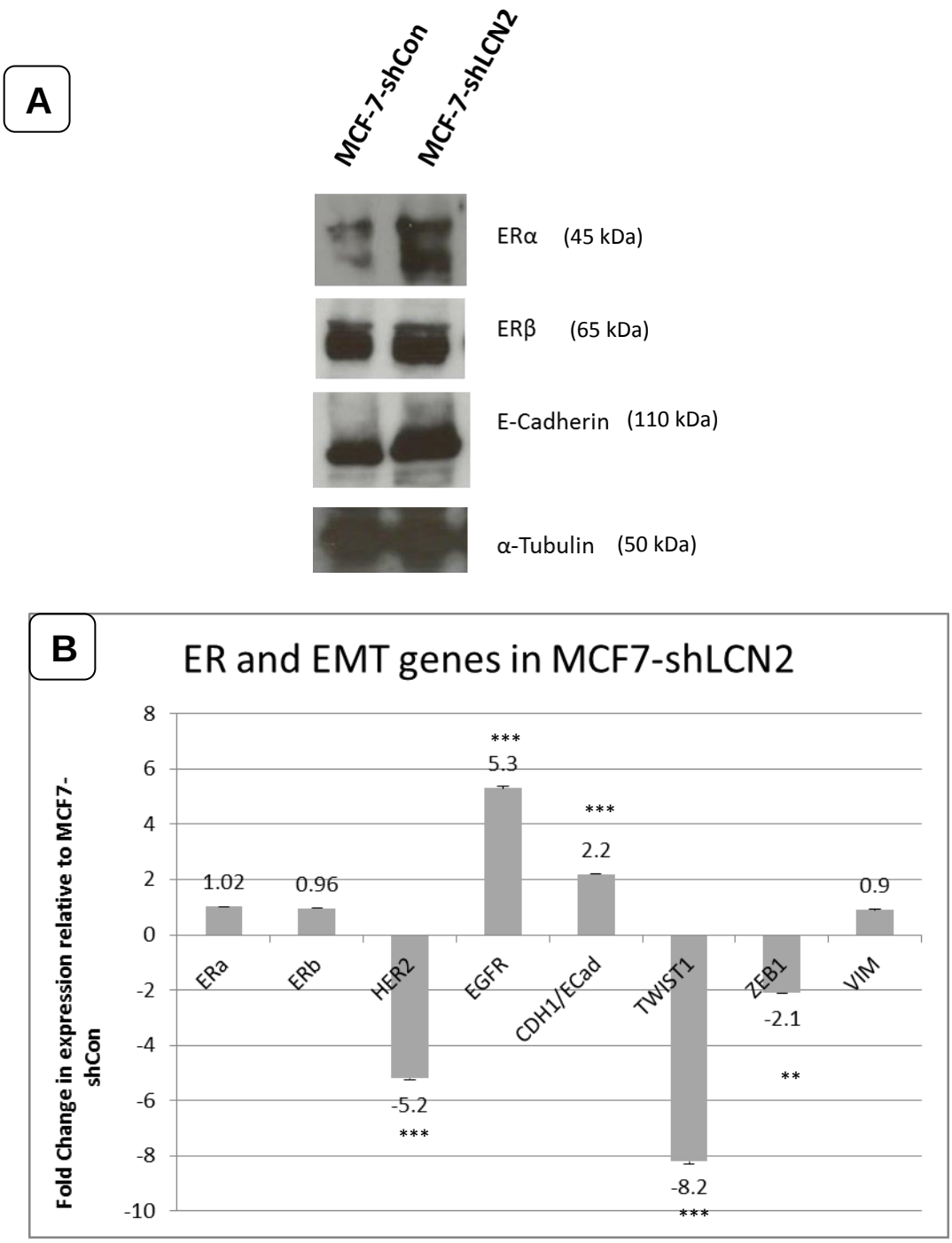

Figure 8.5: Expression of ER and EMT related genes: A- Western blot analysis of ERα, ERβ and E-cadherin in MCF-shLCN2 cells relative to controls. Representative of n=3 blots **B**-qPCR analysis of ERα, ERβ and downstream targets HER2 and EGFR. Also, analysis of gene expression for CDH1 and its negative regulators TWIST1 and ZEB1. All values are relative to expression in MCF7-shCon cells +/- SEM Statistical analysis was carried out using Student's t-test. **p<0.01 ***p<0.001

8.5 mTOR signalling in MCF7-shLCN2 cells . Previously**,** I identified mTOR as a possible effector of LCN2 signalling in PC3-shLCN2 cells, and where p-s6K expression was found to be reduced in PC3-shLCN2 cells (See section 7.2). Therefore I investigated whether mTOR signalling was differentially regulated in MCF7-shLCN2 cells. pMTOR expression itself was unchanged in MCF-7-shLCN2 relative to MCF7-shCon (Figure 8.6), however an increase to expression was observed for p-S6k. p-4E-BP1 also showed a moderate increase although expression was weak in both MCF-7-shLCN2 and MCF-shCon cells. As such, the effects observed in MCF7-shLCN2 cells were opposite of those found in PC3-shLCN2 cells.

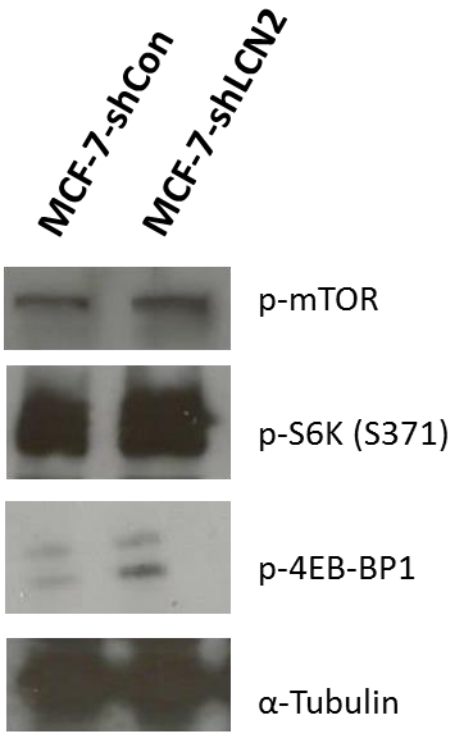

Figure 8.6: mTOR signalling in MCF-7-shLCN2 cells. Western blot analysis of p-mTOR and its downstream targets p-S6K and p-4EB-BP1. (α-Tub is identical to that in figure 8.5A). Data is representative of n=3 experiments.

8.6 DFOX treatment of MCF-7-shLCN2 cells

Previously, I found that chelation of iron by Deferoxamine in PC3 cells elicited a PC3-shLCN2 like morphology (See section 7.3). I therefore aimed to investigate whether a similar effect occurred in MCF7 cells. MCF-7-shCon and MCF-7-shLCN2 cells were treated with 10µg/ml for 48hrs. Treated MCF-7-shCon cells displayed a distinct change in morphology (Figure 8.7), and became flattened and enlarged and in looked visually similar to MCF-7-shLCN2 cells. Notably, there was less apparent effect on MCF-7-shLCN2 cells (Fig 8.7)

MCF7-shCon DFOX-

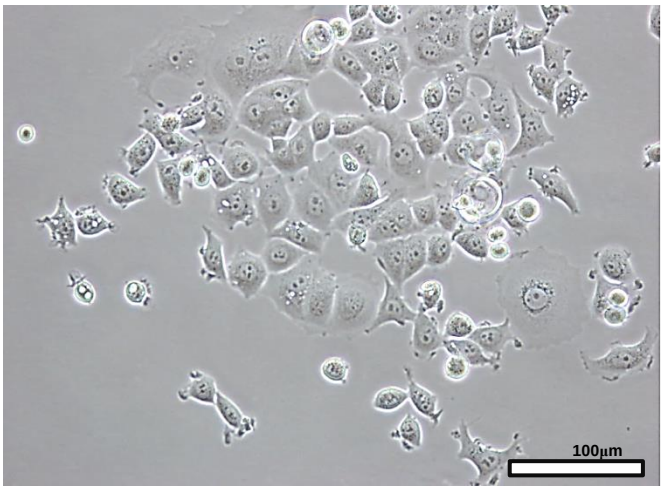

MCF7-shCon DFOX +

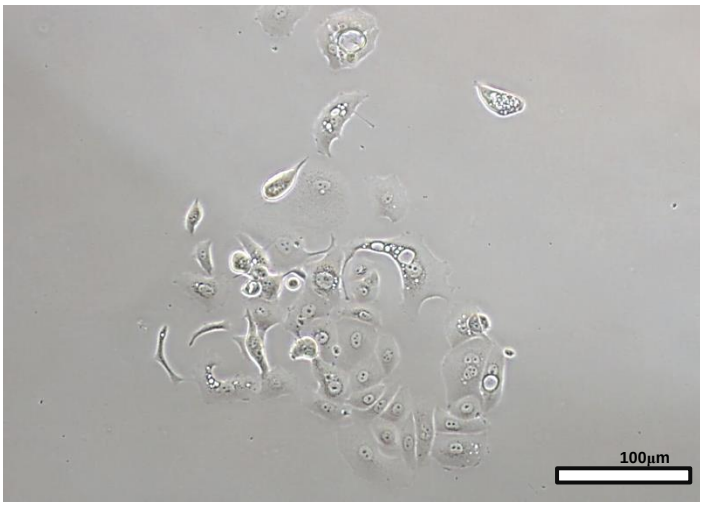

MCF7-shLCN2 DFOX -

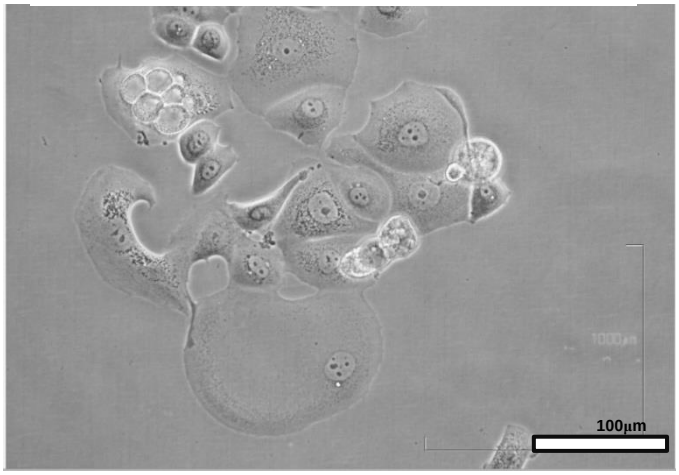

MCF7-shLCN2 DFOX +

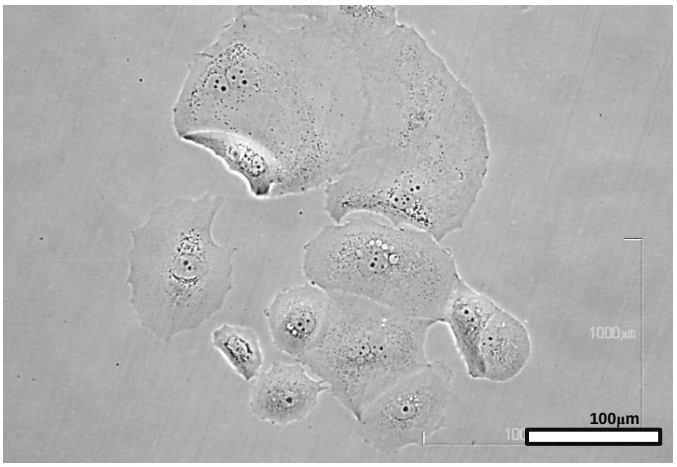

Figure 8.7 Deferoxamine treatment of MCF-7 cells. MCF-7-shCon and MCF-7-shLCN2 cells were treated with 10µM Deferoxamine (DFX) for 48 hours .Following treatment, PC3-shCon cells showed phenotypic change similar to PC3-shLCN2. DFX treated PC3-shLCN2 cells showed a further loss of phase contrast and defined cell edges. X20 magnification, n=3.

Gene expression of DFOX treated MCF7 cells.

Following 48hrs of DFOX treatment, mRNA was extracted from cells and assessed to determine whether there were any effects to gene expression. No significant changes were observed for KDR AGR, CDH1 or KLK6. However, a reduction of 3.8 fold was observed for SPARC in DFOX treated cells (Figure 8.8), a value close to that found in DFOX treated PC3 cells (See figure 7.6). Notably, a decrease of 5.2 fold was recorded for HER2 which was similar to HER2 levels found in MCF7-shLCN2 cells (See Figure 8.5). Therefore, while the changes to gene expression in DFOX treated cells were not as widespread as for PC3-shLCN2 cells (See Fig 7.6), there was a trend that suggests that DFOX treatment of MCF7 cells gives rise to a similar phenotype to MCF7-shLCN2 cells, which indicates that in MCF7 cells at least LCN2 is acting as an iron chelator suppression of LCN2 in MCF7 cells leads to a loss of intracellular iron.

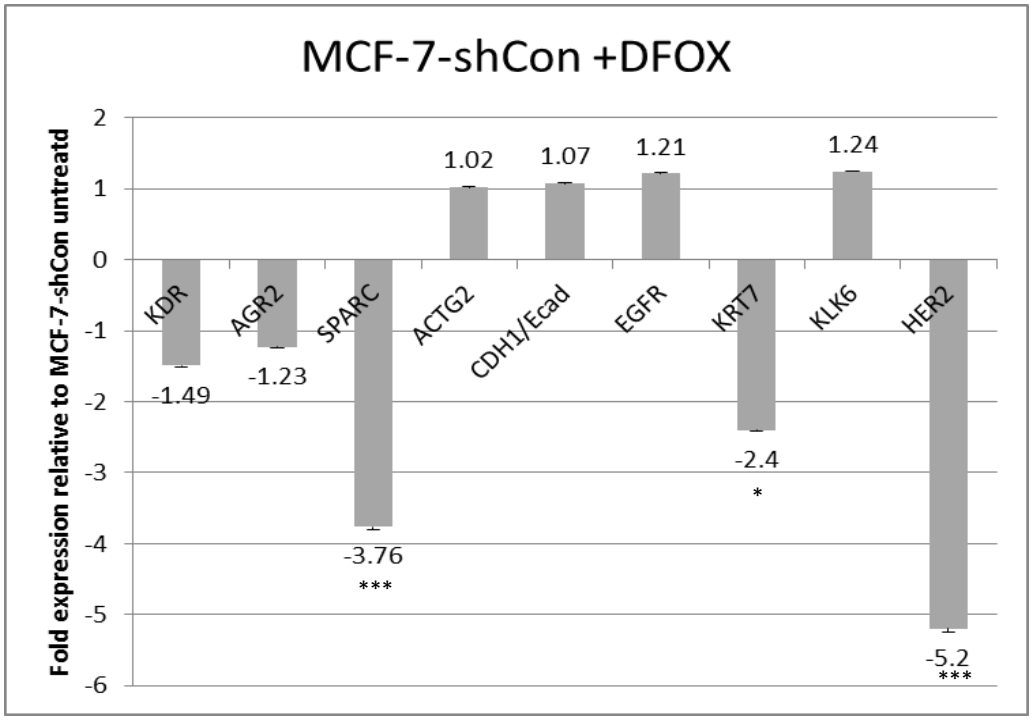

8.8: Gene expression in MCF-7-shCon cells in response to Deferoxamine: MCF-7-shCOn cells were treated with 10μM Deferoxamine (DFX) for 48 hours. qPCR analysis of LCN target genes with the addition of HER2. Values are relative to untreated MCF7-shCon cells +/- SEM Statistical analysis was carried out using Student's t-test. *p<0.05, ***p<0.001.

8.7 Discussion

In a previous publication by Yang et al., 2009, LCN2 was shown to have a negative correlation to both ERα and E-cadherin. This contradicted other studies which have shown that ERα expression represses E-cadherin (Oesterreich et al., 2003). As such, I aimed to investigate whether LCN2 has similar effects in PCa cells compared to the Yang et al. 2009 study in BCa cells. Results presented in this chapter therefore suggest that MCF7 and PC3 cells respond very differently with regards to gene expression when LCN2 is suppressed. However, I also showed that suppression of LCN2 in both cell lines led to an enlarged cell area and that this may be due to the loss of intracellular iron.

In this chapter, it was found that suppression of LCN2 in MCF7 cells resulted in increased expression of genes such as ACTG2 and KLK5, which were previously found to be down-regulated in PC3-shLCN2 cells (See section 6.2). This therefore suggests that these genes are LCN2 targets, but whether these target genes are activated or de-activated differs depending on other factors. That the same gene can have both activating and repressive activity is well known. p53 for instance is particularly well studied in this regards and can both up and down regulate genes depending on their methylation states (Liu and Chen, 2006). Therefore, pre-existing states such as gene methylation may determine whether LCN2 target genes are respond to the lack or presence of LCN2.

Also, I observed opposite effects of LCN2 suppression on the mTOR pathway. Moreover, In PC3 cells, I have shown that treatment with deferoxamine led to a gene expression signature (such as for ACTG2 expression) that was opposite to that found in PC3-shLCN2 cells. However, in MCF7 cells treated with Deferoxamine, the

gene signature was similar to MCF7-shLCN2 cells. When combined therefore, results suggest that there is a fundamental difference between MCF7 and PC3 cells in their response to LCN2. This may be due to the presence of unknown factors which is acts as a repressor in one cell type but as a promoter in the other. However it is also likely that the cell types react differently in response to changes to their intracellular iron levels. LCN2 has been shown to have differing effects in different tissue types, and its effects appear to vary greatly between cell lines, although similar genes such as E-cadherin are commonly associated with LCN2 (Iannetti et al., 2008, Tong et al., 2011). As such, the data in this chapter further demonstrates that LCN2's effects are likely to be dependent on what genes are already active in the cell type. The data also shows that findings in one cell or tissue type should not necessarily be extrapolated to all cells.

In conclusion, the data in this chapter suggests that:

1) Suppression of LCN2 in MCF7 cells leads to a phenotype similar to that of PC3-shLCN2 cells.
2) That while MCF7-shLCN2 cells exhibit a negative correlation to ERα, they also display a negative correlation to E-cadherin
3) Unlike PC3-shLCN2 cells, mTOR pathway activity is increased in MCF7-shLCN2 cells
4) Iron chelation in MCF7 cells gives rise to a phenotype similar to MCF7-shLCN2 cells

Chapter 9: Discussion

9.1 Overview

Prostate cancer is the second leading cause of cancer related deaths in males. The need for understanding how prostate cancer develops, how to detect it and how to treat it is therefore of the utmost importance. Prostate cancer differs to some other forms of the disease in that progression is strongly associated with steroid receptor regulation.

The aim of this study was follow on from work done by Dr. Sandeep Nadendla who demonstrated that ectopic GLI1 led to an androgen independent and EMT like state in LNCaP cells (Nadendla et al 2010). In chapter 3 presented here I subsequently demonstrated that this effect was non reversible and that LNCaP-GLI1 cells maintained an androgen independent phenotype despite GLI1 suppression. Following on from this it was hypothesised that LCN2, which was greatly increased in expression in LNCaP-GLI1 cells was contributing to the androgen independent and EMT phenotype. Through a combination of ectopic expression and targeted suppression, I have demonstrated that contrary to the original hypothesis, LCN2 expression led to increased AR expression and E-cadherin, and was coupled with a negative correlation to ERα.

One of the unresolved questions surrounding LCN2 is whether it is pro- or anti-tumourigenic. In the data presented here, I have demonstrated that rather being simply one or the other, LCN2 demonstrates a range of characteristics. A loss of 3D colony formation in PC3-shLCN2 cells, combined with reduced 2D proliferation are indicative of a pro-tumorigenic activity. On the other hand, an inverse correlation to ERα and E-cadherin (PCa cell lines only) demonstrates an anti-tumorigenic effect. Moreover, ectopic expression of LCN2 did not increase proliferation in LNCaP-LCN2

cells. Also, microarray analysis of PC3-shLCN2 cells revealed both pro- and anti-tumorigenic functions being regulated. Therefore, a simple good or bad label for LCN2 is unsuitable, but may depend on the cancer type. For instance, steroid receptor activity is important in breast and prostate, but is less so in other cancers.

Understanding how LCN2 functions both in normal tissue and cancer is increasing in importance. LCN2 is already used as biomarker for acute kidney injury (Bennett et al., 2008), and has been proposed as a marker for disease progression in breast and pancreatic cancers among others. Gene therapy involving up-regulation of LCN2 has now been used to reduce pancreatic cancer growth (Xu et al., 2013), and is also being trialled for other cancer types. The overall mechanisms of LCN2 function however are still relatively unknown, and there is a lack of consensus particularly with regards to cancer. Many studies on LCN2 have shown opposing effects dependent on tissue type which has further complicated the field. Also, most studies focus on a particular aspect or pathway in cancer and do not provide a more global overview of function. If LCN2 is indeed to be used as either a biomarker or as drug, it is hence important to better understand how LCN2 works across a wide range of cancer types.

While LCN2 has been investigated in breast and pancreatic cancer, the role of LCN2 in prostate cancer has only started to emerge in 2013 (Tung et al., 2013). Given that breast and prostate cancer share steroid receptor signalling as key driving mechanism, the investigation of LCN2 in AR and ER regulation was a logical step. In addition, microarray analysis of PC3-shLCN2 cells revealed many LCN2 linked genes such as SPARC and KLK6 which have not yet been described.

In my study, a key observation was that ectopic expression of LCN2 in LNCaP cells did show changes to steroid receptor regulation, but overall did not show the large changes to proliferation or growth which were seen when LCN2 was suppressed in PC3 and MCF7 cells. One reason for this difference may be due to rate of LCN2 secretion from the cell. In both PC3 and MCF7 cells, high levels of both intracellular and secreted LCN2 were observed. In LNCaP-LCN2 cells however LCN2 was rapidly secreted, which may be in part due to higher LCN2-R expression. This data also suggests that intracellular LCN2 is important for the protein's function, in particular how intracellular LCN2 is influencing iron regulation. High levels of secreted LCN2 were also observed in LNCaP-GLI1 cells. This therefore seems to indicate that there is a characteristic difference in the LNCaP cell line which is not present in PC3 or MCF7 cells. A lack of LCN2 receptor protein in LNCaP cells may also be reducing the effect of LCN2 itself. This may be due to the levels of LCN2 receptor proteins which are able to secrete LCN2. Analysis of intracellular LCN2 protein also showed that both PC3 and MCF7 cells had homodimeric LCN2, whereas LNCaP-LCN2 and LNCaP-GLI1 cells secreted the monomeric forms. This indicates that another factor may be necessary to control LCN2 dimerization or breakdown, although what this factor may be is unknown.

Another potential issue which may be a difference between cell types is post-translational modification. LCN2 has been shown to be glycosylated at numerous sites, although the effects of this glycosylation on function are unknown and in particular whether this affects the 3D structure of the protein (Flower et al., 2000). Evidence of glycosylation was observed using the Santa-Cruz 5G5 antibody which did show evidence of a doublet band in PC3 cells. However this was not detected with other antibodies, and it was not possible to detect the glycosylation state of

LCN2 in LNCaP-LCN2 cells. While a full length LCN2 was transfected into LNCaP cells, it is also possible that the protein was not correctly folded impacting on function.

One key issue with my results was a lack of in-cell imaging by immunofluorescence (IF). The MAB1757 LCN2 antibody from R&D technologies is listed as unsuitable for IF from the company datasheet. Nevertheless, repeated IF optimisation was attempted, but was unable to produce any results and no fluorescence was detected. Indeed, to date no publications have successfully utilised IF for human LCN2 although suitable antibodies have been employed for mouse LCN2 (Langelueddecke et al., 2013). As new antibodies targeting LCN2 become available, this will no doubt elucidate many of its functions

9.1 Post transcriptional effects of LCN2

In these results, I noted that while some genes such as E-cadherin showed expression changes at both the mRNA and protein levels, expression of both AR and ER was regulated at a post-transcriptional level.

Both ER and AR are also regulated post-transcriptionally by a range of micro-RNAs, particularly miR-221, which is up regulated by NF-κB signalling. Data from microarray analysis on PC3-shLCN2 cells did not show any difference in miR-221 expression, or to most other micro-RNAs. However a 3-fold expression was observed for miR-21 which has been shown by to be regulated by androgen receptor and the development of an androgen independent phenotype (Ribas et al, 2009). The role of LCN2 in micro-RNA transcription or function is currently unknown, but would be a worthwhile area of investigation with a more detailed study.

ER and AR are known to be regulated post-transcriptionally and post transnationally through similar mechanisms. Indeed, targeted proteolysis is necessary for both AR and ER function. Upon binding to androgens or estrogens, AR and ER dissociate from HSPs where it can enter the nucleus. Alternatively free AR/ER is targeted for degradation by ubiquitin ligases. This dual action enables cells to finely control the actions of steroid signalling. The balance between signalling and degradation however is still under debate. Studies (Chu at al, 2007) have demonstrated that proteolysis of ER is dependent on the activity of Src. Recent studies have also demonstrated that ER initiates a feedback loop on itself by promoting the expression of proteins which activate E2F-1 which chaperones ER for degradation (Stender et al., 2007). With regards to the data presented in my study, it is possible that altering LCN2 expression is able to influence the levels of proteolysis. Western blots were analysed for both AR and ER breakdown products; unfortunately, the antibodies for ERα and AR did not detect these protein fragments. ERβ did show evidence of breakdown; however results were inconclusive and not pursued further. Whether LCN2 is directly affecting AR/ER degradation or via an intermediary is unknown and microarray analysis on PC3-shLCN2 cells did not reveal any stand-out candidates for regulation. It is also highly likely that LCN2 influences the post-transcriptional regulation of other genes, and hence it would be of interest to perform whole proteome arrays. This may also provide a better picture of exactly how LCN2 is functioning, particularly on other receptors such as progesterone receptor.

9.2 LCN2 signalling pathways

While some of the mechanisms of LCN2 regulation have been studied, there is relatively less data regarding its downstream effects. A key aim of this study was to identify some of the downstream signalling pathways of LCN2. Here I have identified a number of pathways including estrogen receptor and EGFR signalling which were directly affected by LCN2 levels. Notably both EGFR and ER themselves have been shown to up-regulate LCN2 (Tong et al., 2011. Yang et al., 2009) This therefore seems to suggest either bi-directional signalling or a feedback system is active between these genes. With regards to EGFR in particular, I demonstrated that the EGFR inhibitor AG1478 inhibited LCN2 expression, but that in addition, ectopic LCN2 in LNCaP cells increased EGFR expression. AG1478 has previously been shown to inhibit LCN2 expression, however the reverse of LCN2 affecting EGFR has not yet been described in literature.

9.3 Future work

LCN2's role in prostate cancer is still relatively unclear. The results presented in this study provide a number of opportunities for future investigation.

Firstly, if LCN2 does indeed exist as a homodimer within the cell, then this has potential implications for its siderophores binding activities and downstream function. I also noted that dimerised LCN2 appears to be cleaved before being secreted. Further investigation into the processes underlying this change is therefore necessary. It is also worthwhile to see whether this process occurs in vivo as opposed to cell lines. This process is likely to become clearer as better antibodies targeting LCN2 become available In addition, my study did not employ any xenograft

studies in mice. However, recently Tung et al (2013) did perform a limited xenograft which did show reduced tumour growth for PC3-shLCN2 cells in a mouse model. However, no in-depth studies were performed on the tumours, and hence it would be worthwhile to determine factors such as steroid receptor status, metastasis and angiogenesis in further studies.

A further observation which needs to be investigated further is the overall stability of the LCN2 protein. This may be done through siRNA targeted suppression over a much longer time period (e.g. 2 weeks). This would also help identify exactly which pathways are related to LCN2, and in which order they are activated.

In my study, microarray analysis identified the Wnt pathway as being potentially regulated by LCN2. Although LCN2 has been linked to Wnt signalling before, this was as a target gene and not as an effector. It would therefore be worthwhile to investigate fully the role of LCN2 in Wnt signalling, looking at both canonical and non-canonical signalling, and whether any post-translation changes are taking place (e.g. with β-Catenin).

LCN2 is already used as a diagnostic marker for acute kidney injury and post-surgery stress. Testing for LCN2 in blood or urine is steadily becoming cheaper and easier. In prostate cancer, although the PSA test is a good indicator of It cancer stage, it is only indicative of AR expression and thus ignores other factors such as ER expression or the shift to an androgen independent state. It would hence be of great potential interest to examine the levels of LCN2 in prostate cancer patients, either in blood or in urine. LCN2 levels could then be scored against overall prognosis or tumour stage, and correlated to the levels of AR or ER expression in tumours.

Summary of Results

LCN2 forms intracellular dimers	LCN2 is often described as a secreted monomer 24kDa in size. Results showed that intracellular LCN2 appears as a 48kDa dimer which is cleaved before secretion
LCN2 expression negatively correlates to ERα expression	Ectopic expression of LCN2 led to a loss of ERα, whereas shLCN2 in PC3 and MCF7 cells increased ERα expression. This expression was partially restored by recombinant LCN2 protein
LCN2 expression positively correlates to AR	Ectopic expression of LCN2 led to increased AR expression and increased sensitivity to bicalutamide
LCN2- E-cadherin correlation is dependent on cell type	Expression of LCN2 positively correlated to E-cadherin in prostate cells. However E-cadherin was increased in MCF7-shLCN2 cells
LCN2 knockdown leads to phenotypic change	LCN2 suppression in both PC3 and MCF7 cells led to cell enlargement, loss of cell protrusions and effects on cell cycle and loss of nuclear organisation. This may be partially explained by a loss of mTOR signalling.
Downstream signalling for LCN2 is multi-faceted.	Microarray analysis of PC3-shLCN2 cells revealed a wide range of gene expression changes particularly to Wnt, integrin and cadherin signalling.
MCF7-shLCN2 cells had gene expression which was often opposite to that found in PC3-shLCN2 cells	Many genes which were found to be down-regulated in PC3-shLCN2 cells were up-regulated in MCF7-shLCN2 cells and vice versa.
LCN2 has both pro-and anti- tumourigenic properties.	In general, LCN2 appears to demonstrate pro-tumourigenic properties such as to cell cycle and gene expression. However, correlation to ERα expression shows anti-tumourigenic properties as well

References

ABERLE, H., BAUER, A., STAPPERT, J., KISPERT, A. & KEMLER, R. 1997. beta-catenin is a target for the ubiquitin-proteasome pathway. *EMBO J,* 16**,** 3797-804.

ABRAHAMSSON, P. A. 1999. Neuroendocrine differentiation in prostatic carcinoma. *Prostate,* 39**,** 135-48.

AGANI, F. & JIANG, B. H. 2013. Oxygen-independent regulation of HIF-1: novel involvement of PI3K/AKT/mTOR pathway in cancer. *Curr Cancer Drug Targets,* 13**,** 245-51.

ALBERGARIA, A., RIBEIRO, A. S., VIEIRA, A. F., SOUSA, B., NOBRE, A. R., SERUCA, R., SCHMITT, F. & PAREDES, J. 2011. P-cadherin role in normal breast development and cancer. *Int J Dev Biol,* 55**,** 811-22.

ALCEDO, J., ZOU, Y. & NOLL, M. 2000. Posttranscriptional regulation of smoothened is part of a self-correcting mechanism in the Hedgehog signaling system. *Mol Cell,* 6**,** 457-65.

ALDERTON, G. K. 2012. Breast cancer: Reprogramming ERalpha. *Nat Rev Cancer,* 12**,** 79.

ALIMIRAH, F., CHEN, J., BASRAWALA, Z., XIN, H. & CHOUBEY, D. 2006. DU-145 and PC-3 human prostate cancer cell lines express androgen receptor: implications for the androgen receptor functions and regulation. *FEBS Lett,* 580**,** 2294-300.

ARLINGHAUS, R. & LENG, X. 2008. Requirement of lipocalin 2 for chronic myeloid leukemia. *Leuk Lymphoma,* 49**,** 600-3.

ARNOLD, S. A. & BREKKEN, R. A. 2009. SPARC: a matricellular regulator of tumorigenesis. *J Cell Commun Signal,* 3**,** 255-73.

ATTARD, G., RICHARDS, J. & DE BONO, J. S. 2011. New strategies in metastatic prostate cancer: targeting the androgen receptor signaling pathway. *Clin Cancer Res,* 17**,** 1649-57.

BAGSHAW, S. M., BENNETT, M., HAASE, M., HAASE-FIELITZ, A., EGI, M., MORIMATSU, H., D'AMICO, G., GOLDSMITH, D., DEVARAJAN, P. & BELLOMO, R. 2010. Plasma and urine neutrophil gelatinase-associated lipocalin in septic versus non-septic acute kidney injury in critical illness. *Intensive Care Med,* 36**,** 452-61.

BAO, G., CLIFTON, M., HOETTE, T. M., MORI, K., DENG, S. X., QIU, A., VILTARD, M., WILLIAMS, D., PARAGAS, N., LEETE, T., KULKARNI, R., LI, X., LEE, B., KALANDADZE, A., RATNER, A. J., PIZARRO, J. C., SCHMIDT-OTT, K. M., LANDRY, D. W., RAYMOND, K. N., STRONG, R. K. & BARASCH, J. 2010. Iron traffics in circulation bound to a siderocalin (Ngal)-catechol complex. *Nat Chem Biol,* 6**,** 602-9.

BARRESI, V., DI GREGORIO, C., REGGIANI-BONETTI, L., IENI, A., PONZ-DE LEON, M. & BARRESI, G. 2011. Neutrophil gelatinase-associated lipocalin: a new prognostic marker in stage I colorectal carcinoma? *Hum Pathol,* 42**,** 1720-6.

BAUER, M., EICKHOFF, J. C., GOULD, M. N., MUNDHENKE, C., MAASS, N. & FRIEDL, A. 2008. Neutrophil gelatinase-associated lipocalin (NGAL) is a predictor of poor prognosis in human primary breast cancer. *Breast Cancer Res Treat,* 108**,** 389-97.

BAYANI, J. & DIAMANDIS, E. P. 2012. The physiology and pathobiology of human kallikrein-related peptidase 6 (KLK6). *Clin Chem Lab Med,* 50**,** 211-33.

BENNETT, M., DENT, C. L., MA, Q., DASTRALA, S., GRENIER, F., WORKMAN, R., SYED, H., ALI, S., BARASCH, J. & DEVARAJAN, P. 2008. Urine NGAL predicts severity of acute kidney injury after cardiac surgery: a prospective study. *Clin J Am Soc Nephrol,* 3**,** 665-73.

BERNARD, D., POURTIER-MANZANEDO, A., GIL, J. & BEACH, D. H. 2003. Myc confers androgen-independent prostate cancer cell growth. *J Clin Invest,* 112**,** 1724-31.

BERQUIN, I. M., MIN, Y., WU, R., WU, J., PERRY, D., CLINE, J. M., THOMAS, M. J., THORNBURG, T., KULIK, G., SMITH, A., EDWARDS, I. J., D'AGOSTINO, R., ZHANG, H., WU, H., KANG, J. X. & CHEN, Y. Q. 2007. Modulation of prostate cancer genetic risk by omega-3 and omega-6 fatty acids. *J Clin Invest,* 117**,** 1866-75.

BONKHOFF, H. 1998. Neuroendocrine cells in benign and malignant prostate tissue: morphogenesis, proliferation, and androgen receptor status. *Prostate Suppl,* 8**,** 18-22.

BORKHAM-KAMPHORST, E., DREWS, F. & WEISKIRCHEN, R. 2011. Induction of lipocalin-2 expression in acute and chronic experimental liver injury moderated by pro-inflammatory cytokines interleukin-1beta through nuclear factor-kappaB activation. *Liver Int,* 31**,** 656-65.

BRASS, A. L., BARNARD, J., PATAI, B. L., SALVI, D. & RUKSTALIS, D. B. 1995. Androgen up-regulates epidermal growth factor receptor expression and binding affinity in PC3 cell lines expressing the human androgen receptor. *Cancer Res,* 55**,** 3197-203.

BRAY, F., LORTET-TIEULENT, J., FERLAY, J., FORMAN, D. & AUVINEN, A. 2010. Prostate cancer incidence and mortality trends in 37 European countries: an overview. *Eur J Cancer,* 46**,** 3040-52.

BRYCHTOVA, V., VOJTESEK, B. & HRSTKA, R. 2011. Anterior gradient 2: a novel player in tumor cell biology. *Cancer Lett,* 304**,** 1-7.

BUBENDORF, L., SCHOPFER, A., WAGNER, U., SAUTER, G., MOCH, H., WILLI, N., GASSER, T. C. & MIHATSCH, M. J. 2000. Metastatic patterns of prostate cancer: an autopsy study of 1,589 patients. *Hum Pathol,* 31**,** 578-83.

BUMCROT, D. A., TAKADA, R. & MCMAHON, A. P. 1995. Proteolytic processing yields two secreted forms of sonic hedgehog. *Mol Cell Biol,* 15**,** 2294-303.

CARDAMONE, M. D., BARDELLA, C., GUTIERREZ, A., DI CROCE, L., ROSENFELD, M. G., DI RENZO, M. F. & DE BORTOLI, M. 2009. ERalpha as ligand-independent activator of CDH-1 regulates determination and maintenance of epithelial morphology in breast cancer cells. *Proc Natl Acad Sci U S A,* 106**,** 7420-5.

CARNERO, A., BLANCO-APARICIO, C., RENNER, O., LINK, W. & LEAL, J. F. 2008. The PTEN/PI3K/AKT signalling pathway in cancer, therapeutic implications. *Curr Cancer Drug Targets,* 8**,** 187-98.

CHAKRABORTY, S., KAUR, S., GUHA, S. & BATRA, S. K. 2012. The multifaceted roles of neutrophil gelatinase associated lipocalin (NGAL) in inflammation and cancer. *Biochim Biophys Acta,* 1826**,** 129-69.

CHANG, H. H., CHEN, B. Y., WU, C. Y., TSAO, Z. J., CHEN, Y. Y., CHANG, C. P., YANG, C. R. & LIN, D. P. 2011. Hedgehog overexpression leads to the formation of prostate cancer stem cells with metastatic property irrespective of androgen receptor expression in the mouse model. *J Biomed Sci,* 18**,** 6.

CHEN, C., EDELSTEIN, L. C. & GELINAS, C. 2000. The Rel/NF-kappaB family directly activates expression of the apoptosis inhibitor Bcl-x(L). *Mol Cell Biol,* 20**,** 2687-95.

CHEN, M., CARKNER, R. & BUTTYAN, R. 2011. The hedgehog/Gli signaling paradigm in prostate cancer. *Expert Rev Endocrinol Metab,* 6**,** 453-467.

CHEN, M., FEUERSTEIN, M. A., LEVINA, E., BAGHEL, P. S., CARKNER, R. D., TANNER, M. J., SHTUTMAN, M., VACHEROT, F., TERRY, S., DE LA TAILLE, A. & BUTTYAN, R. 2010. Hedgehog/Gli supports androgen signaling in androgen deprived and androgen independent prostate cancer cells. *Mol Cancer,* 9**,** 89.

CHEN, M., TANNER, M., LEVINE, A. C., LEVINA, E., OHOUO, P. & BUTTYAN, R. 2009. Androgenic regulation of hedgehog signaling pathway components in prostate cancer cells. *Cell Cycle,* 8**,** 149-57.

CHEN, W., REN, X. R., NELSON, C. D., BARAK, L. S., CHEN, J. K., BEACHY, P. A., DE SAUVAGE, F. & LEFKOWITZ, R. J. 2004. Activity-dependent internalization of smoothened mediated by beta-arrestin 2 and GRK2. *Science,* 306**,** 2257-60.

CHEN, Z., TROTMAN, L. C., SHAFFER, D., LIN, H. K., DOTAN, Z. A., NIKI, M., KOUTCHER, J. A., SCHER, H. I., LUDWIG, T., GERALD, W., CORDON-CARDO, C. & PANDOLFI, P. P. 2005. Crucial role of p53-dependent cellular senescence in suppression of Pten-deficient tumorigenesis. *Nature,* 436**,** 725-30.

CHESIRE, D. R. & ISAACS, W. B. 2003. Beta-catenin signaling in prostate cancer: an early perspective. *Endocr Relat Cancer,* 10**,** 537-60.

CHOI, J., LEE, H. W. & SUK, K. 2011. Increased plasma levels of lipocalin 2 in mild cognitive impairment. *J Neurol Sci,* 305**,** 28-33.

CLEVERS, H. 2006. Wnt/beta-catenin signaling in development and disease. *Cell,* 127**,** 469-80.

COHEN, R. J., SHANNON, B. A., PHILLIPS, M., MOORIN, R. E., WHEELER, T. M. & GARRETT, K. L. 2008. Central zone carcinoma of the prostate gland: a distinct tumor type with poor prognostic features. *J Urol,* 179**,** 1762-7; discussion 1767.

COLES, M., DIERCKS, T., MUEHLENWEG, B., BARTSCH, S., ZOLZER, V., TSCHESCHE, H. & KESSLER, H. 1999. The solution structure and dynamics of human neutrophil gelatinase-associated lipocalin. *J Mol Biol,* 289**,** 139-57.

COLLINS, A. T., BERRY, P. A., HYDE, C., STOWER, M. J. & MAITLAND, N. J. 2005. Prospective identification of tumorigenic prostate cancer stem cells. *Cancer Res,* 65**,** 10946-51.

COWLAND, J. B., MUTA, T. & BORREGAARD, N. 2006. IL-1beta-specific up-regulation of neutrophil gelatinase-associated lipocalin is controlled by IkappaB-zeta. *J Immunol,* 176**,** 5559-66.

COWLAND, J. B., SORENSEN, O. E., SEHESTED, M. & BORREGAARD, N. 2003. Neutrophil gelatinase-associated lipocalin is up-regulated in human epithelial cells by IL-1 beta, but not by TNF-alpha. *J Immunol,* 171**,** 6630-9.

CREIGHTON, C. J. 2007. A gene transcription signature associated with hormone independence in a subset of both breast and prostate cancers. *BMC Genomics,* 8**,** 199.

DAHMANE, N., LEE, J., ROBINS, P., HELLER, P. & RUIZ I ALTABA, A. 1997. Activation of the transcription factor Gli1 and the Sonic hedgehog signalling pathway in skin tumours. *Nature,* 389**,** 876-81.

DAI, J., HALL, C. L., ESCARA-WILKE, J., MIZOKAMI, A., KELLER, J. M. & KELLER, E. T. 2008. Prostate cancer induces bone metastasis through Wnt-induced bone morphogenetic protein-dependent and independent mechanisms. *Cancer Res,* 68**,** 5785-94.

DAWOOD, S., BROGLIO, K., BUZDAR, A. U., HORTOBAGYI, G. N. & GIORDANO, S. H. 2010. Prognosis of women with metastatic breast cancer by HER2 status and trastuzumab treatment: an institutional-based review. *J Clin Oncol,* 28**,** 92-8.

DEROSA, C. A., FURUSATO, B., SHAHEDUZZAMAN, S., SRIKANTAN, V., WANG, Z., CHEN, Y., SEIFERT, M., RAVINDRANATH, L., YOUNG, D., NAU, M., DOBI, A., WERNER, T., MCLEOD, D. G., VAHEY, M. T., SESTERHENN, I. A., SRIVASTAVA, S. & PETROVICS, G. 2012. Elevated osteonectin/SPARC expression in primary prostate cancer predicts metastatic progression. *Prostate Cancer Prostatic Dis,* 15**,** 150-6.

DEVIREDDY, L. R., GAZIN, C., ZHU, X. & GREEN, M. R. 2005. A cell-surface receptor for lipocalin 24p3 selectively mediates apoptosis and iron uptake. *Cell,* 123**,** 1293-305.

DU, Z. P., YUAN, H. M., WU, B. L., CHANG, J. X., LV, Z., SHEN, J., WU, J. Y., CHEN, H. B., LI, E. M. & XU, L. Y. 2011. Neutrophil gelatinase-associated lipocalin in gastric carcinoma cells and its induction by TPA are controlled by C/EBPbeta. *Biochem Cell Biol,* 89**,** 314-24.

EDINGER, A. L. & THOMPSON, C. B. 2002. Akt maintains cell size and survival by increasing mTOR-dependent nutrient uptake. *Mol Biol Cell,* 13**,** 2276-88.

EGLOFF, A. M., ROTHSTEIN, M. E., SEETHALA, R., SIEGFRIED, J. M., GRANDIS, J. R. & STABILE, L. P. 2009. Cross-talk between estrogen receptor and epidermal growth factor receptor in head and neck squamous cell carcinoma. *Clin Cancer Res,* 15**,** 6529-40.

FELDMAN, B. J. & FELDMAN, D. 2001. The development of androgen-independent prostate cancer. *Nature Reviews Cancer,* 1**,** 34-45.

FERREIRA, A. C., PINTO, V., DA MESQUITA, S., NOVAIS, A., SOUSA, J. C., CORREIA-NEVES, M., SOUSA, N., PALHA, J. A. & MARQUES, F. 2013. Lipocalin-2 is involved in emotional behaviors and cognitive function. *Front Cell Neurosci,* 7**,** 122.

FILARDO, E. J. 2002. Epidermal growth factor receptor (EGFR) transactivation by estrogen via the G-protein-coupled receptor, GPR30: a novel signaling pathway with potential significance for breast cancer. *J Steroid Biochem Mol Biol,* 80**,** 231-8.

FLO, T. H., SMITH, K. D., SATO, S., RODRIGUEZ, D. J., HOLMES, M. A., STRONG, R. K., AKIRA, S. & ADEREM, A. 2004. Lipocalin 2 mediates an innate immune response to bacterial infection by sequestrating iron. *Nature,* 432**,** 917-21.

FLOWER, D. R. 1996. The lipocalin protein family: structure and function. *Biochem J,* 318 (Pt 1)**,** 1-14.

FLOWER, D. R. 2000. Experimentally determined lipocalin structures. *Biochim Biophys Acta,* 1482**,** 46-56.
FLOWER, D. R., NORTH, A. C. & ATTWOOD, T. K. 1991. Mouse oncogene protein 24p3 is a member of the lipocalin protein family. *Biochem Biophys Res Commun,* 180**,** 69-74.
FLOWER, D. R., NORTH, A. C. & SANSOM, C. E. 2000. The lipocalin protein family: structural and sequence overview. *Biochim Biophys Acta,* 1482**,** 9-24.
FU, J., RODOVA, M., ROY, S. K., SHARMA, J., SINGH, K. P., SRIVASTAVA, R. K. & SHANKAR, S. 2013. GANT-61 inhibits pancreatic cancer stem cell growth in vitro and in NOD/SCID/IL2R gamma null mice xenograft. *Cancer Lett,* 330**,** 22-32.
GABBARD, W., MILBRANDT, E. B. & KELLUM, J. A. 2010. NGAL: an emerging tool for predicting severity of AKI is easily detected by a clinical assay. *Crit Care,* 14**,** 318.
GARCIA, J. A. & RINI, B. I. 2012. Castration-resistant prostate cancer: many treatments, many options, many challenges ahead. *Cancer,* 118**,** 2583-93.
GHALI, L., WONG, S. T., GREEN, J., TIDMAN, N. & QUINN, A. G. 1999. Gli1 protein is expressed in basal cell carcinomas, outer root sheath keratinocytes and a subpopulation of mesenchymal cells in normal human skin. *J Invest Dermatol,* 113**,** 595-9.
GHOSH, M. C., GRASS, L., SOOSAIPILLAI, A., SOTIROPOULOU, G. & DIAMANDIS, E. P. 2004. Human kallikrein 6 degrades extracellular matrix proteins and may enhance the metastatic potential of tumour cells. *Tumour Biol,* 25**,** 193-9.
GILMORE, T. D. 2006. Introduction to NF-kappaB: players, pathways, perspectives. *Oncogene,* 25**,** 6680-4.
GIOVANNUCCI, E., ASCHERIO, A., RIMM, E. B., STAMPFER, M. J., COLDITZ, G. A. & WILLETT, W. C. 1995. Intake of carotenoids and retinol in relation to risk of prostate cancer. *J Natl Cancer Inst,* 87**,** 1767-76.
GLAROS, T., FU, Y., XING, J. & LI, L. 2012. Molecular mechanism underlying persistent induction of LCN2 by lipopolysaccharide in kidney fibroblasts. *PLoS One,* 7**,** e34633.
GLASGOW, B. J., ABDURAGIMOV, A. R., GASYMOV, O. K. & YUSIFOV, T. N. 2002. Tear lipocalin: structure, function and molecular mechanisms of action. *Adv Exp Med Biol,* 506**,** 555-65.
GOETZ, D. H., WILLIE, S. T., ARMEN, R. S., BRATT, T., BORREGAARD, N. & STRONG, R. K. 2000. Ligand preference inferred from the structure of neutrophil gelatinase associated lipocalin. *Biochemistry,* 39**,** 1935-41.
GOLDSTEIN, A. S., HUANG, J., GUO, C., GARRAWAY, I. P. & WITTE, O. N. 2010. Identification of a cell of origin for human prostate cancer. *Science,* 329**,** 568-71.
GOLDSTEIN, S. 1990. Replicative senescence: the human fibroblast comes of age. *Science,* 249**,** 1129-33.
GOMEZ-CASADO, C., ROTH-WALTER, F., JENSEN-JAROLIM, E., DIAZ-PERALES, A. & PACIOS, L. F. 2013. Modeling iron-catecholates binding to NGAL protein. *J Mol Graph Model,* 45**,** 111-21.
GONNISSEN, A., ISEBAERT, S. & HAUSTERMANS, K. 2013. Hedgehog signaling in prostate cancer and its therapeutic implication. *Int J Mol Sci,* 14**,** 13979-4007.
GORDON, M. D. & NUSSE, R. 2006. Wnt signaling: multiple pathways, multiple receptors, and multiple transcription factors. *J Biol Chem,* 281**,** 22429-33.
GRAHAM, T. R., ZHAU, H. E., ODERO-MARAH, V. A., OSUNKOYA, A. O., KIMBRO, K. S., TIGHIOUART, M., LIU, T., SIMONS, J. W. & O'REGAN, R. M. 2008. Insulin-like growth factor-I-dependent up-regulation of ZEB1 drives epithelial-to-mesenchymal transition in human prostate cancer cells. *Cancer Res,* 68**,** 2479-88.
GROENEWOUD, M. J. & ZWARTKRUIS, F. J. 2013. Rheb and mammalian target of rapamycin in mitochondrial homoeostasis. *Open Biol,* 3**,** 130185.
GUO, H., ZHANG, Y., BROCKMAN, D. A., HAHN, W., BERNLOHR, D. A. & CHEN, X. 2012. Lipocalin 2 deficiency alters estradiol production and estrogen receptor signaling in female mice. *Endocrinology,* 153**,** 1183-93.
GWIRA, J. A., WEI, F., ISHIBE, S., UELAND, J. M., BARASCH, J. & CANTLEY, L. G. 2005. Expression of neutrophil gelatinase-associated lipocalin regulates epithelial morphogenesis in vitro. *J Biol Chem,* 280**,** 7875-82.

HAASE-FIELITZ, A., BELLOMO, R., DEVARAJAN, P., BENNETT, M., STORY, D., MATALANIS, G., FREI, U., DRAGUN, D. & HAASE, M. 2009. The predictive performance of plasma neutrophil gelatinase-associated lipocalin (NGAL) increases with grade of acute kidney injury. *Nephrol Dial Transplant,* 24**,** 3349-54.

HAASE, M., BELLOMO, R., DEVARAJAN, P., SCHLATTMANN, P., HAASE-FIELITZ, A. & GROUP, N. M.-A. I. 2009. Accuracy of neutrophil gelatinase-associated lipocalin (NGAL) in diagnosis and prognosis in acute kidney injury: a systematic review and meta-analysis. *Am J Kidney Dis,* 54**,** 1012-24.

HARTUPEE, J., LI, X. & HAMILTON, T. 2008. Interleukin 1alpha-induced NFkappaB activation and chemokine mRNA stabilization diverge at IRAK1. *J Biol Chem,* 283**,** 15689-93.

HELDIN, C. H., VANLANDEWIJCK, M. & MOUSTAKAS, A. 2012. Regulation of EMT by TGFbeta in cancer. *FEBS Lett,* 586**,** 1959-70.

HEMMINKI, K. & CHEN, B. 2005. Familial association of prostate cancer with other cancers in the Swedish Family-Cancer Database. *Prostate,* 65**,** 188-94.

HERAWI, M., KAHANE, H., CAVALLO, C. & EPSTEIN, J. I. 2006. Risk of prostate cancer on first re-biopsy within 1 year following a diagnosis of high grade prostatic intraepithelial neoplasia is related to the number of cores sampled. *J Urol,* 175**,** 121-4.

HEUSSLER, H. S. & SURI, M. 2003. Sonic hedgehog. *Mol Pathol,* 56**,** 129-31.

HOLMES, K., ROBERTS, O. L., THOMAS, A. M. & CROSS, M. J. 2007. Vascular endothelial growth factor receptor-2: structure, function, intracellular signalling and therapeutic inhibition. *Cell Signal,* 19**,** 2003-12.

HOROSZEWICZ, J. S., LEONG, S. S., CHU, T. M., WAJSMAN, Z. L., FRIEDMAN, M., PAPSIDERO, L., KIM, U., CHAI, L. S., KAKATI, S., ARYA, S. K. & SANDBERG, A. A. 1980. The LNCaP cell line--a new model for studies on human prostatic carcinoma. *Prog Clin Biol Res,* 37**,** 115-32.

HRABA-RENEVEY, S., TURLER, H., KRESS, M., SALOMON, C. & WEIL, R. 1989. SV40-induced expression of mouse gene 24p3 involves a post-transcriptional mechanism. *Oncogene,* 4**,** 601-8.

HUDSON, C. C., LIU, M., CHIANG, G. G., OTTERNESS, D. M., LOOMIS, D. C., KAPER, F., GIACCIA, A. J. & ABRAHAM, R. T. 2002. Regulation of hypoxia-inducible factor 1alpha expression and function by the mammalian target of rapamycin. *Mol Cell Biol,* 22**,** 7004-14.

HUNCHAREK, M., HADDOCK, K. S., REID, R. & KUPELNICK, B. 2010. Smoking as a risk factor for prostate cancer: a meta-analysis of 24 prospective cohort studies. *Am J Public Health,* 100**,** 693-701.

IANNETTI, A., PACIFICO, F., ACQUAVIVA, R., LAVORGNA, A., CRESCENZI, E., VASCOTTO, C., TELL, G., SALZANO, A. M., SCALONI, A., VUTTARIELLO, E., CHIAPPETTA, G., FORMISANO, S. & LEONARDI, A. 2008. The neutrophil gelatinase-associated lipocalin (NGAL), a NF-kappaB-regulated gene, is a survival factor for thyroid neoplastic cells. *Proc Natl Acad Sci U S A,* 105**,** 14058-63.

INGHAM, P. W., NAKANO, Y. & SEGER, C. 2011. Mechanisms and functions of Hedgehog signalling across the metazoa. *Nat Rev Genet,* 12**,** 393-406.

INOKI, K., LI, Y., ZHU, T., WU, J. & GUAN, K. L. 2002. TSC2 is phosphorylated and inhibited by Akt and suppresses mTOR signalling. *Nat Cell Biol,* 4**,** 648-57.

ITTMANN, M., HUANG, J., RADAELLI, E., MARTIN, P., SIGNORETTI, S., SULLIVAN, R., SIMONS, B. W., WARD, J. M., ROBINSON, B. D., CHU, G. C., LODA, M., THOMAS, G., BOROWSKY, A. & CARDIFF, R. D. 2013. Animal models of human prostate cancer: the consensus report of the New York meeting of the Mouse Models of Human Cancers Consortium Prostate Pathology Committee. *Cancer Res,* 73**,** 2718-36.

JADVAR, H. 2011. Prostate cancer. *Methods Mol Biol,* 727**,** 265-90.

JAIN, G., VOOGDT, C., TOBIAS, A., SPINDLER, K. D., MOLLER, P., CRONAUER, M. V. & MARIENFELD, R. B. 2012. IkappaB kinases modulate the activity of the androgen receptor in prostate carcinoma cell lines. *Neoplasia,* 14**,** 178-89.

JAVELAUD, D., PIERRAT, M. J. & MAUVIEL, A. 2012. Crosstalk between TGF-beta and hedgehog signaling in cancer. *FEBS Lett,* 586**,** 2016-25.

JIAN, L., XIE, L. P., LEE, A. H. & BINNS, C. W. 2004. Protective effect of green tea against prostate cancer: a case-control study in southeast China. *Int J Cancer,* 108**,** 130-5.

JIANG, B., XU, S., HOU, X., PIMENTEL, D. R., BRECHER, P. & COHEN, R. A. 2004. Temporal control of NF-kappaB activation by ERK differentially regulates interleukin-1beta-induced gene expression. *J Biol Chem,* 279**,** 1323-9.

JOHNSON, R. L., ROTHMAN, A. L., XIE, J., GOODRICH, L. V., BARE, J. W., BONIFAS, J. M., QUINN, A. G., MYERS, R. M., COX, D. R., EPSTEIN, E. H., JR. & SCOTT, M. P. 1996. Human homolog of patched, a candidate gene for the basal cell nevus syndrome. *Science,* 272**,** 1668-71.

KAIGHN, M. E., LECHNER, J. F., NARAYAN, K. S. & JONES, L. W. 1978. Prostate carcinoma: tissue culture cell lines. *Natl Cancer Inst Monogr***,** 17-21.

KALLURI, R. & WEINBERG, R. A. 2009. The basics of epithelial-mesenchymal transition. *J Clin Invest,* 119**,** 1420-8.

KARHADKAR, S. S., BOVA, G. S., ABDALLAH, N., DHARA, S., GARDNER, D., MAITRA, A., ISAACS, J. T., BERMAN, D. M. & BEACHY, P. A. 2004. Hedgehog signalling in prostate regeneration, neoplasia and metastasis. *Nature,* 431**,** 707-12.

KARIN, M., CAO, Y., GRETEN, F. R. & LI, Z. W. 2002. NF-kappaB in cancer: from innocent bystander to major culprit. *Nat Rev Cancer,* 2**,** 301-10.

KARLSEN, J. R., BORREGAARD, N. & COWLAND, J. B. 2010. Induction of neutrophil gelatinase-associated lipocalin expression by co-stimulation with interleukin-17 and tumor necrosis factor-alpha is controlled by IkappaB-zeta but neither by C/EBP-beta nor C/EBP-delta. *J Biol Chem,* 285**,** 14088-100.

KAUR, S., BAINE, M. J., GUHA, S., OCHI, N., CHAKRABORTY, S., MALLYA, K., THOMAS, C., CROOK, J., WALLACE, M. B., WOODWARD, T. A., JAIN, M., SINGH, S., SASSON, A. R., SKINNER, V., RAIMONDO, M. & BATRA, S. K. 2013. Neutrophil gelatinase-associated lipocalin, macrophage inhibitory cytokine 1, and carbohydrate antigen 19-9 in pancreatic juice: pathobiologic implications in diagnosing benign and malignant disease of the pancreas. *Pancreas,* 42**,** 494-501.

KAWAUCHI, K., ARAKI, K., TOBIUME, K. & TANAKA, N. 2008. p53 regulates glucose metabolism through an IKK-NF-kappaB pathway and inhibits cell transformation. *Nat Cell Biol,* 10**,** 611-8.

KING, K. J., NICHOLSON, H. D. & ASSINDER, S. J. 2006. Effect of increasing ratio of estrogen: androgen on proliferation of normal human prostate stromal and epithelial cells, and the malignant cell line LNCaP. *Prostate,* 66**,** 105-14.

KINZLER, K. W., BIGNER, S. H., BIGNER, D. D., TRENT, J. M., LAW, M. L., O'BRIEN, S. J., WONG, A. J. & VOGELSTEIN, B. 1987. Identification of an amplified, highly expressed gene in a human glioma. *Science,* 236**,** 70-3.

KINZLER, K. W. & VOGELSTEIN, B. 1990. The GLI gene encodes a nuclear protein which binds specific sequences in the human genome. *Mol Cell Biol,* 10**,** 634-42.

KJELDSEN, L., BAINTON, D. F., SENGELOV, H. & BORREGAARD, N. 1994. Identification of neutrophil gelatinase-associated lipocalin as a novel matrix protein of specific granules in human neutrophils. *Blood,* 83**,** 799-807.

KJELDSEN, L., COWLAND, J. B. & BORREGAARD, N. 2000. Human neutrophil gelatinase-associated lipocalin and homologous proteins in rat and mouse. *Biochim Biophys Acta,* 1482**,** 272-83.

KOBAYASHI, T., SHIMIZU, Y., TERADA, N., YAMASAKI, T., NAKAMURA, E., TODA, Y., NISHIYAMA, H., KAMOTO, T., OGAWA, O. & INOUE, T. 2010. Regulation of androgen receptor transactivity and mTOR-S6 kinase pathway by Rheb in prostate cancer cell proliferation. *Prostate,* 70**,** 866-74.

KOMIYA, Y. & HABAS, R. 2008. Wnt signal transduction pathways. *Organogenesis,* 4**,** 68-75.

KRAUSS, S., CONCORDET, J. P. & INGHAM, P. W. 1993. A functionally conserved homolog of the Drosophila segment polarity gene hh is expressed in tissues with polarizing activity in zebrafish embryos. *Cell,* 75**,** 1431-44.

KYPTA, R. M. & WAXMAN, J. 2012. Wnt/beta-catenin signalling in prostate cancer. *Nat Rev Urol*.

LANDRO, L., DAMAS, J. K., FLO, T. H., HEGGELUND, L., UELAND, T., TJONNFJORD, G. E., ESPEVIK, T., AUKRUST, P. & FROLAND, S. S. 2008. Decreased serum lipocalin-2 levels in human immunodeficiency virus-infected patients: increase during highly active anti-retroviral therapy. *Clin Exp Immunol,* 152**,** 57-63.

LANG, S. H., SHARRARD, R. M., STARK, M., VILLETTE, J. M. & MAITLAND, N. J. 2001. Prostate epithelial cell lines form spheroids with evidence of glandular differentiation in three-dimensional Matrigel cultures. *Br J Cancer,* 85**,** 590-9.

LANGELUEDDECKE, C., ROUSSA, E., FENTON, R. A. & THEVENOD, F. 2013. Expression and function of the lipocalin-2 (24p3/NGAL) receptor in rodent and human intestinal epithelia. *PLoS One,* 8**,** e71586.

LAPLANTE, M. & SABATINI, D. M. 2009. mTOR signaling at a glance. *J Cell Sci,* 122**,** 3589-94.

LAPLANTE, M. & SABATINI, D. M. 2012. mTOR signaling in growth control and disease. *Cell,* 149**,** 274-93.

LAUFER, E., NELSON, C. E., JOHNSON, R. L., MORGAN, B. A. & TABIN, C. 1994. Sonic hedgehog and Fgf-4 act through a signaling cascade and feedback loop to integrate growth and patterning of the developing limb bud. *Cell,* 79**,** 993-1003.

LE ROMANCER, M., POULARD, C., COHEN, P., SENTIS, S., RENOIR, J. M. & CORBO, L. 2011. Cracking the estrogen receptor's posttranslational code in breast tumors. *Endocr Rev,* 32**,** 597-622.

LEE, C. 1996. Role of androgen in prostate growth and regression: stromal-epithelial interaction. *Prostate Suppl,* 6**,** 52-6.

LEE, D. F., KUO, H. P., CHEN, C. T., HSU, J. M., CHOU, C. K., WEI, Y., SUN, H. L., LI, L. Y., PING, B., HUANG, W. C., HE, X., HUNG, J. Y., LAI, C. C., DING, Q., SU, J. L., YANG, J. Y., SAHIN, A. A., HORTOBAGYI, G. N., TSAI, F. J., TSAI, C. H. & HUNG, M. C. 2007. IKK beta suppression of TSC1 links inflammation and tumor angiogenesis via the mTOR pathway. *Cell,* 130**,** 440-55.

LEE, E. K., KIM, H. J., LEE, K. J., LEE, H. J., LEE, J. S., KIM, D. G., HONG, S. W., YOON, Y. & KIM, J. S. 2011. Inhibition of the proliferation and invasion of hepatocellular carcinoma cells by lipocalin 2 through blockade of JNK and PI3K/Akt signaling. *Int J Oncol,* 38**,** 325-33.

LEE, H. J., LEE, E. K., LEE, K. J., HONG, S. W., YOON, Y. & KIM, J. S. 2006. Ectopic expression of neutrophil gelatinase-associated lipocalin suppresses the invasion and liver metastasis of colon cancer cells. *Int J Cancer,* 118**,** 2490-7.

LEE, J., RHEE, M. H., KIM, E. & CHO, J. Y. 2012. BAY 11-7082 is a broad-spectrum inhibitor with anti-inflammatory activity against multiple targets. *Mediators Inflamm,* 2012**,** 416036.

LEISSNER, K. H. & TISELL, L. E. 1979. The weight of the human prostate. *Scand J Urol Nephrol,* 13**,** 137-42.

LENG, X., DING, T., LIN, H., WANG, Y., HU, L., HU, J., FEIG, B., ZHANG, W., PUSZTAI, L., SYMMANS, W. F., WU, Y. & ARLINGHAUS, R. B. 2009. Inhibition of lipocalin 2 impairs breast tumorigenesis and metastasis. *Cancer Res,* 69**,** 8579-84.

LENG, X., LIN, H., DING, T., WANG, Y., WU, Y., KLUMPP, S., SUN, T., ZHOU, Y., MONACO, P., BELMONT, J., ADEREM, A., AKIRA, S., STRONG, R. & ARLINGHAUS, R. 2008. Lipocalin 2 is required for BCR-ABL-induced tumorigenesis. *Oncogene,* 27**,** 6110-9.

LEUNG, L., RADULOVICH, N., ZHU, C. Q., ORGAN, S., BANDARCHI, B., PINTILIE, M., TO, C., PANCHAL, D. & TSAO, M. S. 2012. Lipocalin2 promotes invasion, tumorigenicity and gemcitabine resistance in pancreatic ductal adenocarcinoma. *PLoS One,* 7**,** e46677.

LEVY-LAHAD, E., KRIEGER, M., GOTTFELD, O., RENBAUM, P., KLEIN, G., EISENBERG, S., LAHAD, A., KAUFMAN, B. & CATANE, R. 2000. BRCA1 and BRCA2 mutation carriers as potential candidates for chemoprevention trials. *J Cell Biochem Suppl,* 34**,** 13-8.

LI, H., CHEN, X., CALHOUN-DAVIS, T., CLAYPOOL, K. & TANG, D. G. 2008. PC3 human prostate carcinoma cell holoclones contain self-renewing tumor-initiating cells. *Cancer Res,* 68**,** 1820-5.

LI, J., YEN, C., LIAW, D., PODSYPANINA, K., BOSE, S., WANG, S. I., PUC, J., MILIARESIS, C., RODGERS, L., MCCOMBIE, R., BIGNER, S. H., GIOVANELLA, B. C., ITTMANN, M., TYCKO, B., HIBSHOOSH, H., WIGLER, M. H. & PARSONS, R. 1997. PTEN, a

putative protein tyrosine phosphatase gene mutated in human brain, breast, and prostate cancer. *Science,* 275**,** 1943-7.

LI, S. H., HAWTHORNE, V. S., NEAL, C. L., SANGHERA, S., XU, J., YANG, J., GUO, H., STEEG, P. S. & YU, D. 2009. Upregulation of neutrophil gelatinase-associated lipocalin by ErbB2 through nuclear factor-kappaB activation. *Cancer Res,* 69**,** 9163-8.

LIAO, C. J., LI, P. T., LEE, Y. C., LI, S. H. & CHU, S. T. 2013. Lipocalin 2 induces the epithelial-mesenchymal transition in stressed endometrial epithelial cells: possible correlation with endometriosis development in a mouse model. *Reproduction*.

LILJA, H. 2003. Biology of prostate-specific antigen. *Urology,* 62**,** 27-33.

LIM, R., AHMED, N., BORREGAARD, N., RILEY, C., WAFAI, R., THOMPSON, E. W., QUINN, M. A. & RICE, G. E. 2007. Neutrophil gelatinase-associated lipocalin (NGAL) an early-screening biomarker for ovarian cancer: NGAL is associated with epidermal growth factor-induced epithelio-mesenchymal transition. *Int J Cancer,* 120**,** 2426-34.

LIN, H. H., LIAO, C. J., LEE, Y. C., HU, K. H., MENG, H. W. & CHU, S. T. 2011. Lipocalin-2-induced cytokine production enhances endometrial carcinoma cell survival and migration. *Int J Biol Sci,* 7**,** 74-86.

LIN, P. C., CHIU, Y. L., BANERJEE, S., PARK, K., MOSQUERA, J. M., GIANNOPOULOU, E., ALVES, P., TEWARI, A. K., GERSTEIN, M. B., BELTRAN, H., MELNICK, A. M., ELEMENTO, O., DEMICHELIS, F. & RUBIN, M. A. 2013. Epigenetic repression of miR-31 disrupts androgen receptor homeostasis and contributes to prostate cancer progression. *Cancer Res,* 73**,** 1232-44.

LIU, A. Y., NELSON, P. S., VAN DEN ENGH, G. & HOOD, L. 2002. Human prostate epithelial cell-type cDNA libraries and prostate expression patterns. *Prostate,* 50**,** 92-103.

LIU, C. Z., YANG, J. T., YOON, J. W., VILLAVICENCIO, E., PFENDLER, K., WALTERHOUSE, D. & IANNACCONE, P. 1998. Characterization of the promoter region and genomic organization of GLI, a member of the Sonic hedgehog-Patched signaling pathway. *Gene,* 209**,** 1-11.

LIU, G. & CHEN, X. 2006. Regulation of the p53 transcriptional activity. *J Cell Biochem,* 97**,** 448-58.

LONERGAN, P. E. & TINDALL, D. J. 2011. Androgen receptor signaling in prostate cancer development and progression. *J Carcinog,* 10**,** 20.

MACDONALD, B. T., TAMAI, K. & HE, X. 2009. Wnt/beta-catenin signaling: components, mechanisms, and diseases. *Dev Cell,* 17**,** 9-26.

MAHADEVAN, N. R., RODVOLD, J., ALMANZA, G., PEREZ, A. F., WHEELER, M. C. & ZANETTI, M. 2011. ER stress drives Lipocalin 2 upregulation in prostate cancer cells in an NF-kappaB-dependent manner. *BMC Cancer,* 11**,** 229.

MAK, P., LEAV, I., PURSELL, B., BAE, D., YANG, X., TAGLIENTI, C. A., GOUVIN, L. M., SHARMA, V. M. & MERCURIO, A. M. 2010. ERbeta impedes prostate cancer EMT by destabilizing HIF-1alpha and inhibiting VEGF-mediated snail nuclear localization: implications for Gleason grading. *Cancer Cell,* 17**,** 319-32.

MAKRIS, K., MARKOU, N., EVODIA, E., DIMOPOULOU, E., DRAKOPOULOS, I., NTETSIKA, K., RIZOS, D., BALTOPOULOS, G. & HALIASSOS, A. 2009. Urinary neutrophil gelatinase-associated lipocalin (NGAL) as an early marker of acute kidney injury in critically ill multiple trauma patients. *Clin Chem Lab Med,* 47**,** 79-82.

MALLBRIS, L., O'BRIEN, K. P., HULTHEN, A., SANDSTEDT, B., COWLAND, J. B., BORREGAARD, N. & STAHLE-BACKDAHL, M. 2002. Neutrophil gelatinase-associated lipocalin is a marker for dysregulated keratinocyte differentiation in human skin. *Exp Dermatol,* 11**,** 584-91.

MARIGO, V., JOHNSON, R. L., VORTKAMP, A. & TABIN, C. J. 1996. Sonic hedgehog differentially regulates expression of GLI and GLI3 during limb development. *Dev Biol,* 180**,** 273-83.

MARTI, J., FUSTER, J., SOLA, A. M., HOTTER, G., MOLINA, R., PELEGRINA, A., FERRER, J., DEULOFEU, R., FONDEVILA, C. & GARCIA-VALDECASAS, J. C. 2013. Prognostic value of serum neutrophil gelatinase-associated lipocalin in metastatic and nonmetastatic colorectal cancer. *World J Surg,* 37**,** 1103-9.

MARTINES, A. M., MASEREEUW, R., TJALSMA, H., HOENDEROP, J. G., WETZELS, J. F. & SWINKELS, D. W. 2013. Iron metabolism in the pathogenesis of iron-induced kidney injury. *Nat Rev Nephrol,* 9**,** 385-98.

MATTHEWS, J. & GUSTAFSSON, J. A. 2003. Estrogen signaling: a subtle balance between ER alpha and ER beta. *Mol Interv,* 3**,** 281-92.

MATUSZAK, E. A. & KYPRIANOU, N. 2011. Androgen regulation of epithelial-mesenchymal transition in prostate tumorigenesis. *Expert Rev Endocrinol Metab,* 6**,** 469-482.

MAXWELL, P. & SALNIKOW, K. 2004. HIF-1: an oxygen and metal responsive transcription factor. *Cancer Biol Ther,* 3**,** 29-35.

MAZOR, M., KAWANO, Y., ZHU, H., WAXMAN, J. & KYPTA, R. M. 2004. Inhibition of glycogen synthase kinase-3 represses androgen receptor activity and prostate cancer cell growth. *Oncogene,* 23**,** 7882-92.

MCCABE, N. P., DE, S., VASANJI, A., BRAINARD, J. & BYZOVA, T. V. 2007. Prostate cancer specific integrin alphavbeta3 modulates bone metastatic growth and tissue remodeling. *Oncogene,* 26**,** 6238-43.

MCLAUGHLIN, P. W., TROYER, S., BERRI, S., NARAYANA, V., MEIROWITZ, A., ROBERSON, P. L. & MONTIE, J. 2005. Functional anatomy of the prostate: implications for treatment planning. *Int J Radiat Oncol Biol Phys,* 63**,** 479-91.

MCNEAL, J. E. 1981. The zonal anatomy of the prostate. *Prostate,* 2**,** 35-49.

MERCHANT, A. A. & MATSUI, W. 2010. Targeting Hedgehog--a cancer stem cell pathway. *Clin Cancer Res,* 16**,** 3130-40.

MICALIZZI, D. S., FARABAUGH, S. M. & FORD, H. L. 2010. Epithelial-mesenchymal transition in cancer: parallels between normal development and tumor progression. *J Mammary Gland Biol Neoplasia,* 15**,** 117-34.

MING, J. E., KAUPAS, M. E., ROESSLER, E., BRUNNER, H. G., GOLABI, M., TEKIN, M., STRATTON, R. F., SUJANSKY, E., BALE, S. J. & MUENKE, M. 2002. Mutations in PATCHED-1, the receptor for SONIC HEDGEHOG, are associated with holoprosencephaly. *Hum Genet,* 110**,** 297-301.

MIR, S. U., JIN, L. & CRAVEN, R. J. 2012. Neutrophil gelatinase-associated lipocalin (NGAL) expression is dependent on the tumor-associated sigma-2 receptor S2RPgrmc1. *J Biol Chem,* 287**,** 14494-501.

MIYAMOTO, T., KASHIMA, H., SUZUKI, A., KIKUCHI, N., KONISHI, I., SEKI, N. & SHIOZAWA, T. 2011. Laser-captured microdissection-microarray analysis of the genes involved in endometrial carcinogenesis: stepwise up-regulation of lipocalin2 expression in normal and neoplastic endometria and its functional relevance. *Hum Pathol,* 42**,** 1265-74.

MONIAUX, N., CHAKRABORTY, S., YALNIZ, M., GONZALEZ, J., SHOSTROM, V. K., STANDOP, J., LELE, S. M., OUELLETTE, M., POUR, P. M., SASSON, A. R., BRAND, R. E., HOLLINGSWORTH, M. A., JAIN, M. & BATRA, S. K. 2008. Early diagnosis of pancreatic cancer: neutrophil gelatinase-associated lipocalin as a marker of pancreatic intraepithelial neoplasia. *Br J Cancer,* 98**,** 1540-7.

MONTIRONI, R., MAZZUCCHELLI, R., LOPEZ-BELTRAN, A., CHENG, L. & SCARPELLI, M. 2007. Mechanisms of disease: high-grade prostatic intraepithelial neoplasia and other proposed preneoplastic lesions in the prostate. *Nat Clin Pract Urol,* 4**,** 321-32.

MONTSERRAT, N., GALLARDO, A., ESCUIN, D., CATASUS, L., PRAT, J., GUTIERREZ-AVIGNO, F. J., PEIRO, G., BARNADAS, A. & LERMA, E. 2011. Repression of E-cadherin by SNAIL, ZEB1, and TWIST in invasive ductal carcinomas of the breast: a cooperative effort? *Hum Pathol,* 42**,** 103-10.

MORGAN, T. M., KORECKIJ, T. D. & COREY, E. 2009. Targeted therapy for advanced prostate cancer: inhibition of the PI3K/Akt/mTOR pathway. *Curr Cancer Drug Targets,* 9**,** 237-49.

MULLOR, J. L., DAHMANE, N., SUN, T. & RUIZ I ALTABA, A. 2001. Wnt signals are targets and mediators of Gli function. *Curr Biol,* 11**,** 769-73.

MYERS, R. P. 2000. Structure of the adult prostate from a clinician's standpoint. *Clin Anat,* 13**,** 214-5.

NADENDLA, S. K., HAZAN, A., WARD, M., HARPER, L. J., MOUTASIM, K., BIANCHI, L. S., NAASE, M., GHALI, L., THOMAS, G. J., PROWSE, D. M., PHILPOTT, M. P. & NEILL,

G. W. 2011. GLI1 confers profound phenotypic changes upon LNCaP prostate cancer cells that include the acquisition of a hormone independent state. *PLoS One,* 6**,** e20271.
NADIMINTY, N., LOU, W., SUN, M., CHEN, J., YUE, J., KUNG, H. J., EVANS, C. P., ZHOU, Q. & GAO, A. C. 2010. Aberrant activation of the androgen receptor by NF-kappaB2/p52 in prostate cancer cells. *Cancer Res,* 70**,** 3309-19.
NAUDE, P. J., NYAKAS, C., EIDEN, L. E., AIT-ALI, D., VAN DER HEIDE, R., ENGELBORGHS, S., LUITEN, P. G., DE DEYN, P. P., DEN BOER, J. A. & EISEL, U. L. 2012. Lipocalin 2: novel component of proinflammatory signaling in Alzheimer's disease. *FASEB J,* 26**,** 2811-23.
NDONG, M., KAZAMI, M., SUZUKI, T., UEHARA, M., KATSUMATA, S., INOUE, H., KOBAYASHI, K., TADOKORO, T., SUZUKI, K. & YAMAMOTO, Y. 2009. Iron deficiency down-regulates the Akt/TSC1-TSC2/mammalian Target of Rapamycin signaling pathway in rats and in COS-1 cells. *Nutr Res,* 29**,** 640-7.
NELSON, W. J. & NUSSE, R. 2004. Convergence of Wnt, beta-catenin, and cadherin pathways. *Science,* 303**,** 1483-7.
NIU, J., LI, Z., PENG, B. & CHIAO, P. J. 2004. Identification of an autoregulatory feedback pathway involving interleukin-1alpha in induction of constitutive NF-kappaB activation in pancreatic cancer cells. *J Biol Chem,* 279**,** 16452-62.
NUSSLEIN-VOLHARD, C. & WIESCHAUS, E. 1980. Mutations affecting segment number and polarity in Drosophila. *Nature,* 287**,** 795-801.
O'REILLY, K. E., ROJO, F., SHE, Q. B., SOLIT, D., MILLS, G. B., SMITH, D., LANE, H., HOFMANN, F., HICKLIN, D. J., LUDWIG, D. L., BASELGA, J. & ROSEN, N. 2006. mTOR inhibition induces upstream receptor tyrosine kinase signaling and activates Akt. *Cancer Res,* 66**,** 1500-8.
OESTERREICH, S., DENG, W., JIANG, S., CUI, X., IVANOVA, M., SCHIFF, R., KANG, K., HADSELL, D. L., BEHRENS, J. & LEE, A. V. 2003. Estrogen-mediated down-regulation of E-cadherin in breast cancer cells. *Cancer Res,* 63**,** 5203-8.
OLSEN, C. L., HSU, P. P., GLIENKE, J., RUBANYI, G. M. & BROOKS, A. R. 2004. Hedgehog-interacting protein is highly expressed in endothelial cells but down-regulated during angiogenesis and in several human tumors. *BMC Cancer,* 4**,** 43.
ORABONA, C., DUMOUTIER, L. & RENAULD, J. C. 2001. Interleukin-9 induces 24P3 lipocalin gene expression in murine T cell lymphomas. *Eur Cytokine Netw,* 12**,** 154-61.
OWEN, D. H. & KATZ, D. F. 2005. A review of the physical and chemical properties of human semen and the formulation of a semen simulant. *J Androl,* 26**,** 459-69.
PAN, D., LI, Y., LI, Z., WANG, Y., WANG, P. & LIANG, Y. 2012. Gli inhibitor GANT61 causes apoptosis in myeloid leukemia cells and acts in synergy with rapamycin. *Leuk Res,* 36**,** 742-8.
PARK, S. H., CHEUNG, L. W., WONG, A. S. & LEUNG, P. C. 2008. Estrogen regulates Snail and Slug in the down-regulation of E-cadherin and induces metastatic potential of ovarian cancer cells through estrogen receptor alpha. *Mol Endocrinol,* 22**,** 2085-98.
PATTINGRE, S., ESPERT, L., BIARD-PIECHACZYK, M. & CODOGNO, P. 2008. Regulation of macroautophagy by mTOR and Beclin 1 complexes. *Biochimie,* 90**,** 313-23.
PERKINS, N. D. 2007. Integrating cell-signalling pathways with NF-kappaB and IKK function. *Nat Rev Mol Cell Biol,* 8**,** 49-62.
PIENTA, K. J. & BRADLEY, D. 2006. Mechanisms underlying the development of androgen-independent prostate cancer. *Clin Cancer Res,* 12**,** 1665-71.
PLAYFORD, R. J., BELO, A., POULSOM, R., FITZGERALD, A. J., HARRIS, K., PAWLUCZYK, I., RYON, J., DARBY, T., NILSEN-HAMILTON, M., GHOSH, S. & MARCHBANK, T. 2006. Effects of mouse and human lipocalin homologues 24p3/lcn2 and neutrophil gelatinase-associated lipocalin on gastrointestinal mucosal integrity and repair. *Gastroenterology,* 131**,** 809-17.
RAFFATELLU, M., GEORGE, M. D., AKIYAMA, Y., HORNSBY, M. J., NUCCIO, S. P., PAIXAO, T. A., BUTLER, B. P., CHU, H., SANTOS, R. L., BERGER, T., MAK, T. W., TSOLIS, R. M., BEVINS, C. L., SOLNICK, J. V., DANDEKAR, S. & BAUMLER, A. J. 2009. Lipocalin-2 resistance confers an advantage to Salmonella enterica serotype Typhimurium for growth and survival in the inflamed intestine. *Cell Host Microbe,* 5**,** 476-86.

RAHNAMA, F., SHIMOKAWA, T., LAUTH, M., FINTA, C., KOGERMAN, P., TEGLUND, S., TOFTGARD, R. & ZAPHIROPOULOS, P. G. 2006. Inhibition of GLI1 gene activation by Patched1. *Biochem J,* 394**,** 19-26.

RAMALHO-SANTOS, M., MELTON, D. A. & MCMAHON, A. P. 2000. Hedgehog signals regulate multiple aspects of gastrointestinal development. *Development,* 127**,** 2763-72.

REEBYE, V., QUEROL CANO, L., LAVERY, D. N., BROOKE, G. N., POWELL, S. M., CHOTAI, D., WALKER, M. M., WHITAKER, H. C., WAIT, R., HURST, H. C. & BEVAN, C. L. 2012. Role of the HSP90-associated cochaperone p23 in enhancing activity of the androgen receptor and significance for prostate cancer. *Mol Endocrinol,* 26**,** 1694-706.

REGL, G., NEILL, G. W., EICHBERGER, T., KASPER, M., IKRAM, M. S., KOLLER, J., HINTNER, H., QUINN, A. G., FRISCHAUF, A. M. & ABERGER, F. 2002. Human GLI2 and GLI1 are part of a positive feedback mechanism in Basal Cell Carcinoma. *Oncogene,* 21**,** 5529-39.

REILLY, P. T., TEO, W. L., LOW, M. J., AMOYO-BRION, A. A., DOMINGUEZ-BRAUER, C., ELIA, A. J., BERGER, T., GREICIUS, G., PETTERSSON, S. & MAK, T. W. 2013. Lipocalin 2 performs contrasting, location-dependent roles in APCmin tumor initiation and progression. *Oncogene,* 32**,** 1233-9.

RICHARDSON, D. R. 2005. 24p3 and its receptor: dawn of a new iron age? *Cell,* 123**,** 1175-7.

RIOBO, N. A., LU, K. & EMERSON, C. P., JR. 2006. Hedgehog signal transduction: signal integration and cross talk in development and cancer. *Cell Cycle,* 5**,** 1612-5.

RIUS, J., GUMA, M., SCHACHTRUP, C., AKASSOGLOU, K., ZINKERNAGEL, A. S., NIZET, V., JOHNSON, R. S., HADDAD, G. G. & KARIN, M. 2008. NF-kappaB links innate immunity to the hypoxic response through transcriptional regulation of HIF-1alpha. *Nature,* 453**,** 807-11.

RODDAM, A. W., ALLEN, N. E., APPLEBY, P., KEY, T. J., FERRUCCI, L., CARTER, H. B., METTER, E. J., CHEN, C., WEISS, N. S., FITZPATRICK, A., HSING, A. W., LACEY, J. V., JR., HELZLSOUER, K., RINALDI, S., RIBOLI, E., KAAKS, R., JANSSEN, J. A., WILDHAGEN, M. F., SCHRODER, F. H., PLATZ, E. A., POLLAK, M., GIOVANNUCCI, E., SCHAEFER, C., QUESENBERRY, C. P., JR., VOGELMAN, J. H., SEVERI, G., ENGLISH, D. R., GILES, G. G., STATTIN, P., HALLMANS, G., JOHANSSON, M., CHAN, J. M., GANN, P., OLIVER, S. E., HOLLY, J. M., DONOVAN, J., MEYER, F., BAIRATI, I. & GALAN, P. 2008. Insulin-like growth factors, their binding proteins, and prostate cancer risk: analysis of individual patient data from 12 prospective studies. *Ann Intern Med,* 149**,** 461-71, W83-8.

RUBIN, L. L. & DE SAUVAGE, F. J. 2006. Targeting the Hedgehog pathway in cancer. *Nat Rev Drug Discov,* 5**,** 1026-33.

SANCHEZ-TILLO, E., LAZARO, A., TORRENT, R., CUATRECASAS, M., VAQUERO, E. C., CASTELLS, A., ENGEL, P. & POSTIGO, A. 2010. ZEB1 represses E-cadherin and induces an EMT by recruiting the SWI/SNF chromatin-remodeling protein BRG1. *Oncogene,* 29**,** 3490-500.

SARBASSOV, D. D., ALI, S. M., KIM, D. H., GUERTIN, D. A., LATEK, R. R., ERDJUMENT-BROMAGE, H., TEMPST, P. & SABATINI, D. M. 2004. Rictor, a novel binding partner of mTOR, defines a rapamycin-insensitive and raptor-independent pathway that regulates the cytoskeleton. *Curr Biol,* 14**,** 1296-302.

SARBASSOV, D. D., GUERTIN, D. A., ALI, S. M. & SABATINI, D. M. 2005. Phosphorylation and regulation of Akt/PKB by the rictor-mTOR complex. *Science,* 307**,** 1098-101.

SCHNEIDER, J. G., AMEND, S. R. & WEILBAECHER, K. N. 2011. Integrins and bone metastasis: integrating tumor cell and stromal cell interactions. *Bone,* 48**,** 54-65.

SCHWEIZER, L., RIZZO, C. A., SPIRES, T. E., PLATERO, J. S., WU, Q., LIN, T. A., GOTTARDIS, M. M. & ATTAR, R. M. 2008. The androgen receptor can signal through Wnt/beta-Catenin in prostate cancer cells as an adaptation mechanism to castration levels of androgens. *BMC Cell Biol,* 9**,** 4.

SEN, R. & BALTIMORE, D. 1986. Multiple nuclear factors interact with the immunoglobulin enhancer sequences. *Cell,* 46**,** 705-16.

SENFTLEBEN, U., CAO, Y., XIAO, G., GRETEN, F. R., KRAHN, G., BONIZZI, G., CHEN, Y., HU, Y., FONG, A., SUN, S. C. & KARIN, M. 2001. Activation by IKKalpha of a second, evolutionary conserved, NF-kappa B signaling pathway. *Science,* 293**,** 1495-9.

SHAPIRO, N. I., TRZECIAK, S., HOLLANDER, J. E., BIRKHAHN, R., OTERO, R., OSBORN, T. M., MORETTI, E., NGUYEN, H. B., GUNNERSON, K., MILZMAN, D., GAIESKI, D. F., GOYAL, M., CAIRNS, C. B., KUPFER, K., LEE, S. W. & RIVERS, E. P. 2010. The diagnostic accuracy of plasma neutrophil gelatinase-associated lipocalin in the prediction of acute kidney injury in emergency department patients with suspected sepsis. *Ann Emerg Med,* 56**,** 52-59 e1.

SHAW, G. & PROWSE, D. M. 2008. Inhibition of androgen-independent prostate cancer cell growth is enhanced by combination therapy targeting Hedgehog and ErbB signalling. *Cancer Cell Int,* 8**,** 3.

SHAW, R. J. & CANTLEY, L. C. 2006. Ras, PI(3)K and mTOR signalling controls tumour cell growth. *Nature,* 441**,** 424-30.

SHERWOOD, E. R., THEYER, G., STEINER, G., BERG, L. A., KOZLOWSKI, J. M. & LEE, C. 1991. Differential expression of specific cytokeratin polypeptides in the basal and luminal epithelia of the human prostate. *Prostate,* 18**,** 303-14.

SHIN, D. M., KUCIA, M. & RATAJCZAK, M. Z. 2011. Nuclear and chromatin reorganization during cell senescence and aging - a mini-review. *Gerontology,* 57**,** 76-84.

SHIN, M., MIZOKAMI, A., KIM, J., OFUDE, M., KONAKA, H., KADONO, Y., KITAGAWA, Y., MIWA, S., KUMAKI, M., KELLER, E. T. & NAMIKI, M. 2013. Exogenous SPARC suppresses proliferation and migration of prostate cancer by interacting with integrin beta1. *Prostate,* 73**,** 1159-70.

SIEGEL, R., NAISHADHAM, D. & JEMAL, A. 2013. Cancer statistics, 2013. *CA Cancer J Clin,* 63**,** 11-30.

SIGNORETTI, S., WALTREGNY, D., DILKS, J., ISAAC, B., LIN, D., GARRAWAY, L., YANG, A., MONTIRONI, R., MCKEON, F. & LODA, M. 2000. p63 is a prostate basal cell marker and is required for prostate development. *Am J Pathol,* 157**,** 1769-75.

SIMONS, B. W., HURLEY, P. J., HUANG, Z., ROSS, A. E., MILLER, R., MARCHIONNI, L., BERMAN, D. M. & SCHAEFFER, E. M. 2012. Wnt signaling though beta-catenin is required for prostate lineage specification. *Dev Biol,* 371**,** 246-55.

SLATER, E. P., FENDRICH, V., STRAUCH, K., ROSPLESZCZ, S., RAMASWAMY, A., MATTHAI, E., CHALOUPKA, B., GRESS, T. M., LANGER, P. & BARTSCH, D. K. 2013. LCN2 and TIMP1 as Potential Serum Markers for the Early Detection of Familial Pancreatic Cancer. *Transl Oncol,* 6**,** 99-103.

SMITH, D. S. & CATALONA, W. J. 1994. The nature of prostate cancer detected through prostate specific antigen based screening. *J Urol,* 152**,** 1732-6.

SOBEL, R. E. & SADAR, M. D. 2005. Cell lines used in prostate cancer research: a compendium of old and new lines--part 1. *J Urol,* 173**,** 342-59.

SOMMER, G., WEISE, S., KRALISCH, S., LOSSNER, U., BLUHER, M., STUMVOLL, M. & FASSHAUER, M. 2009. Lipocalin-2 is induced by interleukin-1beta in murine adipocytes in vitro. *J Cell Biochem,* 106**,** 103-8.

SRINIVASAN, G., AITKEN, J. D., ZHANG, B., CARVALHO, F. A., CHASSAING, B., SHASHIDHARAMURTHY, R., BORREGAARD, N., JONES, D. P., GEWIRTZ, A. T. & VIJAY-KUMAR, M. 2012. Lipocalin 2 deficiency dysregulates iron homeostasis and exacerbates endotoxin-induced sepsis. *J Immunol,* 189**,** 1911-9.

STECCA, B., MAS, C., CLEMENT, V., ZBINDEN, M., CORREA, R., PIGUET, V., BEERMANN, F. & RUIZ, I. A. A. 2007. Melanomas require HEDGEHOG-GLI signaling regulated by interactions between GLI1 and the RAS-MEK/AKT pathways. *Proc Natl Acad Sci U S A,* 104**,** 5895-900.

STENDER, J. D., FRASOR, J., KOMM, B., CHANG, K. C., KRAUS, W. L. & KATZENELLENBOGEN, B. S. 2007. Estrogen-regulated gene networks in human breast cancer cells: involvement of E2F1 in the regulation of cell proliferation. *Mol Endocrinol,* 21**,** 2112-23.

STOESZ, S. P., FRIEDL, A., HAAG, J. D., LINDSTROM, M. J., CLARK, G. M. & GOULD, M. N. 1998. Heterogeneous expression of the lipocalin NGAL in primary breast cancers. *Int J Cancer,* 79**,** 565-72.

STONE, K. R., MICKEY, D. D., WUNDERLI, H., MICKEY, G. H. & PAULSON, D. F. 1978. Isolation of a human prostate carcinoma cell line (DU 145). *Int J Cancer,* 21**,** 274-81.

STOYANOVA, T., COOPER, A. R., DRAKE, J. M., LIU, X., ARMSTRONG, A. J., PIENTA, K. J., ZHANG, H., KOHN, D. B., HUANG, J., WITTE, O. N. & GOLDSTEIN, A. S. 2013. Prostate cancer originating in basal cells progresses to adenocarcinoma propagated by luminal-like cells. *Proc Natl Acad Sci U S A,* 110**,** 20111-6.

SU, A. I., WILTSHIRE, T., BATALOV, S., LAPP, H., CHING, K. A., BLOCK, D., ZHANG, J., SODEN, R., HAYAKAWA, M., KREIMAN, G., COOKE, M. P., WALKER, J. R. & HOGENESCH, J. B. 2004. A gene atlas of the mouse and human protein-encoding transcriptomes. *Proc Natl Acad Sci U S A,* 101**,** 6062-7.

SUH, J. & RABSON, A. B. 2004. NF-kappaB activation in human prostate cancer: important mediator or epiphenomenon? *J Cell Biochem,* 91**,** 100-17.

SUN, S. Y., ROSENBERG, L. M., WANG, X., ZHOU, Z., YUE, P., FU, H. & KHURI, F. R. 2005. Activation of Akt and eIF4E survival pathways by rapamycin-mediated mammalian target of rapamycin inhibition. *Cancer Res,* 65**,** 7052-8.

SUN, T., WANG, X., HE, H. H., SWEENEY, C. J., LIU, S. X., BROWN, M., BALK, S., LEE, G. S. & KANTOFF, P. W. 2013. MiR-221 promotes the development of androgen independence in prostate cancer cells via downregulation of HECTD2 and RAB1A. *Oncogene*.

SUN, Y., NIU, J. & HUANG, J. 2009. Neuroendocrine differentiation in prostate cancer. *Am J Transl Res,* 1**,** 148-62.

TABATABAIAN, F., DOUGHERTY, K., DI FULVIO, M. & GOMEZ-CAMBRONERO, J. 2010. Mammalian target of rapamycin (mTOR) and S6 kinase down-regulate phospholipase D2 basal expression and function. *J Biol Chem,* 285**,** 18991-9001.

TAIPALE, J. & BEACHY, P. A. 2001. The Hedgehog and Wnt signalling pathways in cancer. *Nature,* 411**,** 349-54.

TAIPALE, J., CHEN, J. K., COOPER, M. K., WANG, B., MANN, R. K., MILENKOVIC, L., SCOTT, M. P. & BEACHY, P. A. 2000. Effects of oncogenic mutations in Smoothened and Patched can be reversed by cyclopamine. *Nature,* 406**,** 1005-9.

TAMMELA, T. L. 2012. Endocrine prevention and treatment of prostate cancer. *Mol Cell Endocrinol,* 360**,** 59-67.

TEH, M. T., WONG, S. T., NEILL, G. W., GHALI, L. R., PHILPOTT, M. P. & QUINN, A. G. 2002. FOXM1 is a downstream target of Gli1 in basal cell carcinomas. *Cancer Res,* 62**,** 4773-80.

THIERY, J. P., ACLOQUE, H., HUANG, R. Y. & NIETO, M. A. 2009. Epithelial-mesenchymal transitions in development and disease. *Cell,* 139**,** 871-90.

THORSON, P. & HUMPHREY, P. A. 2000. Minimal adenocarcinoma in prostate needle biopsy tissue. *Am J Clin Pathol,* 114**,** 896-909.

TOMITA, K., VAN BOKHOVEN, A., VAN LEENDERS, G. J., RUIJTER, E. T., JANSEN, C. F., BUSSEMAKERS, M. J. & SCHALKEN, J. A. 2000. Cadherin switching in human prostate cancer progression. *Cancer Res,* 60**,** 3650-4.

TONG, Z., CHAKRABORTY, S., SUNG, B., KOOLWAL, P., KAUR, S., AGGARWAL, B. B., MANI, S. A., BRESALIER, R. S., BATRA, S. K. & GUHA, S. 2011. Epidermal growth factor down-regulates the expression of neutrophil gelatinase-associated lipocalin (NGAL) through E-cadherin in pancreatic cancer cells. *Cancer,* 117**,** 2408-18.

TONG, Z., WU, X. & KEHRER, J. P. 2003. Increased expression of the lipocalin 24p3 as an apoptotic mechanism for MK886. *Biochem J,* 372**,** 203-10.

TONG, Z., WU, X., OVCHARENKO, D., ZHU, J., CHEN, C. S. & KEHRER, J. P. 2005. Neutrophil gelatinase-associated lipocalin as a survival factor. *Biochem J,* 391**,** 441-8.

TRAIFFORT, E., DUBOURG, C., FAURE, H., ROGNAN, D., ODENT, S., DUROU, M. R., DAVID, V. & RUAT, M. 2004. Functional characterization of sonic hedgehog mutations associated with holoprosencephaly. *J Biol Chem,* 279**,** 42889-97.

TRAN, C. P., LIN, C., YAMASHIRO, J. & REITER, R. E. 2002. Prostate stem cell antigen is a marker of late intermediate prostate epithelial cells. *Mol Cancer Res,* 1**,** 113-21.

TUNG, M. C., HSIEH, S. C., YANG, S. F., CHENG, C. W., TSAI, R. T., WANG, S. C., HUANG, M. H. & HSIEH, Y. H. 2013. Knockdown of lipocalin-2 suppresses the growth and invasion of prostate cancer cells. *Prostate,* 73**,** 1281-90.

TUXHORN, J. A., AYALA, G. E., SMITH, M. J., SMITH, V. C., DANG, T. D. & ROWLEY, D. R. 2002a. Reactive stroma in human prostate cancer: induction of myofibroblast phenotype and extracellular matrix remodeling. *Clin Cancer Res,* 8**,** 2912-23.

TUXHORN, J. A., MCALHANY, S. J., DANG, T. D., AYALA, G. E. & ROWLEY, D. R. 2002b. Stromal cells promote angiogenesis and growth of human prostate tumors in a differential reactive stroma (DRS) xenograft model. *Cancer Res,* 62**,** 3298-307.

UHLAND, K. 2006. Matriptase and its putative role in cancer. *Cell Mol Life Sci,* 63**,** 2968-78.

VAN BOKHOVEN, A., VARELLA-GARCIA, M., KORCH, C., JOHANNES, W. U., SMITH, E. E., MILLER, H. L., NORDEEN, S. K., MILLER, G. J. & LUCIA, M. S. 2003. Molecular characterization of human prostate carcinoma cell lines. *Prostate,* 57**,** 205-25.

VAN DEN STEEN, P. E., VAN AELST, I., HVIDBERG, V., PICCARD, H., FITEN, P., JACOBSEN, C., MOESTRUP, S. K., FRY, S., ROYLE, L., WORMALD, M. R., WALLIS, R., RUDD, P. M., DWEK, R. A. & OPDENAKKER, G. 2006. The hemopexin and O-glycosylated domains tune gelatinase B/MMP-9 bioavailability via inhibition and binding to cargo receptors. *J Biol Chem,* 281**,** 18626-37.

VASUDEVAN, K. M., GURUMURTHY, S. & RANGNEKAR, V. M. 2004. Suppression of PTEN expression by NF-kappa B prevents apoptosis. *Mol Cell Biol,* 24**,** 1007-21.

VELONAS, V. M., WOO, H. H., REMEDIOS, C. G. & ASSINDER, S. J. 2013. Current status of biomarkers for prostate cancer. *Int J Mol Sci,* 14**,** 11034-60.

VIATOUR, P., BENTIRES-ALJ, M., CHARIOT, A., DEREGOWSKI, V., DE LEVAL, L., MERVILLE, M. P. & BOURS, V. 2003. NF- kappa B2/p100 induces Bcl-2 expression. *Leukemia,* 17**,** 1349-56.

VIAU, A., EL KAROUI, K., LAOUARI, D., BURTIN, M., NGUYEN, C., MORI, K., PILLEBOUT, E., BERGER, T., MAK, T. W., KNEBELMANN, B., FRIEDLANDER, G., BARASCH, J. & TERZI, F. 2010. Lipocalin 2 is essential for chronic kidney disease progression in mice and humans. *J Clin Invest,* 120**,** 4065-76.

VINCENT, T., NEVE, E. P., JOHNSON, J. R., KUKALEV, A., ROJO, F., ALBANELL, J., PIETRAS, K., VIRTANEN, I., PHILIPSON, L., LEOPOLD, P. L., CRYSTAL, R. G., DE HERREROS, A. G., MOUSTAKAS, A., PETTERSSON, R. F. & FUXE, J. 2009. A SNAIL1-SMAD3/4 transcriptional repressor complex promotes TGF-beta mediated epithelial-mesenchymal transition. *Nat Cell Biol,* 11**,** 943-50.

WANG, H. H., WU, M. M., CHAN, M. W., PU, Y. S., CHEN, C. J. & LEE, T. C. 2014. Long-term low-dose exposure of human urothelial cells to sodium arsenite activates lipocalin-2 via promoter hypomethylation. *Arch Toxicol*.

WANG, P., MA, Q., LUO, J., LIU, B., TAN, F., ZHANG, Z. & CHEN, Z. 2009. Nkx3.1 and p27(KIP1) cooperate in proliferation inhibition and apoptosis induction in human androgen-independent prostate cancer cells. *Cancer Invest,* 27**,** 369-75.

WANG, Q., HUANG, C., ZENG, F., XUE, M. & ZHANG, X. 2010. Activation of the Hh pathway in periosteum-derived mesenchymal stem cells induces bone formation in vivo: implication for postnatal bone repair. *Am J Pathol,* 177**,** 3100-11.

WANG, Y. P., YU, G. R., LEE, M. J., LEE, S. Y., CHU, I. S., LEEM, S. H. & KIM, D. G. 2013a. Lipocalin-2 negatively modulates the epithelial-to-mesenchymal transition in hepatocellular carcinoma through the epidermal growth factor (TGF-beta1)/Lcn2/Twist1 pathway. *Hepatology,* 58**,** 1349-61.

WANG, Z. A., MITROFANOVA, A., BERGREN, S. K., ABATE-SHEN, C., CARDIFF, R. D., CALIFANO, A. & SHEN, M. M. 2013b. Lineage analysis of basal epithelial cells reveals their unexpected plasticity and supports a cell-of-origin model for prostate cancer heterogeneity. *Nat Cell Biol,* 15**,** 274-83.

WIRTH, M. P., HAKENBERG, O. W. & FROEHNER, M. 2007. Antiandrogens in the treatment of prostate cancer. *Eur Urol,* 51**,** 306-13; discussion 314.

WU, Y., CHHIPA, R. R., CHENG, J., ZHANG, H., MOHLER, J. L. & IP, C. 2010. Androgen receptor-mTOR crosstalk is regulated by testosterone availability: implication for prostate cancer cell survival. *Anticancer Res,* 30**,** 3895-901.

XIN, L. 2013. Cells of origin for cancer: an updated view from prostate cancer. *Oncogene,* 32**,** 3655-63.

XU, B., ZHENG, W. Y., JIN, D. Y., WANG, D. S., LIU, X. Y. & QIN, X. Y. 2012a. Treatment of pancreatic cancer using an oncolytic virus harboring the lipocalin-2 gene. *Cancer,* 118**,** 5217-26.

XU, J., LAMOUILLE, S. & DERYNCK, R. 2009. TGF-beta-induced epithelial to mesenchymal transition. *Cell Res,* 19**,** 156-72.

XU, Q., MA, P., HU, C., CHEN, L., XUE, L., WANG, Z., LIU, M., ZHU, H., XU, N. & LU, N. 2012b. Overexpression of the DEC1 protein induces senescence in vitro and is related to better survival in esophageal squamous cell carcinoma. *PLoS One,* 7**,** e41862.

XU, Y., CHEN, S. Y., ROSS, K. N. & BALK, S. P. 2006. Androgens induce prostate cancer cell proliferation through mammalian target of rapamycin activation and post-transcriptional increases in cyclin D proteins. *Cancer Res,* 66**,** 7783-92.

YAE, T., TSUCHIHASHI, K., ISHIMOTO, T., MOTOHARA, T., YOSHIKAWA, M., YOSHIDA, G. J., WADA, T., MASUKO, T., MOGUSHI, K., TANAKA, H., OSAWA, T., KANKI, Y., MINAMI, T., ABURATANI, H., OHMURA, M., KUBO, A., SUEMATSU, M., TAKAHASHI, K., SAYA, H. & NAGANO, O. 2012. Alternative splicing of CD44 mRNA by ESRP1 enhances lung colonization of metastatic cancer cell. *Nat Commun,* 3**,** 883.

YAN, L., BORREGAARD, N., KJELDSEN, L. & MOSES, M. A. 2001. The high molecular weight urinary matrix metalloproteinase (MMP) activity is a complex of gelatinase B/MMP-9 and neutrophil gelatinase-associated lipocalin (NGAL). Modulation of MMP-9 activity by NGAL. *J Biol Chem,* 276**,** 37258-65.

YAN, L. & SPITZNAGEL, E. L. 2009. Soy consumption and prostate cancer risk in men: a revisit of a meta-analysis. *Am J Clin Nutr,* 89**,** 1155-63.

YANAI, K., NAKAMURA, M., AKIYOSHI, T., NAGAI, S., WADA, J., KOGA, K., NOSHIRO, H., NAGAI, E., TSUNEYOSHI, M., TANAKA, M. & KATANO, M. 2008. Crosstalk of hedgehog and Wnt pathways in gastric cancer. *Cancer Lett,* 263**,** 145-56.

YANG, F., LI, X., SHARMA, M., SASAKI, C. Y., LONGO, D. L., LIM, B. & SUN, Z. 2002. Linking beta-catenin to androgen-signaling pathway. *J Biol Chem,* 277**,** 11336-44.

YANG, J., BIELENBERG, D. R., RODIG, S. J., DOIRON, R., CLIFTON, M. C., KUNG, A. L., STRONG, R. K., ZURAKOWSKI, D. & MOSES, M. A. 2009. Lipocalin 2 promotes breast cancer progression. *Proc Natl Acad Sci U S A,* 106**,** 3913-8.

YANG, J., MCNEISH, B., BUTTERFIELD, C. & MOSES, M. A. 2013. Lipocalin 2 is a novel regulator of angiogenesis in human breast cancer. *FASEB J,* 27**,** 45-50.

YANG, L., XIE, G., FAN, Q. & XIE, J. 2010. Activation of the hedgehog-signaling pathway in human cancer and the clinical implications. *Oncogene,* 29**,** 469-81.

YE, Y., XIAO, Y., WANG, W., YEARSLEY, K., GAO, J. X., SHETUNI, B. & BARSKY, S. H. 2010. ERalpha signaling through slug regulates E-cadherin and EMT. *Oncogene,* 29**,** 1451-62.

YEAP, B. B., KRUEGER, R. G. & LEEDMAN, P. J. 1999. Differential posttranscriptional regulation of androgen receptor gene expression by androgen in prostate and breast cancer cells. *Endocrinology,* 140**,** 3282-91.

ZHANG, L., ALTUWAIJRI, S., DENG, F., CHEN, L., LAL, P., BHANOT, U. K., KORETS, R., WENSKE, S., LILJA, H. G., CHANG, C., SCHER, H. I. & GERALD, W. L. 2009. NF-kappaB regulates androgen receptor expression and prostate cancer growth. *Am J Pathol,* 175**,** 489-99.

ZHANG, P. X., CHANG, J. X., XIE, J. J., YUAN, H. M., DU, Z. P., ZHANG, F. R., LU, Z., XU, L. Y. & LI, E. M. 2012. Regulation of neutrophil gelatinase-associated lipocalin expression by C/EBPbeta in lung carcinoma cells. *Oncol Lett,* 4**,** 919-924.

ZHAO, C., DAHLMAN-WRIGHT, K. & GUSTAFSSON, J. A. 2008a. Estrogen receptor beta: an overview and update. *Nucl Recept Signal,* 6**,** e003.

ZHAO, J. H., LUO, Y., JIANG, Y. G., HE, D. L. & WU, C. T. 2011. Knockdown of beta-Catenin through shRNA cause a reversal of EMT and metastatic phenotypes induced by HIF-1alpha. *Cancer Invest,* 29**,** 377-82.

ZHAO, J. J., LIN, J., YANG, H., KONG, W., HE, L., MA, X., COPPOLA, D. & CHENG, J. Q. 2008b. MicroRNA-221/222 negatively regulates estrogen receptor alpha and is associated with tamoxifen resistance in breast cancer. *J Biol Chem,* 283**,** 31079-86.

ZHAO, P. & STEPHENS, J. M. 2013. STAT1, NF-kappaB and ERKs play a role in the induction of lipocalin-2 expression in adipocytes. *Mol Metab,* 2**,** 161-70.

ZHOU, Q. & KALDERON, D. 2011. Hedgehog activates fused through phosphorylation to elicit a full spectrum of pathway responses. *Dev Cell,* 20**,** 802-14.

ZHU, H., MAZOR, M., KAWANO, Y., WALKER, M. M., LEUNG, H. Y., ARMSTRONG, K., WAXMAN, J. & KYPTA, R. M. 2004. Analysis of Wnt gene expression in prostate cancer: mutual inhibition by WNT11 and the androgen receptor. *Cancer Res,* 64**,** 7918-26.

ZIEGLER, S., ROHRS, S., TICKENBROCK, L., LANGERAK, A., CHU, S. T., FELDMANN, I., JAKUBOWSKI, N. & MULLER, O. 2007. Lipocalin 24p3 is regulated by the Wnt pathway independent of regulation by iron. *Cancer Genet Cytogenet,* 174**,** 16-23.